REFERENCE ONLY

UNIVERSITY OF LONDON THESIS

Degree PhD Year 2006 Name of Author FENTON M.J

COPYRIGHT

This is a thesis accepted for a Higher Degree of the University of London. It is an unpublished typescript and the copyright is held by the author. All persons consulting the thesis must read and abide by the Copyright Declaration below.

COPYRIGHT DECLARATION

I recognise that the copyright of the above-described thesis rests with the author and that no quotation from it or information derived from it may be published without the prior written consent of the author.

LOANS

Theses may not be lent to individuals, but the Senate House Library may lend a copy to approved libraries within the United Kingdom, for consultation solely on the premises of those libraries. Application should be made to: Inter-Library Loans, Senate House Library, Senate House, Malet Street, London WC1E 7HU.

REPRODUCTION

University of London theses may not be reproduced without explicit written permission from the Senate House Library. Enquiries should be addressed to the Theses Section of the Library. Regulations concerning reproduction vary according to the date of acceptance of the thesis and are listed below as guidelines.

A. Before 1962. Permission granted only upon the prior written consent of the author. (The Senate House Library will provide addresses where possible).

B. 1962 - 1974. In many cases the author has agreed to permit copying upon completion of a Copyright Declaration.

C. 1975 - 1988. Most theses may be copied upon completion of a Copyright Declaration.

D. 1989 onwards. Most theses may be copied.

This thesis comes within category D.

☑ This copy has been deposited in the Library of UCL

☑ This copy has been deposited in the Senate House Library, Senate House, Malet Street, London WC1E 7HU.

The Role of Ageing in Atherogenesis:

Two *In Vivo* Models

Thesis submitted for the degree of
Doctor of Philosophy
at the University of London

by

Mark Fenton MA MB BS MRCP

Department of Medicine
University College London
University of London

November 2005

ProQuest LLC
789 East Eisenhower Parkway
P.O. Box 1346
Ann Arbor, MI 48106-1346

ABSTRACT

Most mammalian cells grown in culture undergo only a limited number of rounds of replicative activity. This exhaustion of proliferative capacity is termed replicative senescence. There is some evidence that replicative senescence may also occur *in vivo*, and it has been postulated that such cellular ageing may contribute to age-related pathologies such as atherosclerosis, and to organismic ageing itself. The aim of this thesis is to explore the associations between replicative senescence, organismic ageing and atherosclerosis.

It was found that a cytochemical assay, senescence-associated β-galactosidase (SA-β-gal), could detect *in vitro* replicative senescence in human endothelial cells (ECs) and rabbit vascular smooth muscle cells (VSMCs).

Endothelial denudation was then undertaken in rabbit carotid arteries, and in some experiments repeated six weeks later. Morphometric analysis of SA-β-gal activity demonstrated that senescent ECs and VSMCs accumulated in the injured vessel wall, a second denudation augmenting this accumulation. Further analysis suggested that these senescent cells showed no proliferative or apoptotic activity.

An animal model of accelerated organismic ageing, the senescence-accelerated prone mouse (SAM-P), and mice from a related strain showing normal ageing (SAM-R), were fed a Western-type diet. Morphometric analysis of lipid deposition in their aortic roots demonstrated increased lipid deposition in SAM-P compared with SAM-R mice, despite lower serum cholesterol levels in SAM-P mice. Study of telomere lengths and SA-β-gal activity showed no evidence of accelerated cellular ageing in SAM-P mice.

It is concluded that cellular ageing can occur in the vasculature, and that a murine strain which ages at an accelerated rate shows a greater susceptibility to atherogenesis. Since no evidence of accelerated cellular ageing was found in this strain, it is postulated that the increased susceptibility of SAM-P mice to atherogenesis, and perhaps also their ageing phenotype, may be attributable to other abnormalities in these mice, such as increased oxidative status.

ACKNOWLEDGEMENTS

Firstly I would like to thank Dr Jorge Erusalimsky for his advice, encouragement and, above all, patience throughout the completion of this thesis. His guidance and support have been invaluable, and I am very grateful for all his help. Secondly, I owe a great debt of gratitude to Professor John Martin for being such a huge source of enthusiasm and support throughout this research.

I am indebted to Mr Steve Barker, whose surgical skill and knowledge were fundamental to the successful completion of the experiments described in Chapter Three. The staff of the Biological Services facility at University College London also provided invaluable help. I am grateful to Keith Miller, Neil Bilbe and David Fish for their advice concerning immunohistochemistry and lipid staining. I am particularly indebted to Felicity Savage for teaching me histological methodologies including the preparation and staining of cryostat sections.

Many thanks must go to Dr Bernd van der Loo for introducing me to cell culture techniques, including immunocytochemistry and *in vitro* β-galactosidase staining. I am extremely grateful to Dr Ying Hong for instructing me in several laboratory techniques including Southern blotting and TUNEL analysis, and for being so encouraging when difficulties were encountered. Likewise I am thankful to Hsiu-Lin Huang for her considerable help with macrophage immunohistochemistry. I would also like to thank Dr Jane Butler for lending her expertise and her pulsed field gel electrophoresis equipment for the analysis of murine telomeres. I am grateful too to Dr David Kurz for helping with the analysis of telomere data. I am particularly grateful to Emma Hawe for her saint-like patience in guiding me through a sea of statistics.

Special mention must go to Dr Anthony Mathur for his friendship and humour, and for proving that thesis-writing can be combined with a career in cardiology.

I would like to thank the British Heart Foundation, whose generous support, in the form of a Junior Research Fellowship, allowed me to conduct these studies.

Lastly I would like to thank my family and friends who have provided such a supportive background to my work. I dedicate this thesis to my parents, who know a lot about language, classics and theology, but are rather weaker on cell biology.

ABBREVIATIONS

4AAP	4-aminoantipyrine
Ab	antibody
ACAT	acyl-CoA:cholesterol acyltransferase
ACE	angiotensin-converting enzyme
ADP	adenosine diphosphate
AGE	advanced glycation end-product
AKR	an inbred mouse strain
AKR/J	the colony of AKR mice maintained at the Jackson Laboratory (Bar Harbor, Maine, USA)
ALP	alkaline phosphatase
A. niger	*Aspergillus niger*
ANOVA	analysis of variance
AP-1	activator protein-1
apoAI	apolipoprotein AI
apoE	apolipoprotein E
ARF	alternative reading frame
Asc	ascorbic acid
ATM	ataxia telangiectasia mutated DNA damage response kinase
ATP	adenosine triphosphate
β-gal	β-galactosidase
bp	base pairs
CCD	charge-coupled device
CD	cluster differentiation
Cdk	cyclin-dependent kinase
CE	cholesterol esterase
C. elegans	*Caenorhabditis elegans*
CHEF	contour-clamped homogeneous field electrophoresis
CO	cholesterol oxidase
CPD	cumulative population doubling
DAB	diaminobenzidine
DAPI	4',6-diamidino-2-phenylindole

DDW	double-distilled water
3,5 DHBS	3,5 dichloro-2-hydroxybenzene
DKC	dyskeratosis congenita
DMEM	Dulbecco's modified Eagle's medium
DMF	dimethylformamide
DNA	deoxyribonucleic acid
DPX	'Distrene-80', Plasticizer, and Xylene
dUTP	deoxyuracil triphosphate
EC	endothelial cell
EDTA	ethylenediamine tetra acetic acid
EEL	external elastic lamina
EGM	endothelial cell growth medium
eNOS	endothelial nitric oxide synthase
ERK	extracellular signal-regulated kinase
FCS	foetal calf serum
g	gravitational force
GK	glycerol kinase
GPO	glycerol phosphate oxidase
h	hour
H&E	haematoxylin and eosin
HAEC	human aortic endothelial cell
HBA	hydroxybenzoic acid
HBSS	Hanks balanced salt solution
HCl	hydrochloric acid
HDF	human diploid fibroblast
HDL	high density lipoprotein
HP	hydrogen peroxide
HRP	horseradish peroxidase
hTERT	human telomerase reverse transcriptase
HUVEC	human umbilical vein endothelial cell
ICAM-1	intercellular adhesion molecule-1
IEL	internal elastic lamina
IFN	interferon

IFN-γ	interferon-gamma
Ig	immunoglobulin
IGF-1	insulin-like growth factor-1
IHD	ischaemic heart disease
IL-1	interleukin-1
IL-1α	interleukin-1 alpha
IL-1β	interleukin-1 beta
IL-6	interleukin-6
IQR	inter-quartile range
kbp	kilo-base pair
kD	kilo-Dalton
LDL	low density lipoprotein
LMP	low melting point
M	molar
MAPK	mitogen-activated protein kinase
MCBD	Molecular and Cellular Developmental Biology
MCP-1	monocyte chemotactic protein-1
min	minute
MLSP	maximum life-span potential
MMP	matrix metalloproteinase
MMP-2	matrix metalloproteinase-2
MoAb	monoclonal antibody
mRNA	messenger ribonucleic acid
mTR	gene encoding mouse telomerase RNA
μM	micromolar
N/A	not applicable
NF-κB	nuclear factor kappa B
NIH	National Institutes of Health
nM	nanomolar
NO	nitric oxide
N/S	not significant (statistically)
NZW	New Zealand White
OxLDL	oxidized low density lipoprotein

PAI-1	plasminogen activator inhibitor-1
PBS	phosphate-buffered saline
PBN	α-phenyl-*t*-butyl nitrone
PCNA	proliferating cell nuclear antigen
PD	population doubling
PDGF	platelet-derived growth factor
PFA	paraformaldehyde
PFG	pulsed field gel
PMSF	phenylmethylsulphonyl fluoride
pRb	retinoblastoma tumour susceptibility gene product
PTCA	percutaneous transluminal coronary angioplasty
RB	retinoblastoma tumour susceptibility gene
RNA	ribonucleic acid
ROS	reactive oxygen species
RT	room temperature
SA-β-gal	senescence-associated beta-galactosidase
SAM	senescence-accelerated mouse
SAM-P	senescence-accelerated prone mouse
SAM-R	senescence-accelerated resistant mouse
SAPK	stress-activated protein kinase
s.d.	one standard deviation
SDS	sodium dodecyl sulphate
sec	seconds
SIPS	stress-induced premature senescence
SM	smooth muscle
SMC	smooth muscle cell
SOD	superoxide dismutase
SSC	standard saline citrate
Str	streptavidin
Str-ALP	streptavidin conjugated with alkaline phosphatase
Str-HRP	streptavidin conjugated with horseradish peroxidase
T lymphocyte	thymus-derived lymphocyte
t-BHP	tert-butylhydroperoxide

TBE	tris base boric acid EDTA buffer
TBS	tris-buffered saline
TdT	terminal deoxynucleotidyl transferase
TE	Tris-EDTA buffer
TERT	telomerase reverse transcriptase
TIMP-1	tissue inhibitor of metalloproteinase-1
TNF	tumour necrosis factor
TNF-α	tumour necrosis factor-alpha
TR	RNA component of telomerase
TRF	terminal restriction fragment
TRF1	TTAGGG repeat binding factor 1
TRF2	TTAGGG repeat binding factor 2
Tris	Tris-(hydroxymethyl)-aminomethane
TUNEL	terminal deoxynucleotidyl transferase -mediated X-dUTP nick end labelling
UCL	University College London
UV	ultraviolet
V	volts
VCAM-1	vascular cell adhesion molecule-1
VEGF	vascular endothelial growth factor
VLDL	very low density lipoprotein
VSMC	vascular smooth muscle cell
v/v	volume to volume ratio
WHHL	Watanabe heritable hyperlipidaemic
WRN	Werner protein
w/v	weight to volume ratio
X-dUTP	hapten-labelled deoxyuracil triphosphate
X-Gal	5-bromo-4-chloro-3-indolyl-beta-galactopyranoside

LIST OF FIGURES AND TABLES

page

CHAPTER ONE

Table 1.1 Pathologies in SAM sub-strains **70**

CHAPTER TWO

Figure 2.1 Processing of excised rabbit carotid arteries **88**

Figure 2.2 Preparation of rabbit carotid artery cross-sections **90**

Table 2.1 Summary of immunohistochemistry protocols used in rabbit carotid artery model **96**

Figure 2.3 Protocols used for detection of β-galactosidase activity in excised rabbit carotid arteries **100**

Table 2.2 Notice used by designated technicians in the management of the UCL colony of SAM mice **103**

Figure 2.4 Preparation of SAM aortic root cross-sections **110**

CHAPTER THREE

Figure 3.1 β-galactosidase staining in confluent early passage HUVECs **121**

Figure 3.2 SA-β-gal staining in early- and late-passage HUVECs **121**

Figure 3.3 Semi-quantitative analysis of SA-β-gal staining in serially passaged HUVECs **122**

Figure 3.4 SA-β-gal staining in early- and late-passage rabbit vascular smooth muscle cells **124**

Figure 3.5 SA-β-gal staining and CD31 labelling in early- and late-passage HUVECs **124**

Figure 3.6 Preliminary protocols for staining for β-galactosidase activity in *ex vivo* tissue **126**

Figure 3.7 Acid β-galactosidase activity in non-denuded rabbit carotid artery **126**

Figure 3.8 Experimental design for rabbit carotid artery denudation studies **131**

Figure 3.9 Morphology of occluded rabbit carotid artery **133**

Figure 3.10 Morphology of control, single- and double-denudation rabbit carotid arteries **135**

Table 3.1 Luminal, neo(intimal) and medial cross-sectional areas of rabbit carotid arteries 137

Figure 3.11 (Neo)intima / media ratios in rabbit carotid arteries 137

Figure 3.12 Endothelial regeneration following denudation injuries in rabbit carotid arteries 138

Figure 3.13 pH dependence of β-galactosidase staining in control rabbit carotid arteries 138

Figure 3.14 SA-β-gal staining in control, single- and double-denudation vessels 140

Figure 3.15 Percentage areas of SA-β-gal staining in the (neo)intima and media of rabbit carotid arteries 142

Figure 3.16 Identification of SA-β-gal-positive cells 144

Figure 3.17 Detection of cellular proliferation and senescence in injured arteries 146

Figure 3.18 TUNEL analysis and SA-β-gal staining in rabbit neointima 147

Figure 3.19 TUNEL analysis and SA-β-gal staining in rabbit media 147

CHAPTER FOUR

Figure 4.1 Phenotypes of SAM-P and SAM-R mice 165

Table 4.1 Weights of SAM mice fed a standard laboratory chow 166

Figure 4.2 Experimental design for SAM atherogenesis study 168

Figure 4.3 Morphology of lipid deposits in C57BL/6 and SAM-P mouse aortic roots (pilot study) 170

Table 4.2 Number of lesions in C57BL/6 and SAM-P mice in pilot study 171

Table 4.3 Extent of Oil red O staining in C57BL/6 and SAM-P mice in the pilot study 172

Figure 4.4 Weights of SAM mice fed the Western-type diet 173

Table 4.4 Serum lipid levels in SAM mice prior to Western-type diet 174

Table 4.5 Serum lipid levels in SAM mice fed a Western-type diet 175

Table 4.6 Serum lipid levels before and after administration of the Western-type diet 176

Figure 4.5 Serum cholesterol and triglyceride levels in SAM mice before and after administration of a Western-type diet 177

Table 4.7 HDL/total cholesterol ratios in young SAM fed a standard chow and in old SAM fed a Western-type diet 179

Figure 4.6 HDL/total cholesterol ratios in SAM mice **179**

Table 4.8 HDL/total cholesterol ratios in old SAM mice fed a standard chow or a Western-type diet **180**

Figure 4.7 Morphology of fatty lesions in SAM-P and SAM-R mice **181**

Table 4.9 Number of lesions in SAM mice fed a Western-type diet **183**

Table 4.10 Median number of lesions in the aortic roots of SAM mice fed a Western-type diet **184**

Table 4.11 Prevalence of lesion types in SAM mice fed a Western-type diet **185**

Table 4.12 Extent of Oil red O staining in SAM mice fed a Western-type diet **187**

Table 4.13 Median areas of Oil red O staining in SAM mice fed a Western-type diet **188**

Figure 4.8 Morphometric analysis of lesion size in SAM mice **189**

Figure 4.9 Macrophages in SAM lipid lesions **191**

Figure 4.10 TRF lengths in SAM-P and SAM-R mice **192**

Table 4.14 TRF lengths in SAM splenic cells **192**

Figure 4.11 SA-β-gal in SAM skin and aorta **194**

CHAPTER FIVE

Figure 5.1 Network of processes associated with atherosclerosis and ageing **231**

TABLE OF CONTENTS

ABSTRACT 2

ACKNOWLEDGEMENTS 3

ABBREVIATIONS 4

LIST OF FIGURES AND TABLES 9

TABLE OF CONTENTS 12

CHAPTER ONE: INTRODUCTION 20

1.1 MECHANISMS UNDERLYING ATHEROSCLEROSIS 21

1.1.1 The development of the atherosclerotic lesion – histology 21

1.1.2 Cells involved in atherogenesis 23
1.1.2.1 Endothelial cells 23
1.1.2.2 Vascular smooth muscle cells 23
1.1.2.3 Monocytes and macrophages 24
1.1.2.4 Platelets 24
1.1.2.5 T lymphocytes 25

1.1.3 Theories of atherogenesis 25
1.1.3.1 The response-to-injury theory 25
1.1.3.2 The lipid theory 26
1.1.3.3 The role of oxidative stress 26
1.1.3.4 The role of hypoxia 27
1.1.3.5 Foetal and infant nutrition 27
1.1.3.6 Monoclonal origin of vascular smooth muscle cells 28
1.1.3.7 Atherogenesis as an inflammatory process 28
1.1.3.8 Putative role of viruses 28
1.1.3.9 Homocysteine 29

1.2 AGEING AS A RISK FACTOR FOR ATHEROSCLEROSIS 29

1.2.1 Physiological changes in the arterial wall with increasing age 29

1.2.2 Evidence for ageing as a risk factor for atherosclerosis 30

1.2.3 Ageing as an independent risk factor for atherosclerosis 31

1.3 MECHANISMS UNDERLYING THE AGEING PROCESS 33

1.3.1 Developmental-genetic theories 33
1.3.1.1 The neuroendocrine theory 34
1.3.1.2 The immunological theory 34
1.3.1.3 Replicative senescence 35

1.3.2 Stochastic theories 35
1.3.2.1 The somatic mutation theory 35
1.3.2.2 The deoxyribonucleic acid repair theory 35
1.3.2.3 The error-catastrophe theory 36
1.3.2.4 Protein cross-linking and advanced glycation end-products 36
1.3.2.5 The role of mitochondrial dysfunction 36
1.3.2.6 The role of free radicals and oxidative stress 37

1.4 REPLICATIVE SENESCENCE 38

1.4.1 Normal regulation of the mammalian cell cycle 38

1.4.2 The phenomenon of replicative senescence 39

1.4.3 Morphological and molecular features of senescent cells 40

1.4.4 Putative mechanisms of replicative senescence 41
1.4.4.1 Telomere shortening in serially passaged cells 41
1.4.4.2 The role of telomerase 42
1.4.4.3 Higher order structure of telomeres 44
1.4.4.4 The effect of changes in telomeric structure on the cell cycle 44

1.4.5 Replicative senescence as a tumour-suppressor mechanism 47

1.4.6 Replicative senescence and organismic ageing 47

1.4.7 Replicative senescence and apoptosis 51

1.4.8 Replicative senescence and atherosclerosis 52
1.4.8.1 Putative role of EC and VSMC senescence in atherosclerosis 52
1.4.8.2 Evidence for EC and VSMC senescence in atherosclerosis 53
1.4.8.3 EC and VSMC proliferation studies 54
1.4.8.4 Telomere studies 54
1.4.8.5 Endothelial denudation studies 55

1.4.9 Detection of senescent cells 55

1.5 OXIDATIVE STRESS 57

1.5.1 Definition 57

1.5.2 The generation and effects of oxidative stress 58

1.5.3 Oxidative stress and organismic ageing 59

1.5.4 Oxidative stress, replicative senescence, and stress-induced premature senescence 60
1.5.4.1 The effects of oxidative status on cellular proliferative activity 60
1.5.4.2 Stress-induced premature senescence 61
1.5.4.3 Relationship between replicative senescence and SIPS 61

1.5.5 Oxidative stress and atherosclerosis 63
1.5.5.1 Epidemiological and dietary studies 63
1.5.5.2 Putative mechanism of action of oxidative stress in atherogenesis 64
1.5.5.3 Atherogenic properties of OxLDL 65
1.5.5.4 Other possible roles for oxidative stress in atherogenesis 66

1.6 EXPERIMENTAL MODELS OF AGEING 66

1.7 THE SENESCENCE-ACCELERATED MOUSE (SAM) 67

1.8 ANIMAL MODELS OF ATHEROSCLEROSIS 69

1.8.1 The C57BL/6 mouse 71

1.8.2 The LDL-receptor deficient mouse 71

1.8.3 The apoE-deficient mouse 71

1.8.4 Rats 72

1.8.5 Rabbits 72

1.8.6 Pigs 72

1.8.7 Non-human primates 72

1.8.8 Denudation models 73

1.9 AIMS OF THE STUDIES DESCRIBED 73

CHAPTER TWO: MATERIALS AND METHODS 74

2.1 MATERIALS 75

2.1.1 Antibodies 75

2.1.2 Kits and reagents used in histology, immunostaining and apoptosis studies 76
2.1.2.1 Kits 76
2.1.2.2 Reagents 76

2.1.3 Kits and reagents used in cell culture and telomere studies 77
2.1.3.1 Kits 77
2.1.3.2 Reagents 77

2.1.4 Other kits, reagents and drugs 78
2.1.4.1 Kits 78
2.1.4.2 Reagents 78
2.1.4.3 Drugs 78

2.1.5 Buffers, solutions and media 79
2.1.5.1 Buffers 79
2.1.5.2 Solutions 79
2.1.5.3 Media 81

2.1.6 Diets 81

2.2 METHODS 82

2.2.1 Home Office Licences for animal research described in this thesis 82

2.2.2 In vitro cell senescence studies 82
2.2.2.1 Culture of HUVECs 82
2.2.2.2 Establishment of rabbit VSMC cultures 83
2.2.2.3 Staining of cell cultures for β-galactosidase activity 84
2.2.2.4 SA-β-gal and CD31 double-staining 85

2.2.3 Studies of cell senescence in rabbit carotid arteries 85
2.2.3.1 Acquisition and maintenance of rabbits 85
2.2.3.2 Denudation of rabbit carotid arteries 86
2.2.3.3 Harvesting of rabbit carotid arteries 87
2.2.3.4 Processing of rabbit carotid arteries, and staining for β-gal activity 87
2.2.3.5 Preparation of arterial cross-sections for further analysis 89
2.2.3.6 Morphological studies: haematoxylin and eosin staining 91
2.2.3.7 Morphometric studies: injury scores, neointima formation and SA-β-gal staining 92
2.2.3.8 Statistical analysis 94

2.2.3.9 Immunohistochemistry 94
2.2.3.10 Detection of apoptotic cells 98
2.2.3.11 Protocols tested during development of *ex vivo* SA-β-gal assay 99

2.2.4 Studies in senescence-accelerated mice 101
2.2.4.1 Establishment and maintenance of a colony of senescence-accelerated mice 101
2.2.4.2 Acquisition and maintenance of C57BL/6 mice 104
2.2.4.3 Administration of a Western-type diet 104
2.2.4.4 Preparation of serum from SAM mice 105
2.2.4.5 Measurement of total serum cholesterol and triglyceride levels in individual SAM mice 105
2.2.4.6 Determination of lipid profiles in pooled sera of SAM mice 107
2.2.4.7 Harvesting, fixation and storage of tissue for analysis of atherogenesis 108
2.2.4.8 Preparation of cryostat cross-sections 108
2.2.4.9 Staining of aortic cross-sections for lipid 109
2.2.4.10 Morphometric analysis of lipid deposition in aortic cross-sections 109
2.2.4.11 Photography of lipid lesions 111
2.2.4.12 Immunohistochemical detection of murine macrophages 111
2.2.4.13 Statistical analysis 112
2.2.4.14 Terminal restriction fragment length analysis 113
2.2.4.15 SA-β-gal staining in tissue from SAM mice 116

CHAPTER THREE: CELL SENESCENCE IN DENUDED RABBIT CAROTID ARTERIES 117

3.1 SECTION ONE: PRELIMINARY EXPERIMENTS 118

3.1.1 Introduction 118

3.1.2 Experimental design 119

3.1.3 Results 120
3.1.3.1 β-galactosidase staining in early passage HUVEC cultures 120
3.1.3.2 SA-β-gal staining in serially passaged HUVEC cultures 120
3.1.3.3 SA-β-gal staining in serially passaged rabbit VSMC cultures 123
3.1.3.4 SA-β-gal and CD31 double-staining in HUVECs 123
3.1.3.5 Development of a protocol for staining rabbit carotid arteries for β-galactosidase activity 123

3.1.4 Discussion of preliminary studies 127

3.2 SECTION TWO: THE DETECTION OF *IN VIVO* SENESCENCE IN THE RABBIT CAROTID ARTERY DENUDATION MODEL 129

3.2.1 Introduction 129

3.2.2 Experimental design 130

3.2.3 Results 132
3.2.3.1 Morphology and morphometry of neointimal lesions in the single- and double-denudation groups 132
3.2.3.2 Detection of SA-β-gal activity in control, single- and double-denudation vessels: qualitative assessment 139
3.2.3.3 Assessment of the accumulation of SA-β-gal-positive cells in denuded vessels 141
3.2.3.4 Identification of SA-β-gal-positive cell types 143
3.2.3.5 Detection of proliferating cells in carotid artery cross-sections 145
3.2.3.6 Detection of apoptotic cells in carotid artery cross-sections 145

3.2.4 Discussion 148
3.2.4.1 Key findings 148
3.2.4.2 Comments on the experimental design 148
3.2.4.3 Discussion of the results 155

3.2.5 Conclusion 161

CHAPTER FOUR: ATHEROGENESIS IN SENESCENCE-ACCELERATED MICE 162

4.1 DESCRIPTION OF THE SAM COLONY ESTABLISHED AT UCL 164

4.2 EXPERIMENTAL DESIGNS FOR THE STUDY OF ATHEROGENESIS IN SAM AND C57BL/6 MICE 167

4.3 RESULTS OF PILOT STUDY COMPARING LIPID DEPOSITION IN SAM-P AND C57BL/6 MICE 169

4.4 RESULTS OF SAM ATHEROGENESIS STUDIES 173

4.4.1 Weight gain of SAM mice on a Western-type diet 173

4.4.2 Serum cholesterol and triglyceride levels in SAM mice 174

4.4.3 HDL/total cholesterol ratios in SAM mice 178

4.4.4 Lipid deposition in the aortic roots of SAM mice fed a Western-type diet 180
4.4.4.1 Morphology of lipid lesions 180
4.4.4.2 Number of lesions per aortic root 182
4.4.4.3 Prevalence of lesions in aortic roots 184
4.4.4.4 Results of morphometric analysis 186

4.4.5 Detection of macrophages in SAM-P and SAM-R aortic roots 190

4.5 RESULTS OF TELOMERE LENGTH ANALYSIS IN SAM MICE 190

4.6 RESULTS OF SA-β-GAL STUDIES IN SAM MICE 193

4.7 DISCUSSION 193

4.7.1 Key findings 193

4.7.2 Comments on the experimental design 195
4.7.2.1 The use of SAM mice in the study of ageing and atherogenesis 195
4.7.2.2 The choice of SAM-P/8 and SAM-R/1 strains 196
4.7.2.3 Choice of the pro-atherogenic diet 197
4.7.2.4 Timing of the initiation of the Western-type diet 198
4.7.2.5 Duration of administration of the Western-type diet 198
4.7.2.6 Measurement of serum lipid profiles 198
4.7.2.7 Tissue harvesting and fixation 199
4.7.2.8 Morphometric analysis of murine aortic roots 199

4.7.3 Discussion of the results 200
4.7.3.1 Preservation of the senescent phenotype 200
4.7.3.2 Susceptibility of SAM-P and SAM-R mice to atherogenesis 200
4.7.3.3 Possible explanations for the greater lesion formation in SAM-P/8 mice 202

4.8 CONCLUSION 211

CHAPTER FIVE: DISCUSSION 212

5.1 SA-β-GAL AS A MARKER OF CELLULAR SENESCENCE 213

5.1.1 Possible weaknesses and limitations 213

5.1.2 Biological rationale for the ability of SA-β-gal to detect senescence 215

5.1.3 Subsequent use of SA-β-gal to detect ex vivo senescence 217

5.2 IMPLICATIONS OF VASCULAR CELL SENESCENCE FOR HUMAN VASCULAR PATHOLOGY 217

5.2.1 Evidence for EC senescence in human atheroma 218

5.2.2 Evidence for VSMC senescence in human atheroma 218

5.2.3 Atherosclerosis as an inflammatory phenomenon 219

5.2.4 Pro-inflammatory properties of senescent ECs 220

5.2.5 Pro-inflammatory properties of senescent VSMCs 220

5.2.6 Putative role of EC senescence in an artery's response to injury 222

5.2.7 Putative role of VSMC senescence in an artery's response to injury 223

5.2.8 Potential widespread effect of a small number of senescent cells 224

5.3 ORGANISMIC AND CELLULAR AGEING, AND ATHEROGENESIS 224

5.3.1 Accelerated ageing and atherogenesis 224

5.3.2 Lack of evidence for enhanced replicative senescence in SAM spleen, skin and aorta 225

5.3.3 Possible interactions between telomere shortening and atherogenesis 226

5.3.4 Oxidative stress and atherogenesis in SAM mice 227

5.3.5 Other possible interactions between organismic ageing and atherogenesis 227

5.3.6 Organismic ageing: an active or a passive process? 228

5.3.7 Processes linking cellular and organismic ageing with atherosclerosis 230

5.4 FUTURE EXPERIMENTS 230

5.4.1 Carotid denudation model 230

5.4.2 SAM model 233

5.4.3 Human studies 235

5.5 CONCLUSION 235

PUBLICATIONS 236

REFERENCES 237

CHAPTER ONE

Introduction

Atherosclerosis is a pathological process which has a variety of clinical manifestations, including ischaemic heart disease (IHD), cerebrovascular disease and peripheral vascular disease. These conditions appear to be markedly age-related in terms of their onset and progression. A number of risk factors have been established for atherosclerosis in general, and for IHD in particular; these include hypertension [Stokes *et al.* 1987], diabetes mellitus [Kannel and McGee 1979], hyperlipidaemia [Zemel and Sowers 1990], smoking [McGill 1988], family history [Friedlander *et al.* 1985] and increased age of the subject. Of these factors, ageing shows the strongest association with lesion extent and severity [McGill 1984, Clarkson *et al.* 1987]. Ironically, when Leonardo da Vinci suggested a causal link between ageing and 'thickening' of blood vessels, his hypothesis was that it was the pathology of the blood vessels which led to ageing, rather than the other way round [cited in Belt 1952].

The aim of this thesis is to explore the relationship between ageing and atherosclerosis using two animal models. By way of introduction, this chapter will firstly describe some of the cellular processes which occur during atherogenesis. Next various theories concerning the aetiology of atherogenesis will be reviewed; in particular, the evidence that ageing and atherosclerosis may be causally linked will be discussed. Mechanisms previously postulated to underlie ageing will then be considered, together with their inter-relationships with those processes thought to underlie atherogenesis. Various animal models which have previously been used to study ageing and atherosclerosis will be described. Finally the more detailed aims of the thesis will be summarized.

1.1 Mechanisms underlying atherosclerosis

Since the experiments described in this thesis concern the effects of ageing at both an organismic and a cellular level on the development of atherosclerosis, it is worth considering in some detail the cellular interactions which take place during atherogenesis.

1.1.1 The development of the atherosclerotic lesion – histology

The earliest lesion of atherosclerosis is the fatty streak; fatty streak formation has been detected as early as foetal development *in utero* [Napoli *et al.* 1997]. Fatty streaks contain predominantly macrophages, but also some vascular smooth muscle cells (VSMCs) [McGill 1968]. Both cell types in the lesion are laden with lipid.

The fatty streak subsequently progresses to the fibrous plaque [reviewed by Ross 1986]. This latter lesion consists of increased numbers of intimal smooth muscle cells (SMCs), together with some macrophages, and other leukocytes including activated lymphocytes. The plaque cells are surrounded by connective tissue matrix, and the lesion contains both intracellular and extracellular lipid. The luminal surface of the plaque consists of a fibrous cap, containing modified SMCs. Monocytes become attached to this luminal surface, usually near the edge of the plaque. Beneath the fibrous cap there may be found necrotic debris, cholesterol crystals and calcification.

The histological sequence of events involved in fatty streak formation, and the subsequent conversion of this lesion into a fibrous plaque, have been studied in detail in cholesterol-fed primates [Faggiotto and Ross 1984] and in humans [Ross 1986].

In the non-human primate studies, the first histological change noted after initiation of an atherogenic diet was the appearance of clusters of leukocytes (mainly monocytes) attached to the arterial luminal surface at scattered sites throughout the vascular tree. Some of these monocytes were subsequently found interposed between endothelial cells (ECs), and later accumulating in clusters in the subendothelial region. Here the monocytes developed into macrophages and accumulated lipid, assuming the phenotype of foam cells. At about this time, VSMCs migrated from the media into the intima and also became laden with lipid. In primates and humans, VSMCs proliferate in the intima, and this proliferation, together with the congregation of foam cells, leads to enlargement of the fatty streak. As VSMCs proliferate, they become the predominant cell type in the intima, and the lesion develops into a fibrous plaque [Faggiotto and Ross 1984, Ross 1986].

Atherosclerotic lesions are considered histologically advanced when their accumulation of lipid, cells and matrix components is accompanied by structural disorganization and derangement of the vessel wall architecture. Extracellular lipid pools increase in size and become confluent, leading to the formation of a well-delineated lipid core. The intimal tissue lying between the lipid core and the endothelial surface becomes progressively more fibrous, eventually forming the fibrous cap [Ross 1986].

At a later stage, microscopic discontinuities emerge in the endothelium, to such an extent that the underlying fatty lesion is exposed to blood in the vessel lumen [Faggiotto and Ross 1984]. This is followed by the adherence and aggregation of

platelets, with the resultant development of mural thrombus. In humans, the fibrous cap is prone to fissure formation, as it contains predominantly proteoglycans and macrophages, and relatively few SMCs [Ross 1986]. Thrombotic encrustations are thought to occur repeatedly on the luminal surface of the lesions, successively overlying newly accumulating lipid; thrombus may thus become incorporated into the plaque, contributing to the structural instability of the lesion and to luminal narrowing [Stary *et al.* 1994]. Subsequent development of haemorrhage into the plaque can result in plaque rupture and vessel occlusion.

1.1.2 Cells involved in atherogenesis

1.1.2.1 Endothelial cells

ECs have various properties which influence the onset and progression of atherogenesis. They bind low density lipoprotein (LDL) via specific receptors [Sawamura *et al.* 1997], and modify it so that it is more readily recognized and ingested by macrophages [Steinberg 1983]. Oxidized lipids in turn induce increased expression of adhesion molecules on ECs, promoting leukocyte attachment [Dart and Chin-Dusting 1999]. ECs also produce vasoactive substances, growth factors and growth inhibitors [Moncada *et al.* 1977, Castellot *et al.* 1982, DiCorleto and Bowen-Pope 1983]; their production and release of nitric oxide (NO) in particular will be discussed later. Some mitotic factors, such as platelet-derived growth factor (PDGF), are produced by human ECs if they are proliferating, but not if they are quiescent [Barrett *et al.* 1984].

1.1.2.2 Vascular smooth muscle cells

The migration and proliferation of VSMCs are important elements in the evolution and enlargement of fatty streaks and fibrous plaques. VSMCs have other properties which appear to be involved in atherogenesis. They can secrete large amounts of connective tissue matrix [Burke and Ross 1979] and accumulate lipid via specific receptors for LDL [Chait *et al.* 1980, Pitas 1990]. They express receptors for PDGF [Bowen-Pope *et al.* 1985], and can respond to chemotactic factors released by ECs [Cucina *et al.* 2003] and activated macrophages [Goetze *et al.* 1999]. They also proliferate in response to stimulation by interleukin-1 (IL-1) [Libby *et al.* 1988]. Their resultant capacity to proliferate and migrate in response to external stimuli is thought to be important in atherogenesis. VSMCs can in turn secrete factors chemotactic for

monocytes [Jauchem *et al.* 1982], and can express the pro-inflammatory mediators intercellular adhesion molecule-1 (ICAM-1) and vascular cell adhesion molecule-1 (VCAM-1) [Shin *et al.* 1996].

VSMCs exhibit two alternative phenotypes: they can exist either in a 'synthetic' or a 'contractile' state [Chamley-Campbell *et al.* 1981]. The phenotype of the cells affects their ability to respond to mitogens and other stimuli.

1.1.2.3 Monocytes and macrophages

As noted above, an early histological finding in atherogenesis is monocyte adhesion to the endothelial surface. Peripheral blood monocytes preferentially adhere to regenerating rather than quiescent ECs *in vitro* [DiCorleto and de la Motte 1985], and to injured rather than intact endothelium *in vivo* [Hansson *et al.* 1981]. The principle mediator of monocyte adhesion and recruitment to the injured vascular wall is thought to be monocyte chemotactic protein-1 (MCP-1) [Kraemer 2000]. Macrophages themselves produce chemotactic agents, including IL-1 and leukotriene B4 [Martin *et al.* 1984], suggesting that as these cells accumulate in the vessel wall, they are able to promote further cellular accumulation.

Macrophages take up lipoproteins via a receptor-mediated mechanism; they possess receptors for both native and modified LDL [Brown and Goldstein 1983, Mazzone *et al.* 1983]. They themselves can oxidize LDL [Parthasarathy *et al.* 1986], rendering it more susceptible to uptake [Steinberg *et al.* 1989]. Other monocyte/macrophage functions which may contribute to atherogenesis include phagocytosis and the synthesis and release of neutral proteases. Macrophages may also be responsible for injuring ECs, bringing about their retraction over the foam cells in fatty streaks [Ross 1986].

1.1.2.4 Platelets

In normal circumstances, platelets are unable to adhere to the arterial endothelium, partly because ECs produce anti-thrombotic substances such as NO, prostacyclin and heparin [Alheid *et al.* 1987]. If platelets do come into contact with subendothelial connective tissue via breaches in the endothelium, they release the contents of their granules [Baumgartner 1972]. These include mitogens such as PDGF [Ross *et al.* 1974], which can induce both migration [Grotendorst *et al.* 1982] and proliferation [Ross *et al.* 1974] of VSMCs. The platelet granules also contain adenosine

diphosphate (ADP) [Mustard and Packham 1975] which can enhance platelet deposition.

1.1.2.5 T lymphocytes

T cells constitute approximately one fifth of the cell population of the fibrous cap, and are also found in the underlying plaque [Jonasson *et al.* 1986]. The entry of T cells into the intima during atherogenesis appears to be mediated by their binding to ICAM-1 [Watanabe and Fan 1998]. T cells are attracted by three chemokines, each inducible by interferon-gamma (IFN-γ): inducible protein-10, monokine induced by IFN-γ, and IFN-inducible T-cell α-chemoattractant [Mach *et al.* 1999]. Intimal T cells may then be activated by interaction with antigens including oxidized LDL and heat-shock proteins [Libby and Aikawa 2002]. Activated T cells can then induce macrophages to release tissue factor, matrix metalloproteinases (MMPs) and pro-inflammatory cytokines, leading potentially to the amplification of the inflammatory response. The T cells themselves appear to polarize into two types: T_H1 cells produce predominantly pro-inflammatory cytokines, while T_H2 cells secrete mainly anti-inflammatory cytokines [reviewed in Libby and Aikawa 2002]. In human atherosclerotic plaques, the T cell response appears to produce predominantly T_H1 cells [Frostegard *et al.* 1999].

1.1.3 Theories of atherogenesis

Over the years, various theories have attempted to explain the initiation and evolution of atherosclerotic lesions. Some of these theories are reviewed below. As will be seen, they are not mutually exclusive, and there are areas of overlap between the mechanisms proposed.

1.1.3.1 The response-to-injury theory

This theory was originally proposed in the nineteenth century, and has more recently been further promoted and modified [Ross and Glomset 1976, Ross 1986]. It suggests that the atherogenic process is triggered by an initial disruption to endothelial integrity. The nature of the agent causing this disruption has been extensively debated, with mechanical injury and chemical insults being putatively implicated. The disruption is believed to be followed by an accumulation of platelets and monocytes at the injury site, and then by the various other cellular interactions detailed above.

The response-to-injury hypothesis, while remaining a widely prevalent view of the aetiology of atherosclerosis, has not gone entirely unchallenged. In particular, it is not always possible to demonstrate physical disruption of the endothelium during the early stages of atherogenesis [Taylor *et al.* 1989, Busse and Fleming 1996]. Indeed in the primate studies detailed above, monocytes appeared to adhere to an intact endothelium [Faggiotto and Ross 1984]. Some authors have taken this as evidence that endothelial denudation does not play any part in plaque initiation [Davies and Woolf 1993], but suggest that it may occur at a later stage, triggering platelet adhesion.

1.1.3.2 The lipid theory

The lipid theory emphasizes the role of circulating lipid in atherogenesis. The potential significance of excess dietary fat in atherogenesis has been recognized for nearly a century [Anitschkow 1913]. The lipid theory arose from the observations that atherosclerotic lesions are lipid-rich, that animals fed a high-cholesterol diet produce lesions similar to human atherosclerotic plaques, and that human populations with high plasma lipid levels show a high incidence of atherosclerosis [Woolf 1977].

Cholesterol and triglycerides are transported in the circulation in the form of lipoproteins, which are spherical particles containing cholesteryl ester and triglyceride, with an outer surface made up of apo-proteins and phospholipids. Up to seventy percent of circulating cholesterol in humans is transported as LDL. This LDL can either be taken up by peripheral tissues (when demand is high, via up-regulation of peripheral LDL receptors), or be cleared by the liver.

It has been proposed that the earliest event in the development of the fatty streak is the transport of LDL into the arterial wall [Navab *et al.* 1996]. This is a concentration-dependent process not requiring receptor-mediated endocytosis [Steinberg *et al.* 1989].

1.1.3.3 The role of oxidative stress

Atherogenesis is thought to be promoted by peroxidation of lipids by oxidative stress [Witztum and Steinberg 1991]. Native LDL is not taken up efficiently by macrophages *in vitro* [Weinstein *et al.* 1976]; prior to uptake, it must first be modified. One such modification involves the progressive oxidation of native LDL to generate a series of forms of LDL termed oxidized LDL (OxLDL) [Witztum 1994]. OxLDL is found in human atherosclerotic lesions, but not in normal arterial tissue [Palinski *et al.* 1989, Ylä-Herttuala *et al.* 1989].

OxLDL has a variety of other properties which render it more atherogenic than native LDL [Steinberg *et al.* 1989], and these will be discussed in detail below. Among these, its cytotoxic capability may contribute to the EC retraction (mentioned earlier) which appears to precede platelet adherence and thrombus formation [Steinberg *et al.* 1989]. There is thus a degree of overlap between the response-to-injury and lipid theories of atherosclerosis, and the postulated involvement of oxidative stress.

1.1.3.4 The role of hypoxia

Hypoxia of the arterial wall has also been implicated in atherogenesis by several investigators [Hueper 1944, Kjeldsen *et al.* 1968, Martin *et al.* 1991]. Inhalation of low oxygen concentrations promoted the development of atherosclerotic lesions in cholesterol-fed rabbits [Kjeldsen *et al.* 1968]. Similarly, when LDL-receptor-deficient rabbits were exposed to either hyperoxic or hypoxic conditions, hypoxic animals developed significantly more severe atheromatous lesions than did those exposed to hyperoxia, despite there being no difference in plasma cholesterol levels between the two groups [Okamoto *et al.* 1983]. Hypoxia can lead to increased expression of PDGF and acyl CoA:cholesterol acyltransferase (ACAT) in the arterial wall, and this has been put forward as a potential mechanism by which localized hypoxia might promote atherogenesis [Martin *et al.* 1991].

At first sight the notion that hypoxia is pro-atherogenic appears to gainsay the theory that oxidative stress is important in the aetiology of atherosclerosis. It is possible, though, that while a generalized increase in oxidative stress in the vessel wall promotes atherogenesis (for example via its modification of LDL to OxLDL), more focal (perhaps microscopic) regions of the vessel wall may become hypoxic (for example through occlusion of the vasa vasorum) leading to a localized release of PDGF and ACAT.

1.1.3.5 Foetal and infant nutrition

Barker *et al.* have proposed that factors in foetal life and infancy determine, to a significant extent, an adult's subsequent risk of developing cardiovascular disease [Barker and Osmond 1986, Barker *et al.* 1989]. They suggested that the foetus' nourishment could 'programme' the development of risk factors such as hypertension, diabetes mellitus and hypercholesterolaemia. This proposition, though, was based entirely on epidemiological data, and no mechanistic explanation was offered. The

theory has subsequently been widely challenged [Elford *et al.* 1991, Paneth and Susser 1995].

1.1.3.6 Monoclonal origin of vascular smooth muscle cells

Evidence has been found that the VSMCs contained within the mature atherosclerotic plaque are monotypic [Benditt and Benditt 1973]. This has led to the theory that the plaque could represent a clonal expansion of the VSMCs in the lesion, and this theory has been supported by other research [Pearson *et al.* 1975]. While clonal expansion of VSMCs may indeed occur, the theory offers no explanation for the trigger which initiates the atherogenic process; nor does it tie in all the cellular and molecular interactions involved in atherogenesis.

1.1.3.7 Atherogenesis as an inflammatory process

As early as the 1950s, it was noted that inflammatory cells were present in experimentally induced atheromatous lesions [Poole and Florey 1958]. The proposition that atherosclerosis should be regarded as an inflammatory process has achieved increasing prominence over the last few years [Libby 2002]. Leukocyte recruitment and pro-inflammatory cytokine expression are prominent features of early atherogenesis. Pro-inflammatory agents such as tumour necrosis factor (TNF) are also atherogenic [Hansson *et al.* 1989]. Atherosclerotic plaques have been shown to contain deposits of immunoglobulins (Igs) [Hollander *et al.* 1979], and end-products of the complement cascade [Vlaicu *et al.* 1985].

OxLDL is itself pro-inflammatory [Lipton *et al.* 1995] and its recognition by T cells can trigger expression of further inflammatory molecules by these lymphocytes [Libby 2002]. Statins, which have been used in clinical practice predominantly for their cholesterol-lowering effect, are now thought to play a role in improving atheromatous plaque stability [Libby and Aikawa 2002], and have been shown to reduce the degree of inflammation in atheromatous lesions, independently of their lipid-lowering effect [Sukhova *et al.* 2002].

1.1.3.8 Putative role of viruses

Various viruses have been implicated in atherogenesis. Herpes simplex virus can alter the metabolism of cellular cholesterol, activate clotting cascades, and induce the infected endothelium to express a receptor for monocytes [Hajjar 1991]. Meanwhile, deliberate infection of chickens with Marek's disease herpes virus induces the

formation of atheroma-like lesions in the coronary arteries and aorta [Fabricant *et al.* 1983]. Furthermore, in heart transplant recipients, there is a strong correlation between cytomegalovirus infection and accelerated atherosclerosis [MacDonald *et al.* 1989]. The role of viral infection in atherosclerosis in otherwise healthy human subjects remains debatable, though.

1.1.3.9 Homocysteine

Hyperhomocysteinaemia is generally recognized as a risk factor for atherosclerotic disease in the coronary, cerebral and peripheral vasculature [Refsum *et al.* 1998, Mangoni *et al.* 2002]. A causal relationship between hyperhomocysteinaemia and atherogenesis remains to be proven, though. Indeed, the most common inherited form of hyperhomocysteinaemia is not associated with increased cardiovascular risk [Brattstrom *et al.* 1998]. Exposure of endothelium to homocysteine leads to EC dysfunction, and it has been postulated that this effect may trigger and influence the progression of atherogenesis [Weiss *et al.* 2002]. Hyperhomocysteinaemia increases expression of tumour necrosis factor-alpha (TNF-α) in coronary arteries, enhancing oxidative stress in the vessel wall via up-regulation of inducible NO synthase [Ungvari *et al.* 2003]; this could have pro-inflammatory and pro-atherogenic effects.

1.2 Ageing as a risk factor for atherosclerosis

This section explores the inter-relationship between ageing and atherosclerosis. In particular it addresses the question of whether atherosclerosis can be regarded as an intrinsic part of the ageing process, or whether ageing is simply a risk factor (either independent or otherwise) for atheroma formation. It begins, though, with an outline of the age-related changes which occur in the arterial wall, even in the absence of atherosclerosis.

1.2.1 Physiological changes in the arterial wall with increasing age

Certain changes occur in non-atherosclerotic arteries with increasing age [Bilato and Crow 1996]. These changes may be regarded as 'physiological'; some begin while the organism is still comparatively young (for example during the second and third decade of life in humans) [McGill *et al.* 1963].

Some of the age-related changes are histological in nature: the total vessel diameter increases, and the intima and media become thickened, partly through the accumulation of extracellular matrix. Elastin tissue content declines (from the age of

thirty years in human coronary arteries [Ahmed 1970]), while collagen becomes more prevalent [Johnson *et al.* 2001a].

Functional changes in the ageing artery include a deterioration in EC function [Celermajer *et al.* 1994], as demonstrated by a decline in endothelium-dependent vasodilation [Gerhard *et al.* 1996]. A decline in synthesis of endothelial NO by systemic arteries with age [Tschudi *et al.* 1996] may have a significant effect on peripheral vascular resistance and therefore on the evolution of hypertension [Luscher *et al.* 1992].

Other age-related changes include increased permeability of the endothelium, and an increased ability of SMCs to migrate towards chemoattractants [Bilato and Crow 1996]. The expression of certain vasoactive substances, such as endothelin-1, and of the pro-atherogenic inducible nitric oxide synthase isoform II, rises in ageing arteries *in vivo* [Goettsch *et al.* 2001]. Furthermore, with age, expression of adhesion molecules and cytokines is increased in ECs, contributing to vascular inflammation [Lusis 2000]. In addition, so-called 'advanced glycation end-products' (AGEs) progressively accumulate with age [Brownlee 1995] as will be discussed in more detail below.

1.2.2 Evidence for ageing as a risk factor for atherosclerosis

As mentioned earlier, ageing appears to be a strong risk factor for atherosclerosis. Epidemiological studies show a clear age-dependence of deaths due to atherosclerotic disease (including IHD, renovascular and cerebrovascular disease) [Kohn 1977]. The risk of death from IHD, for example, rises approximately one hundred-fold between the ages of forty and eighty years [Stationary Office 1996]. Study of mortality data for various clinical pathologies confirms the age-dependence of deaths attributable to atherosclerosis: when all-cause death rates are plotted as a function of age in a semi-log plot, the resultant curve follows an approximately straight line, reflecting the fact that the probability of dying (from any cause) doubles about every eight years after maturity; in contrast, the curve for deaths attributable to atherosclerosis (including IHD) rises more steeply than the all-cause curve, suggesting that these deaths are age-dependent [Kohn 1977].

While mortality data can give a misleading impression of a disease's age-dependence, early clinical and autopsy studies have confirmed an increase in the severity and

prevalence of atherosclerosis with age [Strong and McGill 1962, Heath *et al.* 1973, Zhdanov *et al.* 1973, Vikhert and Zhdanov 1975].

Atherosclerosis is not a universal process; most mammalian species and some human populations age without developing atheromatous lesions [Bierman 1973]. This lack of universality suggests that we should regard atherosclerosis not as an intrinsic part of the ageing process (as some have suggested) but as a disease which may be exacerbated by basic mechanisms underlying ageing [Kohn 1977].

1.2.3 Ageing as an independent risk factor for atherosclerosis

Atherosclerosis involves a whole panoply of cellular and molecular interactions, and these appear to occur on the background of the 'physiological' changes in the ageing arterial wall described above.

In considering whether ageing is an independent risk factor for atherosclerosis, it is necessary to appreciate that simply by ageing, an individual may be exposed to certain established risk factors for a longer period of time, perhaps resulting in an accumulation of damage caused by those factors. For example, correlations have been demonstrated between the severity of atherosclerotic lesion formation and the duration of hypercholesterolaemia [Schmidt *et al.* 1996] and with the number of cigarette pack-years [Whisnant *et al.* 1990].

Furthermore, any disease process which is multifactorial in aetiology will tend to become more prevalent and more severe with age, even if there is no direct mechanism by which ageing itself contributes to either the disease or the risk factors [Bierman 1973]; this is because, with time, the chance of each risk factor emerging will increase, and the number of interactions between the various risk factors will naturally rise. In the case of atherosclerosis, the situation is further complicated by the fact that several of its acknowledged risk factors (in particular hypertension, hyperglycaemia and hypercholesterolaemia) are themselves age-related.

While accepting the above considerations, there is also evidence to suggest that ageing may exert an independent risk on atherosclerosis. Clinical and pathological studies suggest that the commonly accepted risk factors for atherosclerosis (excluding ageing) account for only a fraction of the increase in cardiovascular disease with age: they account for approximately half of the increase in incidence of clinical events [Goldbourt and Neufeld 1986], and about a fifth of the rise in atherosclerotic lesion extent and severity as detected at autopsy [Holme *et al.* 1981]. This would suggest

either that there remain other risk factors as yet unidentified, or that age itself is contributing to the increased risk and severity of disease.

There is further evidence to suggest that ageing may be an independent risk factor for atherosclerosis. For example, generalized atherosclerosis is a feature of premature ageing syndromes such as progeria (Hutchinson-Gilford syndrome) [Baker *et al.* 1981], and Werner's syndrome [Epstein *et al.* 1966]. Similarly, patients with diabetes mellitus (which has been thought of as a disease of accelerated ageing [Kent 1976]) have an earlier onset and more rapid progression of atherosclerosis than non-diabetic subjects [Kohn 1978]. In contrast, though, another syndrome which involves at least some features of premature ageing, dyskeratosis congenita (DKC), is not associated with an increased risk of atherosclerosis [Marciniak *et al.* 2000].

One method which has been used to investigate the independence of ageing as a risk factor for atherosclerosis involves feeding an atherogenic diet, for a specified period of time, to young and old individuals, and then comparing the effects of this diet in the two groups. For example, Orlandi *et al.* fed a 0.2% cholesterol diet for two months to young (two-month old) and old (five- to six-year old) rabbits, and compared the extent of atherogenesis in the aortas of each group. [Orlandi *et al.* 2000]. Fatty streaks were more extensive in the aortas from the older rabbits, even though there was no difference in the lipid profiles between the young and old animals.

Likewise, administration of a high-fat diet to young and old *Cynomolgus* monkeys, produced differing degrees of atherogenesis despite similar lipid profiles in the two groups [Weingand *et al.* 1986]. While young animals developed only fatty streaks, the older group formed more advanced atherosclerotic plaques. *Cynomolgus* monkeys are considered to be one of the most accurate primate models of human atherosclerosis, because of the morphological similarities between their diet-induced lesions and those of man, and also because of their relatively high rate of myocardial infarction [Stary and Malinow 1982].

Similar results, showing more severe diet-induced atherosclerosis in older compared with younger animals, have been reported in other species, including squirrel monkeys [Clarkson *et al.* 1976] and pigeons [Yost and Herman 1988].

Such evidence suggests that ageing can be regarded as an independent risk factor for atherosclerosis, and the question remains as to how this influence may be exerted. In order to explore whether mechanisms exist through which ageing can directly

influence atherosclerosis, it is necessary to consider in some detail the processes believed to underlie ageing, and to determine which of these processes are also involved in atherogenesis.

It has been proposed that organisms may age owing to a trade-off between the evolutionary necessity to produce germ-line cells with extreme accuracy, and the possibility of producing somatic cells with less stringency [Toussaint *et al.* 2000b]; since the somatic cells are produced less stringently (thus saving 'energy'), they are more prone than germ-line cells to mutation and to other cumulative molecular damage, such as that resulting from oxidative stress.

In a similar and related teleological argument, it has been suggested that as the organism is primarily 'designed' (from a Darwinian point of view) to survive long enough to reproduce, ageing may simply result from an in-built redundancy in the design: the organism does not need to survive beyond the reproductive period, and evolutionary energy is not expended in the attempt. One could therefore view ageing as a passive consequence of this conservation of evolutionary energy [Cristofalo 2001]. As will be seen in the following paragraphs, though, there are a multitude of theories which have instead attempted to explain ageing in terms of an active process dependent on various biological mechanisms.

Theories concerning ageing therefore broadly divide into those which concentrate on various intrinsic processes believed to take place within the ageing organism ('developmental-genetic' theories), and those which regard ageing as the result of an accumulation of damage from extrinsic insults ('stochastic' theories) [Cristofalo *et al.* 1994]. Another possibility is that ageing results from a combination of intrinsic processes and extrinsic insults.

1.3 Mechanisms underlying the ageing process

1.3.1 Developmental-genetic theories

According to these theories, organismic ageing is the consequence of genetically programmed and controlled cellular processes which are fundamental to organismic development and maturation. A genetic element in the determination of ageing is suggested by the fact that an organism's maximum life-span potential (MLSP) appears to be a species characteristic, and that there is a greater than one hundred thousand-fold variation in MLSPs between species [Brown 1985]. Further evidence for genetic

control comes from studies involving monozygotic and dizygotic twins, and non-twin siblings. Monozygotic twins show a marked similarity in their life-spans, to an extent not matched by dizygotic twins or non-twin siblings [Jarvik *et al.* 1960].

One criticism of developmental-genetic theories is the observation that while organismic development is a tightly controlled, precise process, the ageing phenotype involves a diverse array of deteriorative changes, and it is difficult to reconcile such a contrast.

Developmental-genetic theories include the neuroendocrine, immunological and replicative senescence theories of ageing.

1.3.1.1 The neuroendocrine theory

This theory attributes ageing to progressive functional decrements in the neuroendocrine system, in particular in the hypothalamic-pituitary-adrenal axis [Finch and Landfield 1985]. One example is the decline in the female reproductive system with age, and its associated systemic pathological effects. Similarly alterations in insulin-sensitivity and growth hormone production may be relevant to the ageing phenotype. Thus, for example, mutations of genes affecting the production of growth hormone and insulin-like growth factor-1 (IGF-1) extend murine life-span [Flurkey *et al.* 2001].

1.3.1.2 The immunological theory

This theory was originally proposed in 1969 [Walford 1969]. It had been observed that the functional capacity of the immune system declines with age [Pisciotta *et al.* 1967], and these early observations have been supported by later research showing, for example, a decreased response of T cells to mitogens with increasing organismic age [Staiano-Coico *et al.* 1984]. The theory suggested that ageing might, at least in part, result from this functional decline (while it was granted that the functional decline might also result from the ageing process). Genetic studies have shown that the MLSPs of various murine strains are related to the expression of specific alleles in the major histocompatibility gene complex [Smith and Walford 1977], suggesting an element of immunogenetic programming in the determination of MLSPs.

Both the immunological and the neuroendocrine theories have been criticized on the grounds that less sophisticated organisms, which do not possess complex control and

defence systems, nevertheless do share several aspects of the ageing phenotype with more advanced organisms.

1.3.1.3 Replicative senescence

The *in vitro* phenomenon of cellular replicative senescence, in which cells grown in culture lose their replicative potential, will be discussed in detail below. As will be seen, replicative senescence may also occur *in vivo*, and there is some evidence to suggest that this cellular process may contribute to ageing of the entire organism.

1.3.2 Stochastic theories

Stochastic theories suggest that organismic ageing results from the progressive accumulation of random damage to vital molecules within the cells of an organism. Such damage might cause sufficient cellular dysfunction to bring about the pathological features associated with ageing. Both actively dividing cells and post-mitotic tissues, such as muscle, nerve and fat cells, could be affected by stochastic damage.

1.3.2.1 The somatic mutation theory

According to this theory, the source of damage to cells is proposed to be background radiation. As early as 1959 it was postulated that since high doses of radiation can induce mutations and shorten organismic life-spans, mutations caused by background levels of radiation may contribute to normal human ageing [Szilard 1959]. Studies of survival curves of radiation-treated rodents suggested that at the doses used, ionizing radiation caused an initial rise in mortality, but did not affect the subsequent rate of ageing [Sacher 1977]. Thus the life-shortening effect of radiation is probably not due to accelerated ageing but to radiation-induced disease.

1.3.2.2 The deoxyribonucleic acid repair theory

This theory, which is related to the somatic mutation theory, attributes ageing to a failure in the normal function of deoxyribonucleic acid (DNA). There may be a failure of DNA repair mechanisms to mend damage caused from a variety of stochastic environmental insults. For example, in one study the ability to repair ultraviolet (UV) radiation-induced DNA damage in cell cultures derived from various species showed a positive correlation with their MLSPs [Hart and Setlow 1974].

1.3.2.3 The error-catastrophe theory

It has been suggested that random errors in protein synthesis may affect those proteins which synthesize DNA and other template molecules; mis-encoded and mis-synthesized proteins would then arise, leading to a magnified knock-on effect [Orgel 1963]. This multiplication of errors could then lead to the development of age-associated pathology.

1.3.2.4 Protein cross-linking and advanced glycation end-products

It has been proposed that when certain post-translational proteins undergo cross-linking, as occurs progressively with age, the function of these molecules is impaired [Kohn 1978]. A particular case of cross-linking involves the process of glycation, the non-enzymatic reaction of glucose with amino groups of proteins. Glycation can lead to the cross-linking of macromolecules such as collagen and osteocalcin, and so to the age-related formation of AGEs (mentioned above in Section 1.2.1) [Brownlee 1995].

AGEs may in turn contribute to age-related pathologies including atherosclerosis. They are capable of triggering the expression of VCAM-1 by ECs [Schmidt *et al.* 1995], as well as trans-endothelial migration of monocytes [Schmidt *et al.* 1993] and SMC chemotaxis [Higashi *et al.* 1997]. When rabbits are injected with AGE-modified rabbit serum albumin, their ascending aortas develop atheromatous lesions [Vlassara *et al.* 1995]. In addition, AGEs on the surface of diabetic erythrocytes can bind to the endothelium, and lead to an increase in oxidative stress in the vessel wall, and this mechanism may underlie some aspects of diabetic vascular complications [Wautier *et al.* 1994]. More recently it has been shown that human ECs grown on glycated collagen show several phenotypic features of premature senescence (a phenomenon discussed in detail below) [Chen *et al.* 2002].

As for the cross-linking theory in general, though, the situation is complicated by the finding that while increased cross-linking leads to impaired cellular and tissue function at some sites, it leads to improved function at others [Hall 1976].

1.3.2.5 The role of mitochondrial dysfunction

Mitochondrial function declines with age [Beckman and Ames 1998a], and mitochondrial decay appears to play a significant role in the ageing process [Hagen *et al.* 1997]. It has been postulated that ageing may be due to the reactive oxygen species (ROS) produced by mitochondria in the electron transport chain, during normal

aerobic metabolism [Miquel *et al.* 1980, Beckman and Ames 1998b]. The term 'ROS' refers both to non-radical derivatives of oxygen such as hydrogen peroxide, and to oxygen-centred radicals such as superoxide ions. ROS not only 'attack' cellular proteins, but are also harmful to the cells' DNA (including mitochondrial DNA); they are also able to modify lipids, and the significance of this process for atherogenesis has been mentioned earlier.

Deletion mutations of the mitochondrial genome accumulate with age, and in animal studies the bioenergetic capacity of mitochondria declines [Cortopassi and Wong 1999], alongside an age-related increase in activation of the mitochondrial permeability transition pore [Mather *et al.* 2000]. When mitochondrial function is ameliorated by feeding the mitochondrial co-enzyme (R)-α-lipoic acid to aged rats, the intracellular build-up of oxidants is reduced, and the age-associated increase in cellular susceptibility to oxidative stress is reversed [Hagen *et al.* 1999, Hagen *et al.* 2000]. It is noteworthy that caloric restriction, a dietary regimen known to prolong life-span in animals, maintains mitochondrial function and lowers oxidant production [Merry 2000].

1.3.2.6 The role of free radicals and oxidative stress

Perhaps most prominent among the stochastic theories of ageing is the free radical theory, which was brought to prominence by Harman [Harman 1956, Harman 1981]. According to this theory, damage is caused to the organism's macromolecules by free radicals – atoms or molecules containing one or more unpaired electrons – including certain ROS and reactive nitrogen species. This damage was proposed to be the principle driving force for ageing. The mechanism of such damage is discussed in more detail below.

It is probable that different mechanisms of ageing operate in different tissues in the body. The heart, for example, may be particularly prone to damage caused by a decline in mitochondrial function: the myocardium is dependent on β-oxidation of fatty acids for energy, and the post-mitotic nature of cardiac myocytes would be expected to allow for greater accumulation of mitochondrial mutations and deletions [Hagen *et al.* 2002].

Among the various theories concerning the aetiology of ageing, two processes in particular warrant more detailed discussion given their potential relevance to

atherosclerosis. The mechanisms of replicative senescence and oxidative stress, and their relevance to ageing and to vascular pathology, are described in the following sections.

1.4 Replicative Senescence

1.4.1 Normal regulation of the mammalian cell cycle

Proliferating cells are usually driven through various check-points in the cell cycle by the activity of certain kinases which act by phosphorylating specific protein substrates. The activity of these kinases is dependent on their association with specific proteins called cyclins, and thus the kinases are referred to as cyclin-dependent kinases (Cdks) [Nigg 1995]. Their activity is modulated by the action of certain Cdk inhibitors [Peter 1997].

The G_1 check-point seems to be particularly important in controlling progression through the cell cycle. Mammalian cells reach a 'restriction point' during G_1: prior to this point they require the presence of growth factors in order to progress through the cell cycle; after it they can continue through the remainder of the cycle without further external stimulation.

The retinoblastoma (RB) gene product, pRb, which plays an important role as a tumour-suppressor protein, is involved in the control of transition from G_1 to S phase (G_1/S transition) [Weinberg 1995, Dyson 1998]. During G_1, E2F transcription factors are bound to pRb, preventing them from binding to DNA and initiating gene transcription. Towards the end of G_1, the pRb subunit of the pRb-E2F complex is phosphorylated by cyclin-Cdk complexes [Buchkovich *et al.* 1989, Sherr 1996, Wagner *et al.* 2001]. The phosphorylated pRb releases its bound E2F, allowing the transcription factor to activate gene expression, contributing to the irreversible entry into S phase.

The level of another tumour-suppressor protein, p53, is usually very low as cells pass through G_1. However, if a cell suffers DNA damage, the level of p53 rises dramatically [Vaziri *et al.* 1997]. p53 then activates the gene which encodes the Cdk inhibitor p21. High levels of p21 in turn lead to activation (via hypophosphorylation) of pRb, which sequesters E2F transcription factors, and so arrests progression through the G_1 check-point. In this way the replication of DNA-damaged cells is halted.

Various mechanisms leading to cell cycle arrest, and the role of other Cdk inhibitors including p16, will be discussed below.

1.4.2 The phenomenon of replicative senescence

The concept of cellular ageing has arisen from studies of cells grown in culture. In the early days of *in vitro* cell culture, it was thought that cells from vertebrate species could undergo an indefinite number of replicative cycles. This theory had arisen from research which appeared to show indefinite subculture of chick cells [Carrel 1912], but this work has subsequently not proved to be reproducible.

Hayflick and Moorhead showed in the early 1960s that when normal human diploid fibroblasts (HDFs) were grown in culture, they underwent only a limited degree of proliferation [Hayflick and Moorhead 1961]; with continual subculture they gradually and inevitably lost their ability to proliferate [Hayflick 1965]. As their replicative capacity was exhausted, and the cells entered a terminally non-dividing state, they were said to undergo 'replicative senescence' [Hayflick and Moorhead 1961, Hayflick 1965]. This property has subsequently been shown to pertain to a variety of human cell types grown in culture [Hayflick and Moorhead 1961, Hayflick 1965, Tassin *et al.* 1979, Thornton *et al.* 1983, Effros and Walford 1984] as well as to cells from other species [Rohme 1981, Stanulis-Praeger 1987]. Replicative senescence is therefore a widespread phenomenon, which is thought to have been evolutionarily conserved from yeast to mammals [Campisi 2001].

Replicative senescence entails an irreversible arrest of cell proliferation and altered cell function. Senescent cells are stably arrested in G_1 [Stein and Dulic 1995, Effros 1996], and are unable to enter the S phase despite exposure to physiological mitogens [Sherwood *et al.* 1988]. The cells remain metabolically active, maintaining the ability to metabolize and synthesize ribonucleic acid (RNA) and protein. Senescent cells usually possess intact DNA replicative machinery, and are able to transduce most signals during mitogenic stimulation [Rittling *et al.* 1986, Goldstein 1990], and yet the cells themselves are unable to resume mitotic activity.

There appear to be differences between species in the stringency with which cell proliferation is limited by replicative senescence. Thus while rodent fibroblasts often 'escape' senescence and spontaneously immortalize, human fibroblasts from normal donors have almost never been reported to immortalize spontaneously [McCormick and Maher 1988].

Only a few higher eukaryotic cell types are thought to be entirely unaffected by replicative senescence. Cells of the germline are capable of continuous replication, as are the immortal cells found within tumours and transformed cell lines; in addition, it has been suggested that some stem cells may not senesce [Campisi 1996].

In cells which do senesce, the onset of senescence is thought to be determined by the number of rounds of cell division that have occurred, rather than by the chronological age of the cultures [Dell'Orco *et al.* 1973]. As a result senescent cells accumulate gradually in culture, the percentage of senescent cells rising as cultures are serially passaged, until eventually all the cells become senescent [Smith and Whitney 1980, Dimri *et al.* 1995].

Replicative senescence should be distinguished from other processes by which cells can withdraw from the cell cycle. One such process is cellular quiescence. Quiescent cells cease to divide under certain culture conditions including nutrient starvation and contact inhibition, but, unlike senescent cells, they maintain their capacity to re-enter the cell cycle upon mitogenic stimulation [Stein *et al.* 1985]. Another process involving withdrawal from the cell cycle is terminal differentiation. Here the failure to proliferate accompanies marked changes in cell phenotype, as part of a programmed process resulting from altered transcriptional regulation. Cells which withdraw from the cell cycle owing to terminal differentiation show different patterns of gene expression and activity from those undergoing replicative senescence [Medrano *et al.* 1994], suggesting that the two processes are indeed distinct.

The onset of senescence does not necessarily lead to cell death. Indeed senescent cells can remain viable and metabolically active for years if maintained with regular changes of culture medium [Matsumura *et al.* 1979, Wang 1995]. There has been some controversy about whether replicative senescence leads to an increased propensity to cell death through apoptosis, and this issue will be discussed in detail below.

1.4.3 Morphological and molecular features of senescent cells

Senescent cells show characteristic changes in morphology and gene expression, and the acquisition of selective changes in differentiated functions [Campisi 1996, Smith and Pereira-Smith 1996]. Morphologically, senescent cells *in vitro* show an increase in size and cytoplasmic vacuolation, the development of polymorphic nuclei, an increase in their nuclear/cytoplasmic ratio, and the development of large lysosomal bodies

[Comings and Okada 1970, Lipetz and Cristofalo 1972, Rosen *et al.* 1981, Repin *et al.* 1984, Nichols *et al.* 1987, Tokunaga *et al.* 1989, Bürrig 1991].

Senescent cells also show altered activity of certain cell-cycle-related enzymes [Chang and Chen 1988, Chen *et al.* 1989] and decreased efficiency of protein synthesis and degradation [Okada and Dice 1984, Dice 1989, Luce and Bunn 1989, Rattan 1991]. They display a high frequency of chromosomal aberrations [Thompson and Holliday 1975].

Several of the differences in gene expression and enzyme activity in senescent cells relate directly to their inability to progress from G_1 to S phase [Stein *et al.* 1991, Dimri and Campisi 1994a and 1994b]. Examples include reduced expression of c-FOS [Seshadri and Campisi 1990], impaired phosphorylation of pRb [Stein *et al.* 1990], and reduced levels of expression of cyclin A [Stein *et al.* 1991], ribonucleotide reductase, histones, proliferating cell nuclear antigen (PCNA) and dihydrofolate reductase [Pang and Chen 1994]. As would be expected in cells which have arrested in G_1, there is also an accumulation of G_1 cyclins [Dulic *et al.* 1993].

The levels of Cdk inhibitors such as p14, p16, p21 and p27 are increased in senescent cells, though the pattern of elevation of particular Cdk inhibitors appears to depend on the species and cell type studied, and on the nature of the trigger leading to senescence [Noda *et al.* 1994, Stein and Dulic 1995, Hara *et al.* 1996, Ben-Porath and Weinberg 2005]. Cdk inhibitors appear to play a causal role in replicative senescence [Xiong *et al.* 1993, el-Deiry *et al.* 1994].

As well as alterations in cell cycle regulatory genes, differential screening of RNA from young and senescent cells, and the use of complementary DNA microarray analysis in senescent cells, have identified alterations in the expression of a variety of other genes: these include those encoding extracellular matrix components and metabolic enzymes [Kumazaki *et al.* 1991, Thweatt *et al.* 1992, Park *et al.* 2001], as well as proteins such as cathepsins (discussed in Chapter Five) [Kamino *et al.* 2003].

1.4.4 Putative mechanisms of replicative senescence

1.4.4.1 Telomere shortening in serially passaged cells

Over thirty years ago it was proposed that the gradual loss of proliferative capacity of replicating cell cultures could be explained by incomplete replication of chromosome ends [Olovnikov 1973]. Since then it has become widely (if not universally) accepted

that replicative senescence in normal somatic cells from higher organisms results from the shortening of chromosomal telomeres [Allsopp *et al.* 1992, Harley and Villeponteau 1995, Campisi 1996]. This shortening has been attributed to the so-called 'end-replication problem', the incomplete replication of the distal 5'-end of the lagging strand during DNA replication [Levy *et al.* 1992].

Telomeres are specialized structures which cap the ends of the chromosomes, protecting the chromosomal ends from degradation and from fusion with other chromosomal ends [Greider 1990, Lee *et al.* 1993]. They comprise multiple repeat sequences of base pairs (bp), complexed with telomeric proteins; in humans and many other organisms, the DNA component of the telomere consists of tandem hexanucleotide repeats of the sequence TTAGGG [Brown 1989]. Their presence distinguishes the normal physiological ends of chromosomes from double-strand breaks; this is thought to be important in determining whether a cell initiates a DNA damage response [Lansdorp *et al.* 2000].

Harley *et al.* provided the first formal demonstration that telomeres shorten during serial passage of cells in culture [Harley *et al.* 1990]; this decrease in length occurred in a replication-dependent manner, and in normal human fibroblasts grown *in vitro* telomeric DNA shortened by approximately fifty bp per population doubling (PD). The rate of telomeric shortening appears to depend on the cell type studied; the rate of loss of telomeric DNA in human ECs, for example, has been measured as approximately 190 bp per PD [Chang and Harley 1995].

It has been suggested that once a critical degree of telomeric shortening is reached, this process is recognized by the cell cycle machinery as DNA damage, leading to a signal to block further replication by exiting the cell cycle [Chang and Harley 1995, Vaziri and Benchimol 1996, Vaziri *et al.* 1997]. For example, certain human T cells become senescent after approximately twenty-five divisions, at a stage when their telomeres have shortened from approximately ten kilo-base pairs (kbp) to approximately five kbp [Effros and Walford 1984, Vaziri *et al.* 1993].

1.4.4.2 The role of telomerase

Telomere attrition is retarded or even prevented in cells immortalized *in vitro* [Counter *et al.* 1994a], in tumour cells [Counter *et al.* 1994b], and in germ-line cells [Wright *et al.* 1996], because these cells express relatively high levels of the enzyme telomerase. In contrast, telomerase is generally absent, or present only at very low levels, in non-

transformed, non-malignant somatic cells [Kim *et al.* 1994]. Non-confluent primary cultures of normal human ECs, for example, express only a low level of telomerase activity, and this activity disappears altogether in quiescent confluent EC cultures [Hsiao *et al.* 1997, Kurz *et al.* 2003]. Low levels of telomerase activity have recently been demonstrated in normal human fibroblasts, and experimental inhibition of this activity led to premature senescence of these cells [Masutomi *et al.* 2003].

Telomerase is composed of two main subunits. An RNA component (TR) serves as a template to synthesize the telomeric DNA sequences; a catalytic component, TERT, shows reverse transcriptase activity [Lingner *et al.* 1997], adding hexameric DNA repeats at the linear ends of eukaryotic chromosomes [Kim *et al.* 1994, Counter *et al.* 1994b, Meyerson *et al.* 1997, Breitschopf *et al.* 2001].

Various telomere-regulating factors appear to be associated with telomere maintenance. These include TTAGGG repeat binding factors 1 and 2 (TRF1 and TRF2) [Smogorzewska *et al.* 2000], tankyrase [Smith *et al.* 1998] and the telomere-associated protein TIN2 [Kim *et al.* 1999]. Expression of these factors varies between species, and to an extent which depends on the replicative age of the cells.

Evidence for a causal role of telomere shortening in replicative senescence has come from studies in which cultures of normal human cell-types (such as fibroblasts and epithelial cells) were transfected with vectors encoding the human version of TERT (hTERT) [Bodnar *et al.* 1998, Vaziri and Benchimol 1998]. While telomerase-negative control cultures showed pronounced senescence, telomerase-expressing clones divided vigorously, and exceeded their normal proliferative life-span by at least twenty PDs, without causing neoplastic transformation [Bodnar *et al.* 1998]; the transfection led to an elongation of telomere length and reduced staining for senescence-associated beta-galactosidase (SA-β-gal) (a marker of replicative senescence discussed below).

A similar extension of replicative life-span has been achieved by the forced expression of hTERT in human arterial ECs [Yang *et al.* 1999]. Transfection of ECs with hTERT leads to preservation of aspects of the pre-senescent phenotype; thus transfection of human aortic endothelial cells (HAECs) with hTERT attenuates the loss of endothelial nitric oxide synthase (eNOS) expression and activity usually seen with serial passages [Matsushita *et al.* 2001]. The introduction of hTERT into human VSMCs likewise extends their replicative life-span, and leads to the preservation of a younger

phenotype [Minamino *et al.* 2001], suggesting that telomere dynamics are relevant to the proliferative capacity of more than one vascular cell type.

The role of telomerase in the prevention of senescence requires further clarification, however, given that some somatic cells exhibit telomere shortening and undergo senescence following rounds of replication, despite expressing telomerase [Broccoli *et al.* 1995, Counter *et al.* 1995]. Conversely, some cell lines can immortalize in the absence of telomerase activity [Murnane *et al.* 1994, Bryan *et al.* 1995].

1.4.4.3 Higher order structure of telomeres

Even if the mitotic clock theory of telomere shortening is accepted, it is not clear which parameter of cellular telomere length is critical in determining when the cell cycle is arrested. It transpires that replicative senescence is induced when telomeres have approximately halved in length [Shay *et al.* 1991a]. Since entry into senescence does not require complete telomere attrition, an alternative trigger for cell cycle arrest must be sought.

One theory proposes that absolute telomere length is less important than the higher-order structure the telomere is able to adopt. In particular, a model has been proposed in which telomeres form so-called 'T-loops' as telomere-related proteins fold the 3' single strand end of the telomere back into double-stranded DNA repeats [Griffith *et al.* 1999]; this configuration, together with the specific binding of proteins such as TRF2 to the T-loop, may protect the G-rich single-strand overhang at the very end of the telomere from degradation and from interactions with signalling proteins.

It has been suggested that when cellular telomerase activity is low, progressive shortening of the telomere in the T-loop may lead to the T-loop's becoming temporarily uncapped, exposing the G-rich single strand of DNA; this uncapping may render the DNA telomerase-accessible, so that if and when telomerase levels subsequently rise, the telomere can become lengthened, and form a T-loop once again [McEachern and Blackburn 1995].

1.4.4.4 The effect of changes in telomeric structure on the cell cycle

The activation pathways leading to the cell cycle arrest found in senescence have proved difficult to elucidate fully; it seems that different pathways are involved, depending on the nature of the trigger for senescence, and the species and cell type being studied.

As described above, replicative senescence appears to result from telomere shortening following rounds of replicative activity. Other forms of senescence, collectively termed stress-induced premature senescence (SIPS), may arise from a variety of other insults to the cell; SIPS is discussed in more detail below.

Various theories have sought to link senescence-related changes in telomeres to the intracellular signalling pathways which bring about cell cycle arrest. It has been proposed that telomere shortening may alter the expression of cell cycle genes located in the vicinity of the telomeres; this has been referred to as the 'telomere position effect'. It seems to apply to replication in yeast [Corda *et al.* 1999], but its role in humans is less easy to establish [Ofir *et al.* 1999].

Telomere loss during replicative senescence may be recognized as a DNA double-strand break, and induce a corresponding check-point response [Chin *et al.* 1999]. It has been mentioned above that if a cell suffers damage to its DNA, the level of p53 rises markedly; p53 may then induce Cdk inhibitors such as p16, p21, and p27, and so bring about arrest in G_1 [McConnell *et al.* 1998, Collado *et al.* 2000, Dai and Enders 2000, Kim *et al.* 2002]. Similarly, several studies have suggested that the cell cycle arrest found in replicative senescence may also be initiated by activation of p53 [Shay *et al.* 1991a, Atadja *et al.* 1995, Vaziri *et al.* 1997]. While activated p53 can induce cell cycle arrest at G_1 and G_2 checkpoints by increasing expression of p21 [el-Deiry *et al.* 1994, Canman *et al.* 1995, Kulju *et al.* 1995], inactivation of p53 delays the onset of replicative senescence [Hara *et al.* 1991, Bond *et al.* 1995]. It has also been demonstrated that an abundance of free single-stranded G-rich telomeric DNA, as might be found when a T-loop becomes uncapped following telomere attrition, can trigger a p53-dependent cell cycle arrest [Saretzki *et al.* 1999].

The activation of p53 appears to be mediated through clusters of damage-response proteins which appear at the telomeres of senescent cells; at the same foci are found activated forms of ATM (ataxia telangiectasia mutated DNA damage response kinase), and its down-stream targets Chk1 and Chk2, which are thought to be the crucial activators of p53 in response to DNA damage [d'Adda di Fagagna *et al.* 2003, Herbig *et al.* 2004].

Inter-species differences in the mechanisms leading to replicative senescence are emphasized by studies in which attempts have been made to prevent the onset of senescence. In murine cells inactivation of either p53 or pRb is sufficient to inhibit

senescence [Harvey *et al.* 1993, Sage *et al.* 2000], suggesting a murine signalling pathway involving sequential activation of p53 and pRb; this pathway is thought to be mediated via increased expression of p21; by contrast, in human cells it appears necessary to inactivate both p53 and pRb in order halt the replicative cycle [Shay *et al.* 1991a, Ben-Porath and Weinberg 2005], implying that p53 may be capable of initiating senescence independently of pRb and p21 activity. The situation is not clear-cut, though, given that in one study involving human fibroblasts, inactivation of p21 appeared sufficient to prevent senescence, without the need for the simultaneous inactivation of p53 [Brown *et al.* 1997].

The Cdk inhibitor p16, which is normally not detectable in adult cells, is over-expressed in senescent cells, and is postulated to be a key regulator of replicative senescence in human cells [Alcorta *et al.* 1996], on the basis of studies which have shown its expression to be markedly elevated in ageing cultures [Wong and Riabowol 1996, Kim *et al.* 2002]. Furthermore, forced over-expression of p16 can induce pre-senescent cells to become senescent [McConnell *et al.* 1998, Dai and Enders 2000], while inactivation of p16 in human cells can significantly delay their senescence [Wei *et al.* 2003]. Activation of p16 provides a mechanism for the activation of pRb without requiring activation of p53. The relevance of this mechanism is emphasized by the finding that, in human cells, forced telomere uncapping by inhibition of TRF2 can cause an induction of p16 and senescence even in the absence of p53 [Smogorzewska and de Lange 2002].

There appear to be two main pathways involved in the initiation of senescence in human cells: when replicative senescence is triggered by telomere attrition and/or T-loop uncapping, a response similar to that involved in a DNA damage response (involving sequential p53, p21 and pRb activation) is initiated; if, by contrast, senescence is triggered by external stresses (for example SIPS resulting from high oxidative stress, as discussed later) it appears to be mediated through activation of pRb by p16, perhaps via the p38-MAPK (mitogen-activated protein kinase) protein [Itahana *et al.* 2003, Iwasa *et al.* 2003, Ben-Porath and Weinberg 2004 and 2005]. This theory is supported by the finding that stress-induced activation of p16 appears to promote the onset of senescence in human cells via a mechanism independent of telomere length [Wei *et al.* 2003].

In murine cells, p16 does not appear to play a significant role in senescence, no matter what its trigger; instead murine cell senescence is mediated via p53 and p21, in a pathway which also involves up-regulation of $p19^{ARF}$ (which is encoded by an alternative transcript of the INK4a locus also responsible for encoding p16) [Itahana *et al.* 2004]. The human equivalent of murine $p19^{ARF}$, $p14^{ARF}$, is up-regulated in senescent human ECs, and is thought to play a role, together with p53, in mediating oxidative stress-induced senescence in these cells [Lundberg *et al.* 2000, Chen *et al.* 2002].

1.4.5 Replicative senescence as a tumour-suppressor mechanism

The suggestion that replicative senescence may play a role as a tumour-suppressor mechanism has arisen from various strands of evidence. Firstly, since senescence prevents multiple rounds of cell replication, it may also reduce the number of opportunities at which defects can arise in the cell genome, reducing the chance of developing the mutations that are required for malignant transformation [Ponten 1976, Sager 1991]. Secondly, oncogenes extend cell replicative life-spans, suggesting that oncogenesis and senescence are opposing mechanisms [Dimri *et al.* 2002]. Thirdly, the p53 and RB genes, both of which are known to be potent tumour-suppressor genes, are involved in the establishment and maintenance of replicative senescence [Shay *et al.* 1991b]. Indeed, mice containing mutations of activators of senescence (such as p53 and p16) are prone to tumourigenesis [Donehower *et al.* 1992, Krimpenfort *et al.* 2001].

Some anti-cancer agents appear to induce a senescence-like phenotype. For example, when mice with lymphomas were treated with cyclophosphamide, their lymphomatous cells underwent replicative senescence *in vivo* [Schmitt *et al.* 2002]; this senescence acted as a barrier to further replication of the tumour cells. Mice bearing tumours whose cells contained an intact machinery for replicative senescence showed a better prognosis in response to chemotherapy than did mice whose tumours contained senescence defects.

1.4.6 Replicative senescence and organismic ageing

It has been postulated that replicative senescence may occur *in vivo*, in tissues where cellular proliferation continues throughout the entire life-span of the organism [Hayflick 1965]. It has further been suggested that *in vivo* cellular senescence may

play a role in such diverse conditions as atherosclerosis, Alzheimer's disease and diabetes mellitus [Tesco *et al.* 1993, Vasile *et al.* 2001, Chen *et al.* 2002]. Hayflick and Moorhead were among the first to observe that senescent cells *in vitro* acquired characteristics of ageing cells *in vivo* [Hayflick and Moorhead 1961], and this observation led to the suggestion that replicative senescence may have a bearing on (or indeed be a cause of) organismic ageing [Hayflick 1965, Finch 1990]. According to this theory, cells which have exhausted their replicative capacity accumulate with age in certain tissues, and, owing to their altered properties, contribute to the development of age-related pathologies [Dimri *et al.* 1995, Campisi 1996].

A direct relationship has been shown between the longevity of several mammalian species and the *in vitro* replicative life-span of their fibroblasts [Rohme 1981, Stanulis-Praeger 1987, Campisi *et al.* 1996]. For example, while fibroblasts from the Galapagos tortoise (which can live for over 100 years) achieve up to 130 PDs in culture, those from the mouse (whose MLSP is approximately three years) manage only up to ten PDs.

Evidence for the occurrence of a decline in cellular replicative capacity with age is found in a variety of studies of human and rodent tissues. Many of these studies have shown an inverse relationship between donor age and the *in vitro* proliferative capacity of their cells [Schneider and Mitsui 1976, Buetow 1985, Stanulis-Praeger 1987, Cristofalo and Pignolo 1993, Campisi *et al.* 1996]. This relationship appears to apply to several cell types [Martin *et al.* 1970, Smith *et al.* 1978, Tassin *et al.* 1979, Effros and Walford 1984, Lipman and Taylor 1987, Blake *et al.* 1997]. Some studies, though, have found either only a weak correlation [Schneider and Mitsui 1976], or no correlation at all [Cristofalo *et al.* 1998]. Nevertheless, the weight of evidence does seem to favour the possibility that ageing donors yield cells with reduced replicative capacity.

Telomere studies generally support this contention. These investigations often employ the measurement of terminal restriction fragments (TRFs); a TRF comprises the telomere itself together with a sub-telomeric region of chromosomal DNA; reduction in TRF length is therefore indicative of telomere shortening. In various human cell types, TRFs in cells from older donors are shorter than those in cells from younger donors [Hastie *et al.* 1990, Allsopp *et al.* 1992, Harley *et al.* 1992, Vaziri *et al.* 1993],

although no such correlation was found in a more recent study of human fibroblasts [Mondello *et al.* 1999].

The study of telomerase-deficient mice might appear to cast doubt on the relevance of telomere shortening to organismic ageing. These mice were genetically engineered by disrupting the mouse TR gene (mTR) [Blasco *et al.* 1997]. Early generations developed without any significant phenotypic abnormalities. Defects were only seen in later generations, and then only in highly proliferative tissues [Rudolph *et al.* 1999]. As will be discussed in Chapter Four, murine telomeres are generally much longer than those found in human cells, and this may explain why early generations of telomerase-deficient mice appear to age normally.

Other studies have compared genetic, biochemical and physiological properties of early- and late-passage cells with those of cells from young and old donors. Some gene expression in senescent cells follows the pattern seen in organismic ageing, with proteins such as fibronectin [Kumazaki *et al.* 1991] and collagenase-1 [West *et al.* 1989] being synthesized in increased quantities in senescent HDFs. The exact pattern of gene expression in senescent cells, though, appears to vary between cell types [Shelton *et al.* 1999]. Cells derived from subjects with progeria or Werner's syndrome share some biochemical and genetic similarities with late-passage cells from normal subjects [Goldstein and Harley 1979, Lecka-Czernik *et al.* 1996], again suggesting a link between cellular and organismic ageing.

Closer study of the genetics of Werner's syndrome has provided further evidence for such a link. Affected individuals have a reduced life-span, and prematurely develop several features of the ageing phenotype, including thinning of the hair, atherosclerosis, osteoporosis and the emergence of malignancies [Ellison *and Pugh* 1955, Epstein *et al.* 1966]. Their cells senesce significantly earlier than age-matched controls [Martin *et al.* 1970, Stanulis-Praeger 1987]. The responsible gene encodes a protein, WRN, which is thought to be involved in telomere maintenance [Li and Comai 2000]. Similarly, cells from subjects affected by progeria have decreased replicative capacity [Goldstein and Harley 1979], and their telomeres are approximately half the length of those in age-matched controls [Allsopp *et al.* 1992].

Study of the clinical syndrome dyskeratosis congenita has also been instructive [Dokal 1999]. Patients have a reduced life-expectancy, and develop premature greying and loss of hair, as well as osteoporosis. Their haematopoietic cells and skin fibroblasts

have a reduced replicative capacity [Dokal *et al.* 1992]. At least some forms of this condition appear to arise from a mutation in a gene which encodes for dyskerin [Heiss *et al.* 1998], a protein which normally stabilizes TR; the resultant disruption in telomerase function appears to be associated with abnormally short telomeric lengths [Marciniak *et al.* 2000]. The fact that subjects with DKC exhibit only certain specific features of premature ageing may result from differences in telomerase activity between their various tissues [Mitchell *et al.* 1999]. It is interesting to note that several of those aspects of the ageing phenotype exhibited by individuals with DKC are shared with mTR-knockout mice: these include the emergence of haematological abnormalities, greying of the hair and an increased incidence of malignancy [Blasco *et al.* 1997, Marciniak *et al.* 2000].

Another human genetic condition, ataxia telangiectasia, is believed to involve inefficient DNA repair, as a result of an inactivating mutation in the p53 kinase, ATM (mentioned earlier in the context of the DNA damage response); fibroblasts from affected individuals show an increased DNA-binding capacity of p53, as well as accelerated telomere shortening and premature replicative senescence in culture [Metcalfe *et al.* 1996, Vaziri *et al.* 1997].

More direct evidence for the accumulation of senescent cells in the ageing organism has arisen from the study of SA-β-gal, a marker of replicative senescence mentioned earlier. Fibroblasts which stain positively for SA-β-gal are found in greater numbers in the skin of elderly subjects than in skin from younger donors [Dimri *et al.* 1995]. The use of SA-β-gal in the detection of senescent cells will be discussed in detail below.

In summary, the reduced replicative capacity and shorter telomeres found in cells from elderly donors, the study of properties of cells from patients with premature ageing syndromes, and the more direct evidence obtained using SA-β-gal, provide a growing body of evidence suggesting that cells with reduced replicative capacity accumulate in the ageing individual.

It is less clear whether such an accumulation contributes to the ageing process. With certain cell types, it is relatively easy to postulate that a reduced proliferative capacity could have a direct influence on age-related pathologies: for example, the age-related attenuation of the proliferative response of T lymphocytes to antigens mentioned earlier [Staiano-Coico *et al.* 1984] could partly explain the decline in immune response observed in the elderly. Similarly, an accumulation of senescent fibroblasts

could explain some pathophysiological changes found in ageing skin: senescent fibroblasts show increased expression of fibronectin and collagenase, and under-expression of the collagenase inhibitor, tissue inhibitor of metalloproteinase-1 (TIMP-1) [West *et al.* 1989, Kumazaki *et al.* 1991, Millis *et al.* 1992], all of which changes could contribute to the thinning and loss of elasticity of ageing skin [Smith and Pereira-Smith 1996]. The extent of the contribution of senescent cells to other ageing pathologies remains debatable, though.

1.4.7 Replicative senescence and apoptosis

It is possible that the postulated accumulation of senescent cells within ageing tissue may in part result from an ability to resist being cleared by the apoptotic process which would usually remove defunct cells. Apoptosis was initially described by Kerr in 1971, as a process which he referred to as 'shrinkage necrosis' [Kerr 1971]. During this genetically-encoded programmed cell death [Alison and Sarraf 1992], cells undergo cytoplasmic shrinkage, together with DNA fragmentation and condensation, leading to the formation of so-called apoptotic bodies [Majno and Joris 1995]. Apoptosis appears to be involved in the regulation of cell numbers in normal tissue [Wyllie 1992]. Some research has suggested that certain cell types, including human fibroblasts, become relatively resistant to apoptosis when they reach replicative senescence [Wang 1995]. Subsequent studies, though, have shown that the susceptibility of senescent cells to apoptosis depends on the nature of the pro-apoptotic signal [Tepper *et al.* 2000], and on the cell type studied. Thus senescent fibroblasts are resistant to apoptosis induced by p53-dependent DNA damage, but are susceptible to p53-independent apoptosis induced by various genotoxic stresses [Seluanov *et al.* 2001]. Furthermore, while senescent human umbilical vein endothelial cells (HUVECs) display a marked increase in spontaneous apoptosis, senescent HDFs do not, even though both cell types show similar accumulations of p16, p21 and p27 [Wagner *et al.* 2001].

In the study by Schmitt *et al.* mentioned earlier [Schmitt *et al.* 2002], the ability of murine lymphomatous cells to enter a senescence programme in response to cyclophosphamide depended on inhibition of their apoptotic pathway by over-expression of the *bcl2* gene. Here replicative senescence and apoptosis appeared to be mutually exclusive responses to an extrinsic insult. Another study has shown that

when pRb is inactivated in senescent cells, the cells undergo apoptosis through a mechanism dependent on E2F [Alexander *et al.* 2003].

Regarding organismic ageing, there is growing evidence to suggest that the ageing process is associated with dysregulation of apoptosis [Warner *et al.* 1997]. Apoptosis is up-regulated during organismic ageing in certain cell types, including cardiac myocytes, hepatocytes, cells of the central nervous system [Higami and Shimokawa 2000], and T lymphocytes [Chrest *et al.* 1995, Aggarwal and Gupta 1998]. It is notable that, with the exception of T cells, these are generally non-dividing cell types; in continuously dividing cells, however, the effects of ageing on apoptosis vary between cell types [Higami and Shimokawa 2000].

1.4.8 Replicative senescence and atherosclerosis

Endothelial [Rosen *et al.* 1981, Maciag *et al.* 1981, Glassberg *et al.* 1982, Thornton *et al.* 1983, Hoshi and McKeehan 1986] and vascular smooth muscle cells [Bierman 1978, Cristofalo and Pignolo 1993] taken from normal tissue have a limited replicative potential when grown *in vitro*.

Evidence that replicative senescence of vascular cells can also occur *in vivo*, and may be involved in atherogenesis, has become increasingly direct over recent years. Suspicion of a connection between cellular ageing and atherosclerosis is raised by the study of premature ageing syndromes, and of other conditions which pre-dispose to atherosclerosis. The decreased *in vitro* replicative capacity of cells derived from subjects with progeria and Werner's syndrome, and the prominence of atherosclerosis in these conditions, have already been mentioned. Similarly, fibroblasts derived from patients with diabetes mellitus (a disease associated with increased atherosclerotic disease) have a lower replicative capacity *in vitro* than cells from non-diabetic subjects [Goldstein *et al.* 1975].

Some *in vitro* studies provide indirect evidence that EC and VSMC senescence may be relevant to atherosclerosis. The pro-atherogenic molecule homocysteine is capable of accelerating EC senescence [Xu *et al.* 2000]. Similarly, OxLDL significantly inhibits telomerase activity in ECs [Breitschopf *et al.* 2001].

1.4.8.1 Putative role of EC and VSMC senescence in atherosclerosis

Senescent ECs *in vitro* show a marked increase in the expression of interleukin-1 alpha (IL-1α) [Maier *et al.* 1990], plasminogen activator inhibitor-1 (PAI-1) [Comi *et*

al. 1995] and ICAM-1 [Maier *et al.* 1993]. These proteins are also over-expressed in atherosclerotic lesions [Moyer *et al.* 1991, Schneiderman *et al.* 1992, van der Wal *et al.* 1992], and have been implicated in the progression of the disease process: IL-1α secretion promotes the adherence of monocytes to the endothelial surface [Bevilacqua *et al.* 1985]; PAI-1 decreases fibrinolytic activity and is thought to have other pro-atherogenic properties [Lupu *et al.* 1993, Christ *et al.* 1997]; ICAM-1 facilitates a number of intercellular interactions in the atherosclerotic plaque, including the entry of T cells into the intima [Watanabe and Fan 1998].

As mentioned earlier, serially passaged ECs show a progressive decline in eNOS expression and activity [Matsushita *et al.* 2001]. Endothelium-derived NO has a protective role against atherosclerosis, through its actions as an inhibitor of platelet adhesion and reactivity, leukocyte adhesion and SMC proliferation [Radomski *et al.* 1987, Mugge *et al.* 1991]. Furthermore, atherosclerotic coronary arteries have lower basal levels of NO secretion than do normal coronary arteries [Chester *et al.* 1990]. It thus seems plausible that EC senescence, if occurring *in vivo*, could contribute to atherogenesis via a decline in endothelial NO production.

Both senescent VSMCs *in vitro* [Christ *et al.* 1997] and VSMCs in atherosclerotic plaques [Lupu *et al.* 1993] synthesize increased levels of PAI-1. Senescent VSMCs also over-express osteopontin and matrix Gla protein, suggesting that VSMCs which have undergone rounds of proliferation *in vivo* may be involved in regulating calcification in vascular lesions [Shanahan *et al.* 1993].

1.4.8.2 Evidence for EC and VSMC senescence in atherosclerosis

The study of *ex vivo* cells and tissue provides rather more direct evidence for a role of vascular cell senescence in atherogenesis. ECs with morphological and karyotypic characteristics typical of senescent cells *in vitro* have been found covering the surface of arterial intimal lesions [Tokunaga *et al.* 1989, Bürrig 1991]. For example, 'giant' ECs have been detected overlying advanced atherosclerotic plaques in human carotid arteries [Bürrig 1991]. Similarly, VSMCs from arterial fibrous plaques share morphological characteristics with senescent cells *in vitro* [Ross 1986, Newby *et al.* 1999]. Furthermore, the conditioned medium of VSMCs derived from atherosclerotic plaques can up-regulate EC synthesis of PAI-1, a property shared with late- (but not early-) passage cultures of normal VSMCs [Christ *et al.* 1997].

1.4.8.3 EC and VSMC proliferation studies

Studies of *in vivo* cellular proliferative rates and *ex vivo* replicative capacity also suggest that vascular cell senescence can occur *in vivo*. Cellular turnover in the human arterial endothelium *in vivo* is generally extremely low [Schwartz and Benditt 1973, Schwartz and Benditt 1976, Hobson and Denekamp 1984]. In a rat model, aortic ECs are essentially quiescent, except at certain 'hot-spots' [Schwartz and Benditt 1977]. Other animal studies have shown that in the bifurcations and branching points of certain arteries, which in humans correspond to atherosclerosis-prone areas, there is an increased rate of EC replication [Wright 1968, Caplan and Schwartz 1973, Stary *et al.* 1992]. These sites are usually exposed to greater haemodynamic forces of shear and stretch [Zarins *et al.* 1990], and here the endothelium may respond with an increase in turnover in an attempt to maintain its integrity [Langille *et al.* 1986]. The question remains as to whether this increased turnover can eventually lead to EC senescence *in vivo*.

Proliferation studies of VSMCs derived from atherosclerotic plaques suggest that they experience a reduction in their replicative capacity [Bennett *et al.* 1995, Lutgens *et al.* 1999]. VSMCs isolated from atherosclerotic plaques and grown in culture rapidly reach senescence, doing so many times more quickly than medial VSMCs taken from non-atherosclerotic arteries [Bennett *et al.* 1995]; these plaque cells are also more prone to apoptosis than normal medial VSMCs. Intimal VSMCs within ruptured plaques also show low levels of proliferation [Lutgens *et al.* 1999], despite their being located within a mitogenic environment [Newby *et al.* 1999], suggesting a loss of replicative capacity.

1.4.8.4 Telomere studies

Studies of telomeric length in cells isolated from vascular tissue have also proved instructive. The rate of telomere shortening is more rapid in ECs derived from iliac arteries than from iliac veins [Chang and Harley 1995]. Similarly, in accordance with the higher rates of EC replication at sites of increased haemodynamic stress, telomere attrition is faster in the distal than in the proximal segment of the abdominal aorta (the distal segment being more prone to atherosclerosis) [Okuda *et al.* 2000]. In this study, the rate of attrition was also higher with increasing donor age. In the following year, the same group demonstrated an inverse correlation between telomere length and donor age in human abdominal aortic ECs [Aviv *et al.* 2001].

Overall these findings suggest that as age advances, vascular cells which have exhausted their replicative capacity may accumulate in clusters in areas prone to atherosclerosis.

1.4.8.5 Endothelial denudation studies

Several studies have investigated the kinetics of the vascular cell proliferative response which follows a breach of the arterial endothelium, in an attempt to understand some of the cellular processes involved in atherosclerosis and the clinical phenomenon of post-angioplasty re-stenosis [Ferns *et al.* 1992]. These studies have usually involved denudation of a region of endothelium by passing a balloon or other device along the luminal surface of the artery. When only a small area of endothelium is injured, the denuded area can be rapidly and totally repaired by replication of the remaining ECs [Reidy and Schwartz 1981]. If a larger area is injured, though, EC replication may not be sufficient to repair the breach [Reidy *et al.* 1983], even after a long period of time [Clowes *et al.* 1986]. This suggests that there is a limit to the amount of EC replication which can occur. In contrast, other research has shown that complete regeneration of large areas of endothelium is possible, provided that the denudation injury is performed without trauma to the media [Lindner *et al.* 1989].

VSMC proliferation also occurs during the intimal thickening induced by mechanical injury to the luminal surface of the vessel, for example following carotid endarterectomy, coronary angioplasty and in endothelial denudation models [Stemerman *et al.* 1982, Davies and Hagen 1994]. It is not known, however, whether this proliferation leads to the accumulation of senescent VSMCs.

1.4.9 Detection of senescent cells

As mentioned earlier, senescent cells in culture show characteristic morphological features. Demonstration of these features, and of an inability of cells to respond to mitogenic stimuli, were once the main methods for identifying senescent cells *in vitro*. Detection of cell senescence *in vivo*, where the morphology of single cells is less easy to assess, and where individual cell growth is difficult to determine, has therefore been problematic. While senescent cells *in vitro* can be identified by their failure to synthesize DNA under optimal growth conditions, *in vivo* DNA synthesis measurements cannot distinguish senescent cells from quiescent or terminally differentiated cells [Dimri *et al.* 1995].

Senescence-associated β-galactosidase, an assay for *in vitro* replicative senescence mentioned earlier, appears to offer the possibility of detecting senescence of individual cells *in vivo* [Dimri *et al.* 1995].

The term β-galactosidase (β-gal) refers to enzymes capable of cleaving β-D-galactose residues in β-D-galactosides. These enzymes are active against a wide range of substrates. The lysosomal isoform of β-gal is optimally detected at a pH varying between 3.0 and 5.0 depending on the species studied, and at pH 4.0 in humans [Morreau *et al.* 1989]; it has therefore been termed acid β-galactosidase [Koldovsky *et al.* 1969]. This acid β-gal activity is detectable in most mammalian cells, regardless of their replicative age [Morreau *et al.* 1989, Dimri *et al.* 1995]. A defect in this enzyme in humans leads to the accumulation of its usual substrates, as is seen in the inherited metabolic disorder G_{M1} gangliosidosis [Mutoh *et al.* 1988]. A bacterial isoform of β-gal has a pH optimum of between 7.4 and 7.5, and is often used as a reporter gene in gene transfer studies [Wakita *et al.* 1991, Cui *et al.* 1994].

Histochemical detection of β-gal activity (at any pH) is usually carried out by incubating cells or tissues with the indigogenic substrate 5-bromo-4-chloro-3-indolyl-β-galactopyranoside (known as X-Gal) [Gossrau *et al.* 1991, Dimri *et al.* 1995, Xu *et al.* 1997]. This substrate, when cleaved by the enzyme, yields an insoluble end-product which appears blue or turquoise under light microscopy.

In 1995, Dimri *et al.* showed that if cultures of human fibroblasts were assayed for β-gal activity at pH 6.0, the enzyme activity appeared to be detected only in senescent cells. This endogenous pH 6.0 activity was therefore termed senescence-associated β-galactosidase (SA-β-gal) [Dimri *et al.* 1995]. Dimri *et al.* demonstrated that this activity was not found in quiescent, terminally differentiated or immortal cells [Dimri *et al.* 1995]. Initially, SA-β-gal was found in senescent cultures of human fibroblasts and keratinocytes [Dimri *et al.* 1995], and of epithelial cells [Bodnar *et al.* 1998], as well as in some human skin biopsies [Dimri *et al.* 1995]. It was not found, though, in senescent cultures of murine fibroblasts, despite being detectable in equivalent cultures derived from rats [Dimri *et al.* 1995]; also, in some cell types, for example adult melanocytes, and sebaceous and eccrine gland cells, β-gal activity was detectable at pH 6.0 whether or not the cells had reached senescence. The ability of the assay to

identify senescent cells therefore appears to depend on the cell type and the species studied.

SA-β-gal has now been widely used to detect cell senescence *in vitro* [for example in studies reported by Serrano *et al.* 1997, Xu *et al.* 1997, Tsukamoto *et al.* 1998, Matsunaga *et al.* 1999]. Its validity as a marker of *in vitro* (let alone *in vivo*) senescence has not gone unchallenged, though, as will be discussed in Chapter Five.

1.5 Oxidative stress

1.5.1 Definition

As alluded to previously (Section 1.3.2.6), according to the 'free radical theory of ageing' [Harman 1956, Harman 1981] organismic ageing is attributable to the progressive and irreversible acquisition of molecular oxidative damage ensuing from normal metabolic reactions occurring in an aerobic environment [Sohal and Allen 1990, Sohal and Weindruch 1996]. Such reactions lead to the continuous generation of ROS including free radicals, mainly from mitochondria; these ROS are believed to be responsible for age-related oxidative damage [Beckman and Ames 1998a]. As well as this physiological production of ROS, increased levels of ROS are generated during certain pathological processes such as ischaemia-reperfusion injury [Welbourn *et al.* 1991] and inflammation [Bragt *et al.* 1980].

Oxidative damage accumulates in the DNA, proteins and lipids of the ageing organism, and leads to cellular dysfunction, and potentially to necrosis or apoptosis [Kurose *et al.* 1997, Naderi *et al.* 2003]. To limit these damaging effects aerobic organisms possess antioxidant defence systems, including enzymes that repair macro-molecular damage [Janssen *et al.* 1993, Demple and Harrison 1994] and a number of mechanisms that 'mop up' ROS [Halliwell and Gutteridge 1989, Sies 1991]; the latter include intrinsic antioxidant enzymes such as catalase, superoxide dismutase (SOD) and glutathione peroxidase, as well as dietary scavengers such as α-tocopherol, ascorbic acid and flavanoids.

When the balance between oxidant and antioxidant processes is altered in favour of the former, there is said to be an increase in the level of oxidative stress, potentially leading to oxidative damage [Sies 1991].

1.5.2 The generation and effects of oxidative stress

The initial radical generated during normal mitochondrial respiration is the superoxide ion. This is metabolized predominantly by mitochondrial SOD [Dionisi *et al.* 1975] to form hydrogen peroxide; some superoxide molecules may also be thrown into the intermembrane space of the mitochondria, where they may be metabolized by cytosolic SOD. Superoxide molecules generated by pathological processes can similarly be metabolized by members of the SOD family, again yielding hydrogen peroxide. Hydrogen peroxide molecules are themselves toxic, but can be metabolized to non-toxic by-products either by catalase or by various peroxidases (including glutathione peroxidase) [Sies 1993]. Hydrogen peroxide may alternatively be metabolized, in the presence of Fe^{2+}, via the Fenton reaction [Imlay *et al.* 1988], to form the hydroxyl radical, which is itself highly toxic.

Superoxide molecules not cleared by the SOD enzyme system are capable of generating further damaging molecules by reactions with other free radicals. They may, for example, react with NO to form peroxynitrite [Beckman *et al.* 1990]. Peroxynitrite, an example of a reactive nitrogen species, may then either decompose to form free radicals including the nitronium ion and hydroxyl ions [Beckman *et al.* 1992], or may itself cause damage to various proteins.

Four subcellular sources of pro-oxidants make a prominent contribution to oxidant stress during ageing [Roy 1997, Beckman and Ames 1998b]; these are mitochondrial and peroxisomal oxidative reactions, microsomal P-450 enzymes, and membrane-associated enzymes such as NAD(P)H oxidase and NO synthase.

Because of their high reactivity, ROS are capable of modifying most biological macromolecules. This damage can be self-perpetuating, as it can lead to the generation of further ROS, themselves capable of inflicting additional damage. The result is an amplification of the initial oxidative insult.

Oxidative damage to DNA is thought to have deleterious effects which contribute to cellular ageing. For example, as will be discussed in detail below, oxidative stress can accelerate the attrition of telomeric DNA which occurs during cell replication; it has been proposed that in this way oxidative stress may augment, or indeed drive cellular senescence.

Oxidative stress is also believed to be involved in the initiation of cell signalling pathways which contribute to various aspects of the ageing phenotype [Lavrovsky *et*

al. 2000]. ROS can up-regulate certain genes whose expression is associated with ageing. For example, ageing has been shown to be associated with a progressive increase in the nuclear level of the activated form of nuclear factor kappa B (NF-κB) in various organs [Spencer *et al.* 1997], and ROS can up-regulate both the expression of this transcription factor, and its transportation to the cell nucleus [Verma and Stevenson 1997]. Similarly, ROS can induce the expression of another transcription factor, activator protein 1 (AP-1), as well as influencing the expression of peroxisome proliferator-activated receptors and other members of the nuclear receptor super-family [Lavrovsky *et al.* 2000]; these various molecules are believed to play important roles in the initiation and maintenance of chronic inflammatory conditions, including the age-related pathologies of rheumatoid arthritis and atherosclerosis.

1.5.3 Oxidative stress and organismic ageing

Most evidence in support of the free radical theory of ageing is correlative and circumstantial. The level of production of free radicals in several organs of various mammalian species is inversely proportional to the MLSPs of these species [Sohal *et al.* 1989]. Conversely, higher levels of some antioxidants, such as SOD, are found in the longer-lived species [Sohal *et al.* 1990].

When levels of intracellular oxidants are measured in cells derived from animals of different ages, higher oxidant levels are found in cells from older animals [Hagen *et al.* 1997]. There is also an age-related increase in the products of oxidative stress [Schleicher *et al.* 1997], including an age-dependent accumulation of oxidized proteins in various tissues [Stadtman 1992], as well as an age-related decline in antioxidant enzymes and molecules [Lykkesfeldt *et al.* 1998].

Various transgenic animal models have been used to explore the theory further. These include fruit-flies over-expressing SOD or catalase [Reveillaud *et al.* 1991, Sohal and Weindruch 1996, Parkes *et al.* 1998], and mice with increased levels of either SOD [Epstein *et al.* 1987] or glutathione peroxidase [Mirault *et al.* 1992]. In these models some extension of the life-span was found: for example, over-expression of SOD in the motorneurones of *Drosophila* increased the organism's life-span by some forty percent [Parkes *et al.* 1998].

An association between oxidative stress and ageing is also suggested by the study of antioxidant mechanisms in subjects with Down's syndrome (trisomy 21). These individuals age prematurely, and have a shortened life expectancy [Kedziora and

Bartosz 1988]. They have an imbalance in their antioxidant enzyme system: they possess three copies of the SOD gene, Sod 1, but only two copies of the gene for glutathione peroxidase [de Haan *et al.* 1996], and in various tissues from Down's syndrome patients SOD activity is raised relative to glutathione peroxidase activity, leading to an accumulation of hydrogen peroxide molecules [Brooksbank and Balazs 1984]. This imbalance may play a role in the premature ageing process itself [Groner *et al.* 1990]. Down's syndrome subjects show an increased susceptibility to lipid peroxidation [Brooksbank and Balazs 1984], and this may contribute to their increased propensity to develop cardiovascular disease.

1.5.4 Oxidative stress, replicative senescence, and stress-induced premature senescence

1.5.4.1 The effects of oxidative status on cellular proliferative activity

Evidence is accumulating that oxidative stress and replicative senescence are inter-related phenomena. Such a relationship was suggested by the early findings that cell proliferation could be inhibited by hyperoxia [Balin *et al.* 1977] and that, conversely, proliferative activity could be prolonged by hypoxia [Packer and Fuehr 1977].

More recently, other interventions which affect the intracellular redox status of dividing cells have been shown to alter their replicative capacity. For example, when cell lines are transfected with Sod 1, increasing the ratio of SOD to glutathione peroxidase and so producing higher levels of hydrogen peroxide and oxidative stress, cellular proliferation is slowed, and there is an alteration in cellular morphology consistent with cellular senescence [de Haan *et al.* 1996].

Markers of oxidative damage to DNA are elevated in senescent HDFs when compared with early-passage cells [Chen *et al.* 1995], suggesting that DNA damage accumulates with rounds of replication. In addition, hyperoxia inhibits proliferation of HDFs, and this effect is associated with accelerated telomere shortening [von Zglinicki *et al.* 1995].

Exposure of HDFs to either hydrogen peroxide or tert-butylhydroperoxide (t-BHP), an organic peroxide which generates ROS, also accelerates telomeric attrition [Dumont *et al.* 2001], while rates of telomeric attrition in fibroblasts are halved when cells are treated with the spin-trapping agent, α-phenyl-*t*-butyl nitrone (PBN) [Chen *et al.* 1995]. Fibroblasts treated with hydrogen peroxide develop short distal single strand

DNA breaks at each replication, and undergo telomeric shortening at a rate related to the accumulation of these breaks [Petersen *et al.* 1998, von Zglinicki *et al.* 2000]. This accumulation of single strand breaks implies not only that telomeric shortening may trigger replicative senescence, but also that telomeres may act as sensors of cumulative oxidative damage [Serra *et al.* 2000, Toussaint *et al.* 2000a].

With regard to vascular cells, hypoxia has been shown to extend the replicative life-span of human VSMCs grown in culture [Minamino *et al.* 2001]; this hypoxia was associated with sustained high levels of hTERT expression. Similarly, exposure of HUVECs to a form of ascorbic acid, Asc2P, which acts as a ROS-scavenger precursor, resulted in a significant reduction in the rate of age-dependent telomere shortening [Furumoto *et al.* 1998]; the cellular replicative life-span was extended, and the cell size enlargement expected in ageing cultures was prevented.

In ECs, the predominant intrinsic defence mechanism against peroxidation appears to be provided by the glutathione redox cycle [Suttorp *et al.* 1986]. It has recently been shown that by increasing intracellular oxidative stress in replicating HUVECs (to a level which does not induce discernible cytotoxic or cytostatic effects) via manipulation of the glutathione redox-cycle, the rate of telomeric attrition is accelerated, and the cells enter a senescent state prematurely [Kurz *et al.* 2004].

1.5.4.2 Stress-induced premature senescence

As well as these effects of oxidative stress on telomere attrition and the emergence of replicative senescence in populations of dividing cells, it is also now recognized that oxidative stress, as well as certain other sub-lethal stresses, can lead to another form of senescence which does not require prior rounds of exhaustive replicative activity. Such stresses include DNA-damaging agents, lack of nutrients and growth factors, oncogenic over-expression, and other metabolic abnormalities [Fairweather *et al.* 1987, Chen and Ames 1994, Serrano *et al.* 1997, Ben-Porath and Weinberg 2004]. These can cause cells to enter the non-dividing state known as stress-induced premature senescence (SIPS) mentioned earlier.

1.5.4.3 Relationship between replicative senescence and SIPS

SIPS and replicative senescence appear to be mediated by two distinct, and yet overlapping mechanisms. A distinction between the two mechanisms is suggested by the responses of cells undergoing either type of senescence to the forced over-

expression of human telomerase: while, as mentioned above, the onset of replicative senescence can be delayed by this intervention [Bodnar *et al.* 1998, Vaziri and Benchimol 1998], the advent of SIPS is not prevented by telomerase over-expression [Gorbunova *et al.* 2002], implying that telomere shortening is not fundamental to the emergence of SIPS. In addition, while replicative senescence is generally considered to cause cell cycle arrest in G_1, oxidative stress has been shown to cause arrest in G_2 in some forms of SIPS [Balin *et al.* 1978, Poot *et al.* 1988] (although other forms of SIPS do appear to lead to arrest in G_1, as will be described below).

Further evidence for the existence of two separate mechanisms leading to two different forms of senescence comes from the study of cultures of human epithelial cells: replicating keratinocytes can undergo SIPS early in the lifetime of the culture, and this arrest is mediated by p16; if p16 expression is silenced by deletion of the p16 locus, keratinocytes will bypass this early SIPS, and continue to replicate until they undergo a later, p53-dependent, replicative senescence [Rheinwald *et al.* 2002]. The emergence of senescence in human cell cultures may thus result from a combination of intrinsic senescence (i.e. telomere-based replicative senescence, acting via p53 and p21) and extrinsic senescence (i.e. SIPS, effected through p16 over-expression) [Herbig *et al.* 2004, Itahana *et al.* 2004]. The relative importance of these two forms of senescence within an individual culture depends not only on the cell type studied, but even on the strain of cells cultured; for example, while WI-38 type human fibroblasts (from the lung) can senesce via both intrinsic and extrinsic mechanisms, BJ type human fibroblasts (from the skin) produce no senescent cells via the p16-based (extrinsic) mechanism, but senesce purely through the p53/p21-telomere-based mechanism [Itahana *et al.* 2003].

Other evidence, though, suggests that there may be a considerable overlap between not only the triggers but also the mechanisms leading to replicative and stress-induced senescence. For example, cells exhibiting either form of senescence share several characteristics, including their morphology, SA-β-gal activity and some abnormalities in cell cycle regulation [Dumont *et al.* 2000, Toussaint *et al.* 2000a]. Thus, when human primary fibroblasts are transfected with activated Ras (which rapidly raises intracellular levels of ROS), cells enter a permanent G_1 arrest, accompanied by accumulation of p53 and p16 [Serrano *et al.* 1997]; this arrest is phenotypically indistinguishable from replicative senescence, and is associated with demonstrable

SA-β-gal activity. The rise in intracellular ROS appears to be a crucial factor in inducing their senescence, in that fibroblasts can be rescued from Ras-induced senescence by scavengers of hydrogen peroxide [Lee *et al.* 1999]. Furthermore, HDFs treated with t-BHP show increased levels of messenger RNA (mRNA) corresponding to genes encoding fibronectin, osteonectin, α1(I)-procollagen, molecules known to be over-expressed in replicatively senescent fibroblasts, and indeed in cells derived from Werner's syndrome subjects [Dumont *et al.* 2000].

It has been proposed that since the intrinsic and extrinsic pathways leading to senescence appear to converge on the activation of p53 and pRb, these two proteins may act as integrators of stress signals, their combined level of activation determining the timing of the onset of senescence [Ben-Porath and Weinberg 2004]. Furthermore, given the overlap between conditions which induce replicative senescence and SIPS, and given the similarity in the characteristics of cells which have undergone either type of senescence, it has been suggested that replicative senescence and SIPS may share the same biological function, and should be regarded as two aspects of a cell's response to physiological stress [Ben-Porath and Weinberg 2004].

1.5.5 Oxidative stress and atherosclerosis

1.5.5.1 Epidemiological and dietary studies

As mentioned previously, it has been proposed that oxidative stress may play a role in the development and progression of atherosclerotic lesions. This theory has partly arisen from epidemiological and nutritional studies. A low prevalence of IHD has been reported in geographical areas where dietary antioxidant intake is high [Diaz *et al.* 1997], or when various antioxidant vitamin supplementation regimes are implemented [Blumberg 1996]. It has also been shown that phenolic substances in red wine are able to inhibit the oxidation of LDL [Frankel *et al.* 1993] and it has been suggested that this might help to explain the relatively low prevalence of coronary artery disease among the French. The epidemiological data relating to dietary antioxidants and IHD risk are not clear-cut, though; in a recent meta-analysis encompassing nine previously studied cohorts, only a weak (negative) correlation was found between dietary antioxidant levels and IHD risk; while dietary supplementation with high doses of vitamin C was associated with a statistically significant reduction in the incidence of major IHD events, vitamin E supplementation failed to show such an effect [Knekt *et al.* 2004].

A causal role for oxidative stress in the development of atherosclerosis has been suggested by studies into the effects of antioxidants in animal models of atherogenesis. Antioxidant administration inhibits the development of early atherogenic lesions in apoE-deficient mice (described below), without having any significant effect on their plasma cholesterol levels [Tangirala *et al.* 1995a]. The antioxidant used in that study, N,N-diphenyl 1,4-phenylenediamine, had a similar effect in cholesterol-fed rabbits, in which it was also shown to protect LDL from oxidation [Sparrow *et al.* 1992]. Similarly, administration of the antioxidant probucol to Watanabe heritable hyperlipidaemic (WHHL) rabbits (which lack functional LDL receptors) led to a dramatic reduction in the rate of atherogenesis [Kita *et al.* 1987], even when the slight hypocholesterolaemic effect of probucol was controlled for by the use of lovastatin in the control group [Carew *et al.* 1987]. A variety of antioxidants have been found to share this capacity to retard early atherogenesis, suggesting that this may be a class effect.

On the other hand, studies in humans have provided less convincing evidence that high antioxidant levels are protective against the progression of atherogenesis. For example, when dietary antioxidant intake and carotid artery intima-media thickness were studied in subjects aged between 45 and 64 years, only among older subjects (those over 55 years of age) was an inverse correlation found between vitamin C intake and average artery wall thickness; in the case of alpha-tocopherol, the inverse relationship was only significant among women, and for carotenoids it was only found among older men, and weakened further after adjustment for potential confounders [Kritchevsky *et al.* 1995]. It seems likely that the less dramatic effect of antioxidants on disease progression seen in humans (compared with their influence in animal models) reflects the complex aetiology of human atherosclerosis.

1.5.5.2 Putative mechanism of action of oxidative stress in atherogenesis

A number of mechanisms have been postulated to act as a potential link between oxidative stress and susceptibility to atherosclerosis. Prominent among these is the 'oxidative modification hypothesis' of atherosclerosis [Witztum 1994] mentioned earlier. According to this theory, oxidative damage to LDL, converting it to OxLDL, renders it more atherogenic than the native lipoprotein [Steinberg 1995].

In atherogenesis, LDL is believed to accumulate in the subendothelial space of arteries, where it is exposed to oxidative agents released from ECs, VSMCs, and,

when present, macrophages and lymphocytes [Morel *et al.* 1984, Witztum and Steinberg 1991]. As a result LDL is mildly oxidized to so-called 'minimally modified LDL' [Navab *et al.* 1996]. This form of LDL induces local vascular cells to release chemoattractants such as MCP-1, as well as granulocyte and macrophage colony-stimulating factors; as a result, monocytes are recruited into the arterial wall, where they differentiate into macrophages [Parhami *et al.* 1993]. Monocytes and macrophages are themselves capable of stimulating further peroxidation of LDL, with the resultant formation of completely oxidized LDL (OxLDL) [Parthasarathy *et al.* 1986]. OxLDL is recognized by scavenger receptors on macrophages, and is internalized to form foam cells [Henriksen *et al.* 1981]. The uptake of OxLDL is not subject to negative-feedback regulation, and therefore results in a massive uptake of cholesterol into the macrophages.

1.5.5.3 Atherogenic properties of OxLDL

Several other properties of OxLDL appear to make it more atherogenic than the native form [Steinberg 1995]. For example OxLDL is chemotactic for circulating monocytes [Quinn *et al.* 1988], and increases monocyte adhesion to the endothelium [Berliner *et al.* 1990] via enhancement of VCAM-1 expression by ECs [Khan *et al.* 1995]. OxLDL also inhibits the egress of monocytes from the arterial wall [Quinn *et al.* 1987]; as a result, once monocytes have crossed the endothelium they become trapped in the vessel wall. OxLDL is cytotoxic for vascular cells, including ECs [Steinberg *et al.* 1989, Witztum and Steinberg 1991], and as a result promotes the release of lipids and lysosomal enzymes into the intimal extracellular space, enhancing the progression of lesion formation [Schwartz *et al.* 1991]. Furthermore, components of OxLDL can induce the production of IL-1 by foam cells [Lipton *et al.* 1995], suggesting a further pro-inflammatory role.

In addition to these actions, OxLDL inhibits endothelium-mediated arterial relaxation [Kugiyama *et al.* 1990] and degrades endothelium-derived NO directly [Chin *et al.* 1992]. Abnormalities in endothelium-derived relaxation have been shown to be associated with the occurrence of atherosclerosis [Ludmer *et al.* 1986], suggesting that the OxLDL-mediated impairment of vasodilation may itself be pro-atherogenic. Indeed the inactivation of NO by oxidative stress, and in particular by superoxide ions, appears to play an important role in vascular pathology generally [Cai and Harrison 2000, Li and Shah 2004].

The susceptibility of LDL to oxidation correlates with the severity of coronary atherosclerosis [Regnstrom *et al.* 1992]. Furthermore, LDL isolated from older subjects shows enhanced susceptibility to oxidation compared with that taken from younger subjects [Walzem *et al.* 1995], suggesting a link between ageing and altered susceptibility to atherosclerosis.

1.5.5.4 Other possible roles for oxidative stress in atherogenesis

There are other mechanisms by which oxidative stress could promote atherosclerosis. These mechanisms may operate in addition to, rather than as alternatives to, the oxidation of LDL. The role of ROS in triggering pro-inflammatory intracellular pathways has already been mentioned (Section 1.5.2), and the resultant inflammation may promote atherogenesis. Oxidative stress can also trigger apoptosis, as mentioned earlier, and it has been suggested that apoptosis may contribute to the formation of the necrotic core of advanced atherosclerotic lesions [Rosenfeld 1998], and to plaque instability [Bennett 1999].

1.6 Experimental models of ageing

A variety of experimental models have been used to study ageing. This variety reflects the difficulty in finding a single model capable of reproducing all aspects of the human ageing process. This in turn is probably a reflection of the complexity of the pathobiological changes involved in human ageing. Experimental models have ranged from cell cultures to non-human primates. Pertinent results from cell culture experiments have been summarized above, and will not be discussed further here.

Studies in yeast have provided valuable insights into mechanisms underlying cellular senescence, as was mentioned earlier in the context of the telomere position effect. Simple organisms such as the fruit-fly *Drosophila melanogaster* [Nusbaum *et al.* 1993] and the nematode *Caenorhabditis elegans* (*C. elegans*) have also been studied in detail. Both are composed, in their adult form, entirely of post-mitotic cells. Genes that extend the life-span of *C. elegans* have been identified [Kenyon 1996], and genetic manipulations of both organisms have been used to influence their ageing [Antebi *et al.* 1998, Rauskolb and Irvine 1999].

A multitude of vertebrates have been used in the study of the various aspects of ageing. They include mice, rats, rabbits, chickens, pigeons, woodchucks, cats, dogs, and non-human primates. Among these, mice have proved a particularly convenient

model, as their natural life-span is approximately thirty times shorter than that of humans [Cristofalo 2001]. Some of these experimental models involve inbred or genetically modified strains.

One such strain is the '*klotho*' mouse [Kuro-o *et al.* 1997]. Mice homozygous for a mutation of the so-called '*klotho* gene' show growth arrest at three to four weeks of age, and die prematurely at approximately nine weeks of age [Nagai and Nabeshima 1997]. They exhibit various age-related pathologies, including skin atrophy, osteoporosis, pulmonary emphysema and cerebellar degeneration, and are being used extensively in ageing research. Their vasculature shows medial calcification and intimal thickening, as well as impairment of endothelium-dependent aortic vasodilatation [Saito *et al.* 1998]. The normal *klotho* gene encodes a membrane protein that shares some sequence homology with the β-glucosidase enzymes of plants and bacteria. An insertional mutation results in severe under-expression of the usual gene product. A human homologue of the *klotho* gene has been isolated, and is situated on the q arm of chromosome 13 [Matsumura *et al.* 1998], a chromosome which contains a number of genes involved in cell growth and replication [Zhang *et al.* 2000].

Another mouse model of ageing is the senescence-accelerated mouse (SAM) [Takeda *et al.* 1981, Takeda *et al.* 1994b]. This model will be described in some detail, as these mice have been used extensively in experiments described in Chapter Four.

1.7 The senescence-accelerated mouse (SAM)

The SAM model has been developed since 1970, and consists of a group of genetically related inbred strains originally derived by selective brother-sister inbreeding at Kyoto University in Japan, from several pairs of AKR/J mice donated by the Jackson Laboratory (Bar Harbor, Maine, USA) in 1968 [Takeda *et al.* 1981, Takeda *et al.* 1991, Hosokawa *et al.* 1997]. AKR mice have been studied for over forty years because of their propensity to develop lymphomas [Siegler and Rich 1963].

It was noticed during the maintenance of the newly-founded Japanese colony of AKR/J mice that certain litters appeared to age at an accelerated rate, and to have a reduced life-expectancy. This property proved to be inheritable. Five litters with such 'severe exhaustion' were chosen as the progenitors of a series termed senescence-accelerated prone mice (SAM-P). Three other litters (also derived from the AKR/J mice) which were considered to show a normal ageing process, were selected as the

progenitors of a series termed senescence-accelerated resistant mice (SAM-R). Selective brother-sister mating was performed within each series, using life-span data and a grading score of their ageing phenotype [Hosokawa 1994, Hosokawa *et al.* 1997]. This grading system assessed the presence and severity of certain criteria believed to be associated with ageing: these included passivity of behaviour, hair loss and coarseness, skin ulceration, lordokyphosis, and the development of ophthalmic lesions (including peri-ophthalmic lesions and cataract formation) [Hosokawa *et al.* 1984]. Mice exhibiting these features to the greatest extent were selected for further breeding to maintain the senescent phenotype within the SAM-P family, while SAM-R mice with the lowest scores were selected for mating.

SAM-P mice have a median life-span of between nine and eleven months, while SAM-R mice have a life-span similar to that of AKR/J mice, that is approximately nineteen months [Takeda *et al.* 1981, Takeda *et al.* 1994b]. These compare with an average life-span in wild-type laboratory mice of twenty-four to thirty months. Takeda *et al.* showed that the rate of decline of survival in SAM-P mice was greater with advancing age compared with the rate in SAM-R mice [Takeda *et al.* 1981]; after analysing body weights and the grading scores of senescence, they concluded that the manifestations of senescence in the SAM-P model did not occur during the animals' developmental stage, but did occur in an accelerated manner following a normal development. They inferred that the SAM-P mice exhibited accelerated, rather than simply premature, ageing [Takeda *et al.* 1981]. While the grading score measuring the emergence of features of the senescent phenotype rose more steeply in SAM-P than SAM-R mice, the scores eventually levelled out: there was no difference between the two strains of mouse in the maximum level of total grading score, but SAM-P mice reached this maximum earlier than did SAM-R mice [Hosokawa *et al.* 1984].

The genetic determinants which originally gave rise to the SAM phenotype are not known. SAM mice show a low incidence of thymic lymphoma compared with AKR/J mice, and so it has been assumed that the genetic background of SAM mice must have deviated from that of their progenitors [Takeda *et al.* 1991]. Indeed analysis of biochemical and immunogenetic markers has confirmed genetic differences between SAM mice and their AKR/J ancestors. It has been deduced that inadvertent outbreeding is likely to have occurred around the time when the progenitors of the SAM-P and SAM-R series were selected and inbreeding was initiated [Hosokawa

1994]. It is still not known which strain may have mated with the original AKR/J mice.

By 1994, selective inbreeding from the original SAM-P and SAM-R litters had led to the emergence of nine SAM-P sub-strains (SAM-P/1 - SAM-P/3 and SAM-P/6 -SAM-P/11) and three SAM-R sub-strains (SAM-R/1, SAM-R/4 and SAM-R/5), other strains having failed to breed successfully [Takeda *et al.* 1994a]; these sub-strains were delineated by the emergence of certain biological characteristics, as shown in Table 1.1 overleaf.

SAM-P mice have been the subject of intensive research ever since their ageing phenotype was recognized. This is mainly because so many of their clinical features correspond to processes and pathologies often found in human ageing. Particularly noteworthy in this context are the development of osteoporosis, cataracts, senile amyloidosis and memory difficulties. Their study has been facilitated by the ready availability of a control group of mice, the SAM-R strain.

Interest in these mice has been compounded by the fact that they show abnormalities in their cell biology which may have aetiological relevance to their ageing phenotype. Thus they show abnormalities in both the replicative capacity of their cells, and in their oxidative status; these abnormalities will be discussed in detail in Chapter Four.

1.8 Animal models of atherosclerosis

Atherogenesis, like ageing, has been studied in several species. As might be expected, those species most closely related phylogenetically to man generally develop lesions most similar to those found in humans. These models include hypercholesterolaemic primates and swine [Ross 1986]. Such models, though, are not readily available experimental tools, nor the most appropriate for every type of study, for both ethical and technical reasons. Other species have also therefore been employed, though these do not always provide the most accurate models.

Mice are being used increasingly in the study of atherosclerosis. Their use has both advantages and disadvantages. Mice are relatively cheap, and readily obtainable. Powerful genetic tools are available in this species which are not applicable in otherwise more suitable models. On the other hand, mice are generally highly resistant to atherogenesis [Witztum 1993, Breslow 1996], and there are important differences between humans and mice in terms of their lipid metabolism: for example, mice lack

Table 1.1 Pathologies in SAM sub-strains

Strain	Pathological phenotype
SAM-P strains	
SAM-P/1	Senile amyloidosis, impaired immune response, lung hyperinflation, hearing impairment
SAM-P/2	Senile and secondary amyloidosis, impaired immune responsiveness
SAM-P/3	Degenerative joint disease of temperomandibular joint
SAM-P/6	Senile osteoporosis
SAM-P/7	Senile amyloidosis, thymoma
SAM-P/8	Deficits in learning and memory
SAM-P/9	Cataract formation
SAM-P/10	Brain atrophy, deficits in learning and memory
SAM-P/11	Senile amyloidosis, contracted kidney
SAM-R strains	
SAM-R/1	Non-thymic lymphoma and histiocytic neoplasm
SAM-R/4	Non-thymic lymphoma and histiocytic neoplasm
SAM-R/5	Nil

Table 1.1 SAM sub-strains were distinguished and defined according to their lineage and according to certain specific pathologies. SAM-P/1, SAM-P/2 and SAM-P/3 sub-strains were developed directly from the original AKR/J mice donated to Kyoto University; SAM-P/6 and SAM-P/9 sub-strains were developed from a SAM-R sub-strain (SAM-R/3) which subsequently failed to breed successfully. SAM-P/7 and SAM-P/8 sub-strains were developed from the SAM-P/1 and SAM-P/2 sub-strains respectively, while SAM-P/10 and SAM-P/11 sub-strains were developed from SAM-P/3 mice. SAM-R/1 mice were developed directly from the AKR/J mice, and subsequently were progenitors of a genetically distinct sub-strain, SAM-R/4. SAM-R/5 mice were developed from a SAM-P sub-strain (SAM-P/4) which subsequently failed to breed successfully.

certain metabolic components, including cholesteryl ester transfer protein and apolipoprotein A, which are found in humans.

1.8.1 The C57BL/6 mouse

Of the inbred murine strains, the C57BL/6 mouse is the most prone to an atherogenic process [Paigen *et al.* 1985], and females are more susceptible than males. To provoke atherosclerosis, even C57BL/6 mice must be fed a highly unphysiological diet, containing not only ten to twenty times the level of cholesterol found in a Western-type diet, but also the unphysiological constituent cholic acid [Paigen *et al.* 1985]. Furthermore, the atheromatous lesions found in C57BL/6 mice occur only in the portion of the aorta adjacent to the aortic valve leaflets, rather than throughout the vascular tree. The lesions resemble the fatty streaks found in early human atherogenesis, and do not progress to more advanced stages such as fibrous cap formation. No coronary artery lesions have been demonstrated in C57BL/6 mice, nor any propensity for lesions to form at bifurcation points [Paigen *et al.* 1985]. There are therefore concerns that the atherogenesis instituted in C57BL/6 mice fed a very high-fat diet may not be a valid model of human atherogenesis.

1.8.2 The LDL-receptor deficient mouse

Other strains of mice which show more marked atherogenesis have been developed through genetic manipulations resulting in alterations of lipoprotein metabolism. LDL-receptor deficient mice develop fatty streaks when fed a Western-type diet [Palinski *et al.* 1995]. These lesions progress to a comparatively advanced stage, including the formation of a lipid-filled necrotic core capped with foam cells, when mice are fed a high-fat, cholic acid-containing diet [Ishibashi *et al.* 1994]. These mice do not develop lesions when fed a low-cholesterol, low-fat diet.

1.8.3 The apoE-deficient mouse

Mice deficient in apolipoprotein E, so called apoE-deficient mice, are yet more prone to atherosclerosis [Plump *et al.* 1992, Zhang *et al.* 1992]. Apo-E usually serves as a ligand through which lipids are cleared from the plasma via receptor-mediated pathways in the liver [Zhang *et al.* 1994]. Apo-E-deficient mice show spontaneous and very marked hypercholesterolaemia even when fed a low-fat diet [Plump *et al.* 1992, Zhang *et al.* 1992]. Furthermore they develop fatty streak lesions which can progress to fibrous plaques, even on a low-fat, low-cholesterol diet free of cholic acid

[Nakashima *et al.* 1994, Reddick *et al.* 1994]. These lesions occur throughout the arterial tree, and their progression is faster when the mice are fed a Western-type diet [Breslow 1993, Witztum 1993].

1.8.4 Rats

Turning to other animal models, rats do not tend to be used for the study of atherosclerosis, as few studies have shown atheromatous plaques in this species. However, some research using cholesterol-fed rats has contributed to our understanding of the role of macrophages in atherogenesis [Joris *et al.* 1983].

1.8.5 Rabbits

Rabbits, in contrast, provide a useful model of early atheromatous lesions. Although normal rabbits do not develop atherosclerosis on a standard diet, administration of a high-fat diet does lead to lesion development in the aorta within a few weeks [Walker *et al.* 1986, Davies and Woolf 1993]; these lesions contain lipid which is almost entirely contained by foam cells, and are thus more similar to fatty streaks than to advanced plaques; a lipid core is not seen, and there is no evidence of plaque rupture.

More advanced lesions are seen in rabbits which possess hereditary defects in their lipid metabolism. In WHHL rabbits, a defect in the LDL receptor causes an inability to bind this lipoprotein, resulting in a marked elevation of serum LDL. This reflects the aetiology of the human condition familial hypercholesterolaemia. In these rabbits, a less unphysiological diet is required to initiate lipid lesion formation than in wild-type rabbits, and the resultant lesions are relatively advanced, containing a lipid core [Buja *et al.* 1990]. WHHL rabbits have also proved useful in highlighting the early role of monocytes in fatty streak formation [Rosenfeld *et al.* 1985].

1.8.6 Pigs

Atherosclerosis in pigs has been studied extensively, partly because porcine coronary artery atheromatous lesions are morphologically similar to those found in man [French *et al.* 1965]. Studies in hypercholesterolaemic swine have also been helpful in elucidating the role of monocytes in atherogenesis, including their evolution into foam cells, and their cellular interactions [Gerrity *et al.* 1979, Gerrity 1981].

1.8.7 Non-human primates

The use of non-human primates has already been mentioned in relation to studies exploring the role of ageing as an independent risk factor for atherosclerosis (Section

1.2.3). Cholesterol-fed monkeys certainly provide a useful model, developing lesions with close similarities to human atherosclerosis [Wissler and Vesselinovitch 1977, Faggiotto and Ross 1984].

1.8.8 Denudation models

Many studies, using several species, have involved mechanical injury to the luminal surface of the arterial wall. Such research has sought to derive insights into clinical phenomena including atherosclerosis and post-angioplasty re-stenosis, and into the effect of certain interventions such as the administration of antioxidants. A denudation model has been used in work described later in this thesis, and more detail about such models is provided in Chapter Three.

1.9 Aims of the studies described

The overall aim of this thesis is to explore the relationship between ageing and cardiovascular disease. Two animal models have been used to study ageing at both an organismic and a cellular level, in particular with regard to the inter-relationship between ageing and atherosclerosis.

In the first model, which involves endothelial denudation of rabbit carotid arteries, the aim has been to find direct evidence that replicative senescence can occur in the vasculature. As has been described above, such evidence has remained elusive. It is known that endothelial denudation injuries are followed by a marked cellular proliferative response. It is hypothesized here that such proliferative activity may lead to the emergence of senescent cells. If vascular cells can indeed senesce *in vivo*, this could have implications for the pathophysiology of human atherosclerotic lesions.

In the second model, the susceptibility of SAM mice to develop atheromatous lesions is studied. If ageing is an independent risk factor for atherogenesis, mice which age in an accelerated manner might be expected to show a greater propensity to atheromatous lesion formation than mice which age at a normal rate.

By studying these two models, the aim of this thesis is to obtain more insight into the relationships between organismic and cellular ageing and atherosclerosis.

CHAPTER TWO

Materials and Methods

2.1 Materials

2.1.1 Antibodies

Alkaline phosphatase-conjugated goat anti-mouse immunoglobulin (Ig)	Dako Ltd, UK
Biotinylated $F(Ab')_2$ fragment of rabbit anti-mouse Ig	Dako Ltd, UK
Biotinylated rabbit anti-rat Ig	Dako Ltd, UK
Mouse anti-*Aspergillus niger* (*A. niger*) glucose oxidase IgG_1, clone DAK-GO1	Dako Ltd, UK
Mouse anti-*A. niger* glucose oxidase IgG_{2a}, clone DAK-GO5	Dako Ltd, UK
Mouse anti-*A. niger* glucose oxidase IgG_{2b}, clone DAK-GO9	Dako Ltd, UK
Mouse anti-CD31, clone JC/70A	Dako Ltd, UK
Mouse anti-PCNA, clone PC10	Dako Ltd, UK
Mouse anti-rabbit CD45, clone L12/201	Serotec, UK
Mouse anti-smooth muscle actin, clone 1A4	Dako Ltd, UK
Rat anti-mouse macrophages/monocytes, clone MOMA-2	Serotec, UK
Rat IgG_{2b} negative control, clone LO-DNP-11	Serotec, UK

2.1.2 Kits and reagents used in histology, immunostaining and apoptosis studies

2.1.2.1 Kits

In Situ Cell Death Detection Kit	Boehringer Mannheim, Germany
Liquid DAB Plus Kit	Dako Ltd, UK
New Fuchsin Chromogenic Substrate System Kit	Dako Ltd, UK

2.1.2.2 Reagents

4',6-diamidino-2-phenylindole (DAPI) in Vectashield™ mounting medium for fluorescence	Vector Laboratories Inc, USA
'Distrene-80', Plasticizer, and Xylene (DPX) mounting medium	BDH Lab Supplies, England
Fast red TR/Napthol AS-MX	Sigma Chemical Co., UK
Glycergel™ mounting medium	Dako Ltd, UK
Hexane	BDH Lab Supplies, England
Levamisole	Dako Ltd, UK
OCT™ compound	RA Lamb Ltd, UK
Oil red O	BDH Lab Supplies, England
Serum-free protein-blocking agent	Dako Ltd, UK
Streptavidin-conjugated alkaline phosphatase	Dako Ltd, UK
Streptavidin-conjugated horseradish peroxidase	Dako Ltd, UK
VECTABOND™ reagent	Vector Laboratories Inc, USA

X-Gal (5-bromo-4-chloro-3-indolyl β-D-galactopyranoside)	Sigma Chemical Co., UK
Xylene	BDH Lab Supplies, England

2.1.3 Kits and reagents used in cell culture and telomere studies

2.1.3.1 Kits

184 Elastomer kit	BDH Lab Supplies, England
TeloQuant™ Telomere Length Assay Kit	Pharmingen, USA

2.1.3.2 Reagents

Hanks balanced salt solution (HBSS)	Clonetics Corp., UK
Lambda ladder pulsed field gel (PFG) marker	New England Biolabs Inc., USA
Low melting point (LMP) agarose	Gibco BRL, UK
Mbo I restriction endonuclease	Gibco BRL, UK
Modified Puck's saline A	Gibco BRL, UK
Phenylmethylsulphonyl fluoride (PMSF)	Sigma Chemical Co., UK
Trypsin Neutralising Solution	Clonetics Corp., UK
Versene (supplied as a 0.53 M solution in isotonically buffered saline)	Gibco BRL, UK

2.1.4 Other kits, reagents and drugs

2.1.4.1 Kits

HDL-Cholesterol Direct cassette	Roche, Switzerland
INFINITY™ Cholesterol Reagent	Sigma Diagnostics
INFINITY™ Triglycerides Reagent	Sigma Diagnostics

2.1.4.2 Reagents

ACCUSET® Liquid Calibrator (A 2539)	Sigma Chemical Co., UK
Cardiolipin controls (C4571 and C4696)	Sigma Chemical Co., UK

2.1.4.3 Drugs

Buprenorphine	Reckitt and Colman Products
Ltd, USA	
Diazepam	Phoenix Pharmaceuticals Ltd USA
Enrofloxacin	Bayer AG, Germany
Fentanyl/fluanisone	Janssen Animal Health, Belgium
Sodium pentobarbital	Rhône Mérieux Ltd, France

Other chemicals were purchased at least at analytical grade, and were purchased from Sigma Chemical Co., UK, or from BDH Lab Supplies, England.

2.1.5 Buffers, solutions and media

2.1.5.1 Buffers

Lysis buffer for telomere study: 0.5 M EDTA pH 8.0, 2% Sarkosyl, 2 mg/ml proteinase K

Phosphate-buffered saline (PBS): Dulbecco's PBS (1X), without calcium, without magnesium (Gibco BRL, UK) containing 0.2 g/L potassium chloride, 0.2 g/L monobasic potassium phosphate, 8 g/L sodium chloride, 1.15 g/L dibasic sodium phosphate.

10 x PBS: Dulbecco's PBS (10X), without calcium, without magnesium (Gibco BRL, UK) containing 2 g/L potassium chloride, 2 g/L monobasic potassium phosphate, 80 g/L sodium chloride, 21.60 g/L $Na_2HPO_4.7H_20$.

0.2 M phosphate buffer: 0.2 M sodium dihydrogen phosphate, 0.2 M disodium hydrogen phosphate, pH 7.4. The buffer was stored in the dark at 4°C for up to 3 months.

0.5 x TBE (tris base boric acid EDTA buffer): 45 mM Tris base, 45 mM boric acid, 1 mM EDTA, pH 8.0.

Tris-buffered saline (TBS): 50 mM Tris base, 150 mM sodium chloride, pH 7.6.

Tris-EDTA (TE) buffer: 10 mM Tris-HCl, 1 mM ethylenediamine tetra acetic acid (EDTA), pH 8.0.

2.1.5.2 Solutions

1% acid alcohol: 1 ml concentrated hydrochloric acid in 99 ml 70% ethanol.

β-galactosidase staining solution (pH 6.0 or 4.0): 5 mM potassium ferrocyanide, 5 mM potassium ferricyanide, 150 mM sodium chloride, 2 mM magnesium chloride, and 40 mM trisodium citrate, titrated either to pH 6.0 with sodium dihydrogen phosphate, or to pH 4.0 with orthophosphoric acid. Solutions titrated to pH 6.0 or pH 4.0 were stored at 4°C protected from light, for up to 3 months.

Eosin solution: 1% (w/v) eosin in distilled water.

Harris' haematoxylin solution: 0.375% (w/v) haematoxylin monohydrate, 7.5% (w/v) ammonium alum, 0.225% (w/v) yellow mercuric acid, 0.4% (v/v) glacial acetic acid, the balance made up with distilled water.

1% LMP agarose: 1 g LMP agarose was dissolved in 100 ml PBS, then heated in a microwave oven to 50°C. The solution was prepared immediately prior to use.

Neutral buffered formalin: 4% formaldehyde, 0.1 M sodium dihydrogen phosphate, 0.1 M disodium hydrogen phosphate, pH 7.4. Stored at RT, and used within 1 month.

Oil red O stock solution: 1 g Oil red O dissolved in 1 litre of isopropanol in a long-necked flask over a water-bath at 56°C for 60 min. The solution was cooled to RT, and stored for up to 6 months at room temperature (RT) in an air-tight bottle.

Oil red O staining solution: 3 parts Oil red O stock solution were mixed with 2 parts distilled water, and left to stand for 5 min at RT. The mixture was filtered, and used immediately.

8% paraformaldehyde stock solution: 40 g paraformaldehyde (PFA) dissolved in 400 ml of distilled water at 80°C, then cooled to room temperature (RT). pH adjusted to 7.4, and volume made up to 500 ml with distilled water. The stock solution was filtered and stored in the dark at 4°C for up to 1 month.

2% or 4% paraformaldehyde / 0.1 M phosphate buffer: These solutions were prepared on the day of use, by dilution of the 8% paraformaldehyde stock solution with appropriate volumes of 0.2 M phosphate buffer and distilled water. The pH of the final solution was re-checked at RT, and if necessary re-adjusted to 7.4.

PMSF working solution: 40 mg PMSF dissolved in 1 ml of isopropanol, then diluted 1000-fold in TE buffer (pH 8.0), yielding a final concentration of PMSF of 40 μg/ml. The solution was prepared immediately prior to use.

Scott's tap water: 0.35% (w/v) sodium bicarbonate, 2% (w/v) magnesium sulphate.

20 x standard saline citrate (SSC): 3 M sodium chloride, 0.3 M Na_3 citrate.$2H_20$, adjusted to pH 7.0 with hydrochloric acid.

1 x SSC / 0.1% sodium dodecyl sulphate (SDS): 50 ml of 20 x SSC, 10 ml of 10% SDS, 940 ml distilled water.

30% sucrose / 0.1 M phosphate buffer: 60 g sucrose dissolved at 80°C in 100 ml of 0.2 M phosphate buffer made up to a final volume of 200 ml with distilled water. The solution was cooled to RT, and the pH adjusted to 7.4. It was then stored in the dark at 4°C for up to 1 month.

Trypsin-EDTA for ECs: 0.025% trypsin / 0.01% EDTA (Clonetics Corp., UK), stored at 4 °C.

Trypsin-EDTA for VSMCs: 0.5 g trypsin / 0.2 g EDTA per litre of modified Puck's saline A.

X-Gal stock solution: 100 mg X-Gal dissolved in 5 ml dimethylformamide (DMF), stored in a glass bottle, protected from light, at -20°C for up to 1 month. Since DMF can dissolve plastic, DMF and the X-Gal stock solution were pipetted using polypropylene tips.

X-Gal working solution (pH 6.0 or 4.0): This solution was prepared immediately prior to use. 1 ml of X-Gal stock solution was added to 19 ml of β-galactosidase staining solution (see above) of the required pH (yielding a 1 mg/ml final concentration of X-Gal). The mixture was filtered (0.22 μm) prior to use.

2.1.5.3 Media

All cell culture media were stored at 4°C.

Dulbecco's modified Eagle's medium (DMEM) with 3.7 g/L sodium bicarbonate buffer and 0.11 g/L sodium pyruvate (Gibco BRL, UK)

DMEM buffered with 20 mM Hepes, pH 7.4 (ICN Biomedicals Ltd, UK)

Endothelial cell growth medium (EGM) culture medium: Modified MCDB 131 medium supplemented with 10 ng/ml human recombinant epidermal growth factor, 1 μg/ml hydrocortisone, 50 μg/ml gentamicin, 50 ng/ml amphotericin B, 12 μg/ml bovine brain extract, and 2% (v/v) foetal bovine serum (EGM, Clonetics Corp., UK).

Dissecting medium for rabbit aortas: DMEM buffered with 20 mM Hepes, pH 7.4 (ICN Biomedicals Ltd, UK) supplemented with 10% foetal calf serum (FCS), 0.1 mM non-essential amino acids, 1 mM sodium pyruvate, 8 mM L-glutamine, 100 U/ml penicillin and 100 μg/ml streptomycin.

VSMC culture medium: DMEM with 3.7 g/L sodium bicarbonate buffer and 0.11 g/L sodium pyruvate (Gibco BRL, UK), supplemented with 20% FCS, 0.1 mM non-essential amino acids, 1 mM sodium pyruvate, 4 mM L-glutamine, 100 U/ml penicillin and 100 mg/ml streptomycin.

2.1.6 Diets

Mouse breeding and maintenance diet (TRM9607): Harlan Teklad, UK (composition: wheat, maize, wheatfeed, HiPro soya, barley, white fishmeal, dry whey, lucerne, dried brewer's yeast, limestone, soya oil, iodised salt, magnesium oxide, mineral and vitamin supplements, methionine, lysine; yielding in g/kg on proximate analysis: crude oil (i.e. fats) 43, crude protein 190, crude fibre 40, cholesterol 0.023. Therefore contains 4.3% fat by weight, 0.0023% cholesterol by weight.

Mouse Western Adjusted Calories diet (TD88137): Harlan Teklad, UK
(composition (g/kg): casein 195, DL-methionine 3.0, sucrose 341.46, corn starch 150.0, anhydrous milkfat 210.0, cholesterol 1.5, cellulose 50.0, mineral mix (AIN-76, 170915) 35.0, calcium carbonate 4.0, vitamin mix (Teklad 40060) 10.0, ethoxyquin 0.04. Therefore contains 21% fat by weight, 0.15% cholesterol by weight.
Guinea pig breeder and maintenance diet (RGP) (used as the standard diet for rabbits studied in the experiments described): Special Diets Service, UK, supplied by Lillico Biotechnology, UK
(contains barley, wheatfeed, oats, linseed cake, fish meal, grass meal, vitamins, major minerals, trace minerals, amino acids; yielding, in g/kg on proximate analysis: crude oil 33, crude protein 187, crude fibre 83)

2.2 Methods

2.2.1 Home Office Licences for animal research described in this thesis

All animal work described in this project was performed under Home Office Personal Licence number 70/14118. The project involving denudation of rabbit carotid arteries was performed under Home Office Project Licence number 70/4540. The breeding and maintenance of the colony of senescence-accelerated mice was carried out under Home Office Project Licence number PPL70/4336, as were the subsequent experiments involving this colony and C57BL/6 mice. All experiments involving animals were performed in full compliance with the Animals (Scientific Procedures) Act 1986, and in accordance with Home Office and University College London (UCL) guidelines.

2.2.2 In vitro cell senescence studies

2.2.2.1 Culture of HUVECs

First passage cryopreserved HUVECs were purchased commercially, and cultured in EGM culture medium at 37°C under 5% CO_2/95% air in a humidified incubator. Cells were plated in six-well plates (Falcon, Becton-Dickinson, UK), at a seeding density of 2,500 cells/cm^2, and the medium was replaced the day after seeding, and subsequently every 48 h. At each passage, the number of cells in the medium removed the day after seeding was counted, and was used to calculate the attachment efficiency, using the

following formula: attachment efficiency = [number of cells seeded – number of cells in the removed medium] / [number of cells seeded]. In most passages, the attachment efficiency was ≥ 0.9.

The cells were grown to confluence (as assessed by light microscopy), and were passaged after trypsinization at weekly intervals: the EGM culture medium was aspirated, and the cells washed in HBSS at RT; cells were then covered with trypsin-EDTA for ECs, and the plates were agitated for 5 min at RT; when cells appeared ready to detach, the plates were tapped to release the majority of cells from the culture surface; the trypsinization reaction was terminated by the addition to each well of Trypsin Neutralising Solution at RT, at a volume equal to that of the trypsin-EDTA in the well; the detached cells were transferred to a sterile 25 ml centrifuge tube; the plates were rinsed with HBSS to collect residual cells, and this rinse was added to the centrifuge tube; the harvested cells were spun at 220 *g* for 5 min (using centrifuge model CR422, Jouan, France) to form a cell pellet; to this pellet 4 to 5 ml of EGM culture medium was added, and the cells were counted using a haemocytometer (Neubauer, Germany); volumes of EGM were then adjusted so that cells could be re-seeded at 2500 cells/cm^2. The number of cumulative population doublings (CPDs) prior to each passage was calculated from cell counts, employing the formula CPD = $\log_2$ ([number of cells harvested] / [number of cells seeded x attachment efficiency]).

2.2.2.2 Establishment of rabbit VSMC cultures

VSMCs were obtained from the thoracic aortas of New Zealand White (NZW) rabbits by the explant technique [Stavri *et al.* 1995, Southgate and Newby 1990, McMurray *et al.* 1991]. An adult male NZW rabbit (Charles River UK Ltd, Kent, UK) was killed by an intravenous overdose (280 mg/kg) of sodium pentobarbital, and the aorta (from the level of the aortic arch to the origins of the renal arteries) was surgically removed using an aseptic and non-traumatic technique. The aorta was placed in the dissecting medium for rabbit aortas (detailed above) in a sterile tissue culture plate. The procedure was then continued in a tissue culture room under a Class II tissue culture hood. Extraneous adventitial tissue was removed using a scalpel, and the vessel was pinned, luminal side up, to a layer of set Sylgard™ encapsulating resin (prepared using the 184 Elastomer kit, BDH, following the manufacturer's instructions). The aortic endothelium was then removed by gentle abrasion with a cell scraper. Squares of media (approximately 1 cm x 1 cm) were cut using a scalpel and forceps. These

squares were divided into regular 1 mm squares using a McIlwain tissue chopper (Mickle Lab Engineering Co. Ltd, UK).

The resultant explants were washed three times in VSMC culture medium, and plated into 100 mm tissue culture plates. Each explant was incubated with 1 ml of VSMC culture medium overnight at 37°C under 5% CO_2/95% air. To those wells where the medial explants had successfully attached to the underlying plastic of the plate, 10 ml of VSMC culture medium were added, and the explants were incubated for a further seven to fourteen days in the tissue culture incubator, until the cultures were semi-confluent. The cell cultures were then trypsinized: the plates were washed three times with Versene at 37°C; 2 ml of trypsin-EDTA for VSMCs was added to each plate, and the plates were agitated for 5 min at RT; the reaction was terminated by the addition to each plate of 10 ml of VSMC culture medium; the cells were then pipetted into a large tissue culture flask. The cells were counted with a haemocytometer, and diluted with VSMC culture medium to give a final concentration of approximately 50,000 cells per ml. The cells were seeded into new 100 mm tissue culture plates at a density of approximately 5 x 10^5 cells / plate. These cells usually re-attached after six to eight hours. After two days (by which time the seeded cells had begun to proliferate), the culture medium was replaced, in order to remove any residual explants carried over with trypsinization, and to remove dead cells. The cultures usually reached confluence four to five days after plating. Cultures were then trypsinized again and serially passaged.

All staining experiments were carried out on confluent cells.

2.2.2.3 Staining of cell cultures for β-galactosidase activity

Cultures of either HUVECs or rabbit VSMCs were washed twice in PBS, and fixed for 3 min at RT with 3% PFA in PBS. After two washes in PBS, cells were incubated for 24 h in X-Gal working solution at 37°C, titrated to either pH 4.0 (for acid β-gal activity) or pH 6.0 (for SA-β-gal) as specified in each experiment described. Following the incubation, cells were washed once in double-distilled water (DDW), dehydrated by passing through graded ethanol solutions (1 min in each of 75, 95 and 100% ethanol solutions), and then air-dried. Cells were viewed under phase contrast or bright-field illumination, using an Axiovert 25 CFL inverted microscope (Carl Zeiss, Germany). SA-β-gal staining was quantified by manual counting: each tissue culture

dish was divided into quarters, and 125 cells were counted in each quarter using a cell counter; the percentage of these 500 cells containing blue precipitate was then calculated. Representative fields were photographed under the inverted microscope, using Kodak Ektachrome 64T colour positive film. In some cases, cultured cells were photographed directly in X-Gal working solution.

2.2.2.4 SA-β-gal and CD31 double-staining

Ethanol-dehydrated SA-β-gal-stained HUVECs were incubated in a humidified chamber at RT for 30 min in a 1:20 dilution of mouse anti-CD31 monoclonal antibody (MoAb) in TBS. Parallel cultures were incubated in an equivalent concentration of isotype-matched (IgG_1) mouse anti-*A. niger* glucose oxidase MoAb, clone DAK-GO1. Cultures were then washed three times in TBS before a 30 min incubation with a 1:20 dilution of alkaline phosphatase-conjugated goat anti-mouse immunoglobulin. After three further washes in TBS, phosphatase activity was visualized using the Dako New Fuchsin Chromogenic Substrate System, according the manufacturer's instructions: equal volumes of the chromogen and an activating solution were mixed together, along with buffered substrate, and with levamisole, an inhibitor of endogenous alkaline phosphatase activity; the cultures were incubated for 5 min in darkness with the resulting substrate solution. This solution was removed, and the cells were washed three times in TBS. The cells were mounted under coverslips using the aqueous mountant Glycergel™. The cells were viewed under bright-field illumination, and photographed as described in the previous paragraph.

2.2.3 Studies of cell senescence in rabbit carotid arteries

2.2.3.1 Acquisition and maintenance of rabbits

Male NZW rabbits weighing between 2.5 and 3.0 kg were obtained from Charles River UK Ltd. These rabbits were between sixteen and seventeen weeks old. Rabbits were delivered to UCL one week prior to the first planned experimental procedure, to allow them time to acclimatize to their new environment. They were housed and maintained in standard conditions: rabbits were housed in individual cages, under temperature control (16 to 20°C) and under a 12-hour light/dark cycle. A standard diet (Special Diet Services guinea pig breeder and maintenance diet, 'RGP', detailed above), containing 3.3% fat by weight, was provided *ad libitum*, as was drinking water.

2.2.3.2 Denudation of rabbit carotid arteries

Prior to each denudation procedure, each rabbit was weighed to allow calculation of appropriate anaesthetic doses. Fentanyl/fluanisone was given intramuscularly at a dose of 0.3 ml/kg. Diazepam (2 mg/kg) was then administered intravenously via the marginal ear vein, while the respiratory rate of the rabbit was observed for evidence of excessive respiratory depression. Where necessary, anaesthesia was 'topped up' by giving a further 0.1 ml/kg of fentanyl/fluanisone after 45 min. Enrofloxacin (10 mg/kg) was administered subcutaneously as prophylaxis against infection.

The depth of anaesthesia was judged by assessing the pupillary light reflex, and the withdrawal response to gentle pinching of the rabbit paw. When the rabbit was fully anaesthetized, it was placed supine on an operating table, and its neck was shaved to reduce the risk of wound contamination. The rabbit was covered with surgical drapes, and kept warm by use of a heated pad below the animal. The animal's arterial oxygen saturation and pulse rate were monitored at five-minute intervals using a pulse oxymeter (IMS, UK) attached to a hind-paw.

All surgery was performed using aseptic technique. A midline incision (approximately 3 cm in length) was made in the rabbit's neck using a scalpel, and the subcutaneous tissues were divided by blunt dissection. The longitudinal strap muscles were incised in the midline to expose the trachea. The right and left common carotid arteries were identified, exposed, and held in silastic slings, taking care to minimize handling of the vessels. The right common carotid artery was gently clamped, and an arteriotomy was made in the vessel using an ophthalmic 'beaver blade', distal to the clamp. A deflated embolectomy catheter (size 2F) (Mantis Surgical Ltd, UK) was inserted via the arteriotomy, and passed 5 cm distally (i.e. cephalically) along the arterial lumen. The balloon of the catheter was then inflated using 0.5 ml of normal saline, and smoothly withdrawn towards the arteriotomy site. When the balloon became visible at the arteriotomy site, it was deflated, re-advanced 5 cm cephalically, re-inflated, and withdrawn again to the arteriotomy site. The deflation, advance, inflation and withdrawal sequence was performed for a third time, before the balloon was finally withdrawn entirely from the artery. While the artery was held under tension using the silastic sling, the arteriotomy incision was closed using a 6/0 proline stitch. The left common carotid artery was then raised from the surrounding tissue in its silastic sling, and the external surface of the artery was gently manipulated with a pair of surgical

forceps, to an extent deemed equivalent to the earlier external manipulation of the right common carotid artery. The silastic slings around each carotid artery were removed, and both common carotid arteries were observed for a few seconds, to check for the presence of pulsatile flow. Muscle and fat layers were then surgically closed using 3/0 vicryl, and the skin was closed using a subcuticular suture.

The rabbit was given buprenorphine (0.3 mg/kg) subcutaneously for post-operative analgesia. The rabbit was then allowed to recover spontaneously from anaesthesia, with fresh bedding in its cage. The animal would usually wake within 30 min of the procedure, and start eating and drinking within an hour.

As will be described in Chapter Three, the denudation procedure described here was performed either once, or on two separate occasions separated by a six-week interval. For each animal both carotid arteries were harvested six weeks after the final denudation procedure had been performed.

2.2.3.3 Harvesting of rabbit carotid arteries

Each rabbit was prepared for surgery and anaesthetized as described in the above section. Once the animal was fully anaesthetized, its neck and thorax were opened surgically via a midline incision, in order to expose the carotid arteries, the heart and the great vessels. The common carotid arteries were identified, and a silastic sling placed around each. Sodium pentobarbital was then given intravenously at a lethal dose (280 mg/kg). The descending thoracic aorta was immediately clamped, and 50 ml of PBS (pH 7.4) was injected into the left ventricle of the heart, using a syringe and a wide-bore needle. This was immediately followed by the injection of 500 ml of 2% PFA in PBS at RT, which was injected into the left ventricle over a 20 min period, using 50 ml syringes. After the first 50 ml of PFA had been injected, the inferior vena cava was divided with a scalpel, to allow excess fluid to be released from the vasculature. When the entire 500 ml of fixative had been injected, the arteriotomy site in the right common carotid artery was identified (by identifying the 6/0 proline suture used for its closure), and the 5 cm portion of artery distal to this site was excised with a scalpel. The equivalent portion of the left common carotid artery was also excised.

2.2.3.4 Processing of rabbit carotid arteries, and staining for β-gal activity

The subsequent processing of the harvested carotid arteries is illustrated in Figure 2.1 overleaf.

Figure 2.1 Processing of excised rabbit carotid arteries

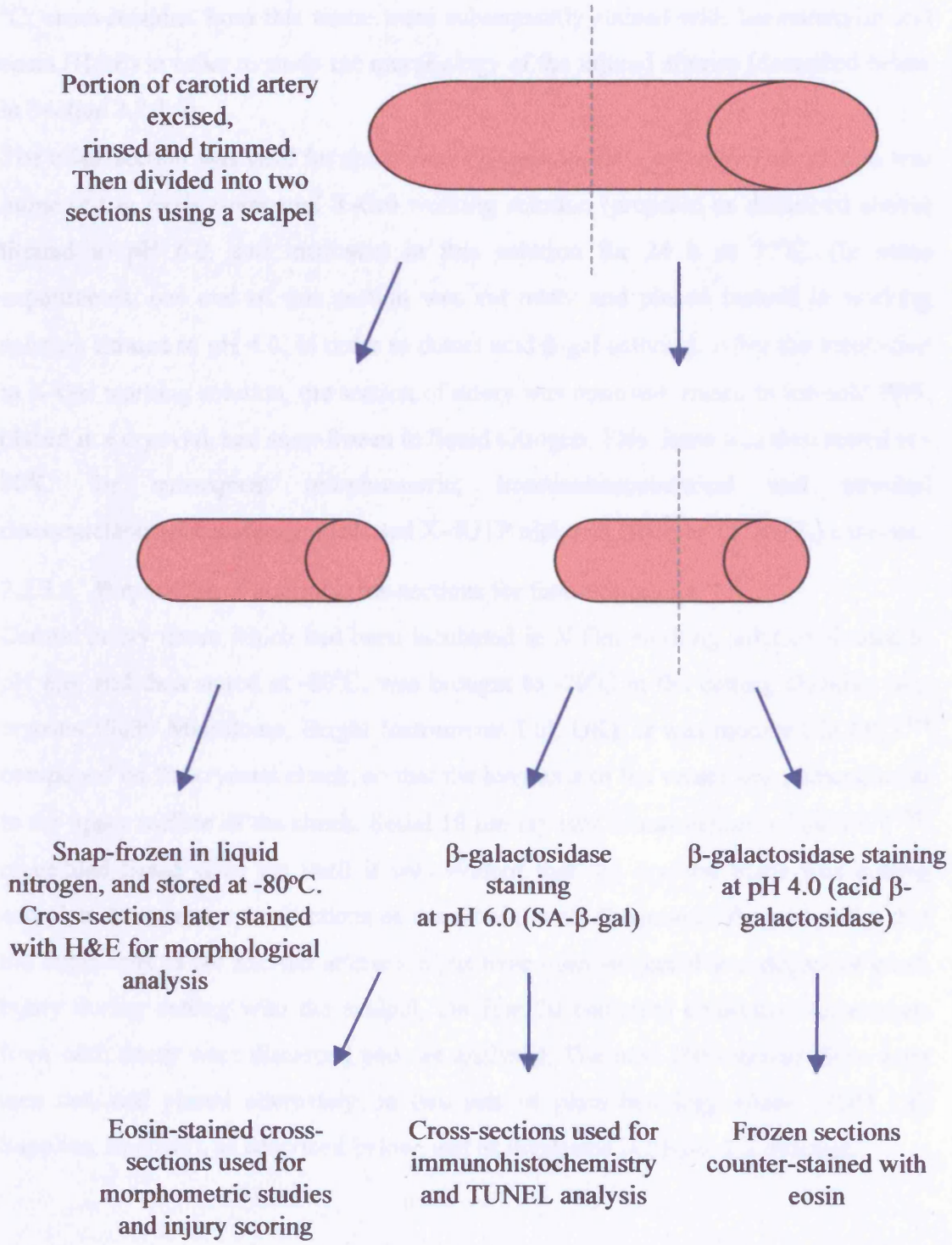

The excised portion of each artery was trimmed of excess peri-adventitial fat using a scalpel and forceps, and rinsed in ice-cold PBS. This tissue was then divided transversely into two sections of approximately equal length using a scalpel.

One section was placed in a cryovial, snap-frozen in liquid nitrogen, and stored at -80 °C; cross-sections from this tissue were subsequently stained with haematoxylin and eosin (H&E) in order to study the morphology of the injured arteries (described below in Section 2.2.3.6).

The other section was used for detection of β-galactosidase activity. This section was immersed in freshly-prepared X-Gal working solution (prepared as described above) titrated to pH 6.0, and incubated in this solution for 24 h at 37°C. (In some experiments, one end of this section was cut away and placed instead in working solution titrated to pH 4.0, in order to detect acid β-gal activity). After the incubation in X-Gal working solution, the section of artery was removed, rinsed in ice-cold PBS, placed in a cryovial, and snap-frozen in liquid nitrogen. This tissue was then stored at -80°C for subsequent morphometric, immunohistochemical and terminal deoxynucleotidyl transferase-mediated X-dUTP nick end labelling (TUNEL) analysis.

2.2.3.5 Preparation of arterial cross-sections for further analysis

Carotid artery tissue which had been incubated in X-Gal working solution titrated to pH 6.0, and then stored at -80°C, was brought to -20°C in the cutting chamber of a cryostat (5030 Microtome, Bright Instruments Ltd, UK). It was mounted in OCT™ compound on the cryostat chuck, so that the long-axis of the vessel was perpendicular to the upper surface of the chuck. Serial 10 μm cryostat cross-sections of the OCT™-embedded tissue were cut until it was evident that the cryostat blade was cutting complete transverse cross-sections of the arterial wall. Because of the possibility that the outer ends of the excised arteries might have been subjected to a degree of crush injury during cutting with the scalpel, the first 20 complete cryostat cross-sections from each artery were discarded and not analysed. The next 100 cross-sections were then cut, and placed alternately on two sets of plain histology slides (BDH Lab Supplies, England), as described below, and as illustrated in Figure 2.2 overleaf.

Figure 2.2 Preparation of rabbit carotid artery cross-sections

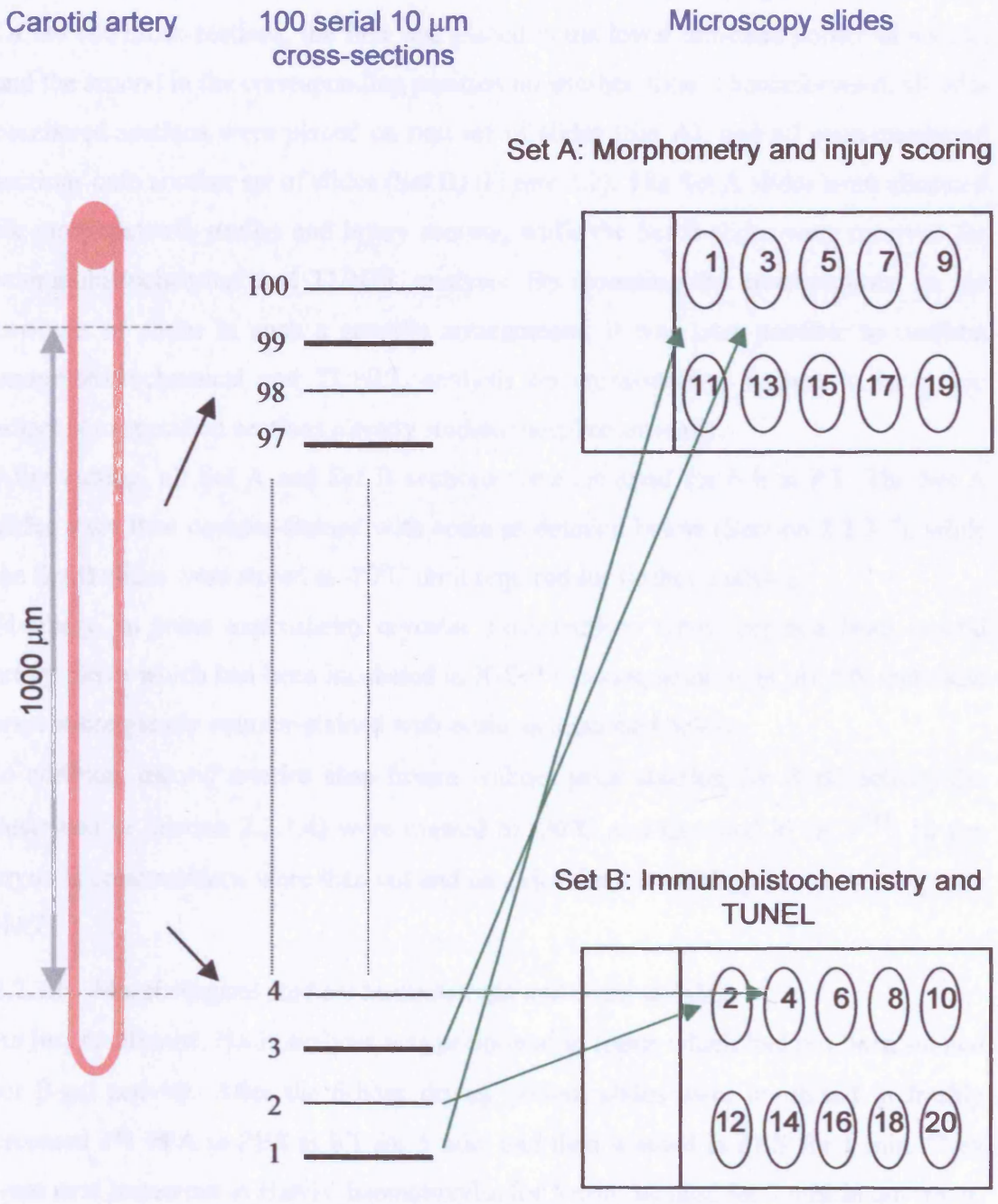

Figure 2.2 One hundred 10 µm cryostat cross-sections were cut from each rabbit carotid artery. Serial cross-sections were distributed onto Set A and Set B slides as illustrated.

Prior to use, these slides had been pre-treated with VECTABOND™ reagent to improve tissue adhesion: slides were immersed in acetone for 5 min at RT, then in 350 ml of acetone containing 7 ml of VECTABOND™ for a further 5 min at RT; they were then washed in water for 30 seconds and left to air-dry overnight.

Of the 100 cross-sections, the first was placed in the lower left-hand corner of a slide, and the second in the corresponding position on another slide. Thenceforward, all odd-numbered sections were placed on one set of slides (Set A), and all even-numbered sections onto another set of slides (Set B) (Figure 2.2). The Set A slides were allocated for morphometric studies and injury scoring, while the Set B slides were reserved for immunohistochemical and TUNEL analysis. By mounting the cross-sections on the two sets of slides in such a specific arrangement, it was later possible to perform immunohistochemical and TUNEL analysis on cross-sections known to have lain adjacent to specified sections already studied morphometrically.

After cutting, all Set A and Set B sections were air-dried for 6 h at RT. The Set A slides were then counter-stained with eosin as detailed below (Section 2.2.3.7), while the Set B slides were stored at -80°C until required for further analysis.

Similarly, in some experiments cryostat cross-sections were prepared from carotid artery tissue which had been incubated in X-Gal working solution at pH 4.0, and these were subsequently counter-stained with eosin as described below.

In addition, carotid arteries snap-frozen without prior staining for β-gal activity (as described in Section 2.2.3.4) were thawed to -20°C and mounted in OCT™; 10 μm cryostat cross-sections were then cut and air-dried for 6 h at RT, prior to staining with H&E.

2.2.3.6 Morphological studies: haematoxylin and eosin staining

As just mentioned, H&E analysis was performed in tissue which had not been stained for β-gal activity. After the 6-hour drying period, slides were immersed in freshly prepared 3% PFA in PBS at RT for 5 min, and then washed in PBS for 1 min. They were next immersed in Harris' haematoxylin for 5 min, washed for 3 min in tap water, differentiated for 6 sec in 1% acid alcohol, then immersed in Scott's tap water for 1 min. The slides were then immersed in eosin solution for 5 min, washed in tap water for 1 min, then passaged through graded ethanol solutions (15 sec in 70%, 30 sec in 100%, then a further 30 sec in 100% ethanol). They were next immersed for 1 min in

xylene, and then re-immersed in fresh xylene for a further 1 min. The sections on the slides were mounted under coverslips in the synthetic resinous mountant DPX.

Slides were viewed under bright-field illumination using an Axiophot 2 microscope (Carl Zeiss, Germany) and were photographed with Kodak Ektachrome 160T colour positive film.

2.2.3.7 Morphometric studies: injury scores, neointima formation and SA-β-gal staining

After the 6-hour drying period mentioned above (Section 2.2.3.5), the slides for morphometric analysis and injury scoring (Set A) were immersed in freshly prepared 3% PFA in PBS at RT for 5 min, rinsed in PBS for 1 min, then immersed in eosin solution for 5 min. They were next washed in tap water for 1 min, then passaged through graded ethanol solutions and xylene as described in the previous paragraph. Sections were again mounted using DPX. Representative sections were viewed and photographed as described for H&E sections.

For each carotid artery, ten cross-sections which would originally have been spaced at 100 μm intervals along the intact vessel were analysed morphometrically (i.e. sections 1, 11, 21, 31 *etc.*). In cases where a section designated to be analysed was either torn or folded, the next intact section was used instead.

These ten cross-sections from each carotid artery were studied using a JVC TK-1281 colour video camera connected to a Nikon LABOPHOT-2 microscope. Morphometric analysis of the cross-sections was performed using a computerized colour image analysis software system (LUCIA M, Version 3.52a, Laboratory Imaging Limited, Czech Republic). The ten cross-sections were analysed for the extent of neointima formation and SA-β-gal staining, and statistical analysis was used to compare the control and treatment groups (as described below).

Injury scores

Cross-sections were scored for the degree of injury using a scoring system devised by Schwartz *et al.* [1992], and adapted by Burchenal *et al.* [1996] for the study of rabbit arteries subjected to balloon angioplasty. According to this system, Grade 0 refers to vessels showing an intact internal elastic lamina (IEL), media and external elastic lamina (EEL). Grade 1 refers to a vessel in which the IEL is lacerated, but without damage to the media or EEL. Grade 2 injury involves disruption of the media, and

Grade 3 injury involves laceration of the EEL. Of the ten cross-sections from each vessel analysed morphometrically, that with the highest neointima/media ratio (assessed as described below) was re-examined under the Nikon microscope, and scored for the extent of injury exhibited; this score was used as the injury score for that vessel.

Neointima formation

Lucia M software (as detailed above) was used to measure the cross-sectional areas bounded by the EEL, the IEL, and the luminal surface of the vessel. The medial cross-sectional area was derived by subtracting the area bounded by the IEL from that bounded by the EEL, while the intimal area was derived by subtracting the luminal area from the area bounded by the IEL. These areas were then used to calculate an intima/media ratio for each cross-section.

This analysis was performed on each of the ten cross-sections from each vessel, and from the ten resultant ratios, a mean intima/media ratio was calculated for that artery. These mean intima/media ratios for each artery were then used to derive mean intima/media ratios for each treatment group of arteries.

While, strictly speaking, the term 'intima' refers to the cell layers within the IEL of uninjured arteries, and the 'neointima' comprises the new cell layers which appear within the IEL following injury to the vessel, in situations where control and denuded vessels are being compared in this thesis, the term 'intima' has often been used to refer to either intimal or neointimal cell layers. Thus, for example, the terms 'intimal thickening' and 'neointima formation' have been used essentially interchangeably.

SA-β-gal staining

The ten Set A cross-sections mentioned above (sections 1, 11, 21, 31 *etc.*) were re-analysed, again using the Lucia M system, to determine the cross-sectional area covered by cells which had developed a blue stain in the X-Gal working solution. Scores of the intimal and medial areas covered by blue cells were made in each cross-section, and these were divided by the intimal and medial cross-sectional areas, respectively, in that cross-section. The resultant fractions were referred to as 'blue/intima' and 'blue/media' respectively. The ten blue/intima and ten blue/media scores were each averaged, to give mean blue/intima and blue/media scores for that

vessel, and were expressed as percentages. These mean percentage areas for each vessel were then used to derive mean percentage areas for each treatment group.

Because blue cells in the adventitia were very sparse, it was possible to perform a count of the number of blue cells in each adventitial cross-section. Again, these counts were averaged in the ten cross-sections per vessel, to give a mean count for that vessel. The counts for each vessel were then used to derive mean counts for each treatment group of rabbits.

Representative examples of β-galactosidase staining were photographed under bright-field illumination using an Axiophot 2 microscope (Carl Zeiss, Germany) and were photographed with Kodak Ektachrome 160T colour positive film.

2.2.3.8 Statistical analysis

(Neo)intima/media ratios were compared statistically using a nested analysis of variance (ANOVA) model, following logarithmic transformation of the data. Nested analysis was required since each animal contributed arteries to more than one group (i.e. to 'control' and 'single', or to 'control' and 'double' groups). Given the low *n* numbers in each group, normal distributions of data cannot be guaranteed, even after log transformation, so *P* values were re-calculated using the non-parametric Wilcoxon rank sum test. The blue/neointima and blue/media percentage areas were compared between the control and single-denudation groups using the Wilcoxon rank sum test, while comparison of these percentage areas between the single- and double-denudation groups was initially performed using ANOVA following log transformation of the data, then re-calculated using the Wilcoxon rank sum test. Statistical analysis was performed using the Intercooled Stata software package (release 6.0), and a value of $P < 0.05$ was considered statistically significant.

2.2.3.9 Immunohistochemistry

Common features of the immunohistochemical protocols used

Immunohistochemical analysis was performed on cross-sections selected from Set B slides from each artery. As mentioned above, these sections had been cut on a cryostat, air-dried for 6 h, then stored at -80°C.

When required, frozen sections were thawed to RT, and circumscribed using a Dako 'Pen for Immunohistochemistry', which contains a material which is water-repellent, and acetone- and alcohol-insoluble. The use of this pen minimizes the volume of

antibody solutions required, as it prevents solution from dispersing away from the tissue section.

All immunohistochemistry involving rabbit arterial cross-sections was performed using mouse monoclonal primary antibodies, following a 30-minute incubation with Dako serum-free protein-blocking agent at RT. In all these studies, a biotinylated $F(Ab')_2$ fragment of rabbit anti-mouse antibody diluted in TBS was used as the secondary agent, and this was in turn detected using streptavidin conjugated with either horseradish peroxidase (HRP) or alkaline phosphatase (ALP), diluted in TBS. Chromogenic substrates were used as tertiary agents to visualize the relevant enzyme activity (see below).

All primary and secondary antibodies were spun at 4000 *g* for 15 min at 4°C (using centrifuge model Mikro 22R, Hettich Zentrifugen, Germany) prior to use, and were diluted as specified in the following paragraphs using TBS. After incubation with each primary, secondary and tertiary agent, slides were washed three times in TBS at 4°C (5 min per wash).

All incubations with primary, secondary and tertiary agents, and with the protein-blocking agent, were performed in a humidified chamber at RT. Incubations with the chromogenic substrates were performed in darkness. After mounting with coverslips, slides were viewed and photographed as described for H&E sections.

The detailed protocols for detection of the various cell types are described below, and are summarized in Table 2.1 overleaf.

Identification of endothelial cells

After thawing of stored tissue cross-sections to RT, slides were immersed in acetone at 4°C for 20 min, then washed three times in TBS. The slides were then treated with 0.6% hydrogen peroxide in TBS at 4°C for 10 min, and subsequently washed three times in TBS at 4°C (5 min per wash). Slides were placed in a humidified chamber, and each cross-section was covered with serum-free protein-blocking agent. After a 30-minute incubation at RT, the protein-blocking solution was removed, and replaced with a 1:20 dilution of mouse anti-CD31 (clone JC/70A), using approximately 250 µl of diluted antibody per section. Parallel sections were covered with a solution of mouse anti-*A. niger* glucose oxidase IgG_1 at an equivalent antibody concentration to the primary antibody, to act as a negative control.

Table 2.1 Summary of immunohistochemistry protocols used in rabbit carotid artery model

Cell type	Fixation	Pre-treatment	Primary Ab, dilution, incubation time	Negative control isotype	Secondary agent dilution, incubation time	Tertiary agent, dilution, incubation time	Chromogen, incubation time
ECs	Acetone, 20 min, 4°C	0.6% HP in TBS, 10 min, 4°C	Anti-CD31, 1:20, 30 min	IgG_1	1:600, 30 min	Str- HRP, 1:500, 30 min	DAB, 10 min
VSMCs	Acetone 20 min, 4°C	N/A	Anti-SM α-actin, 1:100, 30 min	IgG_{2a}	1:300, 30 min	Str-ALP, 1:100, 30 min	Fuchsin, 20 min
Leukocytes, including T cells and monocytes / macrophages	Acetone, 20 min, 4°C	N/A	Anti-CD45, 1:50, 30 min	IgG_1	1:300, 30 min	Str-ALP, 1:100, 30 min	Fuchsin, 20 min
Proliferating cells	4% PFA in TBS for 2 min, then 100% ethanol for 10 min, all at RT	0.6% HP in TBS, 10 min, 4°C	Anti-PCNA, 1:50, 30 min	IgG_{2a}	1:300, 30 min	Str- HRP, 1:500, 30 min	DAB, 10 min

Table 2.1 The table shows the main differences between the immunohistochemical staining protocols used in the rabbit carotid artery denudation model. Abbreviations used: Ab = antibody, DAB = diaminobenzidine, ECs = endothelial cells, HP = hydrogen peroxide, N/A = not applicable, PCNA = proliferating cell nuclear antigen, PFA = paraformaldehyde, SM = smooth muscle, Str-ALP = streptavidin-conjugated alkaline phosphatase, Str-HRP = streptavidin-conjugated horseradish peroxidase, TBS = Tris-buffered saline, VSMCs = vascular smooth muscle cells.

The sections were incubated with the respective antibody for 30 min at RT. The primary antibody (or negative control) was removed, and the slides were washed three times in TBS. Each section was then covered with approximately 250 µl of a 1:600 dilution of biotinylated $F(Ab')_2$ fragment of rabbit anti-mouse antibody. Sections were again incubated in the humidified chamber for 30 min at RT. The secondary agent was removed, and the slides were washed three times in TBS. Sections were then covered with approximately 250 µl of streptavidin-conjugated HRP (Str-HRP), diluted 1:500 in TBS. Slides were incubated for 30 min at RT in the humidified chamber. The tertiary agent was removed, and the slides were washed three times in TBS. Peroxidase activity was visualized using the Liquid DAB Plus kit (Dako Ltd) according to the manufacturer's instructions: one drop of diaminobenzidine (DAB) chromogen was added to 1 ml of buffered substrate, and mixed; the mixture was then used to cover each of the sections to be studied. Slides were incubated in this solution in the humidified chamber for 10 min at RT, in darkness. They were then washed three times in TBS at 4°C (5 min per wash), and sections were mounted under coverslips using Glycergel™.

Identification of vascular smooth muscle cells

VSMCs were detected using a protocol similar to that employed for ECs (Table 2.1). Thawed sections were fixed in acetone and washed three times in TBS as just described, but without the need for subsequent treatment with hydrogen peroxide. Instead, after the TBS washes, the sections were blocked for 30 min with serum-free protein-blocking agent. A 1:100 dilution of mouse anti-smooth muscle α-actin (clone 1A4) was used as the primary antibody, parallel sections being covered with an equivalent antibody concentration of mouse anti-*A. niger* glucose oxidase IgG_{2a} as a negative control. Following incubation in the primary antibody for 30 min at RT, and after three washes in TBS, the sections were covered with a 1:300 dilution of biotinylated $F(Ab')_2$ fragment of rabbit anti-mouse antibody, and incubated with this for 30 min. The secondary agent was removed, and the slides were washed in TBS. Sections were then covered with streptavidin-conjugated alkaline phosphatase (Str-ALP) diluted 1:100 in TBS, and incubated for 30 min at RT. The tertiary agent was removed, and the slides were again washed in TBS. Sections were then covered with Dako New Fuchsin Chromogenic Substrate System solution and levamisole (prepared as described previously (Section 2.2.2.4)). Slides were incubated for 20 min at RT in

darkness. They were then washed three times in TBS at 4°C, and mounted with coverslips, using Glycergel™.

Identification of leukocytes (including monocyte/macrophages and T cells)

The protocol for detection of leukocytes was the same as for the detection of VSMCs, except for the following variations: the primary antibody used was mouse anti-CD45 (clone L12/201), used at a dilution of 1:50, and mouse anti-*A. niger* glucose oxidase IgG_1 was used as the negative control. The secondary agent and the Str-ALP dilutions were as described for smooth muscle α-actin detection, as were the methods of enzyme visualization and mounting of the slides.

Detection of proliferating cells

Proliferating cells were identified using a murine antibody to PCNA (clone PC10). The protocol was similar to that used for the detection of ECs, with the following specific differences. Thawed slides were initially immersed in 4% PFA in TBS at RT for 2 min, then in 100% ethanol at RT for 10 min. Slides were next washed three times in TBS at 4°C, before proceeding through the hydrogen peroxide and protein blocking stages as described for ECs. The anti-PCNA antibody was used at a dilution of 1:50 in TBS. The secondary agent was used at a dilution of 1:300, and the Str-HRP at a dilution of 1:500. Mouse anti-*A. niger* glucose oxidase IgG_{2a} was used as the negative control. As with the ECs, the Liquid DAB Plus kit was used for enzyme visualization.

2.2.3.10 Detection of apoptotic cells

Studies to detect apoptosis were performed on cross-sections selected from the remaining slides of Set B from each artery. Apoptotic cells were detected using TUNEL analysis, employing an '*In Situ* Cell Death Detection Kit' (Boehringer Mannheim) according to the manufacturer's instructions.

Frozen sections were thawed to RT, and then immersed in 4% PFA in PBS at RT for 1 h. After three ten-minute washes in PBS at RT, slides were immersed in 0.1% Triton X-100/0.1% sodium citrate for 2 min at 4°C. After a further three 10-minute washes in PBS at RT, cross-sections were covered with 50 µl of TUNEL staining solution, containing terminal deoxynucleotidyl transferase (TdT) and fluorescein-conjugated deoxyuracil triphosphate (dUTP), and were incubated with this solution in a humidified chamber for one hour at 37°C. After three further 10-minute washes in PBS at RT, the sections were covered with a solution of 4',6-diamidino-2-

phenylindole (DAPI) in Vectashield™ mounting medium for fluorescence detection (Vector Laboratories). The sections were then examined by fluorescence microscopy using an Axiophot 2 microscope fitted with a X63/1.4 numerical aperture Plan Apochromat objective, and fluorescence filter sets appropriate for fluorescein and DAPI (Carl Zeiss, Germany). The sections were also observed under bright-field illumination. Bright field and epifluorescence images were photographed with Kodak Ektachrome 400X colour reversible film. Sections processed with labelling solution without TdT were used as negative controls. Rabbit aortic VSMCs treated with 2 μM staurosporine overnight were used as positive controls.

2.2.3.11 Protocols tested during development of *ex vivo* SA-β-gal assay

In the development of the protocol described above for the detection of endogenous β-gal activity in *ex vivo* rabbit carotid arteries, various preliminary protocols were tested. For these experiments, all β-gal staining was performed at pH 4.0, since this would be expected to detect lysosomal acid β-galactosidase activity in all layers of the vessel wall, regardless of the replicative age of the cells.

Two protocols used in pilot studies are illustrated in Figure 2.3 overleaf, together with the final protocol adopted for the actual SA-β-gal experiments (as described in detail above, in Sections 2.2.3.4, 2.2.3.5 and 2.2.3.6).

Protocol 1

This protocol was similar to that described by Dimri *et al.* for use with human skin samples [Dimri *et al.* 1995]. A rabbit which had had no previous surgery was culled by administration of a lethal dose of sodium pentobarbital, as described above. Its carotid arteries were excised without prior perfusion fixation. After trimming of excess peri-adventitial tissue with a scalpel, the arteries were briefly rinsed in PBS, then snap-frozen in cryovials in liquid nitrogen. The frozen arteries were mounted in OCT™, and transverse 7 μm cross-sections were cut on a cryostat and placed on histology slides. After air-drying for 2 h, these sections were fixed with 1% PFA in PBS at RT for 1 min, and then washed twice (30 sec per wash) in PBS at RT. The slides were then immersed in X-Gal working solution at pH 4.0 for 36 h at 37°C.

Figure 2.3 Protocols used for detection of β-galactosidase activity in excised rabbit carotid arteries

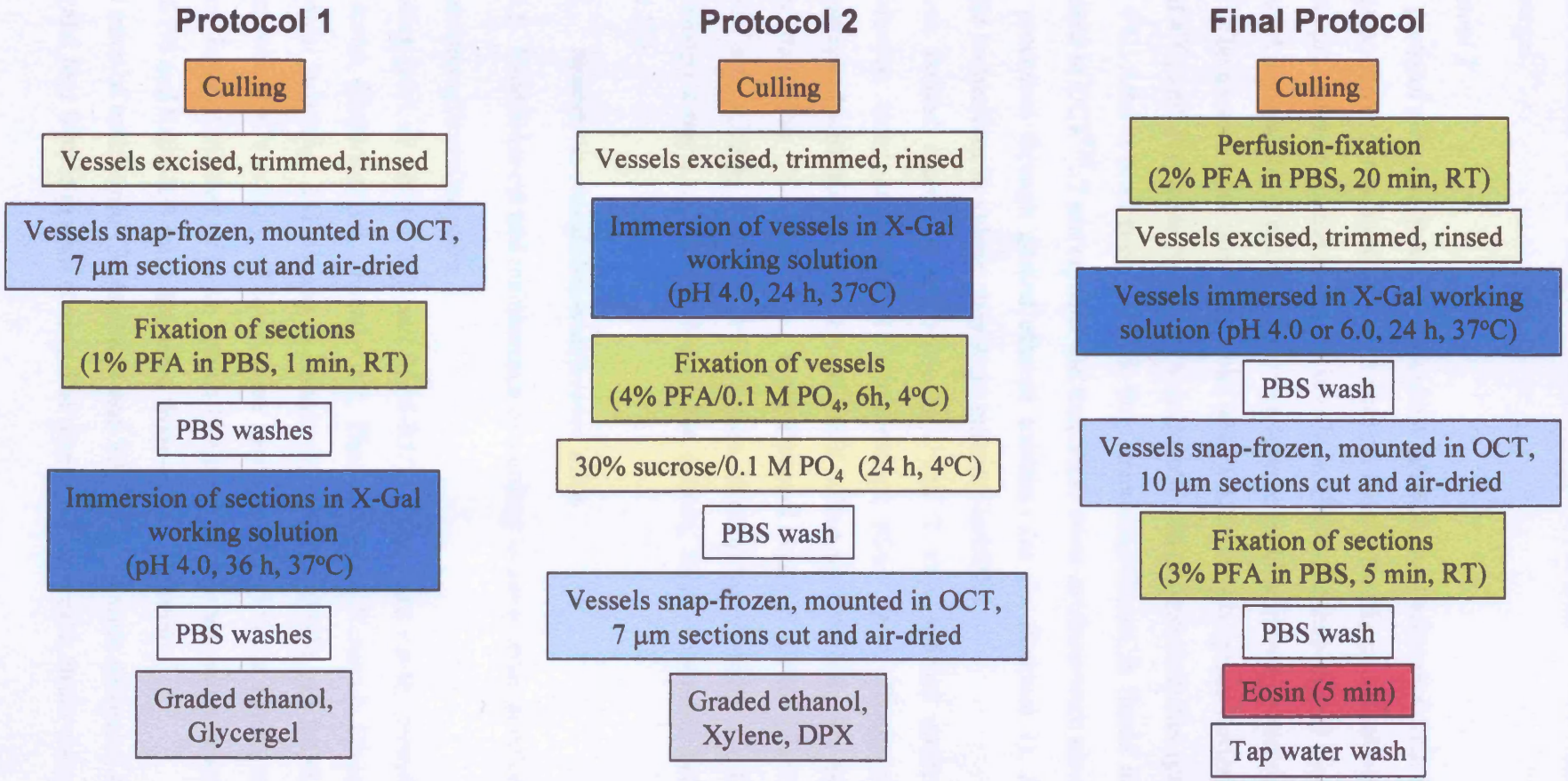

Figure 2.3 Protocol 1 involved immersion of cryostat cross-sections in X-Gal working solution, while in Protocol 2 and the Final Protocol lengths of carotid artery were immersed *in toto* in this solution. The most significant change between Protocol 2 and the Final Protocol was the introduction of perfusion fixation.

After three 5-minute washes in PBS at RT, the slides were passaged through graded ethanol solutions (1 min each in 50%, 70% and 100% ethanol) and then mounted in Glycergel™.

Protocol 2

This protocol was also tested using carotid arteries from animals which had not been perfusion-fixed. Carotid arteries were excised from a freshly culled rabbit, trimmed of excess peri-adventitial tissue, rinsed briefly in PBS, and then placed directly into X-Gal working solution at pH 4.0. The vessels were incubated in this solution for 24 h at 37°C. The arteries were then fixed with 4% PFA/0.1 M phosphate buffer (pH 7.4) for 6 h at 4°C, and next immersed in 30% sucrose/0.1 M phosphate buffer (pH 7.4) for 24 h at 4°C. After a brief rinse in PBS, they were snap-frozen in liquid nitrogen, then mounted in OCT™. 7 μm cryostat-cut transverse cross-sections were air-dried for 2 h, then processed through graded ethanol solutions (as for Protocol 1). After two 1-minute immersions in xylene, they were mounted in DPX.

Tissues stained according to Protocols 1 and 2 were viewed under bright-field illumination using an Axiophot 2 microscope (Carl Zeiss, Germany) and were photographed with Kodak Ektachrome 160T colour positive film. An example of an artery stained at pH 4 using the Final Protocol detailed earlier (Sections 2.2.3.4, 2.2.3.5 and 2.2.3.6, and Figure 2.3) was photographed under an Olympus-BX microscope using a charge-coupled device camera, both as detailed below (Section 2.2.4.12).

2.2.4 Studies in senescence-accelerated mice

2.2.4.1 Establishment and maintenance of a colony of senescence-accelerated mice

Acquisition of breeding pairs

Breeding pairs of SAM-P/8Ta and SAM-R1/Ta mice were kindly provided by Dr M Hosokawa (Experimental Animal Unit, Pharmaceutical Research Division, Takeda Chemical Industries Ltd, Japan) in January 1999. SAM-P/8Ta and SAM-R1/Ta mice are members of a colony of SAM mice maintained at Takeda Chemical Industries, Osaka, Japan. Colonies of these strains had been established using breeding pairs of SAM-P/8 and SAM-R/1 mice delivered from Kyoto University.

Nine mice of each strain (SAM-P/8Ta and SAM-R1/Ta) were delivered to UCL (five male and four female in each strain). The nine mice from each strain were litter-mates.

The SAM-P/8Ta mice were 14 weeks old, and the SAM-R/1Ta mice 16 weeks old, at the time of shipment. All mice were certified free from the following pathogens or diseases: salmonella species, corynebacterium kutscheri, pasteurella pneumotropica, mycoplasma pulmonis, sendai virus, mouse hepatitis virus, minute virus of mice, pneumonia virus of mice, reovirus III and tyzzer.

Housing conditions at UCL

The SAM colony was housed and maintained under standard conditions. After an initial isolation period following transportation from Japan, the breeding pairs were housed in filter racks, under temperature control (20 to 24°C) and under a 12-hour light/dark cycle. Drinking water was provided *ad libitum*. Unless otherwise stated, after weaning mice were fed *ad libitum* with a standard laboratory chow (Harlan Teklad mouse breeding and maintenance diet, TRM9607), which contained 4.3% fat by weight and 0.0023% cholesterol by weight.

The welfare of the mice was checked daily by a designated technician, and 24-hour veterinary cover was available. Since SAM mice are known to develop clinically significant pathologies, a table of clinical end-points was used to provide guidance for the day-to-day care of the colony (Table 2.2, overleaf). Mice were examined daily for any obvious signs of pain or distress, or for the emergence of any of the clinical end-points listed. If these were detected, a decision was made between the veterinary staff and the project licence holders concerning management of the problem, sometimes resorting to culling of affected animals to relieve suffering. In such cases, a Schedule 1 method of killing, as designated by the Animal (Scientific Procedures) Act 1986, was used.

Breeding programme

Six weeks after arrival at UCL, one male mouse from each strain was sacrificed and post-mortems were performed at the Royal Veterinary College, London, to confirm the disease-free status of the colony. The other eight mice in each strain were housed in separate brother-sister pairs, in four boxes. The colony was then allowed to breed, using exclusively brother-sister mating.

Table 2.2 Notice used by designated technicians in the management of the UCL colony of SAM mice

Clinical Sign	Appropriate Action
1. Persistent failure to feed 2. Persistently unresponsive 3. Suspected bone fracture 4. Corneal ulceration 5. Significant skin ulceration 6. Evidence of arthritis of a large joint	Schedule 1 culling
7. 15% decrease in body weight 8. Minor skin ulceration 9. Cataract formation 10. Significant decrease in stride length	Consult veterinary surgeon

Table 2.2 Mice were examined daily for signs of pain or distress, and for the emergence of any of the clinical end-points detailed. If these were found, the above table was used to guide further management. In the case of significant pain or distress, or if severe pathology was discovered, mice were culled without further consultation, using a Schedule 1 method (as designated by the Animal (Scientific Procedures) Act 1986. When less clinically significant pathology was detected, a decision was made between the veterinary staff and the project licence holders as to whether the pathology was likely to improve spontaneously or might improve with appropriate treatment. In cases where it was felt that deterioration was inevitable, mice were culled (using a Schedule 1 method) to avoid further suffering.

In order to preserve the senescent phenotype, new breeding pairs among the SAM-P mice were chosen from those mice that appeared to show most evidence of the ageing phenotype, using a previously described protocol [Hosokawa *et al.* 1997]; the main criteria used were small animal size, loss of fur glossiness, and lack of activity. Inevitably this meant that several of the SAM-P breeding pairs failed to produce litters. In contrast, breeding pairs of SAM-R mice were chosen from those mice that appeared the most healthy. In cases where a breeding pair failed to produce litters, mice were generally re-allocated to other brother-sister pairs in order to maintain the colony.

Litters were weaned at four weeks of age, the male and female offspring being housed in separate cages. In the case of larger litters, mice were further subdivided so that mice were usually housed with three to five animals per cage. Labels on each cage were used to record the date of birth, date of weaning, and dates of death and culling of the mice, together with a record of the emergence of any adverse clinical signs. The size of litters born to breeding pairs was also recorded.

Selected age-matched SAM-P and SAM-R mice were photographed in their cages in order to illustrate differences in size and phenotype between the two strains.

2.2.4.2 Acquisition and maintenance of C57BL/6 mice

A number of male and female C57BL/6 mice were purchased from Harlan UK Ltd, and were housed under identical conditions to those in which SAM mice were maintained. Unless otherwise stated, they were fed *ad libitum* with the same standard laboratory chow (TRM9607) used for SAM mice. Drinking water was again provided *ad libitum*. The C57BL/6 mice were twenty-three weeks old when delivered to UCL.

2.2.4.3 Administration of a Western-type diet

As will be described in Chapter Four, the effect of a relatively high cholesterol diet was assessed in SAM-P, SAM-R and C57BL/6 mice. For these studies a Western-type diet (Harlan Teklad Western Adjusted Calories Diet, TD88137) was employed. This diet is designed to contain the cholesterol and fat content equivalent to a human Western diet, and has been used in several previous studies [Nakashima *et al.* 1994, Palinski *et al.* 1995, Tangirala *et al.* 1995a and b]. It contains 21% fat by weight and 0.15% cholesterol by weight. It does not contain cholic acid. The diet is supplied by the manufacturer as a powder, because of its high fat content. In order to make it more

palatable to the mice, the powder was manually clumped together prior to administration. The diet was administered *ad libitum*, by daily re-stocking of a tray in each cage with excess quantities of the diet. The diet was stored at 4°C prior to stocking of the cages. Mice were weighed at regular intervals during the administration of the diet.

2.2.4.4 Preparation of serum from SAM mice

Prior to bleeding, mice were deprived of food for a 16-hour period. During this time, they had free access to drinking water. On the day of bleeding, mice were warmed to 35°C (for a maximum of 15 min) in a thermostatically heated warm-air chamber (IMS, UK). Venous blood was obtained by making a nick in the superficial tail vein using a scalpel. Approximately 200 µl of venous blood was collected in a V-shaped collecting tube (Microvette CB300, Sarstedt, UK) and immediately stored over ice, in order to inhibit lipoprotein lipase activity. The blood was allowed to clot over 3 h, and was then spun twice, each time at 1000 *g* for 15 min at 4°C (using centrifuge model Mikro 22R). Between the two spins, the blood clot was dispersed using a pipette tip, in order to maximize the yield of serum.

2.2.4.5 Measurement of total serum cholesterol and triglyceride levels in individual SAM mice

Total serum cholesterol

Total cholesterol levels in serum samples from individual mice were assayed using the INFINITY™ Cholesterol Reagent (Sigma Diagnostics, #401-25P). This reagent contains cholesterol oxidase (CO), cholesterol esterase (CE), HRP, 4-aminoantipyrine (4AAP) and hydroxybenzoic acid (HBA). In the presence of this reagent, cholesterol esters are hydrolysed by CE to cholesterol and free fatty acids. The free cholesterol, including that originally present, is oxidized by CO to cholest-4-en-3-one and hydrogen peroxide. The hydrogen peroxide then reacts with HBA and 4AAP, in the presence of HRP, to form a chromophore, quinoneimine dye. The formation of this chromophore can then be detected by its absorbance at 500 nm, and is proportional to the original concentration of cholesterol in the sample.

Serum samples were collected and prepared as described above, stored at -20°C, and individual samples were then analysed in batches. On the day of analysis, the frozen samples were thawed on ice to 4°C. For each sample, 3 µl of serum was added to 300

μl of INFINITY™ Cholesterol Reagent in a 96-well plate, at RT. The plate was incubated at 25°C for 15 min, and then read on a plate-reader (primary wavelength 500 nm, secondary wavelength 660 nm) (Spectra Max 250 plate reader, Molecular Devices Ltd, UK). Experiments were performed in triplicate, and mean concentrations calculated. The plate-reader was calibrated using the ACCUSET® Liquid Calibrator (Sigma Diagnostics) which has a general assigned value of total cholesterol, as measured enzymatically, of 173 mg/dl (4.48 mM). Cardiolipin controls (#C4571 and #C4696, Sigma Diagnostics) of known cholesterol concentrations (175 mg/dl and 283 mg/dl respectively) were analysed with each batch to control for inter-assay variability, and a well containing INFINITY™ Cholesterol Reagent with no added serum was used as a blank.

Serum triglycerides

Serum triglyceride levels in individual SAM serum samples were assayed using the INFINITY™ Triglycerides Reagent (Sigma Diagnostics). This reagent contains lipoprotein lipase, adenosine triphosphate (ATP), glycerol kinase (GK), glycerol phosphate oxidase (GPO), 3,5 dichloro-2-hydroxybenzene (3,5 DHBS), 4-AAP, and HRP. In the presence of this reagent, triglycerides are hydrolysed by lipoprotein lipase to free fatty acids and glycerol. The glycerol is in turn phosphorylated by GK with ATP to glycerol-3-phosphate and ADP. Glycerol-3-phosphate is then oxidized to dihydroxyacetone phosphate by GPO, yielding hydrogen peroxide. The hydrogen peroxide then reacts with 3,5 DHBS and 4AAP, in the presence of HRP, to produce quinoneimine dye, whose absorbance is proportional to the original concentration of triglycerides in the sample. For this assay, the formation of the chromophore is detected by its absorbance at 520 nm.

Because of the potentially deleterious effects of serum lipoprotein lipase activity on triglyceride levels prior to analysis, the assays of triglyceride levels in individual serum samples were performed on freshly obtained serum, within 3 h of venesection. On the day of bleeding and analysis, 3 μl of freshly obtained serum was added to 300 μl of INFINITY™ Triglycerides Reagent in a 96-well plate, at RT. The plate was incubated at 25°C for 15 min, and then read on a Spectra Max 250 plate-reader (primary wavelength 520 nm, secondary wavelength 660 nm). Experiments were performed in triplicate, and mean concentrations calculated. The plate-reader was

again calibrated using the ACCUSET® Liquid Calibrator (see above) which has a general assigned value of total triglycerides, as measured enzymatically, of 105 mg/dl (1.19 mM). Cardiolipin controls (Sigma, #C4571 and #C4696) of known total triglyceride concentrations (119 mg/dl and 297 mg/dl respectively) were again analysed, and a well containing INFINITY™ Triglycerides Reagent with no added serum was used as a blank.

2.2.4.6 Determination of lipid profiles in pooled sera of SAM mice

More detailed lipid profiles were determined in mice fed either a standard laboratory chow or the Western-type diet. Because such studies required at least 100 µl of serum, it was necessary to pool sera from age- and sex- matched mice fed on one or other diet for this analysis.

The pooled samples were subjected to a fully automated cauldron chemistry technique, HDL-Cholesterol Direct, manufactured for use with the COBAS® INTEGRA analyser (both by Roche Diagnostics, Switzerland). The underlying principle was first described by Hino *et al.* [Hino *et al.* 1996]. It relies on coating the surface of lipoproteins with synthetic polyanions. This coating transforms LDL, very low density lipoprotein (VLDL), and chylomicrons into detergent-resistant lipoprotein-polyanion complexes. In contrast, HDL does not form these complexes. Instead, the cholesterol content of the HDL is solubilized by the combined action of the polyanions and a detergent to form micelle complexes. This solubilized cholesterol is oxidized by the sequential action of cholesterol esterase and cholesterol oxidase, to form oxidized cholesterol and hydrogen peroxide. The hydrogen peroxide reacts with N,N-bis(4-sulphobutyl)-m-toluidine and 4-AAP in the presence of HRP, to form quinoneimine dye. The colour intensity of the quinoneimine dye is directly proportional to the HDL-cholesterol concentration in the sample analysed, and is determined by measuring the increase in absorbance at 552 nm. The mechanized analysis thus gives a direct measurement of HDL cholesterol content; it also calculates an estimation of the LDL content, as well as directly measuring total cholesterol and triglyceride levels.

In all cases, this method was used with freshly obtained pooled sera. Individual serum samples were obtained as described above. For same-gender litter mates, equal volumes of sera were pooled together to give a total volume of 100 µl. This 100 µl sample was then analysed by the HDL-Cholesterol Direct cassette in the COBAS

INTEGRA ANALYSER, within 30 min of pooling; the pooled sera were stored at 4°C prior to analysis. HDL/total cholesterol ratios were calculated from the automated measurements of HDL and total cholesterol in each pooled sample.

2.2.4.7 Harvesting, fixation and storage of tissue for analysis of atherogenesis

Some of the studies to be described in Chapter Four involved analysis of lipid deposition in SAM and C57BL/6 aortic roots. At specified time-points, mice were culled by cervical dislocation, and their thoracic and abdominal cavities immediately opened surgically. The heart and aorta were identified, excised as a single piece of tissue, and placed in PBS at RT for one hour; this allows the tissue to relax, facilitating subsequent preparation of cryostat cross-sections [Paigen *et al.* 1987b].

The tissue was then fixed in 4% PFA/0.1 M phosphate (pH 7.4) for 6 h at 4°C. It was next removed, rinsed in PBS, and placed in 30% sucrose/0.1M phosphate (pH 7.4), rendering the tissue more amenable to subsequent cryostat sectioning. The tissue remained in this solution for 20 h at 4°C.

The heart and aorta were then placed on a square of aluminium foil, and the apex of the heart was removed under a dissecting microscope using a scalpel to cut transversely across the ventricles in a plane parallel with the lower tip of each atrial appendage, as described by Paigen *et al.* [Paigen *et al.* 1987b]; subsequent cryostat sectioning parallel with this plane produces true cross-sections of the aortic root.

The apex of each heart was discarded, together with the distal aorta, while the remaining tissue (comprising the base of the heart, the aortic root and the proximal aorta) was covered with OCT™ compound. The tissue, foil and OCT™ were together placed in a beaker of hexane which had been pre-cooled by placing it within another beaker containing liquid nitrogen. This technique minimizes tissue distortion during freezing. Once frozen, the tissue, still attached to the aluminium foil by the frozen OCT™, was placed in a 50 ml Falcon tube, and stored at -80°C.

2.2.4.8 Preparation of cryostat cross-sections

The frozen tissue, coated in OCT™, was brought to -20°C in the cutting chamber of a cryostat. The tissue was then mounted in further OCT™ on a cryostat chuck, with the cut surface of the ventricles uppermost.

Cryostat sections were cut as described by Emeson and Shen [1993]. Serial 10 μm sections were cut through the ventricles, until the left ventricular cavity size was seen

to reduce in size. From this point onwards, individual unstained sections were observed under a light microscope until the valve cusps of the aortic valve first became visible (corresponding to line I in Figure 2.4, overleaf). At this stage, all cryostat cross-sections were mounted onto slides previously treated (as described previously) with VECTABOND™ reagent. Alternate sections were mounted onto separate slides, so that one set of slides (Set A) could be stained for lipid deposits, and the second set (Set B) bearing the adjacent cross-sections, could be used for immunohistochemistry. This distribution of sections was similar to that used in the rabbit carotid study described above, and is illustrated in Figure 2.4.

Sectioning was continued until the valve cusps were no longer visible in the lumen of the aorta, and until the aortic wall had acquired a circular shape. At least 80 serial cross-sections were cut and mounted from each mouse, covering the 800 μm of aortic root distal to line I. The distance along the aorta from the initial appearance of the caudal portion of the valve cusps to their eventual disappearance beyond the tips of the cusps has been reported to be 450-500 μm in C57BL/6 mice [Emeson and Shen 1993], but has not been documented for SAM mice. By checking visually that the valve cusps had disappeared, and by cutting at least 80 cross-sections after line I, it was possible to ensure that the entire aortic root had been cross-sectioned.

2.2.4.9 Staining of aortic cross-sections for lipid

Set A slides were air-dried for 6 h at RT, before being immersed in freshly prepared Oil red O staining solution (see above) for 10 min. They were washed in tap water for 4 min, then counter-stained in Harris' haematoxylin for 1 min. The slides were washed in tap water for a further 10 min, then mounted with coverslips using Glycergel™.

2.2.4.10 Morphometric analysis of lipid deposition in aortic cross-sections

For each aorta, eight cross-sections which would originally have been spaced at 100 μm intervals along the intact aortic root were analysed morphometrically. These sections (i.e. sections 1, 11, 21, 31 *etc.*, all located on the Set A slides) had been stained with Oil red O as described above. As in the rabbit carotid study, if the relevant cross-section was found to be damaged or folded, the next available intact cross-section was used.

Figure 2.4 Preparation of SAM aortic root cross-sections

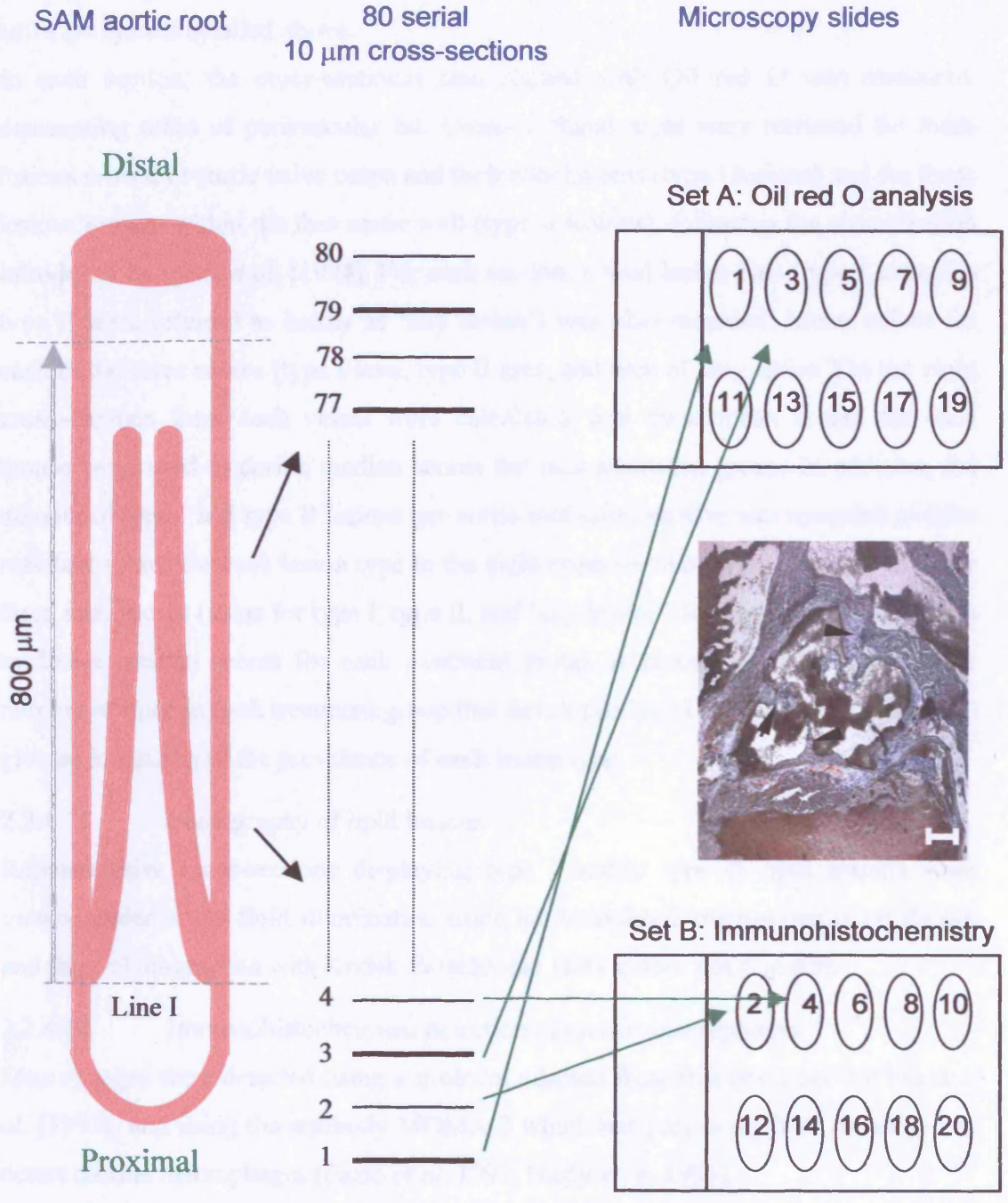

Figure 2.4 80 cryostat sections were cut from each aortic root, starting at line I and continuing distally. Cross-sections were distributed onto Set A and Set B slides as shown. The photomicrograph shows a representative cross-section from a SAM aortic root, stained with Oil red O and haematoxylin, at the level of the valve cusp attachments (arrowheads). Bar = 250 μm.

The eight cross-sections from each aorta were studied using a Nikon LABOPHOT-2 microscope, to which was attached a JVC TK-1281 colour video camera (both as mentioned for the rabbit carotid artery studies). Morphometric analysis of the cross-sections was performed, again using the LUCIA M computerized image analysis software system detailed above.

In each section, the cross-sectional area stained with Oil red O was measured, discounting areas of perivascular fat. Cross-sectional areas were recorded for those lesions related to aortic valve cusps and their attachments (type I lesions) and for those lesions present within the free aortic wall (type II lesions), following the classification introduced by Qiao *et al.* [1994]. For each section, a total lesion area (type I area plus type II area, referred to below as 'any lesion') was also recorded. Mean values for each of the three scores (type I area, type II area, and area of 'any lesion') in the eight cross-sections from each vessel were calculated, and these mean scores for each mouse were used to derive median scores for each treatment group. In addition, the number of type I and type II lesions per aortic root cross-section was recorded and the resultant scores for each lesion type in the eight cross-sections were summated. These three total scores (sums for type I, type II, and 'any lesion') for each mouse were used to derive median scores for each treatment group. A record was also kept of the number of mice in each treatment group that developed type I and/or type II lesions, to give an indication of the prevalence of each lesion type.

2.2.4.11 Photography of lipid lesions

Representative cross-sections displaying type I and/or type II lipid lesions were viewed under bright-field illumination using an Axiophot 2 microscope (Carl Zeiss), and were photographed with Kodak Ektachrome 160T colour positive film.

2.2.4.12 Immunohistochemical detection of murine macrophages

Macrophages were detected using a protocol adapted from that described by Fazio *et al.* [1997], and using the antibody MOMA-2 which has previously been employed to detect murine macrophages [Fazio *et al.* 1997, Hasty *et al.* 1999].

Immunohistochemistry was performed using slides from Set B. These slides had been stored at -80°C. After sections had been thawed to RT, they were further air-dried for 10 min, then immersed in acetone at 4°C for 20 min. After three 30-second washes in

TBS at 4°C, the sections were incubated with Dako serum-free protein-blocking agent in a humidified chamber for 25 min at RT.

The protein-blocking agent was then replaced with the primary antibody, rat anti-mouse macrophages/monocytes, clone MOMA-2 (Serotec, UK) diluted 1:500 in TBS. Rat IgG_{2b}, clone LO-DNP-11 (Serotec, UK), diluted to an equivalent immunoglobulin concentration, was used as a negative control in parallel sections. Sections were incubated with the primary antibody for 30 min, before three further 30-second washes in TBS at 4°C. Sections were next incubated for 30 min at RT with the secondary antibody, biotinylated rabbit anti-rat immunoglobulin (Dako Ltd, UK) diluted 1:300 in TBS. After three further 30-second washes in TBS at 4°C, the sections were incubated for 30 min at RT with Str-ALP, diluted 1:200 in PBS. Following three further 30-second washes in TBS at 4°C, the sections were incubated with 0.01 M Tris buffer, pH 8.0 for 25 min at RT. The buffer was removed and replaced with Fast Red TR/Napthol AS-MX solution (Sigma Chemical Co., UK). The sections were incubated with this solution for 6 min at RT in darkness, then washed three times (30 sec each) in TBS at 4°C. They were then immersed in haematoxylin solution for 50 sec, and then in tap water for 20 min. They were next mounted in Glycergel™, and the slides were sealed with nail varnish. Sections were examined under an Olympus-BX microscope (Olympus Optical Company Ltd, UK), and representative sections were photographed using a charge-coupled device (CCD) camera (Victor Company, Japan).

As with the immunohistochemical experiments described earlier in the chapter, all incubations were performed in a humidified chamber, and all primary and secondary antibodies were spun at 4000 *g* for 15 min at 4°C prior to use.

A score was kept of the percentage of lesions (of any type) which, on adjacent sections, showed immunohistochemical evidence of macrophage invasion.

2.2.4.13 Statistical analysis

SAM weights and litter sizes were compared using a two-tailed unpaired Student's t-test. Total serum cholesterol levels and total triglyceride levels were compared statistically using ANOVA, using the Intercooled Stata software package employed for the rabbit study. Serum triglyceride levels were log-transformed prior to ANOVA, to ensure a normal distribution. HDL/total cholesterol ratios and morphometric data were analysed using the Mann Whitney sign rank test. Lesion counts, and data concerning the prevalence of macrophages in lipid lesions, were analysed using a

Poisson regression model since these data were non-continuous. Lesion prevalence data (again non-continuous) were compared using a Chi-squared test. In all of these analyses, a value of $P < 0.05$ was considered statistically significant.

2.2.4.14 Terminal restriction fragment length analysis

Terminal restriction fragment lengths in splenic cells from SAM-P and SAM-R mice were assayed using pulsed field gel (PFG) electrophoresis, in an adaptation of the protocol described by Kipling and Cooke [1990]. The use of PFG electrophoresis to separate out the TRFs was necessitated by the length of murine telomeres (as discussed in Chapter Four).

Experiments were performed using a TeloQuant™ Telomere Length Assay Kit (Pharmingen, USA), which included a hybridisation buffer, a biotinylated $(TTAGGG)_4$ telomere probe, and a membrane blocking buffer, together with components of a chemiluminescent 'Detection Substrate Working' solution.

In outline, cells were obtained from fresh SAM-P and SAM-R spleens, formed into agarose blocks, and then subjected to digestion of their DNA by the restriction enzyme Mbo I. This enzyme acts as a frequent cutter, and its recognition sequence is not found within the repeated hexamer sequence of the telomere. It therefore cuts the DNA into small fragments, except for the telomeres and subtelomeric regions, which together constitute the terminal restriction fragment. The digested DNA was then separated by PFG electrophoresis and blotted onto a Hybond N^+ membrane. As described below, this membrane was then probed for TTAGGG repeat sequences which were subsequently detected through a chemiluminescence system involving the use of Str-HRP. The average TRF length was then calculated from the position of the detected signal relative to the position of known size standards. The details of the protocol were as follows.

Sample preparation

SAM-P and SAM-R mice of various ages were culled by cervical dislocation, and their spleens removed and placed in ice-cold PBS in individual Petri dishes. Cells were liberated by gently macerating each spleen between two scalpel blades. Tissue debris was removed, and the cells from each spleen were suspended in 10 ml of ice-cold PBS. These samples were then spun at 200 *g* (using centrifuge model CR422) for 10 min at 4°C. The resultant pellets were re-suspended in 3 ml of ice-cold PBS and

counted using a haemocytometer. PBS was added to each sample to adjust the cell concentration of each sample to 25 x 10^6 cells/ml. The diluted cell suspensions were warmed to 50°C, and to each sample an equal volume of molten (50°C) 1% low melting point (LMP) agarose (in PBS) was added. 100 µl aliquots were pipetted into pre-cooled block formers, and left to cool and harden on ice for 20 min. The blocks were then dispensed from the block-formers into lysis buffer (detailed in Section 2.1.5.1). 0.5 ml of lysis buffer was used per block, and the blocks were incubated in this buffer for 48 h at 50°C in a water bath, with gentle agitation every few hours. They were then washed three times (30 min per wash) in Tris-EDTA (TE) (pH 7.5) at 4°C, and then incubated in 50 ml of PMSF working solution (detailed above) for 2 x 30 min at 50°C. After two very brief rinses in ice-cold TE, the blocks were washed for 3 x 15 min in TE at 4°C. The blocks were then stored in 0.5 M EDTA at 4°C.

Restriction enzyme digestion

Blocks from each mouse spleen were washed for 3 x 10 min in TE at 4°C, and then equilibrated in 600 µl of reaction buffer for 90 min. This reaction buffer (supplied together with the restriction endonuclease Mbo I by the manufacturer) contained 50 mM Tris-HCl (pH 8), 10 mM magnesium chloride and 50 mM sodium chloride. The samples were then incubated in 500 µl of reaction buffer containing 10 to 20 units of Mbo I per 100 µl plug, at 37°C overnight.

Pulsed field gel electrophoresis

A gel was prepared (using approximately 150 ml of 1% LMP agarose in 0.5 x TBE) on a PFG electrophoresis apparatus (CHEF-DR II pulsed field electrophoresis system, Bio-Rad, USA). Blocks from each mouse spleen were loaded, together with a high molecular weight ladder (Lambda ladder PFG marker), a control sample containing long telomeres (TeloHI DNA), and a sample of biotinylated lambda DNA digested with the restriction enzyme HindIII (biotinylated λ DNA/HindIII Marker), the latter two agents having been supplied in the Telomere Length Assay Kit mentioned above. The blocks were sealed above with molten 1% LMP agarose. The gel was run for 15 h at 14°C, at 200 V, with pulse parameters of 0.1 to 10 sec, and a start ratio of 1.0.

The gel was then removed and stained in 0.25 µg/ml ethidium bromide (5 µl of 10 mg/ml ethidium bromide diluted in 200 ml of 0.5 x TBE) for 1 h and photographed using a UVP gel documentation system (Ultra-violet Products Ltd, UK).

Transfer to Hybond N^+ membrane

The nucleic acids in the gel were de-purinated in 0.25 M hydrochloric acid for 40 min at RT, and then de-natured in 1.5 M sodium chloride / 0.5 M sodium hydroxide for 2 x 15 min at RT. The gel was then transferred to an MSC charged Hybond-N^+ membrane which had been pre-wetted with DDW and then soaked in the de-naturing solution for 5 min. The transfer was performed overnight. After the well positions had been marked, the membrane was removed, and neutralised by rinsing in 2 x SSC (prepared from 20 x SSC) for 2 x 5 min. It was then cross-linked for 12 sec in a UV crosslinker (Stratalinker, Stratagene Ltd, UK) and allowed to air-dry.

Hybridisation and immunoblotting

The membrane was pre-wetted with 2 x SSC for 5 min, and pre-hybridised at 65°C for 4 h in 14 ml of hybridisation buffer in a hybridisation oven (Techne, UK). 4 µl of 20 ng/ml biotinylated telomere probe was added, and the membrane was hybridised at 65°C overnight. Following two brief rinses in 1 x SSC/0.1% SDS at RT, the membrane was incubated in pre-warmed 1 x SSC/0.1% SDS at 42°C for 2 x 15 min. The membrane was rinsed twice in PBS, then incubated with 30 ml of membrane blocking buffer at RT for 1 h. The blocking buffer was removed, and replaced with 1.5 µl of Str-HRP in 30 ml of fresh blocking buffer. The membrane was incubated in this solution for 1 h at RT, and shaken continuously. After two brief rinses and 3 x 15 min washes in 0.1% Tween-20 in PBS, the membrane was shaken for 5 min in 14 ml of freshly prepared Detection Substrate Working solution. The membrane was then placed between two sheets of plastic wrap, placed in an X-ray film cassette, and exposed to light-sensitive film, which was developed in an automatic developing machine (X-OGRAPHY Compact x2, Medivance Ltd, UK).

Calculation of TRF length

Three gels were run using DNA from mice of various ages. A representative autoradiogram was scanned (using a Hewlett Packard ScanJet 5300C scanner), and a TIFF image obtained. This image was analysed using public domain NIH Image software (version 1.62). This software calculates mean TRF lengths by integrating the signal intensity over the entire TRF distribution as a function of TRF length, using the formula TRF length = $\Sigma(OD_i) / \Sigma(OD_i/L_i)$, where OD_i and L_i are the signal intensity

and TRF length respectively at any position, i, on the autoradiogram. Mean TRF lengths were compared using a Mann Whitney sign rank test.

2.2.4.15 SA-β-gal staining in tissue from SAM mice

Murine tissue was stained for SA-β-gal activity using a protocol which evolved from that used in rabbit carotid arteries. Three- and twelve-month-old SAM-P and SAM-R mice were culled by cervical dislocation. The aorta of each mouse, extending from the arch to the iliac bifurcation, was dissected out using aseptic technique, and extraneous fat removed using a scalpel. The dorsum of each mouse was shaved with a razor blade, and full-thickness squares of dorsal skin (measuring approximately 3 mm x 3 mm) were excised. The aortas and skin squares were rinsed in ice-cold PBS, then immersed in X-Gal working solution titrated to pH 6.0 (or on some occasions at pH 4.0). The tissue was incubated in this solution at 37°C for 24 h, and then rinsed briefly in ice-cold PBS. The samples were then fixed in 4% PFA/0.1 M phosphate buffer (pH 7.5) at 4°C for 6 h, before being immersed in 30% sucrose/0.1 M phosphate buffer (pH 7.4) at 4°C for 36 h. They were next removed from the sucrose solution, coated with liquid OCT™, and rapidly frozen by immersion in hexane which had been pre-cooled in liquid nitrogen. The OCT™-embedded tissue was then stored at -80°C.

10 μm cryostat sections were subsequently cut from the OCT™-embedded tissue, and placed on microscope slides. Tissue was orientated on the cryostat chuck so as to obtain full-thickness cross-sections of the skin, and transverse cross-sections of the aorta. After air-drying for 2 h, the slides were fixed in neutral buffered formalin for 10 min, washed in water for 3 min, and then immersed in eosin solution for 5 min. After washing in tap water for 5 min, sections were air-dried for 2 min, and then mounted under coverslips using Glycergel™. Coverslips were sealed with commercially available nail varnish so as to prevent dehydration of the tissue sections.

CHAPTER THREE

Cell senescence in denuded rabbit carotid arteries

The central aim of the experiments described in this chapter was to determine whether cellular replicative senescence can occur in vascular tissue *in vivo*. The experiments described involved the use of a cytochemical assay, SA-β-gal, which appears to be capable of detecting senescent cells both in culture and in certain *ex vivo* tissue samples [Dimri *et al.* 1995].

The chapter is divided into two sections. Section One begins with a description of preliminary *in vitro* studies carried out to establish whether SA-β-gal is capable of identifying replicative senescence in vascular cells (ECs and VSMCs). It concludes with an account of the adaptation of this assay for the study of *ex vivo* rabbit vascular tissue samples.

Section Two describes the use of the adapted assay in a rabbit carotid artery denudation model. The assay was used to detect senescent cells in carotid arteries which had been subjected to either a single endothelial denudation, or to two serial denudations. Morphological and morphometric studies were used to establish the extent of endothelial regeneration and neointimal formation following the denudation procedures. Immunohistochemistry was used to determine which cell types exhibited SA-β-gal activity. The results of experiments designed to discriminate between senescent, apoptotic and proliferating cells in the vessel wall are also described.

3.1 Section One: Preliminary experiments

3.1.1 Introduction

The use of SA-β-gal to detect senescent cells in culture has been described in Chapter One. This assay involves the detection, at pH 6.0, of the activity of the enzyme β-galactosidase. The use of this assay to identify senescent cells appears to be applicable only to certain cell types, and only in certain species.

Dimri *et al.* have commented that later passages of HUVECs show greater numbers of SA-β-gal-positive cells than do early passages, though no data were provided to support the contention that the assay was identifying senescent cells in these cultures [Dimri *et al.* 1995]: they did not describe the relationship between passage number and SA-β-gal-positivity in detail, nor did they give evidence that SA-β-gal-positivity correlated with a senescent phenotype.

In addition, prior to the current study, the use of SA-β-gal to detect senescence in VSMCs of any species, or in rabbit cells of any type, had not been described.

The aims of the cell culture studies described in this section were to confirm that the SA-β-gal assay does indeed specifically identify senescence in endothelial and vascular smooth muscle cells, and also to establish whether the assay is an effective marker of senescence in cells derived from rabbits. A further goal was to establish whether SA-β-gal staining was compatible with subsequent immunocytochemical identification of cell types. The aim of the remaining experiments in this section was to adapt the cellular β-gal staining protocol for use in excised rabbit arterial tissue.

3.1.2 Experimental design

As described in Chapter Two (Sections 2.2.2.1 and 2.2.2.2), first passage cryopreserved HUVECs, and rabbit VSMCs obtained by the explant technique, were grown in culture and serially passaged.

In initial experiments, early passage cultures of HUVECs were stained for β-gal activity at pH 4.0, to assess whether, as with other mammalian cells [Morreau *et al.* 1989, Dimri *et al.* 1995], acid β-gal activity is detectable in 'young' cultures. The assay was then performed in other similarly 'young' HUVECs at pH 6.0, in order to establish whether this led to more selective staining.

Other HUVECs were serially passaged, and the prevalence of cells staining positively for β-gal activity at pH 6.0 (i.e. for SA-β-gal) was determined. The relationship between the accumulation of SA-β-gal-positive cells and the decline in cell density at confluence was studied, and the morphology of cells showing SA-β-gal activity was noted. Similarly, SA-β-gal activity was assayed in serially passaged rabbit VSMCs.

Immunocytochemistry was next used to detect the EC surface antigen CD31 in early- and late-passage HUVEC cultures which had already been stained for SA-β-gal.

The experiments designed to adapt the cellular SA-β-gal assay for use in rabbit vascular tissue involved staining non-injured rabbit carotid arteries for β-gal activity. The aim was to develop a protocol which could detect β-gal activity (if present) in all layers of the vessel wall, while providing optimal preservation of the vessel wall architecture. Various modifications were made to the original protocol described by

Dimri *et al.* for use with skin biopsies [Dimri *et al.* 1995], including the introduction of perfusion fixation.

3.1.3 Results

3.1.3.1 β-galactosidase staining in early passage HUVEC cultures

As described in Chapter One (Section 1.4.9) β-gal activity can be detected by the enzyme's ability to cleave the indigogenic substrate 5-bromo-4-chloro-3-indolyl-β-galactopyranoside (X-gal) to leave a blue end-product [Gossrau *et al.* 1991, Dimri *et al.* 1995]. An endogenous lysosomal enzyme activity is detected at pH 4.0, and this activity is found in most mammalian cell types, regardless of the replicative age of the cells [Morreau *et al.* 1989, Dimri *et al.* 1995].

Figure 3.1 Panel A (overleaf) shows the result of incubating confluent early-passage HUVECs with X-gal working solution at pH 4.0. As indicated in this photomicrograph, all the cells in the culture exhibited dark blue staining. In contrast, Figure 3.1 Panel B shows the result of staining early-passage HUVECs at pH 6.0. Under these conditions, only occasional cells displayed an accumulation of blue precipitate. A frequent finding in these experiments was that those cells staining positively for β-gal activity at pH 6.0 (SA-β-gal activity) were larger than the non-staining cells in the same dish, as is illustrated in this panel.

3.1.3.2 SA-β-gal staining in serially passaged HUVEC cultures

The prevalence of SA-β-gal staining in serially passaged HUVECs was then investigated.

Figure 3.2 (overleaf) shows SA-β-gal staining in early-passage (Panel A) and late-passage (Panel B) HUVECs. While very few early passage cells stained for SA-β-gal, it was evident that by late passages the majority of cells showed positive staining. Comparison of the two panels, which show cells at the same magnification, reveals an increase in size of the HUVECs in later cultures.

Figure 3.1 β-galactosidase staining in confluent early passage HUVECs

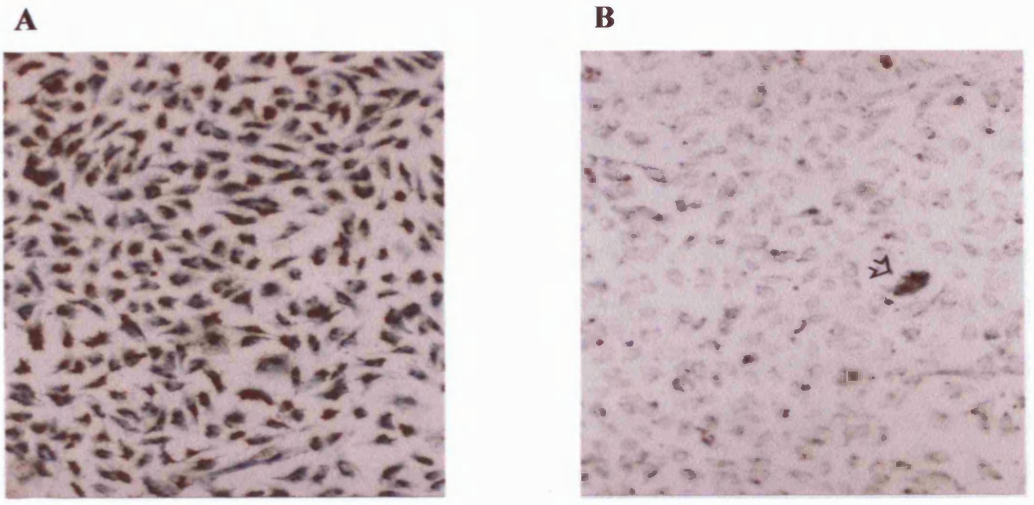

Figure 3.1 Representative photomicrographs showing early passage ECs stained for β-gal activity. Panel A shows staining at pH 4.0, detecting acid β-gal activity; all cells show positive (blue) staining. In contrast, the ECs shown in Panel B were stained at pH 6.0, to detect SA- β-gal activity; only one EC in this culture (marked with an arrow) shows strong blue staining, and this cell appears larger than the surrounding ECs. Both photomicrographs were taken under bright field illumination using an Axiovert 25 CFL inverted microscope with a 10X objective.

Figure 3.2 SA-β-gal staining in early- and late-passage HUVECs

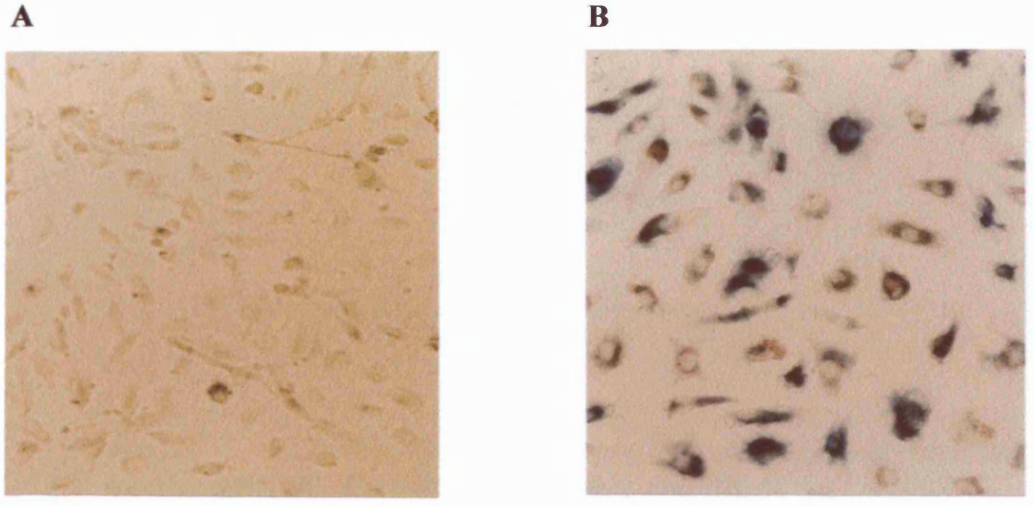

Figure 3.2 Photomicrographs showing early- (Panel A) and late- (Panel B) passage ECs stained for SA-β-gal activity. In Panel A, very few early-passage ECs show positive (blue) staining. In contrast, the majority of late-passage ECs in Panel B stain positively for SA-β-gal. Both photomicrographs were taken in staining solution under bright field illumination using an Axiovert 25 CFL inverted microscope with a 20X objective. Comparison of the two photomicrographs shows the increase in cell size in later passages.

Figure 3.3 shows the percentage of SA-β-gal-positive cells in each culture dish plotted against cumulative population doublings (CPDs). As shown, until approximately 32 CPDs, the percentage of cells staining for SA-β-gal activity remained low, at less than 20%, though even in these early passages there appeared to be a trend for the percentage to rise with increasing CPDs. Beyond 32 CPDs, however, there was a dramatic rise in the percentage of cells staining for SA-β-gal, reaching approximately 62% at about 38 CPDs. Also shown on this graph is the decline in cell density at confluence with serial passages. This decline suggests a pronounced increase in mean cell size in later passages, and suggests that the cultures were approaching senescence. It is notable that the dramatic rise in SA-β-gal staining appears to coincide with a sudden acceleration in the decline of cell density at confluence.

Figure 3.3 Semi-quantitative analysis of SA-β-gal staining in serially passaged HUVECs

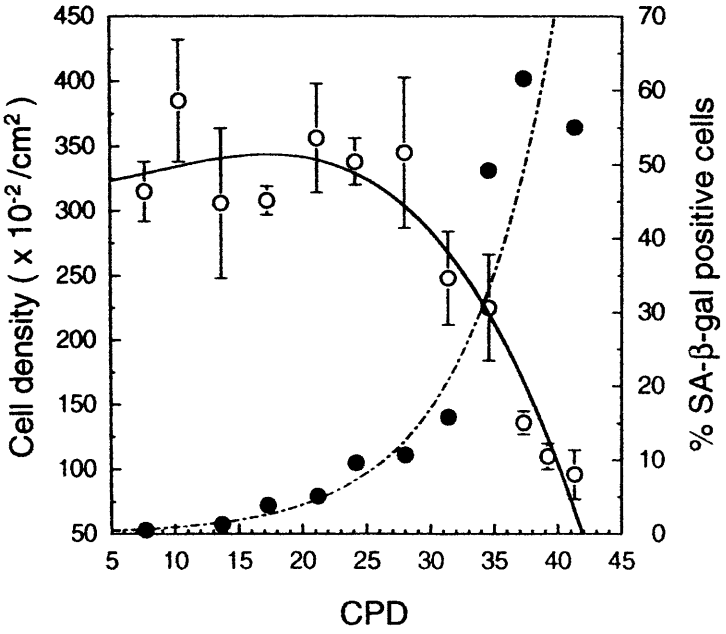

Figure 3.3 HUVECs were grown to confluence, and serially passaged at weekly intervals. Harvested cells were counted at each passage, as described in Chapter Two. Parallel cultures were stained for SA-β-gal activity. In this graph the cell density at confluence (white circles) and the percentage of HUVECs staining positively for SA-β-gal (black circles) are shown as a function of the cumulative population doublings (CPDs) at each passage. Values for cell density are the mean of replicate dishes ± s.d..

3.1.3.3 SA-β-gal staining in serially passaged rabbit VSMC cultures

Rabbit VSMCs were obtained by the explant technique and serially passaged. In contrast to HUVECs, rabbit VSMCs lost their proliferative capacity after only three to four passages. When primary cultures of rabbit VSMCs were stained for SA-β-gal, no positive staining was observed, either in the central area of confluent cells surrounding the explant, or at the leading edge of growth (Figure 3.4, Panel A, overleaf). In contrast, the majority of third-passage VSMCs showed positive SA-β-gal staining (Figure 3.4, Panel B). Again, comparison of the two panels demonstrates the increase in size of the later passage cells. In the later cultures, those cells which stained blue also showed a veil-like appearance and irregularities of cellular shape.

3.1.3.4 SA-β-gal and CD31 double-staining in HUVECs

Immunocytochemistry was used to detect the EC surface antigen CD31 in early- and late-passage HUVEC cultures which had been stained for SA-β-gal activity. The antigen-antibody complexes were visualized using an ALP-conjugated secondary antibody in combination with the chromogenic substrate fuchsin. Figure 3.5 (overleaf) shows representative results of these experiments. Both early- (Panel A) and late- (Panel B) passage HUVEC cultures showed a similar intensity of CD31 labelling (the pink/red colour of fuchsin). The increase in cell size in late-passage HUVECs is again evident in the figure. From Panel B it is clear that SA-β-gal staining was still easily detectable despite the CD31 counter-stain, and that, conversely, detection of CD31 was not significantly impaired by prior staining for β-gal activity. Parallel cultures stained with a negative-control primary antibody at an equivalent immunoglobulin dilution did not show positive counter-staining (data not shown).

3.1.3.5 Development of a protocol for staining rabbit carotid arteries for β-galactosidase activity

Dimri *et al.* have described a protocol for detecting SA-β-gal activity in excised samples of human skin [Dimri *et al.* 1995]. In Chapter Two details are given of two preliminary protocols used in the adaptation of Dimri's method for use in excised rabbit vascular tissue (Section 2.2.3.11). In these preliminary protocols, incubation with X-gal working solution was performed at pH 4.0, in order to detect the ubiquitous

Figure 3.4 **SA-β-gal staining in early- and late-passage rabbit vascular smooth muscle cells**

A B

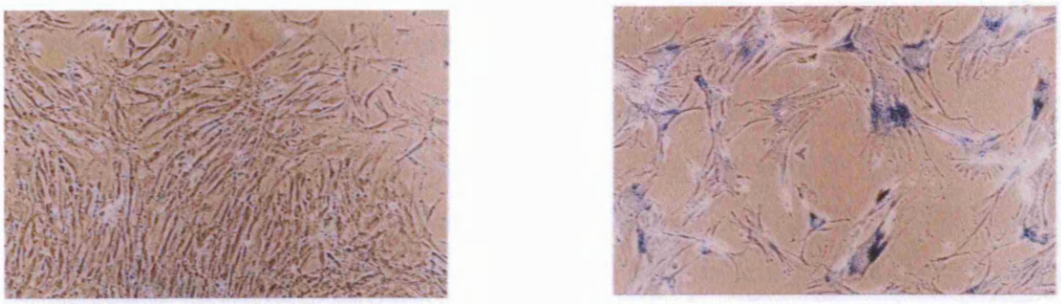

Figure 3.4 Representative photomicrographs showing early- (Panel A) and late- (Panel B) passage rabbit VSMCs stained for SA-β-gal activity. Panel A shows rabbit VSMCs outgrowing from an aortic media explant, which is adjacent to the area of confluent growth but outside the photographic field. These primary culture cells show no blue staining, either in the area of tightly packed cells or at the leading edge of growth. In contrast, the majority of third-passage VSMCs shown in Panel B stain positively for SA-β-gal; these cells show the giant size and veil-like appearance of senescent VSMCs. Phase-contrast photomicrographs were taken using an Axiovert 25 CFL inverted microscope with a 10X objective.

Figure 3.5 **SA-β-gal staining and CD31 labelling in early- and late-passage HUVECs**

A B

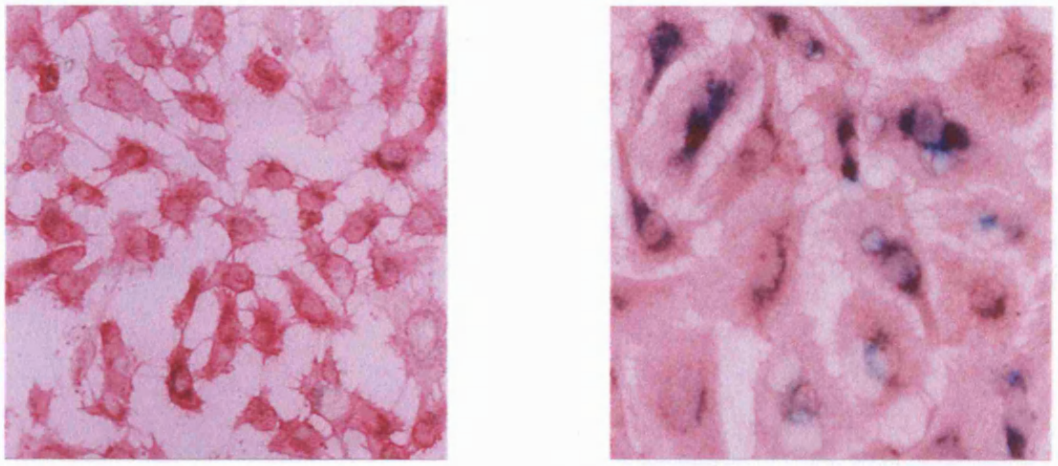

Figure 3.5 Representative photomicrographs showing early- (Panel A) and late- (Panel B) passage HUVECs stained for SA-β-gal activity (blue stain), and labelled for CD31 by immunocytochemistry (pink stain). In Panel A no passage 3 cells show blue staining. In contrast, the majority of passage 11 HUVECs in Panel B stain positively for SA-β-gal. The SA-β-gal staining appears to be localized predominantly in or around the nuclei. Both photomicrographs were taken under bright field illumination using an Axiovert 25 CFL inverted microscope with a 20X objective.

acid β-gal activity which was expected to be present in cells throughout the vessel wall; testing of the various protocols at this pH would therefore indicate the extent of tissue penetration by the working solution, and allow an assessment of the compatibility of tissue fixation with β-gal detection.

Protocol 1

The first protocol used (Protocol 1, Figure 2.3) was almost identical to that described by Dimri *et al.* for use with skin samples [Dimri *et al.* 1995]. It involved snap-freezing excised rabbit carotid arteries and preparing cryostat-cut cross-sections. These sections were fixed in PFA, incubated in X-Gal working solution at pH 4.0, passaged through graded ethanol solutions, and mounted on histology slides. The only difference from Dimri's protocol was that a longer immersion in X-Gal working solution was used (24 h, rather than an overnight immersion) in order to allow time for permeation of the working solution through the thicker cross-sections used in the rabbit study (7 μm, rather than 4 μm in the Dimri study). Figure 3.6 Panel A (overleaf) shows a representative cross-section processed according to this protocol. As shown, no blue staining was detected in any layer of the vessel wall.

Protocol 2

Since various minor adaptations to Protocol 1 failed to yield any improvement in β-gal staining, a fundamental change was instituted in the staining protocol. In Protocol 2 (Figure 2.3), freshly excised carotid arteries were immersed *in toto* in X-gal working solution (again at pH 4.0) for 24 h at 37°C. They were subsequently fixed in PFA and snap-frozen. Cryostat sections were cut, air-dried, and mounted in DPX. Figure 3.6 Panel B shows a representative section of carotid artery stained using this protocol. Blue staining is observed in all layers of the vessel wall, and the intensity of staining appears homogeneous throughout the artery.

Figure 3.6 Preliminary protocols for staining for β-galactosidase activity in *ex vivo* tissue

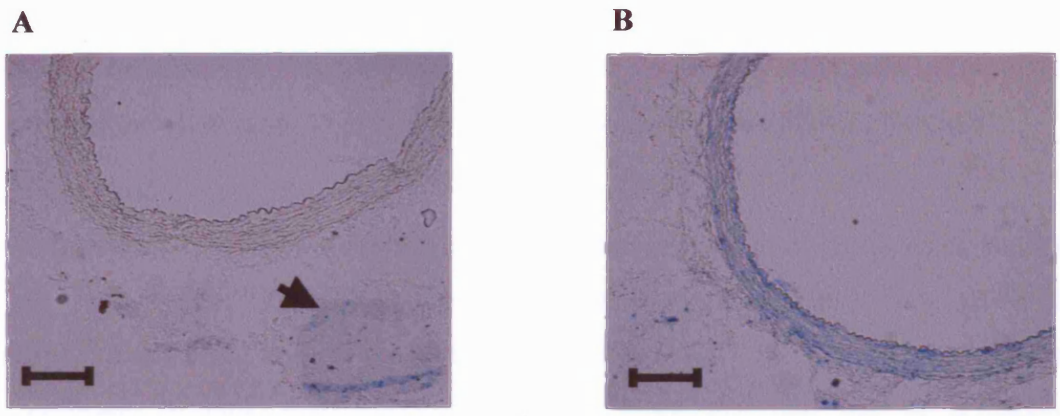

Figure 3.6 Panel A shows a representative carotid artery cross-section stained for β-gal activity using Protocol 1, as detailed in Figure 2.3; in this protocol, cryostat cross-sections were immersed in X-Gal working solution at pH 4.0. As shown, no positive (blue) staining was detected in any layer of the arterial wall. The area of positive staining marked with an arrow was believed from its size and position to be the vagus nerve. Panel B shows a carotid artery cross-section prepared using Protocol 2, as detailed in Figure 2.3; in this protocol carotid arteries were immersed *in toto* in X-Gal working solution at pH 4.0. While positive staining was demonstrated throughout the vessel wall, preservation of tissue structure was poor. Bar = 125 μm.

Figure 3.7 Acid β-galactosidase activity in non-denuded rabbit carotid artery

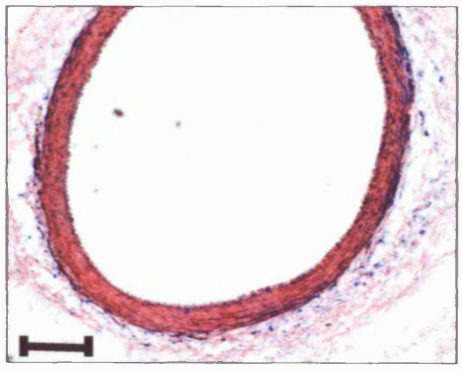

Figure 3.7 The photomicrograph shows a representative rabbit carotid artery cross-section stained following the Final Protocol detailed in Figure 2.3 and summarized overleaf. According to this protocol rabbits were perfusion-fixed, and their carotid arteries were immersed *in toto* in X-Gal working solution (in this case at pH 4.0); cryostat cross-sections were prepared, and counter-stained with eosin. As shown, at pH 4.0, blue staining was demonstrable throughout the vessel wall. The introduction of perfusion fixation significantly improved the preservation of vessel wall integrity. Bar = 125 μm.

Thus, *in toto* immersion of fresh tissue in X-Gal working solution appeared to yield strong β-gal staining. This protocol, though, was not adopted as it stood, because light microscopy of H&E-stained cross-sections revealed very poor preservation of the EC layer (data not shown). This finding suggested that fixation of tissue prior to excision would be required in order to preserve the integrity of the endothelial monolayer.

Final Protocol

In the protocol eventually adopted for the subsequent balloon denudation studies ('Final Protocol' in Figure 2.3), therefore, rabbits were perfusion-fixed prior to excision of the carotid arteries (as described in Section 2.2.3.3). 2% PFA was used as the perfusate because preliminary experiments suggested that use of a higher concentration of the fixative rendered subsequent frozen sections brittle and non-adherent to histology slides. After perfusion fixation, the carotid arteries were excised, immersed *in toto* in X-Gal working solution for 24 h, and then snap-frozen. 10 μm cryostat sections were further fixed in PFA, counter-stained with eosin, and mounted in DPX; these thicker sections provided better preservation of vessel structure than the 7 μm sections used earlier. Figure 3.7 (previous page) shows a representative section from an artery stained in this way. The section again shows blue staining of cells throughout the entire vessel wall. This finding is in agreement with the contention that lysosomal β-gal activity is relatively ubiquitous, and that the tissue was adequately permeated by X-gal working solution. As will be shown below, this protocol preserved endothelial integrity, as demonstrated by immunohistochemical detection of CD31.

3.1.4 Discussion of preliminary studies

The cell culture studies described above demonstrate that β-gal activity can be detected at pH 6.0 in vascular cells. As well as confirming the increase in this SA-β-gal staining in late-passage HUVECs as previously reported by Dimri *et al.*, the results strongly suggest that this enzyme marker specifically identifies cellular senescence in endothelial and vascular smooth muscle cells. This conclusion is suggested by the following findings: firstly, in serially passaged HUVECs, an abrupt rise in the percentage of cells staining positively for SA-β-gal coincided with a sharp decline in the cell density at confluence, indicating that the emergence of positive staining corresponded with an increase in mean cell size, a feature of senescent ECs in culture [Johnson and Longenecker 1982]; similarly, the finding that individual SA-β-gal-

positive HUVECs and rabbit VSMCs appear larger than their non-staining neighbours, and in the case of VSMCs show the veil-like appearance and irregular shape previously described in senescent VSMCs [Dartsch *et al.* 1990], further supports the contention that this enzyme activity specifically detects senescence in vascular cells.

The widespread β-gal staining at pH 4.0 in young HUVECs, and the almost complete absence of staining at pH 6.0 in these cells, are in accordance with the proposition that while all early passage HUVECs contain lysosomal β-gal activity, only selected cells harbour SA-β-gal activity. Dimri *et al.* have similarly reported the presence of occasional SA-β-gal-positive cells in early passages of human fibroblasts [Dimri *et al.* 1995]. The explanation for the occurrence of SA-β-gal-positive cells in early passages remains unclear, but it is possible that they are either cell contaminants (i.e. senescent cells from other cultures), or cells which have senesced via a mechanism other than replicative senescence; one such mechanism might be SIPS, a process discussed in Chapter One.

Conversely, it is notable that even in cultures containing large numbers of senescent cells, a substantial proportion of cells appeared still to be pre-senescent, in that they did not stain positively for SA-β-gal. This finding may reflect inter-cell variability in proliferative rates. Alternatively the SA-β-gal-negative cells may be cells which have been rendered quiescent (by either intrinsic or extrinsic signals), and which have therefore failed to reach senescence.

It was striking that rabbit VSMCs reached senescence after fewer passages than did human ECs. This finding could have a number of explanations. If the telomere theory of replicative senescence is valid, one might attribute the observed difference in proliferative activity between the two cell types to a difference in their mean telomere length. There is no published data concerning the telomere length of rabbit VSMCs, and so a direct comparison of TRF length between rabbit VSMCs and HUVECs is not possible. HUVECs are thought to have a mean TRF length of 14 kbp in neonates, and have been found to senesce when their TRF lengths reach approximately 6 kbp [Chang and Harley 1995]. TRF length has been measured in preparations of cells from human aortic intima and media (presumed, but not proven, to be predominantly VSMCs); in preparations from one-month-old subjects, mean TRF lengths were approximately 7 kbp, this parameter falling to approximately 5 kbp in eighty-year-old subjects [Okuda *et al.* 2000]. In humans then, neonatal HUVECs appear to have longer TRFs than do

one-month-old VSMCs. It would be unwise, though, to extend this comparison to rabbit VSMCs without further investigation; given that mice have substantially longer telomeres than do humans (as detailed in Chapter Four), it is evident that there can be significant inter-species differences in telomere length even in equivalent cell types. The speed with which rabbit VSMCs reach senescence, compared with HUVECs, may relate either to a shorter TRF length prior to the onset of proliferative activity, or may reflect a greater degree of telomere attrition with each round of replication. Alternatively, there may be other factors, not related to telomere dynamics, which halt rabbit VSMC after only a few passages. These factors may be either intrinsic biological signalling mechanisms, such as over-expression of Cdk inhibitors, or may be artefactual constraints related to the culture conditions in which the cells were grown.

Establishment of the compatibility of CD31 staining with SA-β-gal detection was important for the planned study of excised rabbit carotid artery specimens. As mentioned in Chapter One (Section 1.4.3) senescent cells show alterations in gene expression and protein synthesis. It was therefore necessary to confirm that senescent ECs continue to express CD31. Furthermore, the results show that fuchsin does not mask SA-β-gal staining, and that this might therefore be a suitable chromogen for use in the rabbit carotid artery model. This experiment therefore suggested that the combination of CD31 labelling and SA-β-gal staining might be used to detect senescent ECs.

The adaptations in the staining procedure described above for use in excised rabbit arterial tissue yielded a protocol capable of detecting endogenous β-gal activity throughout the vessel wall while maintaining arterial architecture.

3.2 Section Two: The detection of *in vivo* senescence in the rabbit carotid artery denudation model

3.2.1 Introduction

As has been discussed in Chapter One (Section 1.4.6), it has been suggested that the *in vitro* phenomenon of replicative senescence may also occur *in vivo*. Recently the use of SA-β-gal has confirmed the emergence of senescent cells in tissues where rates of cell turnover are relatively high, such as normal skin, healing venous ulcers, and

hyperplastic prostate glands [Dimri *et al.* 1995, Mendez *et al.* 1998, Choi *et al.* 2000]. In contrast, in tissues where rates of cell turnover are low, such as in the blood vessel wall [Schwartz *et al.* 1980, Hobson and Denekamp 1984], the suggestion that senescent cells may accumulate *in vivo* has remained controversial [Reidy *et al.* 1983, Clowes *et al.* 1986, Lindner *et al.* 1989].

As also mentioned in Chapter One, one tool for studying the replicative capacity of vascular cells has been the use of endothelial denudation models. Following mechanical injury to the luminal surface of the arterial wall, a proliferative response occurs, involving both endothelial and vascular smooth muscle cells [Reidy and Schwartz 1981, Stemerman *et al.* 1982]. More recent research has shown that repetition of the denudation injury leads to a further wave of endothelial and VSMC proliferation [Azuma *et al.* 1995]. If senescence of cells in the vasculature can occur at all *in vivo*, one might therefore expect it to emerge following repetitive injury of the luminal surface of the arterial wall, where vascular cells will have undergone an unusually high number of rounds of replication.

The main aim of the experiments described in this section was to use the SA-β-gal assay to establish whether the proliferative response provoked by an endothelial denudation injury could indeed lead to the accumulation of senescent cells *in vivo*. If this proved to be the case, a further goal would be to discover whether a second denudation injury would result in a more marked accumulation of senescent cells than a single injury. The next aim was to identify which, if any, cell types expressed SA-β-gal activity *in vivo*. The final aim was to study the relationship between these putatively senescent cells and the occurrence of proliferative and apoptotic activity in the vessel wall.

3.2.2 Experimental design

The final protocol for tissue harvesting and β-gal staining described above (Final Protocol in Figure 2.3) was used to look for cellular senescence in two groups of adult male NZW rabbits (as illustrated in Figure 3.8 overleaf). The first group, referred to as the 'single-denudation' group, consisted of six adult rabbits which were subjected to a single trans-luminal injury of the right common carotid artery, and culled six weeks later.

Figure 3.8 Experimental design for rabbit carotid artery denudation studies

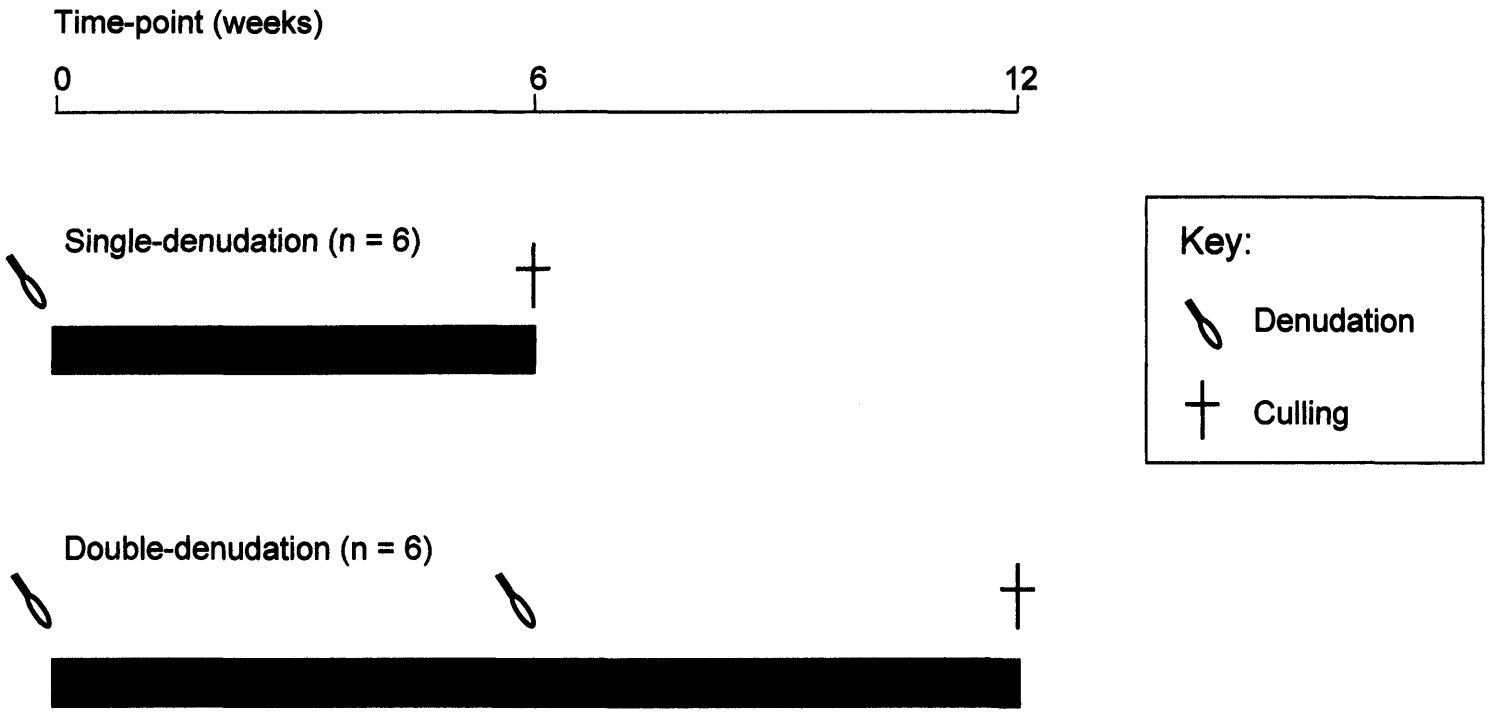

Figure 3.8 Twelve Male New Zealand White animals were divided into two groups: the single-denudation group underwent denudation of the right carotid artery, and were culled six weeks later; the double-denudation rabbits underwent two denudations to the right carotid artery, six weeks apart, and were culled six weeks after the second denudation. The left carotid arteries from both groups of mice were sham-operated, and acted as the control group.

The second group, referred to as the 'double-denudation' group, consisted of six age-matched rabbits which were subjected to two trans-luminal injuries of the right common carotid artery, with a six-week interval between the two procedures; these animals were culled six weeks after the second denudation. In both groups, at the time of each denudation to the right common carotid artery, the left common carotid artery was sham-operated (as detailed in Section 2.2.3.2) to act as a control; the resultant sham-operated arteries are henceforward referred to as the 'control' group.

After culling, each rabbit was perfusion-fixed, and the common carotid arteries were excised. The tissue was processed as detailed earlier (Section 2.2.3.4 and Figure 2.1). Cryostat-cut sections were prepared, and used for morphological and morphometric analysis. The degree of injury caused to each vessel was assessed according to a grading score, and the extent of intimal hyperplasia was measured morphometrically. Morphometric analysis was also used to determine the extent of staining for SA-β-gal activity in the various layers of the arterial wall. Other sections were used for immunohistochemical analysis, in order to identify the cell types showing SA-β-gal activity, and to determine whether these cells also showed evidence of proliferative activity. Further sections were subjected to TUNEL analysis, to establish whether the cells showing SA-β-gal activity also showed evidence of apoptotic activity.

Data concerning the extent of intimal hyperplasia and the prevalence of SA-β-gal staining were compared between groups using statistical analysis, as described in Chapter Two (Section 2.2.3.8).

3.2.3 Results

3.2.3.1 Morphology and morphometry of neointimal lesions in the single- and double-denudation groups

Morphology

H&E staining was used to study the morphology of cross-sections from control and denuded arteries. Neointimal formation occurred in all twelve denuded arteries. In two single-denudation arteries, and two double-denudation arteries, the injured vessel had become completely occluded by the time of culling. This occlusion appeared to consist of a combination of neointimal cells and acellular material, possibly including thrombus. This finding was in keeping with the results of Bosmans *et al.*, who found occlusive thrombus in approximately 30% of their rabbit carotid arteries following

balloon angioplasty [Bosmans *et al.* 1997]. Since in the four occluded vessels in the current study there was severe disruption of the architecture of the vessel, with loss of the integrity of the IEL, re-modelling of the vessel wall, and neovascularization of the occluding material, as shown in Figure 3.9, these arteries and their sham-operated controls were omitted from further study.

Figure 3.9 Morphology of occluded rabbit carotid artery

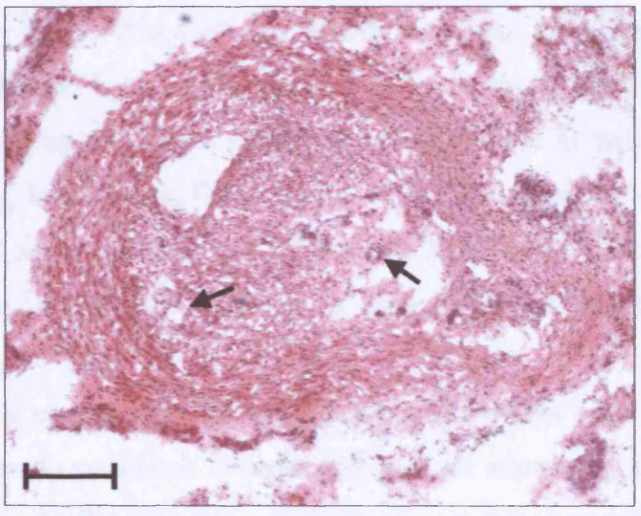

Figure 3.9 shows a representative cross-section of a rabbit carotid artery found to be occluded six weeks after a denudation injury. The tissue has been stained with haematoxylin and eosin. The vessel wall architecture is markedly disrupted, and the lumen is almost entirely filled with cellular and acellular material. Arrows show examples of re-canalization by new vessels. Bar = 125 μm.

The remaining eight denuded vessels (four single-denudation and four double-denudation) were patent at the time of culling. These eight vessels, together with their corresponding control arteries, were used for all further analysis described below.

Injury Scores

Injury scores were determined in the eight denuded arteries which remained patent at the time of culling. As described in Chapter Two (Section 2.2.3.9) the injury score for each vessel was determined by analysis of the cross-section for that vessel which showed the greatest degree of neointima formation. Using this method, among the single-denudation vessels, three had an injury score of grade 0, possessing an intact

IEL; the fourth vessel had a score of grade 1, with laceration of the IEL, but with intact deeper structures. Similarly, among the double-denudation group, three vessels showed grade 0 injury, while one showed grade 1 injury. Thus the single- and double-denudation groups appeared to have sustained equivalent degrees of injury.

Neointimal appearance in single- and double-denudation vessels

Figure 3.10 (overleaf) shows representative cryostat cross-sections, stained with H&E, from control, single- and double-denudation vessels. Panel A shows a typical sham-operated control vessel. Although not clearly seen with H&E staining, the lumen of the vessel is bordered by a single layer of ECs, which lie adjacent to the IEL. It is known from previous work that a small number of VSMCs lie within the rabbit intima, sometimes lying between duplicate layers of the IEL [Kockx *et al.* 1992], though again this is not obvious in Figure 3.10. Outside the IEL, the concentric VSMC layers of the media are clearly seen, and these are separated from the surrounding adventitia by the EEL.

Panel B shows a cross-section of carotid artery six weeks after a single denudation injury. A concentric neointima is seen, and appears somewhat less cellular than the underlying media. In Panel C, the neointima of a double-denudation vessel is shown. Again a neointima has formed, and this appears thicker than the single-denudation neointima shown in Panel B.

In single denudation vessels, the majority of neointimal VSMCs appeared to be aligned axially in the vessel wall. By contrast, after a second denudation, the neointima appeared stratified, containing two layers of cells (see, for example, Panel C): the deeper layer consisted of cells aligned axially, while the more superficial layer contained cells oriented circumferentially, and so perpendicular to the cells in the deeper intimal layer. The possible significance of this finding will be discussed below.

Figure 3.10 Morphology of control, single- and double-denudation rabbit carotid arteries

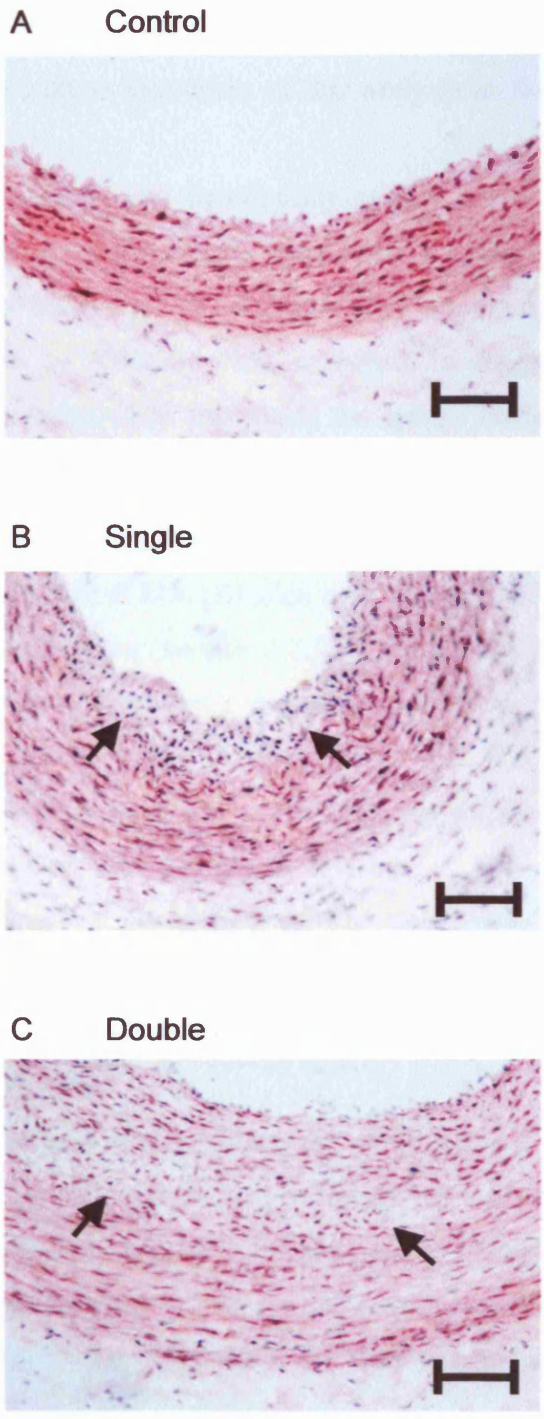

Figure 3.10 Photomicrographs of representative cross-sections from control (Panel A), single- (Panel B), and double-denudation (Panel C) rabbit carotid arteries. Sections were stained with haematoxylin and eosin. Arrows in Panels B and C indicate the internal elastic lamina of each injured vessel. The neointima in Panel C appears stratified: the more superficial cells appear to be aligned parallel with medial cells; the deeper neointimal cells appear more disorganized. Bar = 80 μm.

Morphometric analysis of neointimal and medial size

As mentioned in Chapter Two, (neo)intima/medial ratios were used as a surrogate marker of the VSMC proliferative response to the mechanical insult. Table 3.1 and Figure 3.11 (both overleaf) show the results of this analysis in the eight injured and eight control vessels.

As shown, neointimal formation was significantly greater in the double-denudation than in the single-denudation vessels, whether measured as neointimal cross-sectional area ($P = 0.003$), or as a fraction of the corresponding medial area ($P = 0.008$ by nested ANOVA, $P = 0.02$ by Wilcoxon rank sum test). In contrast, no statistically significant difference was found when comparing the medial cross-sectional areas of the vessels in the single- and double-denudation groups.

Extent of re-endothelialization in single- and double-denudation arteries

CD31, which is used as a marker of ECs [Albelda *et al.* 1990], was detected in *ex vivo* arteries as described in Chapter Two (Section 2.2.3.9). Figure 3.12 Panel A (page 138) shows a representative cross-section from a sham-operated artery, immunostained for CD31. The continuous brown stain circumscribing the lumen of the vessel demonstrates the presence of an intact EC layer. Similar results were obtained with randomly selected sections from the other control arteries.

Previous research has shown that the balloon catheter denudation procedure used in the current study leads to complete removal of the EC layer [Reidy *et al.* 1983]; this finding was confirmed in preliminary studies for this project using CD31 immunostaining (data not shown).

When single-denudation vessels were studied six weeks after a denudation injury (Figure 3.12 Panel B), an intact (or very nearly intact) layer of CD31 staining was demonstrated, suggesting that in the time between the denudation procedure and culling, complete re-endothelialization of the denuded surface had been achieved. The section shown is representative of the findings in the other single-denudation vessels.

Table 3.1 Luminal, (neo)intimal and medial cross-sectional areas of rabbit carotid arteries

Cross-sectional areas	Lumen	(Neo) intima	Media	(Neo)intima/ media ratio
Control (n=8)	9.76 ± 2.29	0.09 ± 0.02	4.21 ± 0.62	0.02 ± 0.01
Single (n=4)	7.35 ± 4.22	1.22 ± 0.38	4.21 ± 0.73	0.29 ± 0.10
Double (n=4)	9.61 ± 2.71	6.54 ± 3.02	4.16 ± 1.34	1.79 ± 0.91
P value (Control v. Single)	0.91	0.07	0.22	0.00005
P value (Single v. Double)	0.40	0.003	0.95	0.008

Table 3.1 The table shows the luminal, (neo)intimal and medial cross-sectional areas of control, single-denudation and double-denudation rabbit carotid arteries, together with the (neo)intima/media ratios for these vessels. Areas are expressed as mean ± s.d. (x 10^5 μm^2). (Neo)intima/media ratios are expressed as mean fractional values. Areas and ratios are rounded to two decimal places. *P* values were calculated using a nested ANOVA following log transformation of the data.

Figure 3.11 (Neo)intima / media ratios in rabbit carotid arteries

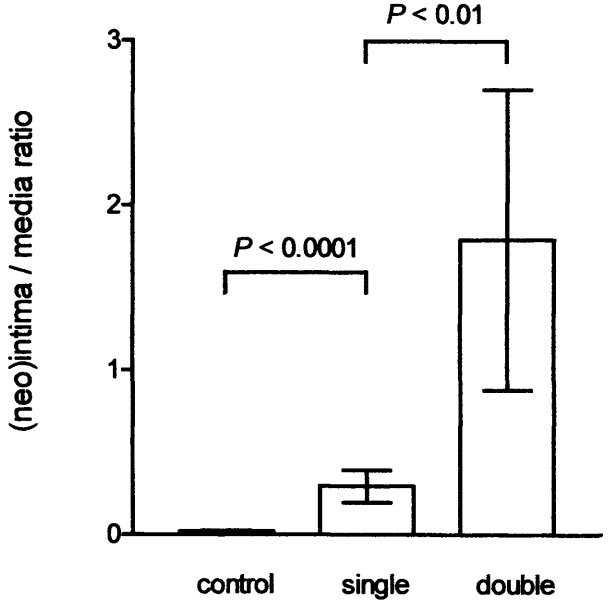

Figure 3.11 The graph illustrates the (neo)intima/media ratios of control, single- and double-denudation rabbit carotid arteries, using data from Table 3.1. Ratios are expressed as mean fractional values ± s.d.. *P* values were calculated using a nested ANOVA following log transformation of the raw data.

Figure 3.12 **Endothelial regeneration following denudation injuries in rabbit carotid arteries**

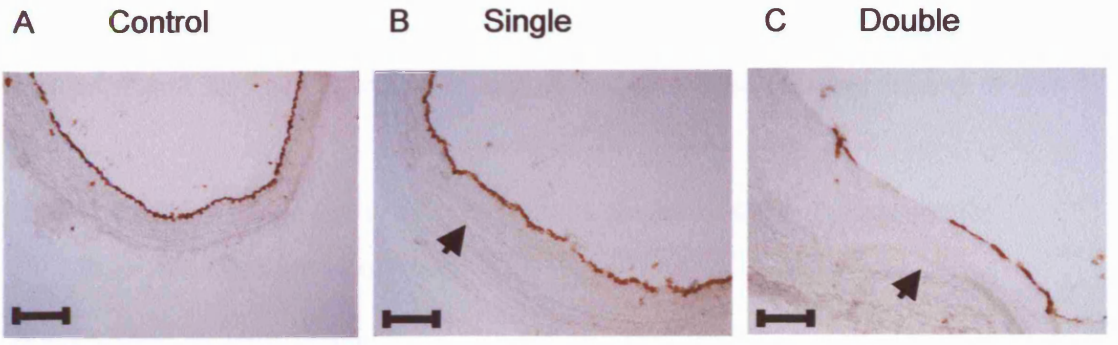

Figure 3.12 Photomicrographs of representative cross-sections from control (Panel A), single- (Panel B), and double-denudation (Panel C) rabbit carotid arteries immunostained for the EC surface antigen CD31 (brown stain). In single-denudation vessels the EC layer was consistently intact (or near-intact) six weeks after injury, while large areas devoid of endothelium were found in double-denudation vessels. Arrows in Panels B and C indicate the IELs of the injured vessels. Bar = 125 μm.

Figure 3.13 **pH dependence of β-galactosidase staining in control rabbit carotid arteries**

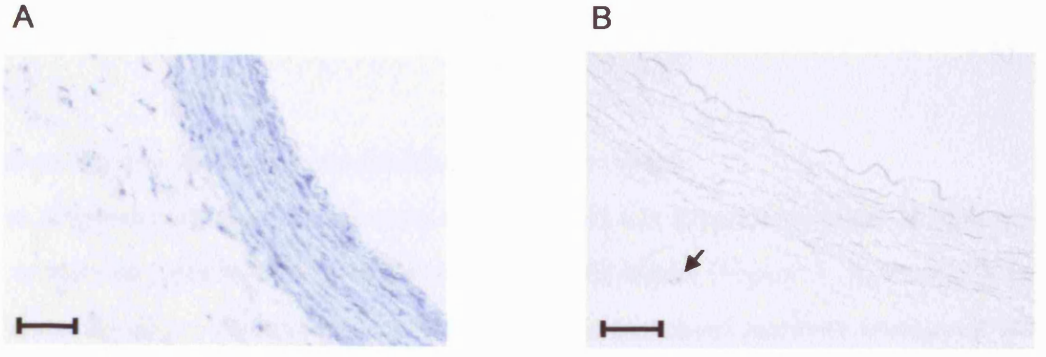

Figure 3.13 Representative photomicrographs showing control rabbit carotid arteries stained for β-galactosidase activity at pH 4.0 (Panel A) and pH 6.0 (Panel B). In Panel A positive staining is present throughout the vessel wall, reflecting the ubiquitous presence of acid β-gal activity. In contrast only occasional cells showed positive staining (see arrow in Panel B) when control vessels were stained for SA-β-gal activity; in control arteries these rare cells were found either in the adventitia or the media, but never bordering the vessel lumen. Bar = 80 μm.

Figure 3.12 Panel C shows a representative cross-section from a double-denudation vessel, stained for CD31 six weeks after the second injury. In contrast to the findings in single-denudation vessels, there are marked discontinuities in the EC layer, suggesting a failure of complete re-endothelialization. Indeed complete re-endothelialization was not observed in any of the double-denudation vessels in this study.

3.2.3.2 Detection of SA-β-gal activity in control, single- and double-denudation vessels: qualitative assessment

SA-β-gal activity in control arteries

As described previously, when sham-operated carotid arteries were stained for β-gal activity at pH 4.0, positive staining was detected in all layers of the vessel wall (Section 3.1.3.5 and Figure 3.7). A similar result, this time without an eosin counter-stain, is illustrated in Figure 3.13 Panel A (page 138). By contrast, Figure 3.13 Panel B shows a representative section from a control vessel stained for β-gal activity at pH 6.0 (SA-β-gal). Here no positive staining is seen in the intima or media, and only a single blue cell is seen in the adventitia. Indeed, in all the control vessels stained for SA-β-gal, only occasional blue cells were found in the adventitia, and the finding of blue cells in the media was even rarer. In no control vessels were blue cells found in the intima.

Panels A and D of Figure 3.14 (overleaf) show a further example of the rarity (or, as in this case, absence) of SA-β-gal staining in control arteries, here with an eosin counter-stain.

SA-β-gal activity in single- and double-denudation vessels

When single-denudation vessels were stained at pH 6.0, an accumulation of blue cells was consistently demonstrable in the neointima and media (Figure 3.14, Panels B and E). These SA-β-gal-positive cells, while present in increased numbers compared with control arteries, were still relatively rare, and tended to be found as isolated cells, scattered apparently randomly in the layers of the neointima and media, with no evident tendency to form clusters.

Figure 3.14 SA-β-gal staining in control, single- and double-denudation vessels

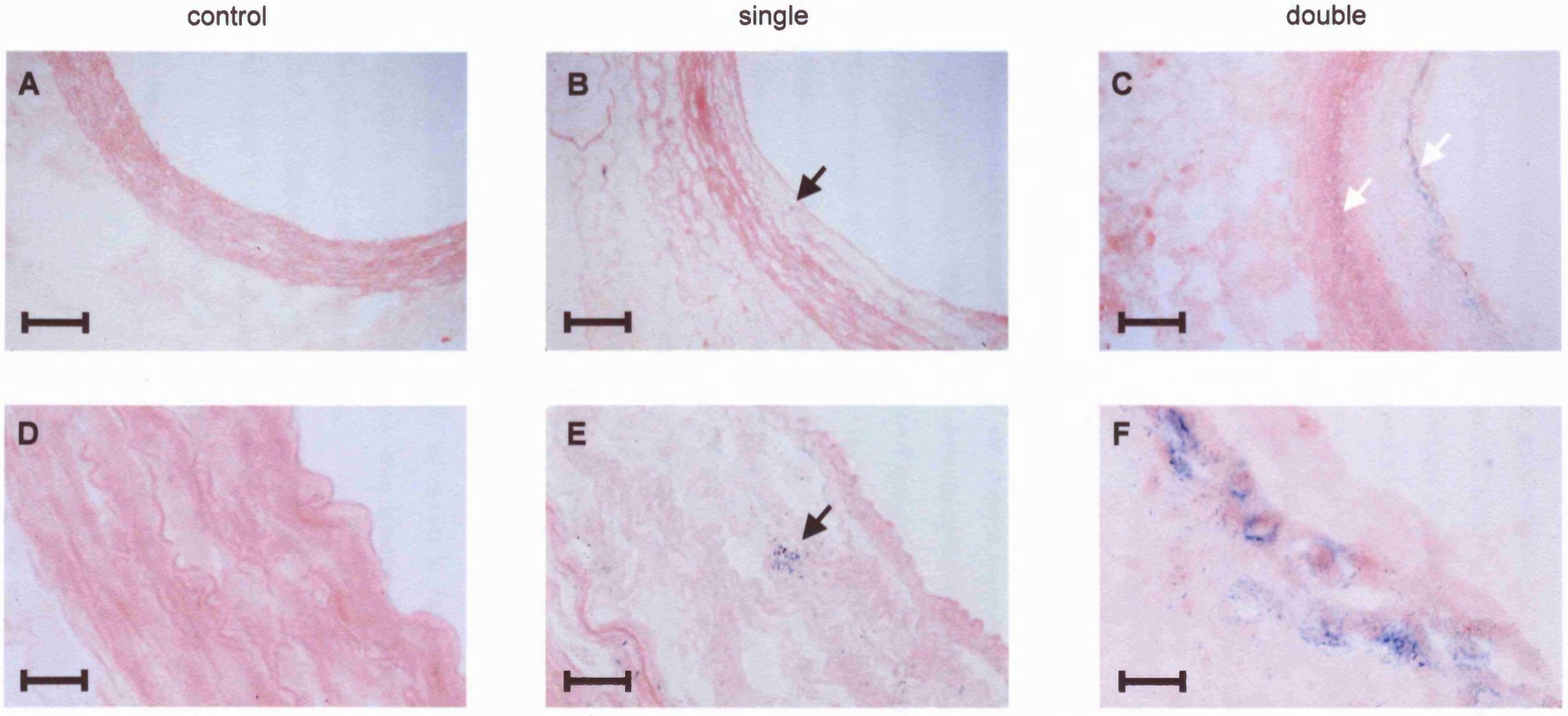

Figure 3.14 Photomicrographs showing SA-β-gal staining in representative carotid artery cross-sections from control (Panels A and D), single- (Panels B and E) and double-denudation (Panels C and F) vessels, counter-stained with eosin. Panels D, E and F show at high-power areas close to the vessel lumen within Panels A, B and C respectively. The black arrows in Panels B and E indicate a single positively-stained cell in the neointima of a single-denudation artery. In Panel C two layers of blue cells (white arrows) are seen in a double-denudation vessel: one near the luminal border of the neointima and one in the region of the IEL. Bar = 160 μm in Panels A, B and C, and 20 μm in Panels D, E and F.

In double-denudation vessels, however, the accumulation of SA-β-gal-positive cells was markedly increased, and these cells appeared either as a discontinuous layer near the luminal border of the neointima, or in clusters distributed at various depths in the neointima and media (Panels C and F of Figure 3.14).

In both single- and double-denudation vessels, a few scattered SA-β-gal-positive cells were found in the adventitia, but these occurred as rare isolated cells.

3.2.3.3 Assessment of the accumulation of SA-β-gal-positive cells in denuded vessels

The extent of SA-β-gal activity in the carotid arteries was assessed morphometrically, as described in Chapter Two (Section 2.2.3.7), and was expressed as the percentages of neointimal and medial cross-sectional areas occupied by blue cells.

Figure 3.15 (overleaf) shows the results of this analysis. As mentioned above, no blue cells were detected in the intima of any of the control arteries, and in these vessels only a negligible percentage of the medial cross-sectional area was occupied by blue cells. After a single denudation, sufficient SA-β-gal-positive cells emerged to occupy a measurable percentage of the neointimal cross-sectional area (Figure 3.15, Panel A). A second denudation led to a further accumulation of SA-β-gal-positive cells in the neointima, the percentage of neointimal cross-sectional area covered by blue cells rising from 0.06% to 0.99% ($P < 0.001$ by nested ANOVA, $P = 0.02$ by Wilcoxon rank sum test). Similarly, the percentage of medial area covered by blue cells rose from 0.00068% to 0.01% after a single denudation, and to 0.11% after a second injury ($P < 0.02$ by nested ANOVA, $P = 0.02$ by Wilcoxon rank sum test) (Figure 3.15, Panel B).

The progressive increase in medial occupation by blue cells appeared to parallel the accompanying rise in neointimal occupation (as shown in Figure 3.15), although the percentage of media occupied by blue cells was always markedly lower than the corresponding percentage of neointimal area.

As mentioned in Chapter Two, the occurrence of SA-β-gal-positive cells in the adventitia of vessels in all three groups was assessed by counting individual cells. The mean numbers of SA-β-gal-positive cells per cross-section in the control, single- and double-denudation groups were 2.4, 1.7 and 2.2 respectively.

Figure 3.15 Percentage areas of SA-β-gal staining in the (neo)intima and media of rabbit carotid arteries

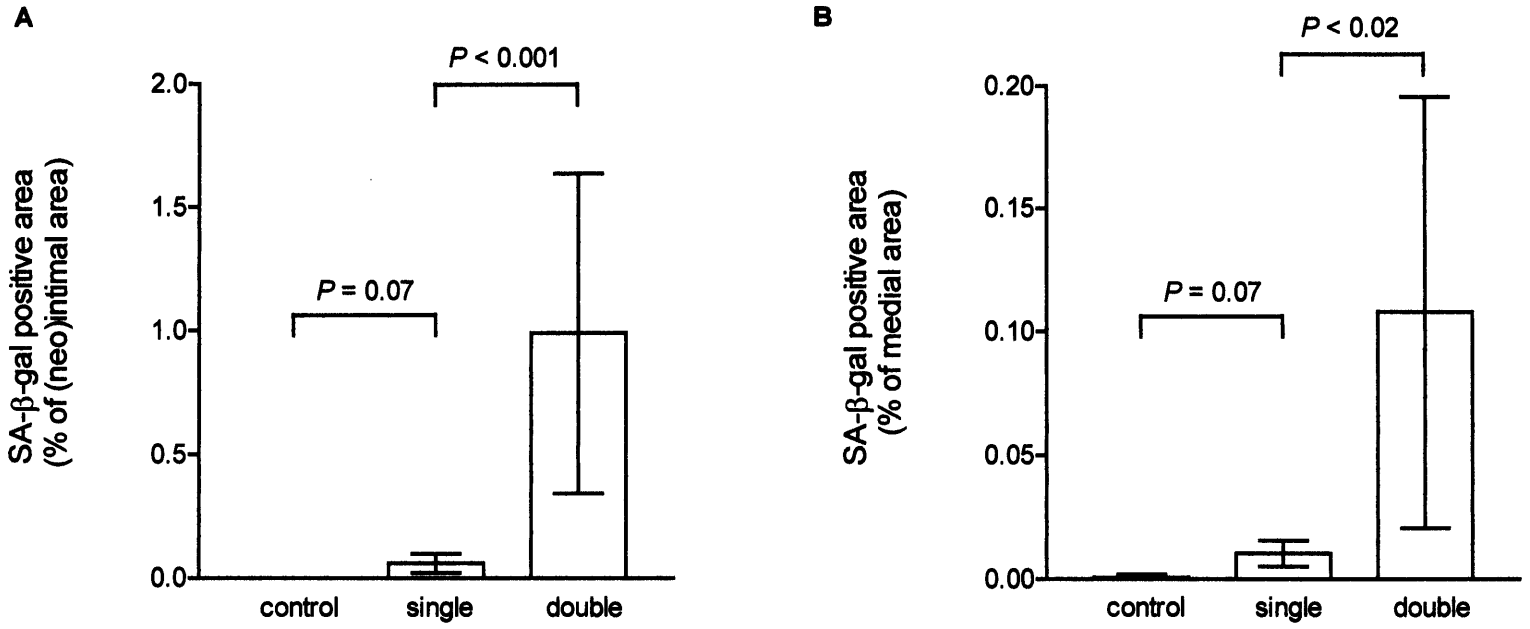

Figure 3.15 illustrates the percentages of (neo)intimal (Graph A) and medial (Graph B) areas covered by SA-β-gal-positive cells in control, single- and double-denudation rabbit carotid arteries. Percentages are shown as mean values +/- s.d.. *P* values for comparisons between control- and single-denudation percentages were calculated using the Wilcoxon rank sum test, since data were non-parametric and zero values in the control group precluded log transformation. *P* values for comparisons between single- and double-denudation vessels were calculated using a nested ANOVA following log transformation of the data; when *P* values were re-calculated using non-parametric tests, differences between single- and double-denudation groups remained statistically significant for both neointimas and medias.

3.2.3.4 Identification of SA-β-gal-positive cell types

Immunohistochemistry was used to determine which cell types expressed SA-β-gal activity in the carotid artery cross-sections. Antibodies were used to detect the presence of CD31 (for ECs), smooth muscle α-actin (for VSMCs), and CD45 (a leukocyte marker found on all white cells, including T lymphocytes [Lefrancois *et al.* 1986] and cells of the monocyte/macrophage lineage [Kurtin *et al.* 1985]).

CD31 labelling

When single- and double-denudation vessels which had been stained for SA-β-gal activity were immunostained for CD31, cells were detectable which co-stained for SA-β-gal activity and the presence of CD31 (as shown in Figure 3.16, Panels A and B, overleaf). These co-staining cells were more numerous in double-denudation than in single-denudation vessels, assessed qualitatively. These cells bordered the vessel lumen, and in the double-denudation vessels tended to be found in regions neighbouring discontinuities in the endothelium, as is illustrated in the figure.

Smooth muscle α-actin labelling

Panels C and D of Figure 3.16 show a representative example of smooth muscle α-actin labelling in a double-denudation vessel. As shown, numerous cells were detected which co-stained for SA-β-gal activity and for smooth muscle α-actin. Such cells were detected in both the neointima and the media, and the clusters of blue cells in the neointima of double-denudation vessels (mentioned above) were found to co-stain for smooth muscle α-actin. Similar co-staining was found in the neointima and media of single-denudation vessels, though as mentioned above, blue cells were rarer in these arteries than in double-denudation vessels.

CD45 labelling

Study of near-adjacent sections stained for either CD31 or smooth muscle α-actin suggested that all the blue cells in these sections stained positively for one or other of these antigens. Nevertheless, immunohistochemical detection of CD45 was undertaken in order to establish whether leukocytes might also express SA-β-gal activity.

Figure 3.16 Identification of SA-β-gal-positive cell types

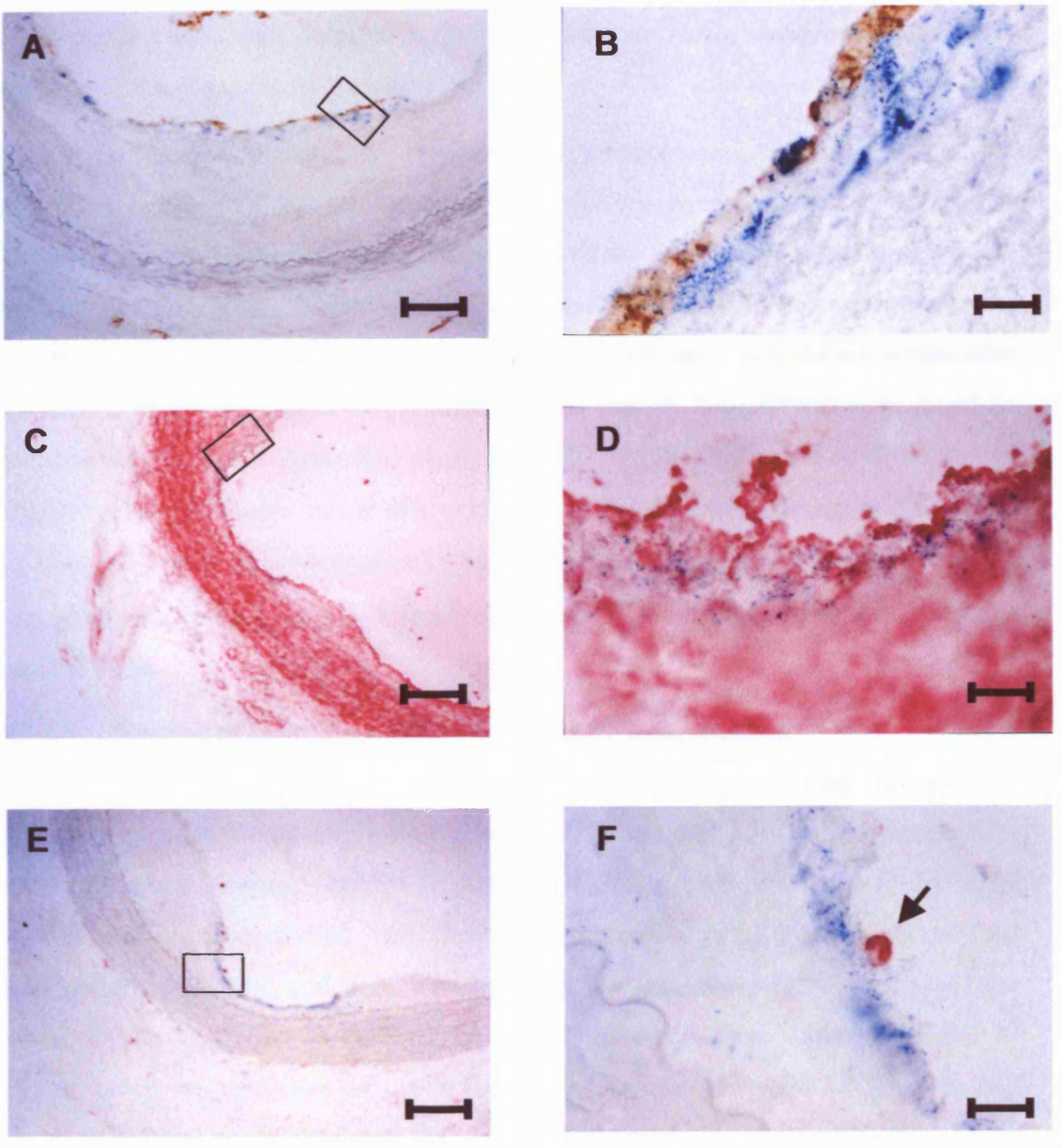

Figure 3.16 Photomicrographs showing immunostaining for CD31 (Panels A and B, brown), smooth muscle α-actin (Panels C and D, red) and CD45 (Panels E and F, red) in representative double-denudation rabbit carotid artery cross-sections. Panels B, D and F show at high-power the boxed areas in Panels A, C and E respectively. The SA-β-gal (blue) staining co-localizes with the immunostaining in Panels B and D, but not in Panel F. The arrow in Panel F indicates a CD45-positive cell apparently adhering to SA-β-gal-positive cells in the neointima; these blue cells were found, in adjacent cross-sections, to be VSMCs. Bar = 160 μm in Panels A, C and E, and 20 μm in Panels B, D and F.

Panels E and F of Figure 3.16 show a representative result from these experiments. No SA-β-gal-positive cells in any sections studied (from either single- or double-denudation vessels) showed CD45 labelling. Instead, as illustrated in the figure, some CD45-positive cells were detected in the lumen, adjacent to the vessel wall, apparently adhering to SA-β-gal-positive cells.

3.2.3.5 Detection of proliferating cells in carotid artery cross-sections

Immunohistochemistry was also used to detect proliferating cells in double-denudation carotid arteries; several cross-sections from each of the four double-denudation vessels were stained for PCNA. These sections contained a low but measurable number of PCNA-positive cells, suggesting residual cellular proliferative activity six weeks after the second injury. Figures 3.17 (overleaf) shows that PCNA-positive cells could be detected in both the neointima (Panels A, B and C) and the media (Panel D) of injured arteries. Although these vessels also contained a considerable number of SA-β-gal-positive cells, none of these blue cells was found to stain positively for PCNA. There was no apparent relationship between the location of proliferating cells and SA-β-gal-positive cells.

3.2.3.6 Detection of apoptotic cells in carotid artery cross-sections

Cross-sections from double-denudation arteries were labelled using the TUNEL technique in order to detect apoptotic cells. Figures 3.18 and 3.19 (both on page 147) show representative results of this analysis. TUNEL-positive cells were found in all arterial cross-sections studied. They were few in number (ranging from one to four cells per cross-section), and were found in both the neointima (Figure 3.18) and the media (Figure 3.19). The TUNEL-positive nuclei tended to show a marked degree of fragmentation, as confirmed on DAPI fluorescent staining (Figure 3.18 Panel B, and Figure 3.19 Panel B), suggesting that they were late apoptotic cells.

As mentioned above, a large number of SA-β-gal-positive cells were found near the luminal border of the neointima of double-denudation vessels. In none of the sections studied with TUNEL analysis was any TUNEL-positivity found in this region of the vessel wall. Indeed, it was notable that despite an extensive survey of the sections analysed, including sections containing large numbers of SA-β-gal-positive cells, no cells were detected which displayed both TUNEL- and SA-β-gal-positivity.

Figure 3.17 Detection of cellular proliferation and senescence in injured arteries

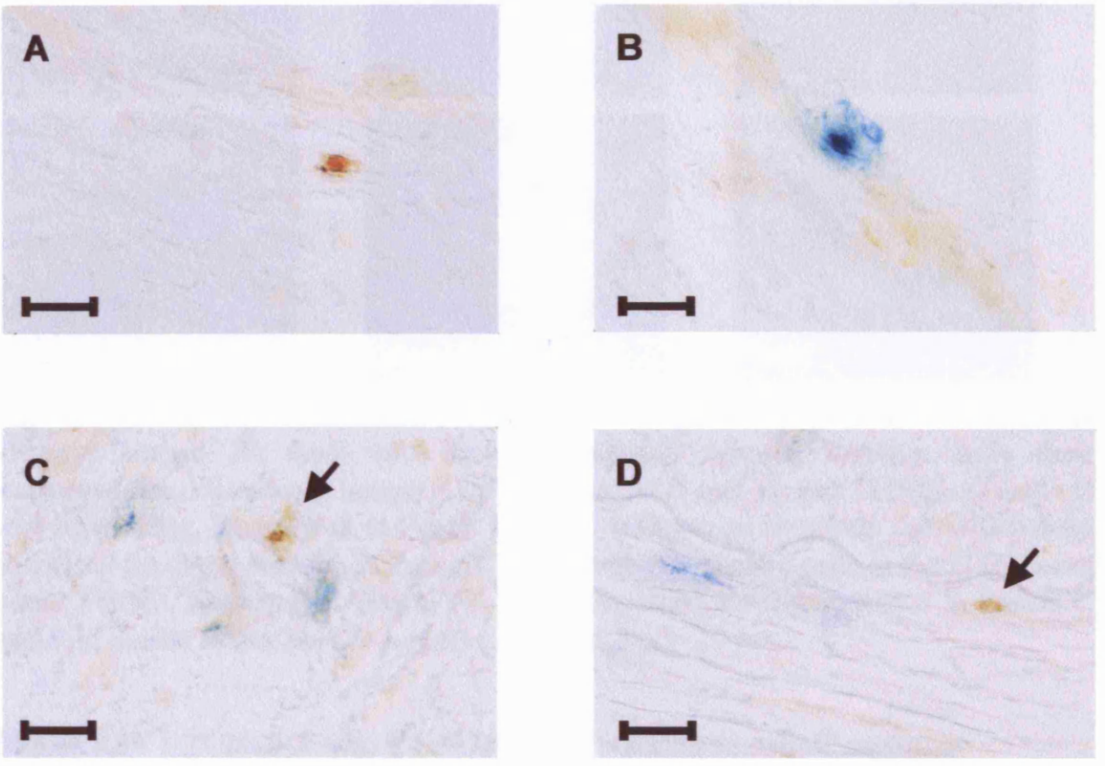

Figure 3.17 Photomicrographs showing immunostaining for PCNA (brown) in representative double-denudation rabbit carotid artery cross-sections. The upper panels show an isolated PCNA-positive cell (Panel A) and an isolated SA-β-gal-positive cell (blue, Panel B), both in the neointima. The lower panels show areas of neointima (Panel C) and media (Panel D) where proliferating cells (arrows) and senescent cells are found in close proximity. The SA-β-gal staining does not co-localize with the PCNA immunostaining. Bar = 10 μm in Panels A, B and C, and 12.5 μm in Panel D.

Figure 3.18 TUNEL analysis and SA-β-gal staining in rabbit neointima

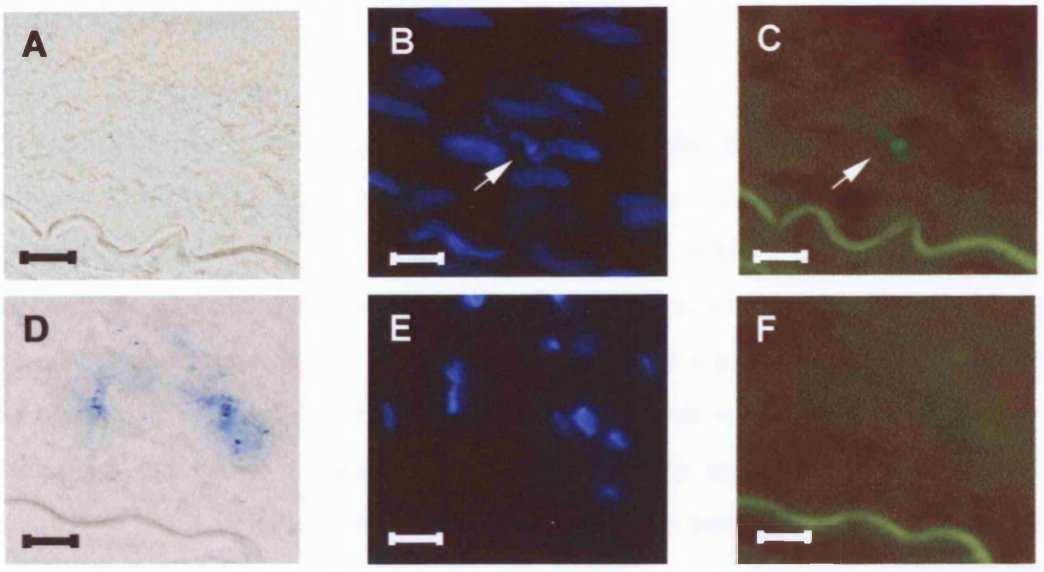

Figure 3.18 shows representative bright-field images of two areas of neointima (Panels A and D) from two double-denudation vessels, together with their corresponding fluorescent images of DAPI (Panels B and E) and TUNEL (Panels C and F) staining. The arrows in Panels B and C indicate an apoptotic cell which does not show SA-β-gal staining in Panel A. The SA-β-gal-positive cells in Panel D do not show TUNEL fluorescence (Panel F). The background autofluorescence in Panels C and F is similar to that seen in negative controls. Bar = 10 μm.

Figure 3.19 TUNEL analysis and SA-β-gal staining in rabbit media

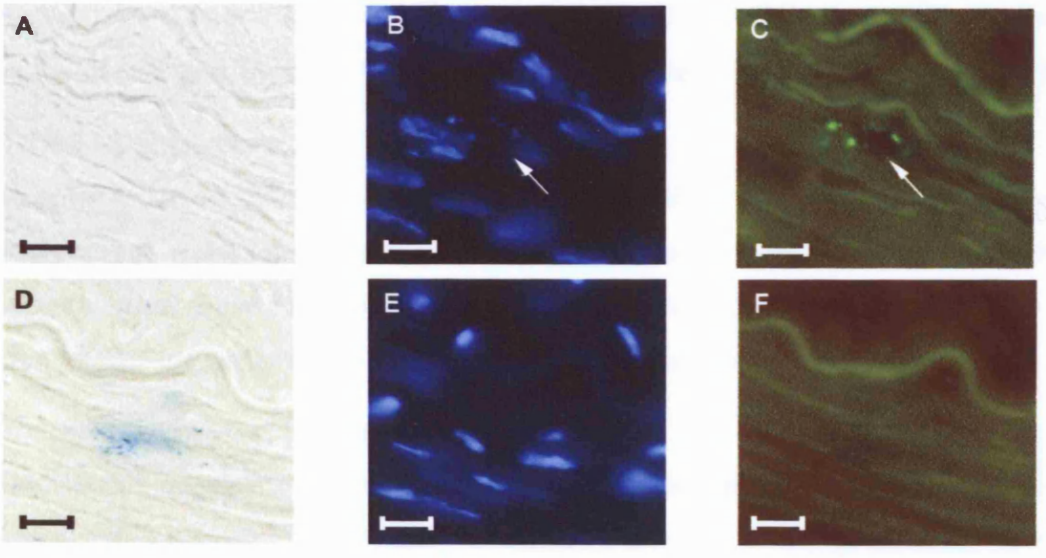

Figure 3.19 shows bright field images of two areas of media (Panels A and D) from two double-denudation vessels, together with their corresponding fluorescent images of DAPI (Panels B and E) and TUNEL (Panels C and F) staining. The arrows in Panels B and C indicate an apoptotic cell which does not show SA-β-gal staining in Panel A. The SA-β-gal-positive cell in Panel D does not show TUNEL fluorescence (Panel F). The background autofluorescence in Panels C and F is similar to that seen in negative controls. Bar = 10 μm.

3.2.4 Discussion

3.2.4.1 Key findings

The results of the *in vivo* experiments described in this chapter can be summarized as follows. In those vessels which did not become totally occluded, the denudation injury used in this study led to a consistent degree of injury, with no (or minimal) disruption of the IEL. Morphometric studies showed that a second denudation injury led to a greater degree of neointima formation than a single injury, while the medial cross-sectional area was not significantly affected by denudation injuries. Furthermore, the neointima of vessels denuded twice had a stratified appearance, with an apparent difference in the alignment of the neointimal cells in the superficial and deep layers. The endothelial layer completely regenerated after a single denudation, but failed to do so after a second injury. Staining of control vessels at pH 6.0 showed only very occasional cells expressing SA-β-gal activity, and these cells were confined to the media and adventitia; after a single denudation small numbers of SA-β-gal-positive cells were also found in the neointima; their numbers in the neointima and media increased following a second denudation. Immunohistochemistry confirmed that these SA-β-gal-positive cells were endothelial and vascular smooth muscle cells, and that they did not express PCNA. TUNEL analysis showed that while apoptosis was present in the arterial wall, it occurred in cells distinct from those showing SA-β-gal activity.

3.2.4.2 Comments on the experimental design

In order to discuss the implications of the above findings, it is worth firstly reviewing the changes which are known to occur in the arterial wall following denudation injuries, since these data informed the design of the experiments described in this chapter, and are useful in the interpretation of the results given above.

The use of endothelial denudation models

Endothelial denudation models have been used extensively over the last twenty-five years; they have employed a variety of different arteries (including the iliac, femoral, carotid, and coronary arteries, as well as the aorta) in a number of species (including mouse, rat, rabbit and pig) [for example: Reidy *et al.* 1982, Clowes *et al.* 1986, Weidinger *et al.* 1990, Schneider *et al.* 1993, Burchenal *et al.* 1996, Bosmans *et al.* 1997, Perlman *et al.* 1997, Hutter *et al.* 2003]. Such research has often been undertaken in order to study the clinical scenario of post-angioplasty re-stenosis.

Because the injury leads to intimal hyperplasia, a process which also occurs in atherosclerosis, denudation studies have also been used to investigate certain aspects of atherogenesis [for example: Moore *et al.* 1982, Lindner and Reidy 1991, Niimi *et al.* 1994, Efendy *et al.* 1997, Dzau *et al.* 2002].

Histological changes following denudation injuries

The changes in the arterial wall which follow endothelial denudation can be summarized as follows. Almost immediately after removal of the endothelium, platelets [Groves *et al.* 1979] and leukocytes [Reidy and Silver 1985] adhere to the luminal surface of the vessel wall. As noted previously, platelets contain mitogens and chemoattractants for VSMCs (such as PDGF), as well as pro-thrombotic agents. Leukocytes enter the vessel wall, and are subsequently found in the gradually developing neointima [Ferns *et al.* 1991]. A few of these are neutrophils [Jonasson *et al.* 1988, Verheyen *et al.* 1988], while others are T cells [Jonasson *et al.* 1988], suggesting an inflammatory element to the vessel wall response. Macrophages have also been detected in the neointima formed following denudation injury in some normocholesterolaemic animals, and these cells can become foam cells if the animals have been fed a high-cholesterol diet [Verheyen *et al.* 1988]. Macrophage invasion is in fact not found in the neointimas of normocholesterolaemic rabbits [Azuma *et al.* 1995].

Another major component of the vessel's response to injury comprises proliferation of VSMCs within the media, migration of VSMCs from the media to the neointima, and their further proliferation within this newly-forming layer [Clowes *et al.* 1983, Clowes and Schwartz 1985]. These changes have been attributed to the release of chemoattractants and growth factors released by activated platelets adhering to the denuded vessel wall [Fingerle *et al.* 1989] and to the release of cytokines by other cells [Liu *et al.* 1989]. Basic fibroblast growth factor, released from dead vascular cells, has been postulated to be the major mitogen controlling the proliferation of VSMCs following trans-luminal injury [Lindner and Reidy 1991]. Other mediators involved in the promotion of intimal proliferation and matrix accumulation include transforming growth factor-β, angiotensin II, epidermal growth factor, and IGF-factor 1 [reviewed in Dzau *et al.* 2002].

Bone marrow-derived cells may contribute to neointimal SMC content. Female C57BL/6 have been subjected to total body irradiation, and then transfused with

marrow cells from congenic male donors; after endothelial denudation of their iliac arteries, approximately half of the neointimal α-smooth muscle actin-containing cells are of male donor origin, suggesting that they originate in the bone marrow [Campbell *et al.* 2001]. Stromal cell-derived factor-1α, which is involved in the mobilization and homing of stem cells, has been demonstrated in the neointima of apoE-deficient mice, while systemically-injected peripheral blood progenitor cells are recruited to neointimal lesions after vascular injury [Schober *et al.* 2003].

There is a heterogeneity in the proliferative capacity of medial VSMCs [Haudenschild and Grunwald 1985]; of those VSMCs which migrate to the neointima, only fifty percent subsequently proliferate [Clowes and Schwartz 1985]. There is also a well-documented alteration in the VSMC phenotype following denudation injury: this apparently reversible change involves a move from a contractile towards a synthetic phenotype, with a loss of myofilament density, and the development of large quantities of endoplasmic reticulum and free ribosomes [Manderson *et al.* 1989], decreased desmin and increased vimentin expression [Kocher *et al.* 1984], and a change from α-actin to β-actin expression [Barja *et al.* 1986].

In areas of incomplete re-endothelialization, the luminal border of the vessel wall becomes lined with phenotypically altered VSMCs, which form a layer which has been termed a 'pseudoendothelium' [Reidy 1985]. These cells again show a decline in myofilament density. The pseudoendothelium is non-thrombotic, but lacks the permeability barrier properties of the normal endothelium. The presence of such a pseudoendothelium does not retard the rate of re-endothelialization of an area denuded by balloon injury [Reidy 1988].

Denudation injuries lead to a wave of apoptotic activity [Han *et al.* 1995, Bochaton-Piallat *et al.* 1995, Perlman *et al.* 1997]. In the media, this wave starts very soon after the mechanical insult: in one study, involving balloon denudation of rat carotid arteries and rabbit external iliac arteries, up to 70% of medial VSMCs were apoptotic within thirty minutes of the injury [Perlman *et al.* 1997]; the extent of apoptosis in the media then declined sharply over the following few hours. A wave of apoptosis is also observed in the developing neointima; this wave reaches its peak between one and three weeks after the denudation, depending on the model studied [Han *et al.* 1995, Bochaton-Piallat *et al.* 1995]. In the rat model, the wave of neointimal apoptotic activity has disappeared by six weeks after the denudation injury [Bochaton-Piallat *et*

al. 1995]. The time-course of the apoptotic wave in the rabbit carotid model has not been fully characterized.

ROS may play a role in the promotion of apoptosis in denuded vessels. An intracellular rise in ROS levels can mediate p53-dependent apoptosis *in vitro* [Johnson *et al.* 1996]. More recently, increased oxidative stress has been detected in the injured vessel wall using an assay of glutathione levels in denuded rabbit carotid arteries [Pollman *et al.* 1999], and this alteration of the redox status was associated with induction of pro-apoptotic stress-activated protein kinases (SAPK). Medial VSMCs were more susceptible to apoptosis than their neointimal counterparts [Pollman *et al.* 1999].

Following denudation injuries ECs proliferate and migrate into the denuded area from neighbouring regions of the vessel; in a rat denudation model a combination of EC migration and proliferation caused a sheet of regenerating endothelium to advance at approximately 70 μm per day in the circumferential direction, and about six times faster axially [Haudenschild and Schwartz 1979].

Nearly thirty years ago it was observed that areas which re-endothelialized earliest developed least intimal thickening [Stemerman *et al.* 1977]. Re-endothelialization appears to inhibit both migration and proliferation of VSMCs. Thus in a rat denudation model, VSMCs migrated into the intima only in those areas not re-covered by regenerating endothelium seven days after injury [Haudenschild and Schwartz 1979]; in another denudation model, rates of VSMC proliferation in the intima were lower in re-endothelialized than in persistently denuded areas [Clowes *et al.* 1983]. Conversely, repeated endothelial removal promotes subsequent intimal thickening [Niimi *et al.* 1994]. Recently over-expression of a specific inhibitor of EC growth, endostatin, in a mouse arterial denudation model, has been shown to retard re-endothelialization, and this retardation was associated with increased neointima formation [Hutter *et al.* 2003].

A potential mechanism for the interaction between endothelial denudation and intimal hyperplasia is suggested by *in vitro* evidence that ECs can inhibit VSMC proliferation via NO signalling [Scott-Burden *et al.* 1993], and that serial passage of ECs leads to a progressive decline in eNOS activity [Matsushita *et al.* 2001]. It has been suggested that the decline in NO secretion by ECs which follows denudation injuries [Niimi *et al.* 1994], or the suppression of their NO production by ROS [Jaimes *et al.* 2001], may

remove one inhibitory control on VSMC proliferation and migration [Dzau *et al.* 2002].

Previous studies involving balloon injury to the rabbit carotid artery

The histological changes described so far are thought to occur in most endothelial denudation models. The rabbit carotid artery model employed in the current study has been used extensively in previous investigations [for example: Reidy *et al.* 1983, Reidy 1988, Manderson *et al.* 1989, Azuma *et al.* 1990, Niimi *et al.* 1994, Azuma *et al.* 1995, Bosmans *et al.* 1997, Efendy *et al.* 1997, Pollman *et al.* 1999, Rosenthal *et al.* 2002, Herdeg *et al.* 2003, Francis *et al.* 2003].

The model was first used by Reidy *et al.* specifically to explore the question of whether rabbit ECs have a limited replicative life-span *in vivo* [Reidy *et al.* 1983]. It had previously been noted that after denudation of rabbit aortas, EC replication halted after fourteen days of vigorous proliferative activity [Reidy *et al.* 1982]. Attention then turned to the carotid artery, since the more straightforward anatomy at this latter site (not complicated by multiple branch-points) simplified the study of endothelial re-growth. Following balloon denudation of the carotid artery (using a 2F saline-filled embolectomy catheter, as employed in the current study), endothelial re-growth progressed from either end of the vessel, but, as in the aorta, stopped after fourteen days, leaving an area still devoid of endothelium [Reidy *et al.* 1983]. A second catheter injury (this time effected by passing a nylon catheter along the artery, removing a zone of endothelium approximately ten cells wide) led to further EC replication, but ECs did not spread or migrate to cover the previously denuded area. This second proliferative response was cited as evidence that the initial cessation of replicative activity had not been caused by replicative senescence [Reidy *et al.* 1983]. It did not exclude the possibility, though, that the original halt in endothelial re-coverage was caused by a combination of contact inhibition occurring in central areas of the partially regenerated endothelium, and replicative senescence occurring at the leading edge of endothelial regrowth. If this were the case, the re-activation of replication by a second injury could be explained by the release from contact inhibition of non-senescent cells in the re-denuded area.

Azuma *et al.* have studied the kinetics of re-endothelialization in this model in more detail [Azuma *et al.* 1990]. They found that one week after injury, approximately 30% of the arterial luminal surface was covered with regenerating ECs, this percentage

rising to 95% by four weeks; by six weeks after the injury full endothelial coverage had been achieved. In this study it was found that regenerated ECs differed from 'native' cells in that they were elongated in shape and irregularly orientated. There was also evidence of EC dysfunction, as manifested by impaired endothelium-dependent relaxation in response to acetylcholine. Intimal thickening and VSMC proliferation were also noted, and no evidence was found of lipid accumulation in the arterial wall.

In a later study using the rabbit model, the same group performed two balloon denudations of the right carotid artery six weeks apart, then culled the animals two weeks after the second injury [Niimi *et al.* 1994]. Following this protocol, they found that full endothelial coverage had been achieved within two weeks of the second injury, suggesting that re-endothelialization proceeded more rapidly following a double- than a single-denudation. They also noted that intimal thickening became more pronounced after the second denudation injury, and speculated that this might result from reduced production of NO by the endothelium.

In a further study, the same group performed balloon denudation of the right carotid arteries of a group of ten-week-old Japanese White rabbits; six weeks later they injured both the right and left carotid arteries [Azuma *et al.* 1995]. They then used scanning electron microscopy and immunohistochemistry to investigate the resultant EC and VSMC proliferative responses. Cells expressing PCNA were detected in both the neointima and the media within twenty-four hours of a single denudation; their number rose dramatically over the next forty-eight hours, then gradually declined almost to basal levels over the following four to six weeks. In contrast, after a second denudation injury, there was a more pronounced and more prolonged proliferative response in both the neointima and the media, such that a substantial number of cells still showed evidence of proliferative activity in both layers six weeks after the second injury, although the wave did appear to have peaked two weeks earlier. After a double injury, the proliferative response in the neointima was more pronounced, and occurred earlier, than that in the media.

When rabbits whose carotid arteries have undergone endothelial denudation are subsequently fed a high cholesterol diet, lipid is deposited in the neointima [Efendy *et al.* 1997]; the neointima contains a peri-luminal layer of densely populated cells, a central lipid-rich layer, and a deeper VSMC-rich region. The rabbit carotid balloon

denudation model has therefore sometimes been used in the study of atherogenesis. It has subsequently also been employed to evaluate the potential benefits of agents as diverse as brachytherapy, sulphated oligosaccharides, retinoids and garlic extract [Efendy *et al.* 1997, Rosenthal *et al.* 2002, Herdeg *et al.* 2003, Francis *et al.* 2003] in the context of either atherosclerosis or post-angioplasty re-stenosis.

Benefits of using the rabbit carotid denudation model in the current study

There were several reasons for choosing the rabbit carotid artery denudation model in particular in the current study. Firstly, as just detailed, the kinetics of the proliferative response to balloon injury in this model have previously been documented in detail. This was important in a study primarily designed to investigate an attenuation of proliferative capacity. Secondly, the capacity for rabbits to undergo repeated arterial denudation meant that the proliferative response could be re-triggered, and therefore prolonged, by a second injury. The size of rabbit carotid arteries, and the virtually complete de-endothelialization known to occur following the standard balloon denudation [Reidy *et al.* 1983], meant that the second injury could safely be regarded as affecting the site already injured. Another benefit of the model is that it affords a readily-available control, using sham operations of the contralateral carotid artery.

Further comments concerning the experimental design and methods used

The use of a six-week interval between denudation injuries, and between the final injury and culling, was based on the studies detailed above, showing that such an interval allows time for a full-blown proliferative response to occur (and indeed to begin to decline) [Azuma *et al.* 1990, Niimi *et al.* 1994, Azuma *et al.* 1995].

The prevalence of SA-β-gal-positive cells in the neointima and media was expressed in terms of the percentage areas of neointima and media covered by blue cells. Percentage areas were used in preference to absolute areas in order to control for variations in arterial size between animals. The use of individual cell counts was considered, but it was found in preliminary experiments that the use of a counter-stain to detect cell nuclei made the SA-β-gal staining difficult to visualize.

In the immunohistochemical studies, the two staining kits (the New Fuchsin Chromogenic Substrate System and the Liquid DAB Plus kits) were each tested on carotid artery cross-sections to determine which method gave the most effective staining for each cell type investigated. For example, while the fuchsin system was

able to detect rabbit ECs (in the same way as it had labelled HUVECs in the *in vitro* studies), it in fact proved less effective than the DAB system in demonstrating the presence (or absence) of a continuous endothelium in excised arteries.

TUNEL has been employed since 1992 for the detection of programmed cell death, and relies on the incorporation of dUTP (conjugated with agents such as fluorescein or biotin) at sites of DNA breaks, as are found in the fragmented DNA of apoptotic cells [Gavrieli *et al.* 1992]. The role of TUNEL in detecting apoptosis in vascular tissue has been established since it was used to detect apoptotic VSMCs in human atherosclerotic plaques [Geng and Libby 1995], and its use in balloon-injured rabbit carotid artery has been described more recently [Kamenz *et al.* 2000].

3.2.4.3 Discussion of the results

The aim of the *ex vivo* experiments described in this chapter was to assess whether a cellular proliferative response to a denudation injury could lead to the emergence of senescent cells. It was important to characterize the nature of the proliferative responses to single- and double-denudation injuries in order to correlate these with the development of senescence. The EC proliferative response was assessed by immunohistochemical detection of CD31; (neo)intima/media ratios were used as an indication (though not a direct measurement) of the degree of VSMC proliferation. In addition, the presence of proliferating cells six weeks after a double-denudation was detected by staining for PCNA, and the results of this analysis will be discussed later in this Section.

If the proliferative response and the occurrence of senescence were to be compared between the single- and double-denudation groups, it was desirable that the severity of the initial trauma to the vessel wall should be similar in each group. The similarity of the injury scores in the eight denuded arteries which did not occlude suggests that the balloon catheter technique employed in the current study delivered a comparatively consistent mechanical insult.

EC proliferative response to denudation injury

There were clear-cut differences in the vascular cell proliferative response to injury following single- and double-denudations. Complete re-endothelialization occurred after a single denudation, but not after a second injury. The complete re-endothelialization six weeks after a single injury in this model is consistent with the

findings of Azuma *et al.* mentioned earlier [Azuma *et al.* 1990]. It also corresponds with research mentioned in Chapter One, showing that complete regeneration of large areas of endothelium can be achieved in rat carotid arteries, provided that the denudation injury is performed without trauma to the media [Lindner *et al.* 1989]. As mentioned above, most of the arteries in the current study showed an intact IEL after injury, and so complete repair of the endothelium might be expected. As mentioned earlier, Reidy *et al.* have described incomplete re-endothelialization of the rabbit carotid artery up to twelve weeks after endothelial denudation with a 2F saline-filled embolectomy catheter [Reidy *et al.* 1983]; in that study, though, the entire length of the common carotid artery, from the aorta to the bifurcation of the internal and external carotid arteries was denuded, while a much shorter section was injured in the current experiments.

The failure of the endothelium to regenerate completely after a second injury in this study could be interpreted as a failure of the ECs to continue to proliferate as a result of replicative senescence. On the other hand, as mentioned earlier (Section 3.2.4.2), Reidy *et al.* argued that their ability to re-stimulate EC replication through a second denudation injury [Reidy *et al.* 1983] disproved the theory that the initial cessation in EC replication was caused by replicative senescence. Thus, for direct evidence of *in vivo* EC senescence, one must turn to the SA-β-gal experiments discussed below.

The failure of complete re-endothelialization in double-denudation vessels in the current study might appear to be inconsistent with previous research using this model, showing total re-endothelialization two weeks after a second denudation [Niimi *et al.* 1994, Azuma *et al.* 1995]. These two cited studies, though, employed a balloon catheter inflated with air, while the balloon used in the current study was filled with saline. It is possible that the use of saline in the balloon leads to a more stringent removal of ECs, resulting in a more extensive area of denudation. As a result a larger number of EC doublings would be required to re-cover the exposed area. If the onset of senescence prevents these extra replications from occurring (particularly after a second denudation, when some proliferative capacity may have been expended repairing the initial injury), the luminal surface could remain denuded.

VSMC proliferative response to denudation injury

Turning to the VSMC proliferative response, neointimal sizes attained in the current study were similar to those reported in previous cell proliferation research using the

same animal model [Azuma *et al.* 1995]. Neointimal size can be used only as an indicator (and not a direct measure) of the VSMC proliferative response, since the neointimal bulk compromises not only VSMCs, but also other cell types (such as neutrophils, T cells and macrophages) and extracellular matrix.

Even given this qualification, the consistent finding that neointima/media ratios following double-denudation injuries were greater than those following single denudation injuries, at very least suggests an increased VSMC proliferative response following the second denudation. This concurs with the finding of Azuma *et al.* mentioned earlier, that a second denudation injury led to a more persistent and extensive wave of cell proliferation within the neointima and media than did a single denudation [Azuma *et al.* 1995]. The apparent stratification of the double-denudation neointima raises another possibility, though: the second denudation injury may have left some of the original neointima intact, so that the observed rise in neointima/media ratio after a second injury may simply have resulted from the superimposition of a second neointima on the remains of the first.

The stratification within the double-denudation neointima has not been described previously. Regenerating ECs in injured rabbit arteries fail to align themselves axially, parallel with blood flow; they have variable sizes and irregular shapes, raising the possibility that their misalignment reflects senescence-related changes in cell-to-cell interactions [Reidy *et al.* 1983, Weidinger *et al.* 1990]. The stratification of the double-denudation neointimas in rabbit carotid arteries may reflect an equivalent alteration in the properties of VSMCs which are the product of a double proliferative response: some of these neointimal cells, having reached senescence, may have lost their ability to form normal intercellular interactions, and may also influence the behaviour of neighbouring cells, disrupting the homogeneity of the surrounding neointima.

The emergence of senescent cells in denuded arteries

Turning to the experiments involving staining for SA-β-gal activity, the almost complete absence of positive staining in control arteries stained at pH 6.0 (compared with the widespread staining at pH 4.0) demonstrates, at the very least, that β-gal activity in intact rabbit arteries shows a pH-specificity similar to that displayed by non-senescent human skin fibroblasts, HUVECs and rabbit VSMCs in culture. It is

tempting to deduce that it also demonstrates that intact rabbit carotid arteries contain very few, if any, senescent cells.

As will be discussed in Chapter Five, SA-β-gal has not been universally accepted as a marker of replicative senescence. For the purposes of the following discussion, the assumption will be made (as it was by Dimri *et al.*) that the selective ability of SA-β-gal to detect senescent cells *in vitro* is mirrored in *ex vivo* tissue [Dimri *et al.* 1995].

Given the low rates of cell turnover in the normal arterial wall, it is not surprising that only very scarce SA-β-gal-positive (senescent) cells were detected in control arteries. The emergence of SA-β-gal-positive cells in the neointima and media of denuded arteries appears to mirror the gradual appearance of such cells in serially-passaged *in vitro* cultures, strengthening the inference that the blue-stained cells in the vessel wall are indeed senescent.

The emergence of senescent cells in a vessel recovering from a mechanical injury would make mechanistic sense. The telomeric theory of replicative senescence suggests that for cells to become senescent, they must have undergone a certain number of cell divisions. The wave of proliferative activity which occurs after a denudation injury may lead to sufficient rounds of replicative activity to allow senescence to emerge. In the case of the endothelium, ECs bordering the area recently denuded by the second of two sequential injuries might themselves be the product of rounds of EC replication ensuing from the first injury; if so these ECs would be expected to have partially exhausted their replicative capacity, and so might reach the limit of their replicative potential before achieving complete repair of the breach in the endothelium. Similarly, the fact that a second denudation led to a dramatic increase in the percentage area of neointima and media covered by SA-β-gal-positive cells could be explained if the second wave of proliferative activity in the vessel wall involved cells whose replicative capacity had already been partially depleted following the initial denudation.

The finding that SA-β-gal-positive cells were observed in the adventitia reflects the increasingly appreciated fact that the adventitia is not an inert outer envelope of the artery, but is actively involved in processes such as vessel re-modelling [Stenmark *et al.* 2002]. Following endothelial denudation injuries, the adventitia contains a significant population of proliferating cells, some of which migrate to the neointima and acquire characteristics of myofibroblasts [Shi *et al.* 1996]. It seems plausible that

the occasional SA-β-gal-positive cells found in the adventitia of injured arteries in the current study might result from such proliferative activity.

Most of the blue cells found in single- and double-denudation vessels were located in the neointima. If positive staining is indeed a manifestation of senescence, this finding could have various explanations. Firstly, the majority of proliferative activity in the injured arterial wall may occur in the neointima, as is suggested by quantitative analysis of PCNA detection [Azuma *et al.* 1995]. Alternatively, or in addition, those cells which proliferate in the neointima may do so at a greater rate than cells in the media, or may intrinsically have reduced replicative capacity compared with their medial equivalents; this could be explained by the notion that VSMCs undergo some rounds of proliferation in the media, migrate to the neointima, and then undergo further cell divisions [as suggested in Clowes *et al.* 1983, Clowes and Schwartz 1985].

The demonstration of more senescence in the neointima than in the media of the injured artery has parallels in atherosclerotic lesions. As mentioned in Chapter One, VSMCs derived from fibrous plaques show reduced proliferative capacity compared with cells from the underlying media [Ross 1986, Bennett *et al.* 1995]. Similarly, intimal cells from arteries known to be susceptible to atherosclerosis show more marked age-related telomere attrition than do intimal cells from arteries which are usually free of disease; in contrast, no difference is found in the age-related rate of telomere loss between medial cells from the two types of artery [Chang and Harley 1995].

Immunohistochemistry showed that in the current study most of the SA-β-gal-positive cells in the injured vessels were VSMCs, and that a minority were ECs. The demonstration that the SA-β-gal-positive cells were not leukocytes or macrophages was in itself important, since these cell types contain a significant number of lysosomes, and it might be expected that their lysosomal content could be detectable by staining for β-gal activity even at the sub-optimal pH of 6.0.

Replicative senescence or SIPS?

While it is tempting to attribute the presence of senescent vascular cells to telomeric attrition resulting from rounds of proliferative activity, another explanation for the emergence of SA-β-gal-positive cells must be considered. In Chapter One (Section 1.5.4.2) it was mentioned that manipulation of a cell's redox status could result in

SIPS, a process which does not involve prior rounds of replicative activity and telomeric attrition, but which may result from other forms of DNA damage. *Ex vivo* mechanical injury to dissected rings of rabbit iliofemoral artery leads to increased oxidative stress in the tissue [Souza *et al.* 2000]. Furthermore, balloon-induced injury to porcine coronary arteries *in vivo* leads to an early increase in superoxide production via a mechanism dependent on the activity of NAD(P)H oxidase [Shi *et al.* 2001], the major enzymatic source of intracellular ROS in vascular cells [Pagano *et al.* 1995]. This raises the possibility that mechanical injury to the arterial wall may, via a localized increase in oxidative stress, lead to stress-induced premature senescence of vascular cells, which, given the *in vitro* experiments of Dumont *et al.* mentioned in Chapter One, may explain the emergence of SA-β-gal activity in the current study [Dumont *et al.* 2000].

Previous experimental data suggest that other agents are also capable of inducing SIPS in vascular cells: for example, when early passage HUVECs are grown in culture on glycated extracellular matrix proteins, they show some features of premature senescence, including SA-β-gal expression, without having undergone telomeric attrition [Chen *et al.* 2002]. While such proteins were not used in the rabbit carotid artery experiments, the results of Chen *et al.* do emphasize that SA-β-gal expression by ECs can occur via mechanisms other than replicative senescence.

Proliferative and apoptotic activity in the injured vessel wall

Arterial cross-sections were immunostained for PCNA, a 36 kD nuclear protein associated with the cell cycle. Nuclear PCNA immunoreactivity is found in the proliferative component of normal tissues [Hall *et al.* 1990], and has, as mentioned above, been used previously as a marker of proliferative activity in the rabbit carotid model [Azuma *et al.* 1995]. The immunohistochemical demonstration of cells still proliferating in the vessel wall six weeks after a double-denudation injury in the current study was consistent with findings from that earlier research [Azuma *et al.* 1995]; any discrepancy in the relative abundance of proliferating cells in the two studies may reflect the fact that Azuma *et al.* used a larger balloon (3F, rather than 2F in the current study), and may thus have caused a more traumatic injury.

Several sections from each of the four double-denudation arteries were examined, so that, although there were relatively few PCNA-positive cells in each section, in all a considerable number of PCNA-positive cells were observed, together with a large

number of SA-β-gal-positive cells. Despite this, no examples were found of cells staining positively for PCNA while also exhibiting SA-β-gal activity. Instead PCNA-positive and SA-β-gal-positive cells co-existed in the same vessel, but formed two distinct populations. This suggests that cell proliferation and senescence can coincide temporally in the same tissue, and that SA-β-gal identifies cells which are not dividing. Any dual-staining within a single cell for both PCNA and SA-β-gal would strongly have argued against the validity of SA-β-gal as a marker of senescent cells.

As mentioned in Chapter One (Section 1.4.7), the relationship between replicative senescence and apoptosis has been the subject of some debate. Several studies have reported the occurrence of apoptosis during neointima formation [Han *et al.* 1995, Bochaton-Piallat *et al.* 1995, Perlman *et al.* 1997, Malik *et al.* 1998].

The TUNEL results described in this chapter suggest that the apoptotic cells are distinct from those undergoing senescence: no evidence for co-staining with SA-β-gal and TUNEL was found, despite an extensive study of the double-denudation vessels. This would support (though admittedly not prove) the contention that senescent rabbit vascular cells are resistant to apoptosis. It would also suggest that, in these cell types at least, apoptosis is not an inevitable consequence of senescence.

The sparsity of apoptotic cells in the vessel walls in this study is consistent with previous research which has shown that the wave of apoptosis which follows a denudation injury has subsided considerably only four weeks after the mechanical insult [Bochaton-Piallat *et al.* 1995, Kollum *et al.* 1997]. It also concurs with the suggestion that following a second denudation injury, neointimal cells are relatively resistant to death by apoptosis [Pollman *et al.* 1999].

3.2.5 Conclusion

The results described in this section strongly suggest that endothelial and vascular smooth muscle cells are able to undergo senescence *in vivo* following an endothelial denudation injury, and that the prevalence of senescent cells can be increased by repeated injury to the arterial wall. The senescent cells do not appear to be prone to apoptosis.

The pathological and clinical implications of the emergence of senescent cells in the vessel wall will be discussed in Chapter Five.

CHAPTER FOUR

Atherogenesis in senescence-accelerated mice

The experiments described in Chapter Three were designed to explore whether cellular ageing can occur in the vasculature. In contrast, the studies detailed in this chapter used an animal model of accelerated organismic ageing to investigate whether an ageing phenotype, *per se*, is associated with increased susceptibility to atherogenesis. Additional experiments were performed to look for evidence of accelerated cellular ageing in this model.

To these ends, two related strains of mice, senescence-accelerated prone (SAM-P) and senescence-accelerated resistant (SAM-R), were studied; the origin of these strains has been described in Chapter One (Section 1.7).

In the only previously published study looking for evidence of susceptibility to atherosclerosis in this model [Yagi *et al.* 1995], microscopy of the thoracic aortas of SAM mice fed a physiological murine diet revealed subendothelial invasion by macrophages in SAM-P but not SAM-R vessels; furthermore, when the aortic walls were analysed for their content of lipid peroxides, triglycerides and cholesterol, all three parameters were found to be higher in SAM-P than in SAM-R aortas. These findings were taken as an indication that SAM-P mice might be more prone to atherogenesis than SAM-R mice, although no atheromatous lesions were demonstrated in either strain.

In the current study, SAM-P and SAM-R mice were fed a diet with a higher fat and cholesterol content than that used by Yagi *et al.*, in an attempt to provoke a more marked atherogenic response. The susceptibility of each murine strain to atherosclerosis was assessed by measuring the extent of lipid deposition in their aortic roots. Immunohistochemical studies were carried out to look for evidence of macrophage infiltration in the arterial wall. Serum cholesterol and triglyceride levels were measured in each strain, in order to establish whether any observed difference in lipid lesion formation could be attributed to inter-strain differences in serum lipid levels. In a pilot study, lipid deposition was compared in SAM-P mice and C57BL/6 mice, an inbred strain known to be relatively susceptible to atherogenesis [Paigen *et al.* 1985]. In further studies, two markers of cellular replicative senescence, telomere shortening and SA-β-gal activity, were used to investigate SAM cells and tissue samples for evidence of accelerated cellular ageing.

This chapter begins with a brief description of the SAM colony maintained at UCL. The protocols for the studies of atheroma formation in SAM-P, SAM-R and C57BL/6

mice are given, and the results of these studies are then reported in detail. The results of the telomere and SA-β-gal studies are then described, and the chapter ends with a discussion of all the results obtained from studies of the murine model.

4.1 Description of the SAM colony established at UCL

All four of the original SAM-P breeding pairs produced litters, while one of the four SAM-R breeding pairs failed to breed. Another SAM-R breeding pair produced several litters, but all these offspring were eaten by their parents while still pups. The remaining two SAM-R breeding pairs bred successfully. In subsequent generations, most newly-formed SAM-P and SAM-R breeding pairs successfully produced litters. The mean litter size was slightly larger for SAM-R mice (7.9 pups per litter) than for SAM-P mice (7.0 pups per litter), though this difference did not reach statistical significance ($P = 0.26$).

Maintenance of the senescent phenotype in SAM-P mice was judged qualitatively by assessing fur glossiness and the incidence of senescence-associated pathologies. A quantitative assessment was made on the basis of the weight of the SAM-P and SAM-R strains. Unfortunately, meaningful data concerning the life-spans of the generations of SAM mice used in this project could not be produced; insufficient numbers of mice from the generations studied reached the end of their natural life-spans. Mice died 'early' for a variety of reasons: several were culled for this study and for related work; others were culled to relieve suffering from senescence-related pathologies or other illnesses; other mice were injured by fighting with litter mates, and were either found dead or were culled to relieve suffering.

Figure 4.1 (overleaf) shows the phenotypes of age-matched female SAM-P and SAM-R mice, fed a standard laboratory chow (the 'mouse breeding and maintenance diet' described in Chapter Two) since weaning. As shown, female SAM-P mice were smaller than their SAM-R counterparts, and showed loss of fur glossiness. Similar differences in phenotype were found between male SAM-P and SAM-R mice.

Figure 4.1 Phenotypes of SAM-P and SAM-R mice

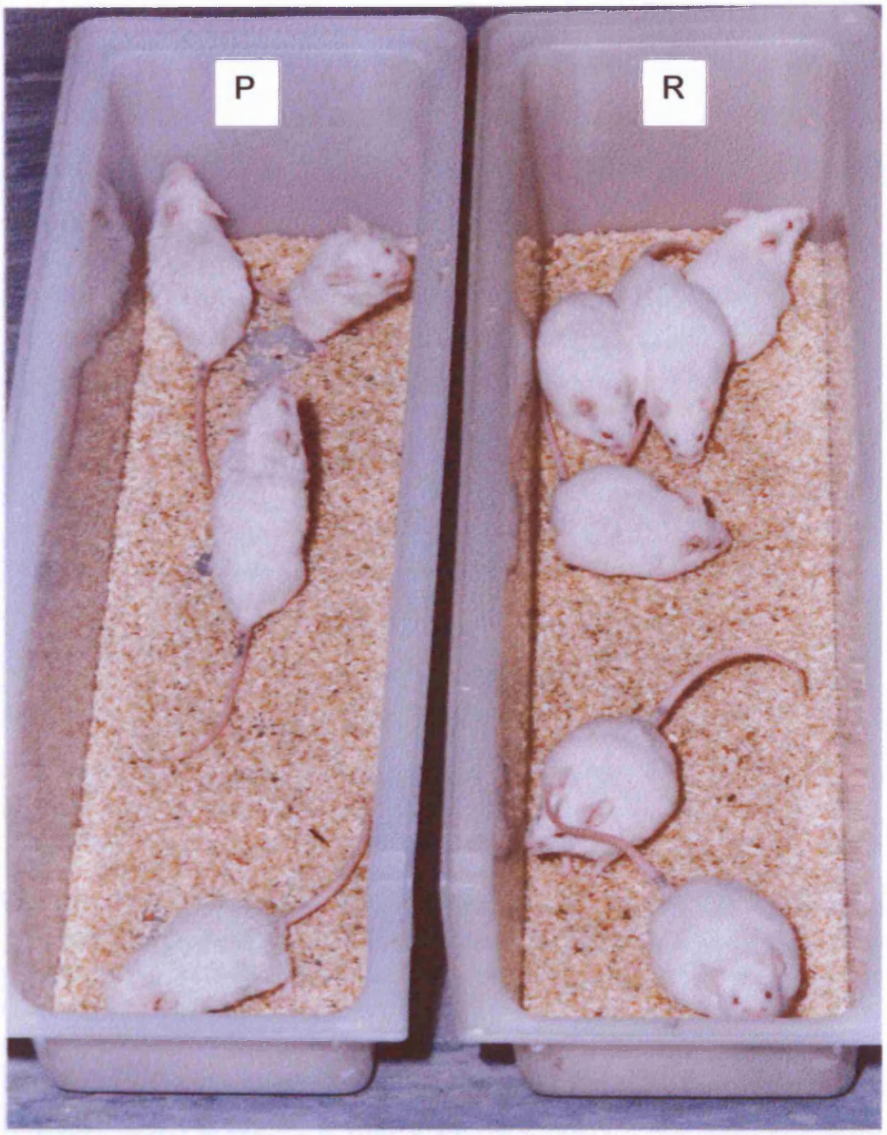

Figure 4.1 The figure shows female SAM-P (left box) and SAM-R mice (right box), photographed at forty-five weeks of age. They had been fed a standard laboratory chow since weaning. The SAM-P mice are smaller than their SAM-R counterparts, and show loss of fur glossiness.

The smaller size of SAM-P mice is also illustrated by the weights at twenty-eight weeks of age of fourteen SAM-P and fourteen SAM-R mice fed the standard laboratory chow since weaning (Table 4.1); these mice would subsequently be fed the Western-type diet. Female mice tended to be smaller than their male counterparts in both strains (a feature common to many other murine strains). Male and female SAM-P mice were smaller than age- and sex-matched SAM-R mice, the differences in each case reaching statistical significance.

Table 4.1 Weights of SAM mice fed a standard laboratory chow

	Male	**Female**
SAM-R	36.2 ± 1.7 g (n=8)	29.8 ± 5.8 g (n=6)
SAM-P	27.0 ± 2.6 g (n=7)	23.1 ± 2.8 g (n=7)
***P* value**	< 0.00001	0.02

Table 4.1 The table shows the mean weights (± s.d.) of 28-week-old SAM mice fed a standard laboratory chow since weaning at four weeks of age. *P* values were calculated using a two-tailed unpaired t-test, assuming equal variance (as had been demonstrated using Bartlet's test).

Age-related pathologies were more common in SAM-P than in SAM-R mice. 12 SAM-P mice (from a total of 178 SAM-P mice in the colony) developed peri-ophthalmic lesions (erythema and swelling), and this sign was not found in any of the 187 SAM-R mice in the colony. Four SAM-P were culled at less than one year of age because of skin ulceration and exhaustion; only one SAM-R mouse was culled to relieve suffering. This mouse, one of the original breeders transported from Japan, was culled at eighty weeks of age, and this was because it showed signs of exhaustion.

SAM-P mice in general showed reduced levels of activity compared with the SAM-R mice, but this was not formally assessed at UCL. Similarly, facilities for testing learning and memory in the SAM mice were not available, and so this element of their ageing phenotype was not assessed as part of this project.

4.2 Experimental designs for the study of atherogenesis in SAM and C57BL/6 mice

Two studies of atherogenesis were undertaken: a pilot study comparing atherogenesis in C57BL/6 and SAM-P mice, and a more detailed study comparing atherogenesis in SAM-P and SAM-R mice.

The pilot study was designed to establish whether SAM mice could tolerate a Western-type diet, and to give an indication of the relative susceptibility of SAM-P and C57BL/6 mice to atherogenesis. The 'Mouse Western Adjusted Calories Diet' (detailed in Chapter Two) was fed *ad libitum* to seven male SAM-P mice, and to seven C57BL/6 mice (two male, five female), from twenty-four weeks of age, for twelve weeks. Until the initiation of this Western-type diet, SAM-P and C57BL/6 mice had been fed the standard laboratory chow from weaning onwards. The mice were culled at the end of the administration of the Western-type diet, and their hearts and aortas were harvested, processed and analysed for the extent of lipid deposition in their aortic roots (as described in Chapter Two, Section 2.2.4.10). Parameters measured included the number of lesions detected in each aortic root, and the area of Oil red O staining in each aortic root cross-section.

The experimental design for the study comparing atherogenesis in SAM-P and SAM-R mice, is illustrated in Figure 4.2 overleaf. Fourteen SAM-P (seven male, seven female) and fourteen SAM-R (eight male, six female) age-matched mice were weaned at four weeks of age, then fed the standard laboratory chow until reaching twenty-eight weeks of age. For the following seventeen weeks these mice were fed the Western-type diet *ad libitum*.

As illustrated in Figure 4.2, venous blood samples were obtained from these mice one week before, and sixteen weeks after starting the Western-type diet. These samples were analysed for the serum cholesterol and triglyceride levels of individual mice. In addition, pooled serum samples prepared from the blood taken sixteen weeks after starting the Western-type diet were used to determine HDL/total cholesterol ratios on this diet. (This analysis was not possible one week before starting the diet, as the automated analyser was not available at that time-point).

Figure 4.2 Experimental design for SAM atherogenesis study

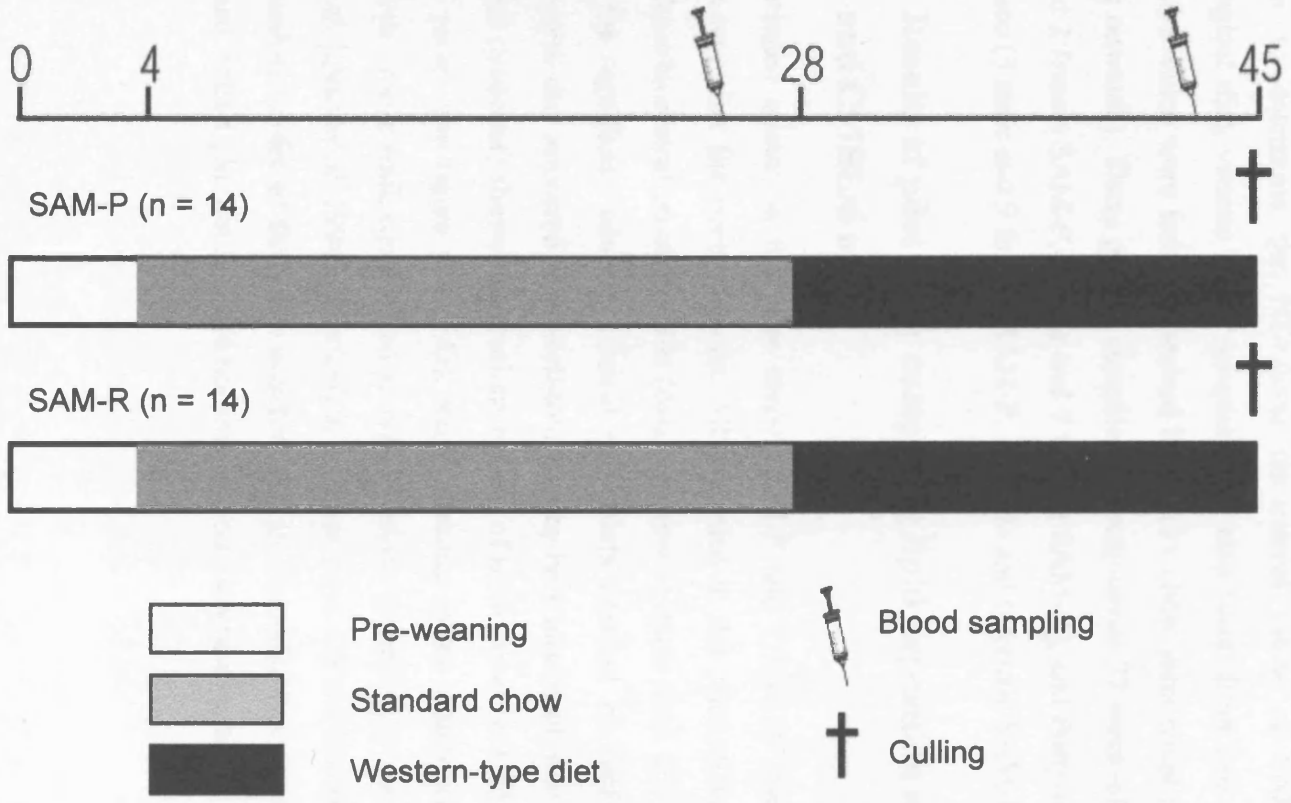

Figure 4.2 14 SAM-P and 14 SAM-R mice were weaned at 4 weeks of age, fed a standard laboratory chow for the next 24 weeks, and then fed a Western-type diet until culling at 45 weeks of age. Venous blood samples were taken at 27 and 44 weeks of age to allow the measurement of serum lipid levels in individual mice. Some of the blood taken at 44 weeks of age was used to prepare pooled serum samples for the assessment of HDL/total cholesterol levels in each group. After culling, SAM aortic roots were analysed for lipid deposition and macrophage invasion.

The mice were weighed at intervals during the administration of the high-cholesterol diet (at 0, 5, 10 and 15 weeks on the diet) in order to assess the relative ability of the SAM-P and SAM-R mice to thrive on this diet.

All mice were culled at forty-five weeks of age, and their hearts and aortas were harvested for further analysis, including morphometric studies and immunohistochemistry.

In order to determine the HDL/total cholesterol ratios of SAM mice fed a physiological diet, venous blood samples were also taken from two other groups of SAM mice which were fed the standard laboratory chow throughout their lives (from weaning onwards). These groups comprised twenty-seven 27-week-old SAM mice (9 male and 2 female SAM-P, 9 male and 7 female SAM-R), and thirty-one 44-week-old SAM mice (3 male and 9 female SAM-P, 13 male and 6 female SAM-R).

4.3 Results of pilot study comparing lipid deposition in SAM-P and C57BL/6 mice

As mentioned above, in the pilot study SAM-P and C57BL/6 mice were fed the Western-type diet for twelve weeks. All the mice in the pilot study gained weight during the administration of this diet (data not shown); none died, and none developed any of the significant adverse clinical end-points detailed in Table 2.2. Thus the Western-type diet appeared to be well-tolerated by both strains of mouse.

Figure 4.3 (overleaf) shows lipid lesions typical of those found in C57BL/6 and SAM-P aortic roots. The figure shows Oil red O staining in the attachments of the valve cusps to the aortic wall, categorized as type I lesions according to the classification of Qiao *et al.* [Qiao *et al.* 1994] described in Chapter Two. Oil red O was typically found at the luminal border of the valve attachments, as illustrated here. Lesions were 'flat' rather than 'raised', in that they did not impinge on the vessel lumen.

Figure 4.3 Morphology of lipid deposits in C57BL/6 and SAM-P mouse aortic roots (pilot study)

A C57BL/6 (low magnification)

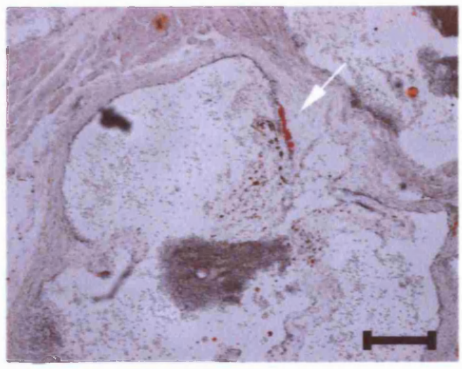

B C57BL/6 (high magnification)

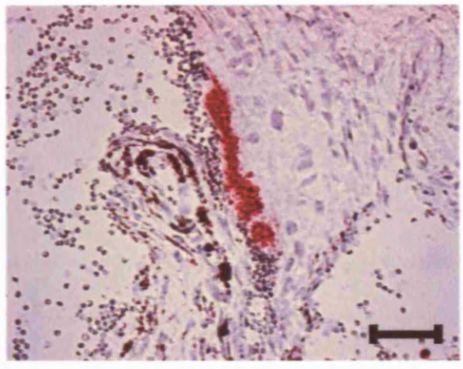

C SAM-P (high magnification)

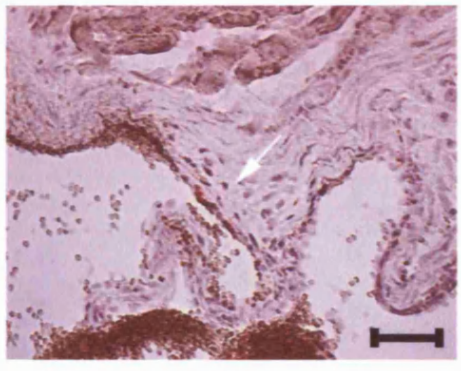

Figure 4.3 Photomicrographs of representative cross-sections from C57BL/6 (Panels A and B) and SAM-P (Panel C) aortic roots, stained with Oil red O (red) and counter-stained with haematoxylin (blue). These mice had been fed the Western-type diet for 12 weeks. Panel A shows the structure of a typical murine aortic root at the level of the aortic valve cusps. The arrow in Panel A indicates Oil red O staining in one of the valve cusp attachments; this type I lesion is shown at higher power in Panel B. The arrow in Panel C indicates a similar type I lesion in a SAM-P cusp attachment. Bar = 125 μm in Panel A, and 30 μm in Panels B and C.

Table 4.2 shows the total number of lipid lesions found in the aortic roots of these mice, calculated as described in Chapter Two (Section 2.2.4.10). While all C57BL/6 and SAM-P mice developed type I lipid lesions, no type II lesions (lesions in the free aortic wall) were detected in either mouse strain in this pilot study. There was no statistically significant difference between the number of type I lesions found in C57BL/6 and SAM-P mice (with median values of 3 lesions (inter-quartile range (IQR): 1-6) in C57BL/6 mice, and 6 lesions (IQR: 4-6) in SAM-P mice, $P = 0.07$).

Table 4.2 Number of lesions in C57BL/6 and SAM-P mice in pilot study

Mouse strain, designation and gender	Type I lesions	Type II lesions
C57BL/6		
#1 (M)	6	0
#2 (M)	3	0
#3 (F)	1	0
#4 (F)	7	0
#5 (F)	1	0
#6 (F)	2	0
#7 (F)	4	0
SAM-P/8		
#1 (M)	1	0
#2 (M)	4	0
#3 (M)	6	0
#4 (M)	5	0
#5 (M)	6	0
#6 (M)	6	0
#7 (M)	10	0

Table 4.2 shows the total number of fatty lesions in the aortic roots of the C57BL/6 and SAM-P mice investigated in the pilot study, calculated as described in Chapter Two. These mice were fed the Western-type diet for twelve weeks, starting at twenty-four weeks of age.

The mean areas stained with Oil red O in the eight cross-sections from each aortic root are given in Table 4.3. There was no statistically significant difference between C57BL/6 and SAM-P mice in terms of the cross-sectional areas of type I lipid deposition (median values of 329.7 μm^2 (IQR: 111.1-406.7) in C57BL/6 mice, and 87.9 μm^2 (IQR: 79.5-227.5) in SAM-P mice, $P = 0.28$). In summary, lipid deposition on a Western-type diet therefore appeared similar in C57BL/6 and SAM-P mice in this small study, whether assessed by lesion type, lesion number, or lesion area.

Table 4.3 Extent of Oil red O staining in C57BL/6 and SAM-P mice in the pilot study

Mouse strain, designation and gender	Type I lesions	Type II lesions
C57BL/6		
#1 (M)	1010.3	0
#2 (M)	406.7	0
#3 (F)	9.7	0
#4 (F)	396.1	0
#5 (F)	185.3	0
#6 (F)	111.1	0
#7 (F)	329.7	0
SAM-P/8		
#1 (M)	82.9	0
#2 (M)	61.1	0
#3 (M)	227.5	0
#4 (M)	79.5	0
#5 (M)	87.9	0
#6 (M)	115.7	0
#7 (M)	1435.7	0

Table 4.3 shows the mean area stained with Oil red O (in μm^2, accurate to one decimal place) in the eight cross-sections from each C57BL/6 and SAM-P aortic root investigated in the pilot study. Within each group of mice, the mean areas of type I lipid deposition were distributed non-parametrically.

4.4 Results of SAM atherogenesis studies

4.4.1 Weight gain of SAM mice on a Western-type diet

Figure 4.4 shows the weight gain of the fourteen SAM-P and fourteen SAM-R mice fed the Western-type diet for seventeen weeks. Each subgroup (male and female, SAM-P and SAM-R) gained weight on this diet.

Figure 4.4 Weights of SAM mice fed the Western-type diet

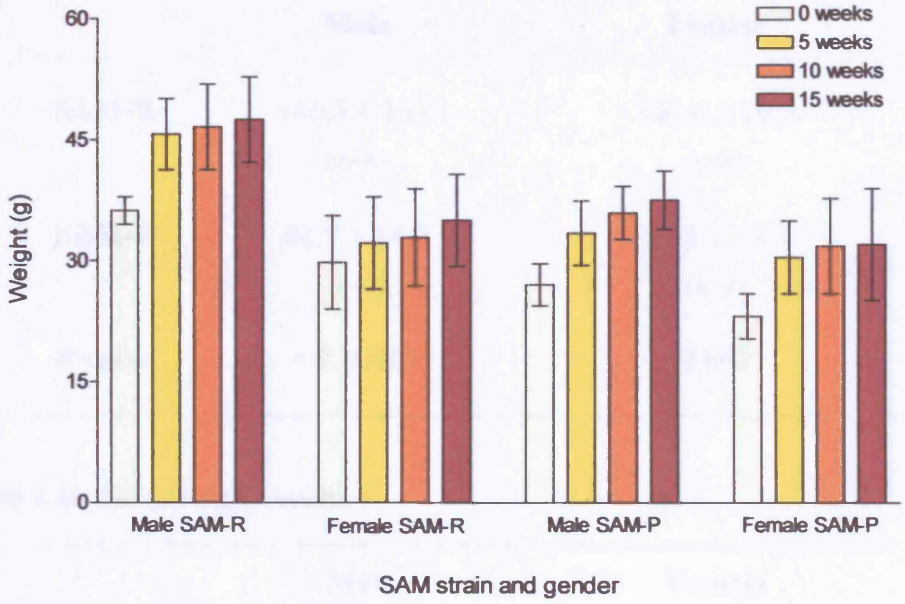

Figure 4.4 SAM mice were fed the Western-type diet for 17 weeks, beginning at 28 weeks of age. The graph shows the weights of these mice (expressed as mean values ± s.d. for each strain- and gender-matched group) at the initiation of the diet (0 weeks) and at 5-weekly intervals thereafter. As shown, mice of both strains, and of either gender, gained weight on the experimental diet.

4.4.2 Serum cholesterol and triglyceride levels in SAM mice

Tables 4.4 shows the total serum cholesterol and triglyceride levels in these fourteen SAM-P and fourteen SAM-R mice at 27 weeks of age. At this stage they had been fed the standard laboratory chow since weaning at four weeks of age, and would subsequently be fed this chow for another week, followed by the Western-type diet for seventeen weeks (as illustrated in Figure 4.2).

Table 4.4 Serum lipid levels in SAM mice prior to Western-type diet

Table 4.4a Serum cholesterol

	Male	**Female**
SAM-R	166.3 ± 16.4 (n=8)	146.6 ± 39.6 (n=6)
SAM-P	91.7 ± 14.7 (n=7)	84.3 ± 13.6 (n=7)
***P* value**	< 0.00001	0.002

Table 4.4b Serum triglycerides

	Male	**Female**
SAM-R	50.7 ± 14.0 (n=8)	42.4 ± 10.0 (n=6)
SAM-P	70.5 ± 32.0 (n=7)	96.1 ± 23.2 (n=7)
***P* value**	0.25	0.0001

Tables 4.4a and **4.4b** show, respectively, the serum cholesterol and triglyceride levels in the four groups of mice (male and female, SAM-P and SAM-R) at twenty-seven weeks of age. Lipid levels are expressed as mean values ± s.d., and are given in mg/dl. *P* values were calculated using ANOVA, with a log transformation of triglyceride values to ensure a normal distribution.

Serum cholesterol levels were lower in SAM-P than in SAM-R mice, whether male or female mice were studied. Within each strain, there was a tendency for male mice to have a higher serum cholesterol level than their female counterparts, though no statistically significant inter-gender differences were detected. Serum triglyceride levels, in contrast, tended to be higher among SAM-P than SAM-R mice, whether male or female mice were studied (Table 4.4b). No statistically significant inter-gender differences in serum triglyceride levels were detected in either strain.

Table 4.5 shows the lipid levels in the same group of SAM mice, now measured at forty-four weeks of age, by which time they had received the Western-type diet for sixteen weeks.

Table 4.5 Serum lipid levels in SAM mice fed a Western-type diet

Table 4.5a Serum cholesterol

	Male	**Female**
SAM-R	286.8 ± 45.7 (n=8)	259.2 ± 23.8 (n=6)
SAM-P	150.8 ± 15.6 (n=7)	175.8 ± 26.9 (n=7)
***P* value**	< 0.0005	< 0.0001

Table 4.5b Serum triglycerides

	Male	**Female**
SAM-R	173.3 ± 106.3 (n=8)	89.2 ± 42.6 (n=6)
SAM-P	156.1 ± 32.3 (n=7)	169.9 ± 92.7 (n=7)
***P* value**	0.92	0.09

Tables 4.5a and **4.5b** show the serum lipid levels in the SAM mice at forty-four weeks of age. These mice had been fed the standard laboratory chow for twenty-four weeks, and then the Western-type diet for the next sixteen weeks. Lipid levels (in mg/dl) are expressed as mean values ± s.d.. *P* values were calculated by ANOVA, with log transformation of triglyceride values.

Figure 4.5 Serum cholesterol and triglyceride levels in SAM mice before and after administration of a Western-type diet

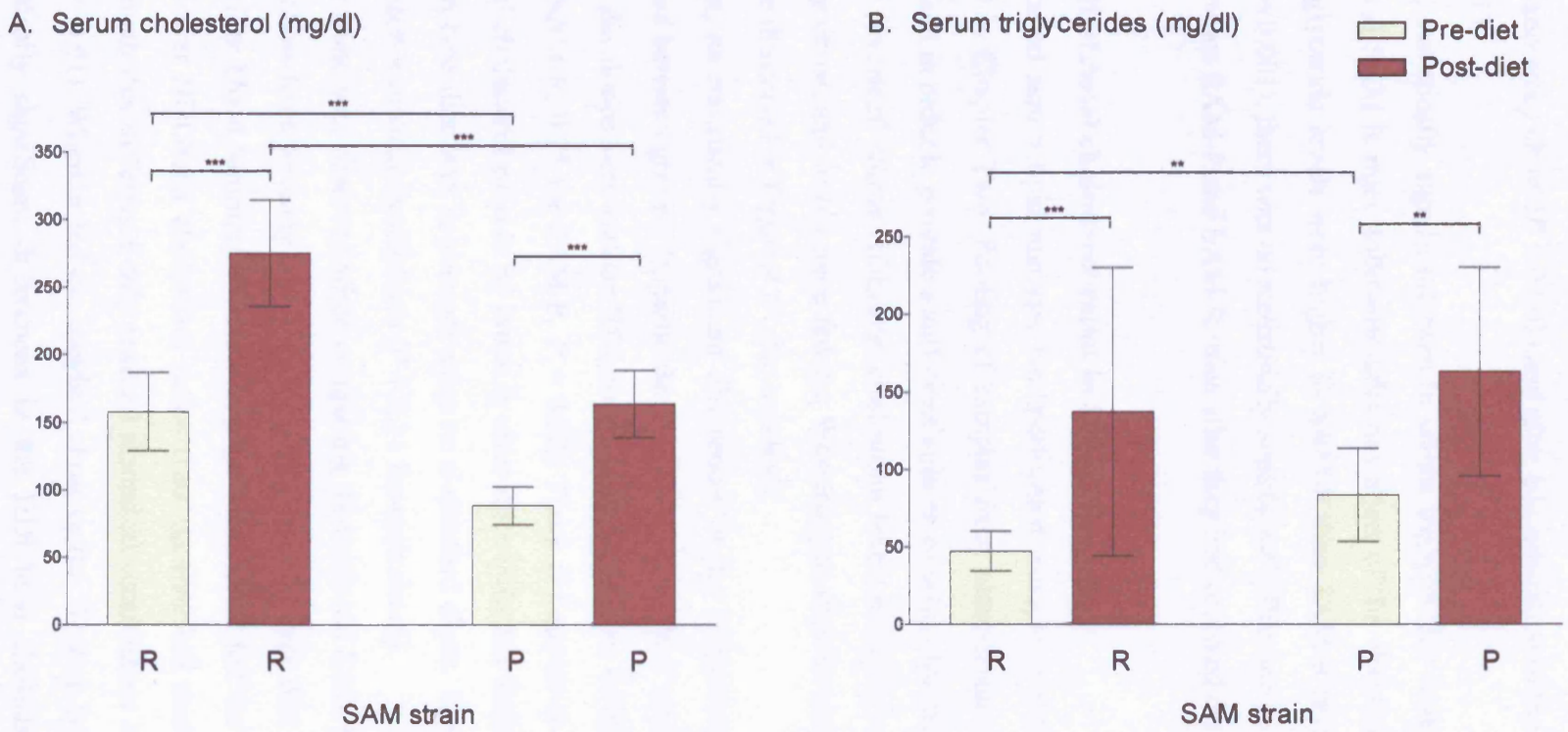

Figure 4.5 Graph A shows the serum cholesterol, and Graph B the serum triglyceride levels, of 14 SAM-P and 14 SAM-R mice before and after administration of a Western-type diet. Pre-diet samples were taken from 27-week-old mice which had been fed a standard laboratory chow since weaning. Post-diet samples were taken when the same mice had reached 44 weeks of age; they had been fed the standard laboratory chow from weaning until 28 weeks of age, and thenceforward the Western-type diet. Serum cholesterol and triglyceride levels (in mg/dl) are expressed as mean values +/- s.d.. ** = $P<0.01$, *** = $P<0.001$ by ANOVA.

As shown, administration of the Western-type diet led to parallel, statistically significant increases in the serum cholesterol levels of SAM-P and SAM-R mice. SAM-P mice showed lower total cholesterol levels than SAM-R mice, both on the standard laboratory chow ($P < 0.001$) and after administration of the Western-type diet ($P < 0.001$).

Similarly, statistically significant rises in serum triglycerides were observed in both SAM-P and SAM-R mice following administration of the Western-type diet. While serum triglyceride levels were higher in SAM-P than SAM-R mice on the standard chow ($P = 0.001$), there was no statistically significant difference in serum triglyceride levels between SAM-P and SAM-R mice after they had received the Western-type diet ($P = 0.2$).

4.4.3 HDL/total cholesterol ratios in SAM mice

More detailed serum lipid analysis was performed using an automated analyser, as described in Chapter Two. Pooling of samples from same-strain, same-gender mice was required in order to provide a sufficient volume of serum for the analyser.

Table 4.7 (overleaf) shows HDL/total cholesterol levels in young mice fed a standard laboratory chow, and in old mice fed the Western-type diet for sixteen weeks. These results are illustrated in Figure 4.6 (also overleaf).

As shown, no statistically significant differences in the HDL/total cholesterol ratios were found between groups. In particular, SAM-R and SAM-P mice fed the Western-type diet developed very similar HDL/total cholesterol ratios (with median values of 0.72 for SAM-R, 0.75 for SAM-P, $P = 0.38$). There did appear to be a trend for the HDL/total cholesterol ratio to be lower in older mice (whether SAM-P or SAM-R) on a Western-type diet than in younger mice on a standard chow, though this difference did not reach statistical significance ($P = 0.11$ for each strain).

A similar trend was observed when comparing 44-week-old SAM mice either fed the standard chow from weaning onwards, or fed the Western-type diet for the last sixteen weeks before blood sampling (Table 4.8, page 180). Mice fed the Western-type diet showed lower HDL/total cholesterol ratios than age-matched mice fed the standard chow, though this difference only reached statistical significance among the SAM-R mice ($P = 0.01$). Whether fed the standard chow or the Western-type diet, there were no statistically significant differences in the HDL/total cholesterol between age-matched SAM-P and SAM-R mice.

Table 4.7 HDL/total cholesterol ratios in young SAM fed a standard chow and in old SAM fed a Western-type diet

	27-week-old mice Standard chow	44-week-old mice Western-type diet	*P* value
SAM-R	0.92 (IQR: 0.90-0.92, n=3)	0.72 (IQR: 0.67-0.77, n=4)	0.11
SAM-P	0.86 (IQR: 0.76-0.88, n=3)	0.75 (IQR: 0.72-0.80, n=4)	0.11
***P* value**	0.05	0.38	

Table 4.7 shows the HDL/total cholesterol ratios in pooled sera from four groups of mice: 11 young SAM-P and 16 young SAM-R mice had been fed the standard laboratory chow from weaning onwards; 14 old SAM-P and 14 old SAM-R mice had been fed the standard chow for 24 weeks from weaning, and then the Western-type diet for the next 16 weeks. For each group, HDL/total cholesterol ratios were measured in 3 or 4 pooled samples (see n values provided). Median ratios and IQRs were calculated for each group of mice. *P* values were calculated using the Mann-Whitney sign rank test.

Figure 4.6 HDL/Total cholesterol ratios in SAM mice

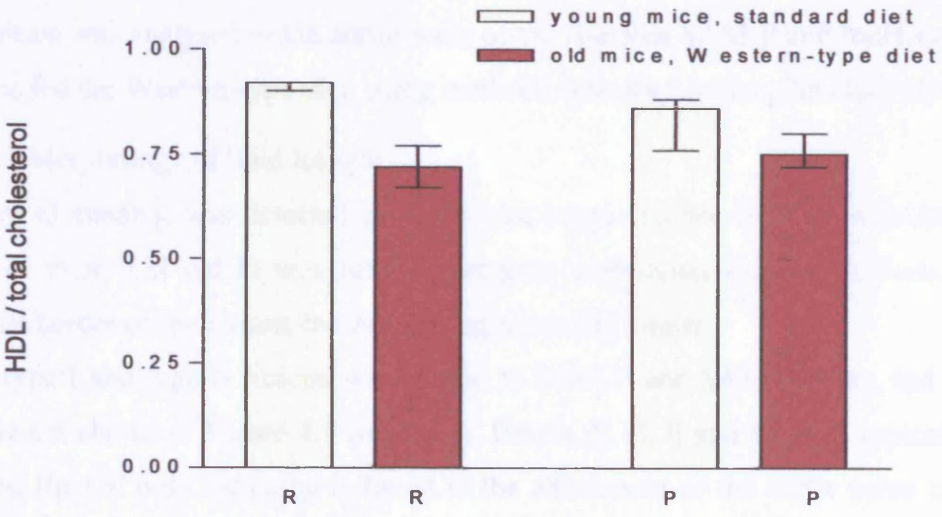

Figure 4.6 illustrates the median HDL/total cholesterol ratios (± IQR) in pooled sera from the four groups of mice detailed in the legend to Table 4.7. No statistically significant differences were found between strain- or diet-matched groups.

Table 4.8 HDL/total cholesterol ratios in old SAM mice fed a standard chow or a Western-type diet

	44-week-old mice Standard chow	44-week-old mice Western-type diet	*P* value
SAM-R	0.89 (IQR: 0.84-0.94, n=6)	0.72 (IQR: 0.67-0.77, n=4)	0.01
SAM-P	0.86 (IQR: 0.81-0.86, n=3)	0.75 (IQR: 0.72-0.80, n=4)	0.07
***P* value**	0.52	0.38	

Table 4.8 Sera were pooled from four groups of old mice: 12 SAM-P and 19 SAM-R mice had been fed the standard laboratory chow from weaning onwards; 14 SAM-P and 14 SAM-R mice had been fed the standard chow for 24 weeks from weaning, and then the Western-type diet for 16 weeks. For each group, HDL/total cholesterol ratios were measured in between 3 and 6 pooled samples. Median ratios, inter-quartile ranges and *P* values were calculated as described for Table 4.7.

4.4.4 Lipid deposition in the aortic roots of SAM mice fed a Western-type diet

In order to compare the susceptibility to atherogenesis of the two SAM strains, lipid deposition was analysed in the aortic roots of the fourteen SAM-P and fourteen SAM-R mice fed the Western-type diet, using methods described in the pilot study above.

4.4.4.1 Morphology of lipid lesions

Oil red O staining was detected in aortic root cross-sections from both SAM-P and SAM-R mice. Oil red O was found in regions underlying the endothelium, at the luminal border of the intima, but not impinging on the lumen.

Both type I and type II lesions were found in SAM-P and SAM-R mice, and typical lesions are shown in Figure 4.7 (overleaf). Panels A, C, E and G show typical type I lesions; the Oil red O staining is found in the attachment of the aortic valve cusps to the aortic wall. Panels B, D, F and H show typical type II lesions; the Oil red O is found at the luminal border of the free aortic wall, bearing no relation to any of the valve cusp attachments. As shown, SAM-R Oil red O deposits tended to be smaller and fainter than deposits in SAM-P mice.

Figure 4.7 **Morphology of fatty lesions in SAM-P and SAM-R mice**

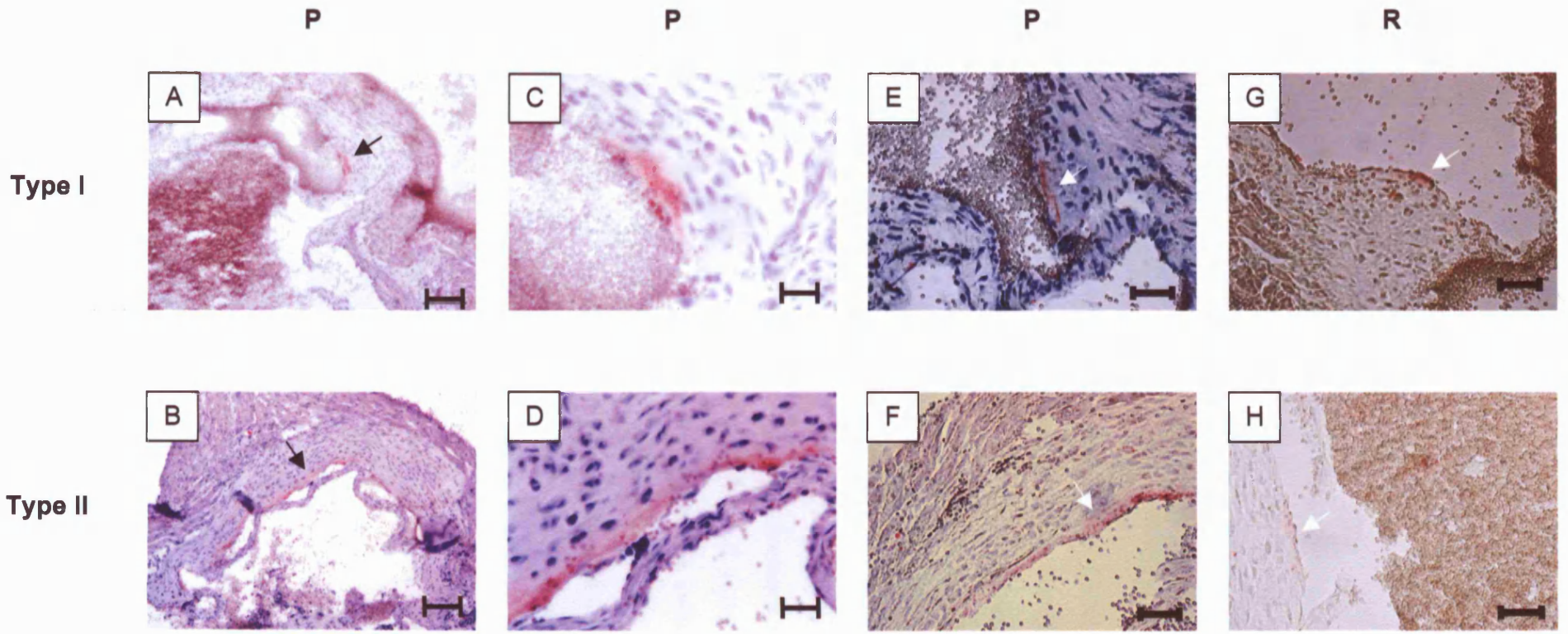

Figure 4.7 Photomicrographs of representative fatty lesions in SAM aortic roots. Panel A shows a SAM-P type I lesion situated on the attachment of an aortic valve leaflet. Panel B shows a SAM-P type II lesion in the aortic free wall. Panels C and D show magnified views of the areas indicated by black arrows in Panels A and B respectively. Panels E and F show other examples of SAM-P type I and type II lesions respectively. Panels G and H show SAM-R type I and type II lesions respectively, indicated by white arrows. Panels A-D were photographed under an Axiophot 2 microscope. Panels E-H were photographed using a CCD camera attached to an Olympus-BX microscope. Bar = 100 μm in Panels A and B, 25 μm in Panels C, D, E and G, and 50μm in Panels F and H.

The lipid lesions appeared to have reduced cellularity (as judged by the paucity of haematoxylin-stained nuclei in these regions) compared with the surrounding tissue. No evidence was found of more complex lesions.

4.4.4.2 Number of lesions per aortic root

As in the pilot study, the number of distinct lesions in each of eight aortic root cross-sections was recorded, categorized as either type I or type II lesions; a score was also kept of the number of lesions of any type. These three scores from the eight cross-sections were then summated, to give three total scores for each mouse. Table 4.9 (overleaf) shows the results of this analysis.

Using this method, a lesion extending along the length of the aortic root, and therefore appearing in more than one analysed cross-section, was scored for each time it appeared in an aortic root cross-section, so that, strictly speaking, the table does not record the actual number of lesions in the aortic root, but merely gives an indication of the true figure. For convenience though, and with this qualification in mind, the scores for each aortic root are referred to henceforward as the 'number of lesions' per aortic root.

It is evident from Table 4.9 that type II lesions were less common than type I lesions, in both SAM-P and SAM-R mice. The data for each SAM-R group (male and female) are heavily skewed, each group containing a single mouse (a male mouse designated #1, and a female mouse designated #4) with a high number of lesions compared with the remainder of their respective groups. When these cross-sections were re-examined, it was noted that the lesions in these two mice were small compared with the less numerous lesions found in other SAM-R mice, so that the cross-sectional area of Oil red O staining per aortic root was in fact typical of that found among the other SAM-R mice (see below). Furthermore, the lipid profiles of these two mice were unremarkable when compared with those of the other SAM-R mice.

Since there were no statistically significant inter-gender differences in lesion counts in each strain of mouse, SAM-P were compared with SAM-R mice irrespective of gender. The data in Table 4.9 were used to calculate the median number of lesions per aortic root in each group.

Table 4.9 Number of lesions in SAM mice fed a Western-type diet

SAM gender, strain, and designation	Any lesion	Type I lesions	Type II lesions
Male SAM-R			
#1	5	5	0
#2	1	0	1
#3	0	0	0
#4	0	0	0
#5	1	1	0
#6	0	0	0
#7	0	0	0
#8	1	1	0
Female SAM-R			
#1	1	1	0
#2	1	1	0
#3	0	0	0
#4	7	7	0
#5	0	0	0
#6	2	2	0
Male SAM-P			
#1	6	4	2
#2	6	5	1
#3	2	1	1
#4	2	0	2
#5	1	1	0
#6	2	2	0
#7	0	0	0
Female SAM-P			
#1	0	0	0
#2	3	1	2
#3	5	5	0
#4	4	4	0
#5	2	2	0
#6	1	1	0
#7	1	0	1

Table 4.9 shows the total number of fatty lesions in the aortic roots of the 14 SAM-P and 14 SAM-R mice fed the Western-type diet for 17 weeks, calculated as described in Chapter Two.

Table 4.10 shows the results of this analysis. SAM-P mice developed a greater number of lesions of any type than did SAM-R mice (P = 0.03). Similarly, SAM-P mice developed more type II lesions than did SAM-R mice (P = 0.04). There was, however, no statistically significant difference in the number of type I lesions found in the two strains of mouse (P = 0.23).

Table 4.10 Median number of lesions in the aortic roots of SAM mice fed a Western-type diet

	Any lesion	Type I	Type II
SAM-R	1 (IQR: 0-1) (mean 1.36)	0.5 (IQR: 0-1) (mean 1.29)	0 (IQR: 0-0) (mean 0.07)
SAM-P	2 (IQR: 1-4) (mean 2.50)	1 (IQR: 0-4) (mean 1.86)	0 (IQR: 0-1) (mean 0.64)
***P* value**	0.03	0.23	0.04

Table 4.10 shows the median number of lesions (classified as type I and type II lesions, and lesions of any type) in the 28 SAM mice fed the Western-type diet for 17 weeks. Inter-quartile ranges are given in brackets. These values were calculated using the non-parametric data in Table 4.9. Mean values for each group are also provided, to emphasize the fact that type II lipid deposition was found in both SAM-P and SAM-R aortic roots in this experiment. P values were calculated using Poisson regression analysis.

4.4.4.3 Prevalence of lesions in aortic roots

An alternative approach to assessing the extent of atherogenesis in SAM mice involved determining how many mice in each group developed each type of lesion. The results of this analysis are given in Table 4.11 (overleaf), each field in the table showing the number of mice developing each lesion type, as a fraction of the number of mice within the specified group.

Table 4.11 Prevalence of lesion types in SAM mice fed a Western-type diet

	Any lesion			Type I lesions			Type II lesions		
Gender	**M**	**F**	**M and F**	**M**	**F**	**M and F**	**M**	**F**	**M and F**
SAM-R	4/8	4/6	**8/14**	3/8	4/6	**7/14**	1/8	0/6	**1/14**
SAM-P	6/7	6/7	**12/14**	5/7	5/7	**10/14**	4/7	2/7	**6/14**
***P* value**	N/S	N/S	**0.1**	N/S	N/S	**0.25**	N/S	N/S	**0.03**

Table 4.11 shows the number of mice displaying lesions of each specified type, as a fraction of the number of mice in each group. For example, 3 of the 8 male SAM-R mice developed type I lesions, while 6 of the 14 SAM-P mice of either gender developed type II lesions. *P* values were calculated using a Chi-squared test. Abbreviation: N/S = statistically non-significant.

12 of the 14 SAM-P mice developed fatty lesions of any type, compared with 8 of the 14 SAM-R mice, this difference not reaching statistical significance ($P = 0.1$). 10 of the SAM-P mice developed type I lesions, compared with 7 of the SAM-R mice, again without reaching statistical significance ($P = 0.25$). More strikingly, there was a statistically significant difference in the proportions of mice developing type II lesions, (6 of the SAM-P mice, compared with a single SAM-R mouse, $P = 0.03$).

4.4.4.4 Results of morphometric analysis

The mean areas stained with Oil red O in the eight cross-sections from each SAM-P and SAM-R aortic root are given in Table 4.12 (overleaf). Using the data in Table 4.12, Table 4.13 (page 188) shows the median area per cross-section covered by Oil red O for each treatment group, categorized according to lesion type. Data from male and female mice have been combined within each group. Since the data in Table 4.12 are non-parametric, groups were compared statistically using median values and non-parametric tests, yielding the *P* values given in Table 4.13.

SAM-P mice showed a greater extent of fatty lesions development than SAM-R mice, as assessed by the cross-sectional area of Oil red O staining in lesions of any type ($P = 0.003$). This difference appeared to be partly accounted for by a statistically significant difference in type II lesion formation ($P = 0.03$); SAM-P mice also appeared to show more extensive type I lipid lesion formation than SAM-R mice, but this difference did not reach statistical significance ($P = 0.17$).

It will be noted that although type II lipid deposition occurred in both SAM-P and SAM-R mice, and was more extensive in SAM-P than SAM-R mice (as noted above), median lesion areas in each group were identical (0.0 in each case, because of the number of mice in each group where no type II lipid deposition was found). Graphic depiction of median areas of type II lesion areas in the two groups might thus be misleading, failing to demonstrate the calculated difference between the two groups. For the sake of illustration, therefore, the graph in Figure 4.8 (page 189) uses the mean lesion areas (± s.d.) also provided in Table 4.13; the *P* values quoted in the graph remain those given in Table 4.13, having been calculated from the (appropriate) non-parametric test, the Mann-Whitney sign rank test.

Table 4.12 Extent of Oil red O staining in SAM mice fed a Western-type diet

SAM gender, strain, and designation	Any lesion	Type I lesions	Type II lesions
Male SAM-R			
#1	37.8	37.8	0
#2	20.2	0	20.2
#3	0	0	0
#4	0	0	0
#5	13.6	13.6	0
#6	0	0	0
#7	0	0	0
#8	33.3	33.3	0
Female SAM-R			
#1	76.8	76.8	0
#2	115.2	115.2	0
#3	0	0	0
#4	111.3	111.3	0
#5	0	0	0
#6	48.9	48.9	0
Male SAM-P			
#1	38.6	37.8	0.7
#2	290.6	92.9	197.7
#3	311.2	20.7	290.5
#4	288.6	0	288.6
#5	66.8	66.8	0
#6	118.3	118.3	0
#7	0	0	0
Female SAM-P			
#1	0	0	0
#2	260.6	9.2	251.4
#3	180.5	180.5	0
#4	423.9	423.9	0
#5	36.8	36.8	0
#6	134.6	134.6	0
#7	144.4	0	144.4

Table 4.12 shows the mean areas stained with Oil red O (in μm^2, accurate to one decimal place) in the eight cross-sections from each of the aortic roots of the 14 SAM-P and 14 SAM-R mice fed the Western-type diet for 17 weeks.

Table 4.13 Median areas of Oil red O staining in SAM mice fed a Western-type diet

	Any lesion	Type I	Type II
SAM-R	16.9 (IQR: 0.0-48.9) (mean 32.6±41.3)	6.8 (IQR: 0.0-48.9) (mean 31.2±42.1)	0.0 (IQR: 0.0-0.0) (mean 1.4±5.4)
SAM-P	139.5 (IQR: 38.6-288.6) (mean 163.9±132.7)	37.3 (IQR: 0.0-118.3) (mean 80.1±114.7)	0.0 (IQR: 0.0-197.7) (mean 83.8±121.7)
***P* value**	0.003	0.17	0.03

Table 4.13 shows the extent of Oil red O staining (in μm^2) in the aortic roots of the 28 SAM mice fed the Western-type diet for 17 weeks. Areas were calculated using the non-parametric data in Table 4.12, and are expressed as median values together with their inter-quartile ranges. Mean values (± s.d.) for each group are also provided, to illustrate that type II lipid deposition was detected in both murine strains. *P* values were calculated using the Mann-Whitney sign rank test.

Figure 4.8 Morphometric analysis of lesion size in SAM mice

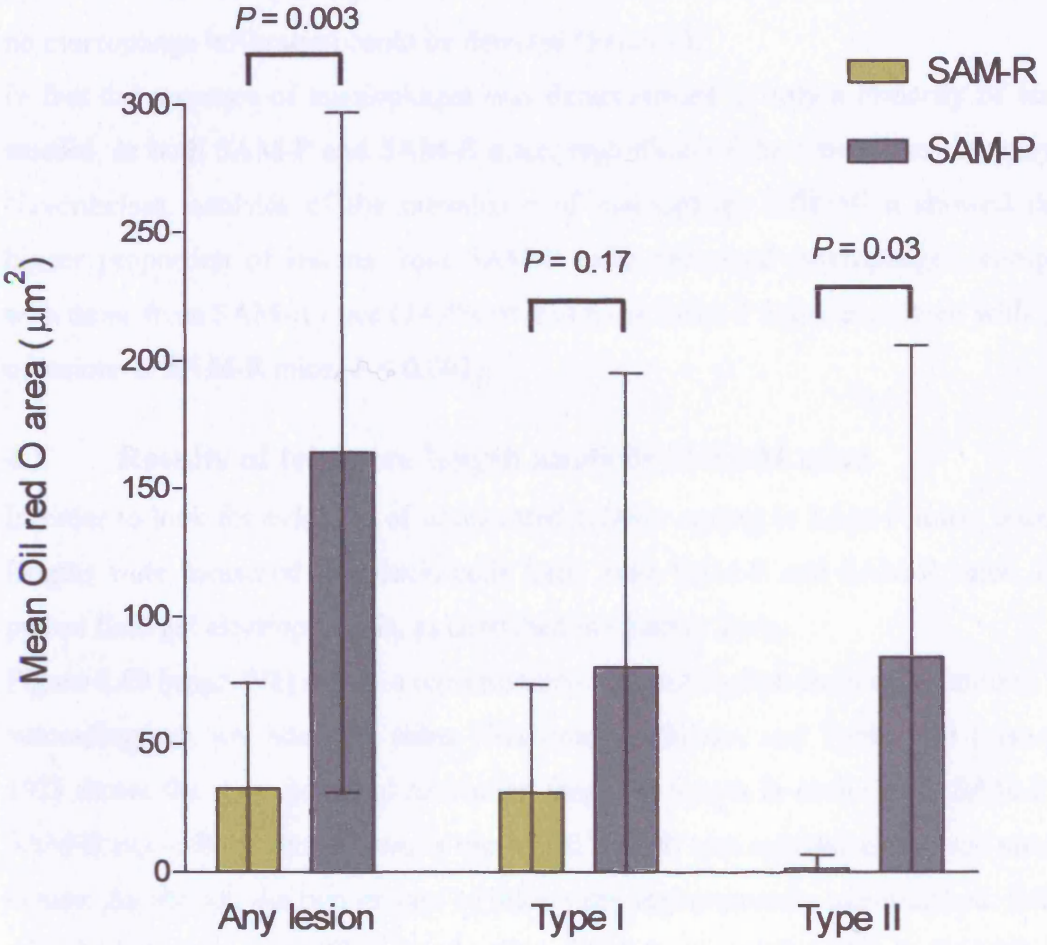

Figure 4.8 shows the mean areas (in μm^2, ± s.d.) of Oil red O staining in aortic root cross-sections from SAM-P and SAM-R mice fed the Western-type diet, categorized according to lesion type. As described in the text, *P* values were calculated using the Mann Whitney sign rank test.

4.4.5 Detection of macrophages in SAM-P and SAM-R aortic roots

Aortic root cross-sections adjacent to those showing lipid deposition were analysed for the presence of macrophages using immunohistochemistry, in an attempt to establish whether the lipid lesions were indeed a manifestation of early atherogenesis.

Figure 4.9 (overleaf) shows representative type I (Panel A) and type II (Panel C) lesions in SAM-P mice, containing macrophages (Panels B and D, respectively). The figure also shows a lipid deposit in the aortic root of a SAM-R mouse (Panel E) where no macrophage infiltration could be detected (Panel F).

In fact the presence of macrophages was demonstrated in only a minority of lesions studied, in both SAM-P and SAM-R mice, regardless of the type of lesion analysed. Nevertheless, analysis of the prevalence of macrophage infiltration showed that a higher proportion of lesions from SAM-P mice contained macrophages, compared with those from SAM-R mice (24.4% of lesions in SAM-P mice, compared with 9.7% of lesions in SAM-R mice, $P < 0.001$).

4.5 Results of telomere length analysis in SAM mice

In order to look for evidence of accelerated cellular ageing in SAM-P mice, telomere lengths were measured in splenic cells from male SAM-P and SAM-R mice, using pulsed field gel electrophoresis, as described in Chapter Two.

Figure 4.10 (page 192) shows a representative autoradiograph from these studies. This autoradiograph was analysed using NIH Image software, and Table 4.14 (also page 192) shows the mean terminal restriction fragment length in each of the SAM-P and SAM-R mice; from these values, a mean TRF length was calculated for each strain of mouse. As shown, the two groups of mice were approximately age-matched. SAM-P mice had shorter mean TRF lengths than SAM-R mice (53.4 kbp in SAM-P mice versus 64.4 kbp in SAM-R mice, $P = 0.02$, Mann-Whitney sign rank test). There was no evidence of a correlation between mean TRF length and age, in either SAM-P or SAM-R mice (Spearman rank correlation coefficient 0.19, $P = 0.65$).

Figure 4.9 Macrophages in SAM lipid lesions

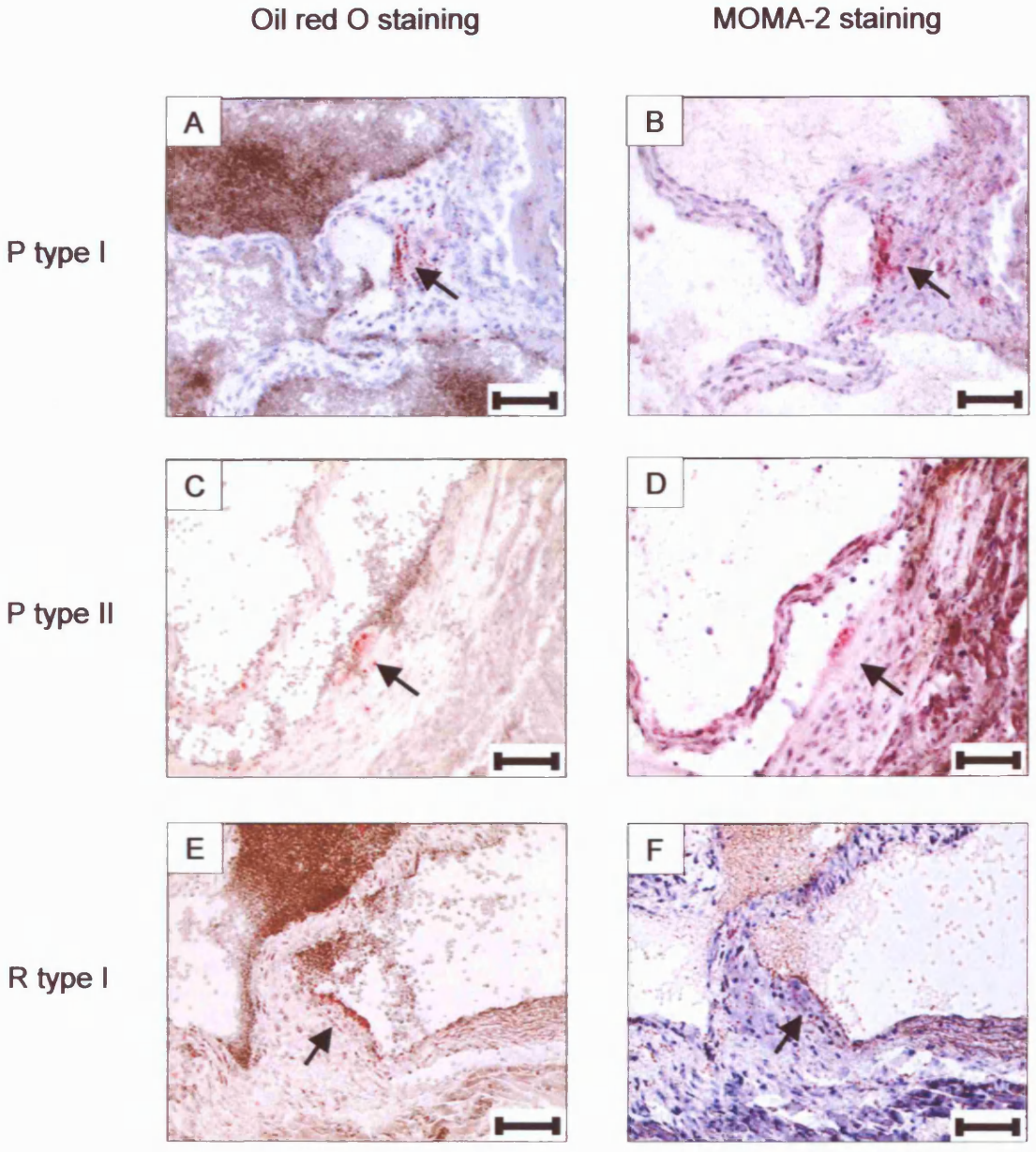

Figure 4.9 Photomicrographs show representative aortic root cross-sections stained with Oil red O (left-hand column) and MOMA-2 (right-hand column), all counter-stained with haematoxylin. Panels B, D and F show sections adjacent to those in Panels A, C and E respectively. The illustrated SAM-P type I lesion (Panel A, arrow) and SAM-P type II lesion (Panel C, arrow) contain macrophages (red stain indicated by arrows in Panels B and D respectively), while the SAM-R type I lesion shown in Panel E (arrow) does not (Panel F, arrow). Bar = 60 μm. As detailed in the text, only a minority of SAM-P and SAM-R lesions exhibited macrophage infiltration.

Figure 4.10 TRF lengths in SAM-P and SAM-R mice

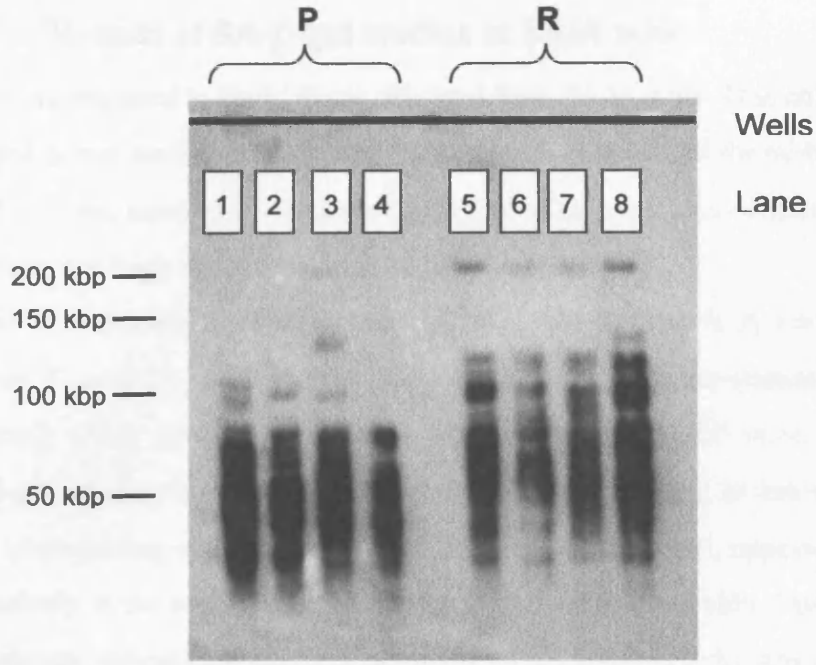

Figure 4.10 shows a representative autoradiograph from the gels run to measure SAM TRF lengths. Lanes 1-4 contain DNA from SAM-P mice of the following ages respectively: 21 days, 21 days, 294 days and 120 days. Lanes 5-8 contain DNA from SAM-R mice of the following ages respectively: 21 days, 21 days, 269 days and 127 days. The mice studied in lanes 1-4 were therefore approximately age-matched with those studied in lanes 5-7.

Table 4.14 TRF lengths in SAM splenic cells

Mouse strain	Age (days)	Mean TRF length (kbp)
SAM-R	21	62.9
SAM-R	21	64.3
SAM-R	127	67.2
SAM-R	269	63.1
Mean		**64.4**
SAM-P	21	53.3
SAM-P	21	52.5
SAM-P	120	52.4
SAM-P	294	55.2
Mean		**53.4**

Table 4.14 shows the mean TRF lengths in SAM mice of various ages, calculated using NIH Image software to analyse the gel shown in Figure 4.10.

4.6 Results of SA-β-gal studies in SAM mice

SA-β-gal was used to study tissue obtained from SAM mice. This enzyme activity was assayed in murine tissue using a protocol similar to that used for rabbit carotid arteries. SA-β-gal was assayed in vascular tissue and skin, examples of tissues which usually have low and high rates of cellular turnover respectively.

Figure 4.11 Panels A-D show sections of SAM-R (Panels A and B) and SAM-P (Panels C and D) skin, stained for SA-β-gal and counter-stained with eosin (see overleaf); these samples were taken from twelve-month-old mice. In SAM-R skin, SA-β-gal staining was usually undetectable; in a few cases, as illustrated in Panel B, faint blue staining could be seen; such staining, when found, appeared to be localized exclusively in the eccrine and sebaceous glands. In SAM-P skin, from both young and old animals, strong blue staining indicative of SA-β-gal activity was seen in the dermis of all samples analysed; again staining in all cases was detected only in the eccrine and sebaceous glands (Panel D). There was no discernible age-related increase in the intensity of staining among either SAM-P or SAM-R mice.

A representative SAM-P aortic cross-section stained for SA-β-gal is shown in Figure 4.11 Panels E and F; as shown, no blue staining was detected in this aorta from a twelve-month old mouse. Indeed, no positive SA-β-gal staining was found in any aortic sections from SAM-P or SAM-R mice irrespective of their age, despite employing several variations to the staining protocol, and despite the fact that β-gal activity was detectable at pH 4.0.

4.7 Discussion

4.7.1 Key findings

The results described in this chapter can be summarized as follows. SAM-P mice were more susceptible than SAM-R mice to fatty lesion development, as assessed by analysis of the cross-sectional area of Oil red O staining in the aortic roots of each strain. SAM-P mice showed a greater extent of Oil red O staining in lesions of any type (i.e. type I and type II combined), and the greater extent of type II lesion development in SAM-P mice (compared with SAM-R mice) also reached statistical significance.

Figure 4.11 SA-β-gal staining in SAM skin and aorta

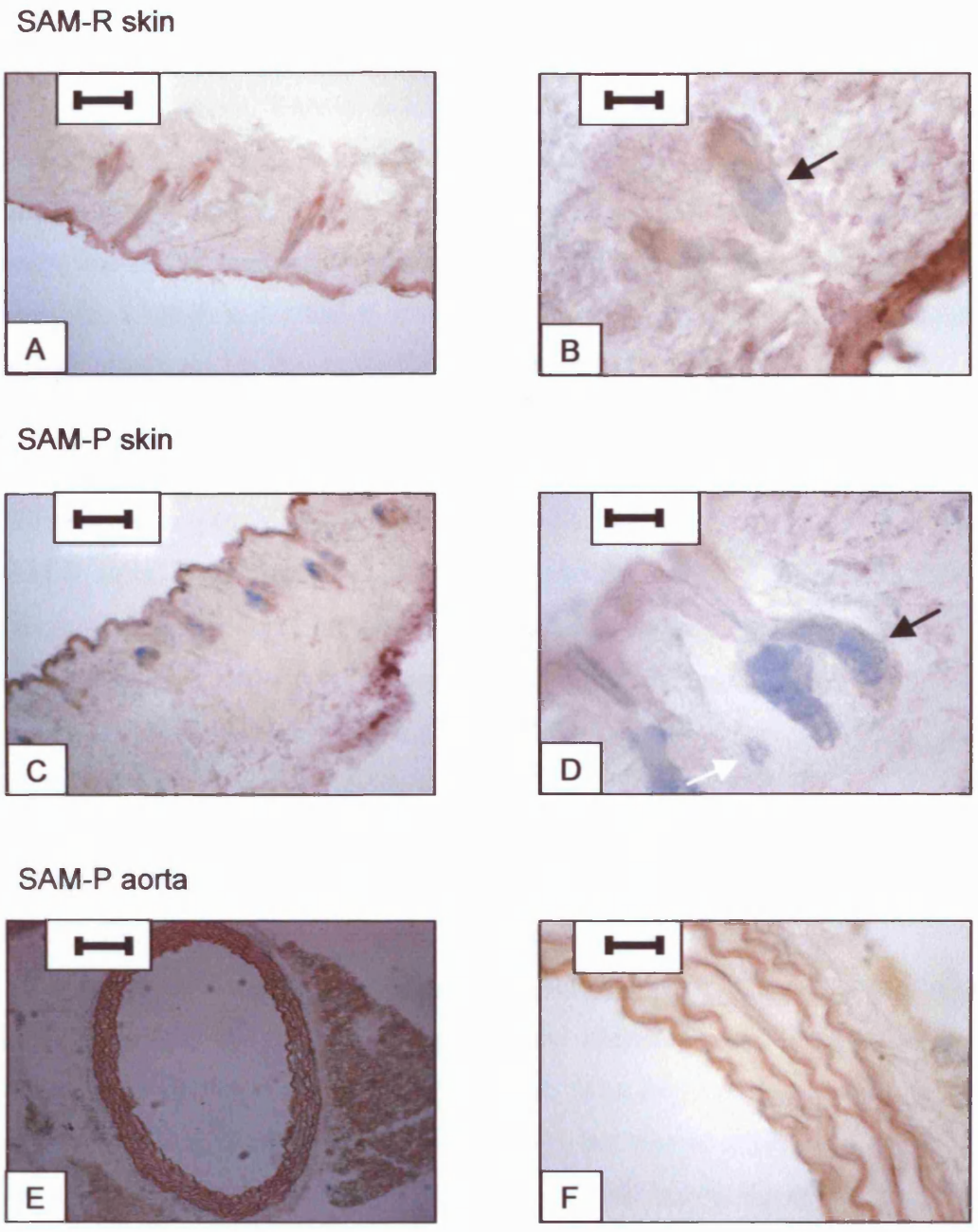

Figure 4.11 Panels A-F show SA-β-gal staining in SAM tissue at low- (Panels A, C and E) and high- (Panels B, D and F) magnification. In SAM-R skin only very faint blue staining is found in the sebaceous glands (arrow in Panel B). In SAM-P skin stronger blue staining is seen in the sebaceous and eccrine glands (black and white arrows, respectively, in Panel D). No SA-β-gal staining was detectable in SAM-P aortas (Panels E and F); nor was it found in SAM-R aortas (data not shown). Bar = 160 μm in Panels A and C, 40 μm in Panels B and D, 100 μm in Panel E, and 25 μm in Panel F.

Furthermore, a greater proportion of SAM-P mice than of SAM-R mice developed type II lesions. SAM-P mice also developed a greater number of lesions per aortic root (as defined above), and in particular a greater number of type II lesions, than SAM-R mice.

On a standard chow, SAM-P mice had lower serum cholesterol levels but higher serum triglyceride levels than SAM-R mice. After administration of the Western-type diet, SAM-P and SAM-R mice showed parallel increases in their serum cholesterol levels, and serum triglyceride levels in the two strains rose to similar levels in each strain. In SAM-P and SAM-R mice, the HDL/total cholesterol ratio was similar, whether mice were fed the standard chow or the Western-type diet.

Immunohistochemistry confirmed the presence of macrophages in the lipid deposits, and macrophage invasion occurred more frequently in SAM-P than in SAM-R lesions.

TRF analysis in splenic cells showed that SAM-P telomeres were shorter than those of SAM-R mice. There was no discernible shortening of SAM telomere length with increasing age. SA-β-gal activity was detected strongly in SAM-P, but only very faintly (if at all) in SAM-R skin; the staining in SAM skin was, though, confined to the sebaceous and eccrine glands. SA-β-gal activity was not detected in vascular tissue from either SAM strain.

4.7.2 Comments on the experimental design

4.7.2.1 The use of SAM mice in the study of ageing and atherogenesis

The main aim of this study was to establish whether a phenotype of accelerated ageing is associated with an increased susceptibility to atherosclerosis. The SAM model was chosen for use in this study for several reasons. Most importantly, it provides not only a strain exhibiting accelerated ageing (SAM-P), but also an appropriate control strain (SAM-R) sharing a similar genetic background. Furthermore, the ageing phenotype of SAM-P mice includes several characteristics found in human ageing. Indeed the research group which established the original SAM colony have pointed out that certain clinical and pathological features (namely osteoporosis, degenerative joint disease, cataract formation, and hearing impairment) which have elsewhere been described as "inevitable disorders as a direct consequence of physiologic senescence" [Cotran *et al.* 1989] are all found in the SAM model [Takeda *et al.* 1994a].

The genetic background of SAM mice may provide a further advantage for their use in the study of atherogenesis. SAM mice are derived, as mentioned in Chapter One, from AKR/J mice. In a previous study of the relative susceptibility of ten inbred murine strains to atheroma formation on a high-fat diet, the AKR/J strain was the fourth most susceptible, behind C57BL/6J, C57L/J and DBA/2J, as assessed by lesion size and number in the aortic root [Paigen *et al.* 1985]. It is a matter for speculation whether this susceptibility may have been handed down to their descendants, the SAM mice.

The use of murine models in general to study either ageing or atherosclerosis is open to criticism. Murine cells contain much longer telomeres than do human cells, with TRFs of up to 150 kilo-bases in mice, compared with TRF lengths of five to ten kilo-bases in humans [Kipling and Cooke 1990]. This difference alone may suggest that different mechanisms underlie the ageing processes in the two species. Similarly, differences in lipid metabolism between mice and humans (discussed below), together with the relative athero-resistance of most murine strains, suggest that murine atherogenesis does not exactly replicate human disease. Nevertheless, as discussed in detail in Chapter One (Sections 1.8.1, 1.8.2 and 1.8.3) mice have been extensively used in the study of atherosclerosis, partly because of their ready availability, and partly because of the well-established techniques developed to measure the extent of lesion formation.

4.7.2.2 The choice of SAM-P/8 and SAM-R/1 strains

SAM-P/8 mice show many of the typical features of the SAM-P ageing phenotype, including the development of hair loss, lack of fur glossiness, periophthalmic lesions, and spinal lordokyphosis [Hosokawa 1994]. Their median survival time mice has been quoted as between 10.0 [Takeda *et al.* 1994a] and 12.1 [Takeda *et al.* 1991] months. SAM-P/8 mice have been the subject of several studies investigating derangement of oxidative stress as part of the ageing phenotype [Zhao *et al.* 1990, Edamatsu *et al.* 1995, Butterfield *et al.* 1997]; it has been shown that manipulation of the oxidative status of these mice can affect their life-span [Edamatsu *et al.* 1995].

SAM-R/1 mice have been used as a control strain in several studies, whether in comparison with SAM-P/8 mice [Zhao *et al.* 1990, Yoshino *et al.* 1994a, Butterfield *et al.* 1997, Han *et al.* 1998, Kurokawa *et al.* 1998, Ye *et al.* 2002], SAM-P/1 mice [Kohno *et al.* 1985, Yagi *et al.* 1988, Nisitani *et al.* 1990, Yagi *et al.* 1995, Park *et al.* 1996, Odagiri *et al.* 1998], SAM-P/6 mice [Jilka *et al.* 1996] or SAM-P/11 mice

[Hosokawa *et al.* 1994, Nakamoto *et al.* 1994, Zhu *et al.* 2001]. Their median survival time has been quoted as between 18.9 [Takeda *et al.* 1994a] and 19.0 [Takeda *et al.* 1991] months. They may develop non-thymic lymphoma or histiocytic neoplasms, but do not exhibit features of the accelerated ageing phenotype [Takeda *et al.* 1991].

The groups of SAM-P and SAM-R mice fed the Western-type diet had slightly different compositions in terms of their male-female mix. This was necessitated by the limited number of age-matched SAM-P and SAM-R mice available in the new colony at UCL. In fact the lack of statistically significant inter-gender differences in serum lipid levels, or in aortic root lipid deposition in SAM mice, meant that the discrepancy in group composition did not influence the overall finding of increased lipid deposition in SAM-P compared with SAM-R mice.

4.7.2.3 Choice of the pro-atherogenic diet

For the reasons given in the introduction to this chapter, the diet chosen for the current study had a higher fat and cholesterol diet than that employed by Yagi *et al.* [Yagi *et al.* 1995]. The Western-type diet used here has previously been employed in several studies of atherogenesis in mice [Nakashima *et al.* 1994, Palinski *et al.* 1995, Tangirala *et al.* 1995a and b]. Administration of this diet results in the development of fatty streaks in LDL-receptor-deficient mice [Palinski *et al.* 1995]; in ApoE-deficient mice more advanced lesions develop, to the extent of fibrous plaque formation [Nakashima *et al.* 1994, Tangirala *et al.* 1995b].

This diet was used in preference to those with a higher fat content for a variety of reasons. Firstly, it was considered desirable that the experimental diet should be as close as possible to a physiological murine diet in terms of its fat content, while still provoking atherogenesis. Secondly, many of the higher-cholesterol diets contain cholic acid, which promotes atherogenesis by inhibiting cholesterol 7α-hydroxylase, an enzyme which in mice is involved in the clearance of cholesterol from the body [Dueland *et al.* 1993]; the Western-type diet did not contain this unphysiological constituent. Furthermore, many of the very high cholesterol diets are unpalatable to mice despite various modifications in their formulation to increase their appeal. Since SAM-P mice generally thrive less well than SAM-R mice, it was important that their diet should be as palatable as possible, so that both strains would feed freely, and so that there should be no in-built bias, with one strain eating more food than the other.

4.7.2.4 Timing of the initiation of the Western-type diet

When the severity of organismic ageing is scored serially in SAM-P and SAM-R mice, a divergence in the ageing phenotype between the two families of mice becomes evident at six months of age [Hosokawa *et al.* 1994], and this divergence becomes more marked over the following weeks. By administering the experimental diet when the mice reached twenty-eight weeks of age, it was intended that the pro-atherogenic stimulus should coincide with the period of accelerated organismic ageing, thus allowing the two processes to interact.

4.7.2.5 Duration of administration of the Western-type diet

Given the absence of overt atherogenesis in SAM mice fed a standard chow for five months [Yagi *et al.* 1995], SAM mice were exposed to the pro-atherogenic stimulus for as long as possible after the chosen initiation date. The seventeen-week administration time was a compromise between this goal and the need for mice to survive until the end of the treatment period. One concern was that administration of a high-fat diet might reduce the SAM life-span, particularly as a previous study has shown, conversely, that chronic caloric restriction can prolong the life-span of SAM mice [Kohno *et al.* 1985].

4.7.2.6 Measurement of serum lipid profiles

Measurement of lipid profiles should if possible be performed using fresh samples, since lipoprotein lipase activity within stored serum can affect triglyceride levels in particular. On the other hand, it was also desirable that sera from all mice from a particular time-point should be assayed simultaneously so as to eliminate the possibility of inter-assay variability. Serum triglyceride levels were therefore analysed in freshly obtained samples, using cardiolipin controls to check for inter-assay variability, while serum cholesterol levels were measured in batches of frozen sera from age-matched mice.

The use of an automated cauldron chemistry technique for the analysis of HDL/total cholesterol ratios has the advantage that it can be used with very small volumes (100μl) of serum. The method is accurate, according to the manufacturer, for serum samples with a total lipid content of up to 1000 mg/dl.

4.7.2.7 Tissue harvesting and fixation

In several studies of murine atherogenesis, perfusion fixation has been employed to preserve vessel and lesion architecture [Zhang *et al.* 1994, Tangirala *et al.* 1995b, Groot *et al.* 1996]. In other similar studies, though, perfusion fixation has not been used [Stewart-Phillips and Lough 1991, Lin *et al.* 1995, Fyfe *et al.* 1994], even when such studies were designed specifically to compare susceptibility to atherosclerosis between various murine strains [Paigen *et al.* 1985, Qiao *et al.* 1994]. Perfusion fixation was not undertaken in the current study of SAM mice because it was felt that the physical manipulation of the murine heart involved in positioning the perfusion catheter might in fact disrupt the integrity of the aortic root.

While it is possible that the absence of perfusion fixation might itself lead to a distortion of the aortic tissue at the moment of culling, and might therefore affect the results of morphometric analysis, it was felt that by treating all the tissues from SAM-P and SAM-R mice identically, valid comparisons could still be drawn between the two strains. Emeson and Shen have used equivalent reasoning to justify omission of perfusion fixation in a study of atheroma formation in C57BL/6 aortic roots [Emeson and Shen 1993].

4.7.2.8 Morphometric analysis of murine aortic roots

The degree of atherogenesis in each mouse was assessed by studying the cross-sectional area of lipid lesions in the aortic root. This approach was developed in 1985 [Paigen *et al.* 1985], and subsequently further refined [Paigen *et al.* 1987b], as a means of determining the susceptibility of various murine strains to atherosclerosis. Initially the appropriateness of this method for the study of human atherosclerosis was questioned, because the location and appearance of murine lesions appeared to differ from those in humans. Nevertheless the approach proved useful in studies investigating genetic loci that distinguished atherosclerosis-prone from atherosclerosis-resistant mice [Paigen *et al.* 1987a], and the model began to gain acceptance. It has become a standard tool for comparing susceptibility to atherosclerosis in different murine strains [Paigen *et al.* 1985, Qiao *et al.* 1994], and for investigating the effects of various interventions (such as dietary, pharmacological and genetic modifications) on the atherogenic process [Zhang *et al.* 1992 and 1994, Emeson and Shen 1993, Emeson *et al.* 1995, Marotti *et al.* 1993, Reddick *et al.* 1994, Lin *et al.* 1995, Tangirala *et al.* 1995a and 1995b, Groot *et al.* 1996].

Furthermore, the degree of lipid lesion development in the aortic root has been shown, in certain mouse strains, to correlate well with the overall extent of atherosclerosis in the remainder of the vascular tree [Tangirala *et al.* 1995b], suggesting that under pro-atherogenic conditions, lesion formation in the aortic root and throughout the vasculature as a whole are determined by common pathological factors. This finding has been used to justify employing aortic root analysis as an indicator of an animal's overall susceptibility to atherogenesis [Tangirala *et al.* 1995b].

The use of Oil red O to detect lipid deposition in murine aortic roots is also well-established [Paigen *et al.* 1985, Emeson and Shen 1993, Emeson *et al.* 1995, Fyfe *et al.* 1994, Qiao *et al.* 1994, Reddick *et al.* 1994, Zhang *et al.* 1994, Lin *et al.* 1995, Groot *et al.* 1996]. Oil red O is a non-ionic, hydrophobic azo dye. The rationale for its use for detecting lipid is that the dye is more soluble in lipid than it is in the solvent (isopropanol).

The classification of lesions as type I or type II deposits, introduced by Qiao *et al.* [Qiao *et al.* 1994], was described in Chapter Two; Paigen *et al.* had previously drawn a distinction between these two lesion types [Paigen *et al.* 1987b], but had not applied the 'type I' and 'type II' designations introduced later by Qiao *et al.*. The significance of the distinction between the two lesion types is discussed below.

4.7.3 Discussion of the results

4.7.3.1 Preservation of the senescent phenotype

The appearance of the mice, and the incidence of senescence-related pathologies, suggest that the senescent phenotype was maintained in the colony of SAM-P mice. The lower weight of SAM-P mice compared with age- and sex-matched SAM-R mice was a consistent finding, and was preserved whether mice were fed a standard chow or the atherogenic Western-type diet. It is well-recognized that without scrupulous selectivity of brother-sister mating (ensuring that the most exhausted-looking SAM-P sibling pairs are bred together, and conversely that the healthiest SAM-R pairs are matched) the senescent phenotype can easily be lost [Hosokawa *et al.* 1997].

4.7.3.2 Susceptibility of SAM-P and SAM-R mice to atherogenesis

The amount of lipid deposition in the SAM aorta roots was analysed using a variety of approaches. Lesion counts and morphometric analysis of lesion size suggested a greater susceptibility to atherogenesis in SAM-P than in SAM-R mice, while no

statistically significant difference was found in prevalence of lesion formation between the two strains.

It has previously been suggested that type I lesions (related to the valve cusps and their attachments) are not an accurate reflection of the atherogenic process in mouse models, while type II lesions (on the aortic free wall) are more discriminating, giving a more accurate and more reproducible indication of the degree of atherogenesis in the remainder of the vascular tree [Paigen *et al.* 1987b]. Furthermore, type II lesions are considered more relevant to the pathology of human disease, which involves lesions in free arterial walls [Paigen *et al.* 1987b]. In C57BL/6 mice fed a high-cholesterol diet, lesions in the aortic free wall (later designated type II lesions by Qiao *et al.* [Qiao *et al.* 1994]) were typically filled with foam cells, invaded the underlying media, had a raised endothelium, and bulged into the aortic lumen [Paigen *et al.* 1987b]; in the same model, lesions confined to the valve cusp (later termed type I lesions) remained small and did not invade the underlying media.

It is therefore interesting to note that for each of the three parameters measured in the current study (number of lesions per aortic root, prevalence of lesion formation, and cross-sectional lesion area) statistically significant differences between SAM-P and SAM-R mice were found only in the lesion type considered to be a better indicator of an animal's susceptibility to atherosclerosis, and to be more representative of human disease.

Macrophages are not normally present in the murine arterial wall [Qiao *et al.* 1994], so the demonstration of macrophages coincident with Oil red O staining (albeit on adjacent cross-sections) suggests that the fatty lesions were the product of a pathological process involving cellular infiltration of the vessel wall, and it seems reasonable to infer that this process was atherogenesis. The presence of macrophages militates against the possibility that the Oil red O staining was merely artefactual.

The absence of macrophages in other Oil red O-staining lesions does not exclude the possibility that these too were atheromatous lesions; the detected lipid may either represent extracellular lipid pools which might, at a later stage, be invaded by macrophages, or alternatively this lipid may have been taken up already by VSMCs.

Further experiments are required to investigate whether lipid deposition in the SAM aortic root correlates with the degree of atheroma formation elsewhere in the vasculature of this strain. Some preliminary experiments were performed for this

thesis, in which whole aortas (from the aortic root to the iliac bifurcation) were excised from other SAM mice fed the Western-type diet, opened length-wise, and immersed in Oil red O staining solution. Employing this method, no clearly defined lipid lesions were seen in either SAM-P or SAM-R aortas (data not shown). This is not surprising, as even lesions in the SAM aortic root (the site most prone to atherogenesis in many murine strains) were microscopic.

The fatty lesions demonstrated in both SAM strains were small, particularly in comparison with the lesions which develop in atherosclerosis-prone strains fed a very high-fat diet. The fact that neither SAM strain developed large lesions does not, though, invalidate the finding of statistically significant differences in lesion formation between the two SAM strains. It is interesting to note that on the Western-type diet lesion size was comparable between SAM-P and C57BL/6 aortic roots. It would be interesting to determine how large lesions would grow if SAM-P mice were fed a diet with the higher cholesterol and fat levels usually employed in studies of atherogenesis in the C57BL/6 model.

The current study investigated susceptibility to atherogenesis in only two SAM strains (P/8 and R/1). Before any firm inferences can be drawn from this study concerning the relationship between accelerated ageing and atherosclerosis, further studies need to be undertaken to confirm that the observed differences apply to other SAM-P and SAM-R strains.

4.7.3.3 Possible explanations for the greater lesion formation in SAM-P/8 mice

The apparently greater susceptibility of SAM-P/8 mice to atherogenesis compared with SAM-R/1 mice could be attributed to a variety of causes. Since the SAM-P/8 and SAM-R/1 mice were housed and maintained in identical conditions, and were fed an identical diet, it seems reasonable to infer that the greater susceptibility of SAM-P/8 mice to atherosclerosis is an intrinsic biological property which has probably arisen as one aspect of their senescent phenotype.

Ultimately, atherosclerosis results from an interaction of blood constituents with components of the arterial wall. The difference in susceptibility to atherogenesis between the two murine strains is therefore likely to arise from differences either in their blood constituents or in the properties of their vessel walls. Alternatively, there may be a difference in the microenvironment in which the blood constituents interact with the arterial wall; one influence on this microenvironment could be the oxidative

status of the vessel wall. It is also possible that other acknowledged risk factors for atherosclerosis are more prominent in one SAM strain than the other, and of the various explanations for the greater susceptibility to atherogenesis of SAM-P mice, this possibility is addressed first below.

Blood pressure and diabetes in SAM mice

Since in humans hypertension and diabetes mellitus are two of the main established risk factors for atherosclerosis [Kannel and McGee 1979, Stokes *et al.* 1987], it is important to consider the possibility that the apparent difference in susceptibility to atherogenesis between SAM-P and SAM-R strains may result from differences in their blood pressure and/or serum glucose levels.

In fact evidence from a study comparing blood pressures in SAM-P/8 and SAM-R/1 mice argues against a prominent role for hypertension as a pro-atherogenic factor in SAM-P mice [Han *et al.* 1998]. Young SAM-P/8 and SAM-R/1 mice have similar blood pressures, and while the blood pressure of SAM-R/1 mice remains approximately constant throughout their life, the blood pressure of SAM-P/8 mice actually falls after approximately six months of age.

Furthermore, in a study looking at age-related changes in the thoracic aortas of SAM-P/11 and SAM-R/1 mice, the more marked histological changes found in the vasculature of SAM-P11 mice (detailed below) developed over the first nine months of their lives, during which time the blood pressures of the SAM-P/11 and SAM-R/1 mice were indistinguishable [Zhu *et al.* 2001].

The prevalence of diabetes mellitus in SAM-P and SAM-R mice has not been documented in the literature to date, and serum glucose levels in these mice have not been systematically compared. In fact the only relevant published study suggests that SAM-P/8 hearts are more sensitive than SAM-R/1 hearts to insulin [Kurokawa *et al.* 1998], suggesting, if anything, that SAM-R/1 mice are likely to be the more insulin-resistant (and therefore more glucose-intolerant) strain. Determination of the relative prevalence of diabetes mellitus in the two SAM strains is clearly necessary in order to clarify whether this disease may be involved in the pathology of SAM mice.

Serum lipid profiles in SAM mice

A third major risk factor for human atherosclerosis is hypercholesterolaemia [Zemel and Sowers 1990]. It was therefore necessary to establish whether the relative

susceptibility to atherogenesis of SAM-P mice could be attributed to an abnormality in their serum lipid profile. A comparison of the serum lipid profiles of SAM-P/8 and SAM-R/1 mice fed a standard laboratory chow or a high-fat diet had not previously been published.

In the current study, on a standard laboratory chow SAM-P/8 mice had lower serum total cholesterol levels but higher serum triglyceride levels than SAM-R/1 mice at twenty-seven weeks of age. Similarly, when SAM-P/1 and SAM-R/1 mice were fed a standard chow [Yoshino *et al.* 1994a], SAM-P/1 mice tended to show lower total cholesterol and higher serum triglycerides levels than SAM-R/1 mice, though these differences reached statistical significance only at a few time-points in the course of their lives.

Administration of a high-fat diet has been shown to raise the serum lipid levels in several strains of mouse [Nakashima *et al.* 1994, Qiao *et al.* 1994]. Similarly in the present study, administration of the Western-type diet led to statistically significant increases in the serum cholesterol and triglyceride levels in both SAM-P/8 and SAM-R/1 mice. After sixteen weeks on this diet, SAM-P/8 mice still had lower serum cholesterol levels than SAM-R/1 mice, but the two strains now had similar triglyceride levels.

Since SAM-P/8 mice showed lower serum cholesterol levels than SAM-R/1 mice both before and after administration of the Western-type diet, the greater accumulation of lipid in SAM-P/8 aortic roots cannot be explained by the total serum cholesterol level of these mice. The greater susceptibility of SAM-P mice also occurred despite a convergence of serum triglyceride levels between the two murine strains.

HDL/total cholesterol ratios were similar in SAM-P/8 and SAM-R/1 mice fed either the standard chow or the Western-type diet. In humans, HDL removes cholesterol from the peripheral tissues and from lipid deposits in the arterial wall, transporting it back to the liver for further degradation and subsequent excretion in bile; this process is known as 'reverse cholesterol transport'. As a result, subjects with high HDL cholesterol levels (especially those in whom the total/HDL cholesterol ratio is less than 4.5) achieve a protective effect against atherosclerosis [Miller 1987, Assmann and Gotto 2004]. The ratio of total/HDL cholesterol is therefore used in clinical practice as part of the assessment of a subject's cardiovascular risk.

Similarly, in several inbred strains of mouse fed a high-cholesterol diet, HDL levels are inversely proportional to the degree of atherosclerotic lesion formation in their aortic roots [Nishina *et al.* 1993]. There are, though, reasons to question whether the role of murine HDL is analogous to that of human HDL.

In humans, HDL cholesterol constitutes only a minority of total cholesterol levels, the majority being made up of LDL. By contrast, in mice HDL is the most abundant cholesterol-carrying particle [Rubin and Smith 1994], and this applies to SAM-P/1 and SAM-R/1 mice [Komura *et al.* 1994]. In the present study, HDL also constituted the majority of total cholesterol in SAM-P/8 and SAM-R/1 mice whether fed a standard chow or a Western-type diet.

The major protein associated with HDL (in both humans and mice) is apolipoprotein AI (apoAI), and the concentration of this apolipoprotein is the major determinant of HDL concentration. If the human *apoAI* gene is over-expressed in transgenic mice of strains usually susceptible to atherosclerosis, this manipulation leads to an elevation in their HDL levels, and renders the mice resistant to atherogenesis [Rubin *et al.* 1991]. On the other hand, although mice created with an inactive *apoAI* gene have a significantly lower HDL concentration than wild-type mice, they do not display increased susceptibility to atherosclerosis [Li *et al.* 1993]. It is generally felt, though, that HDL particles do perform an anti-atherosclerotic protective role in mice at least approximately analogous to that in humans [Rubin and Smith 1994, Rigotti *et al.* 1997].

When C57BL/6 mice are fed a high cholesterol diet their total plasma cholesterol rises and their HDL cholesterol falls; their HDL/total cholesterol ratio consequently falls dramatically [Emeson *et al.* 1995] and mice develop atheromatous lesions in the aortic root. This atherogenesis is thought to be largely attributable to the reduction in HDL levels [Paigen *et al.* 1987a, LeBoeuf *et al.* 1990]. After various interventions, though, such as the addition of alcohol to the high-fat diet, the extent of atherosclerosis does not appear to correlate with the HDL/total cholesterol ratio [Emeson *et al.* 1995]. Clearly this casts some doubt on the ability of this ratio to predict susceptibility to atherosclerosis in certain situations.

In the present study, the similarity between SAM-P and SAM-R mice in terms of their HDL/total cholesterol ratios when fed either diet, combined with their parallel increases in serum cholesterol and triglycerides and the lower cholesterol levels in

SAM-P mice, suggest that any observed difference in fatty lesion formation cannot easily be attributed to differences in lipid profile between the two strains.

Histological changes in the SAM arterial wall

As mentioned above, one possible explanation for the apparent increased susceptibility of SAM-P mice to atherogenesis may relate to intrinsic changes in the arterial wall. Histological differences have been described between the arteries of SAM-P and SAM-R mice.

With age, there is an increase in aortic wall thickness in SAM mice (as indeed there is in humans [Virmani *et al.* 1991]), and this thickening is more pronounced in SAM-P than SAM-R mice [Zhu *et al.* 2001]. Age-related aortic wall thickening in humans has been attributed to the accumulation of extracellular matrix within the subintima and media of the vessel [Cooper *et al.* 1994]. Similarly, in SAM mice there is an increase in the abundance of collagen fibres between the VSMCs, together with breakage and disorganization of the elastic laminae; the VSMCs undergo hypertrophy, but their number in the media falls significantly [Zhu *et al.* 2001]. These changes are observed earlier and are more exaggerated in SAM-P than SAM-R mice, and, as mentioned earlier, cannot be attributed to differences in blood pressure between the two strains. Zhu *et al.* found no evidence of amyloid or lipid deposition in either SAM-P or SAM-R aortas [Zhu *et al.* 2001].

Such differences in vessel wall architecture between SAM-P and SAM-R mice may well contribute to, or indeed be a manifestation of, a difference in susceptibility to atherosclerosis. They may arise from factors 'extrinsic' to the vessel wall, such as high serum glucose levels in the lumen; alternatively, they may arise from 'intrinsic' differences in vascular cell biology between the two strains.

The previous chapter dealt with the question of whether cellular replicative senescence occurs in the vasculature in a pathological situation. It is now worth considering whether the accelerated ageing of SAM-P mice might be accompanied by accelerated ageing at a cellular level, and whether any such loss of cellular replicative capacity might contribute to an increased susceptibility to atherosclerosis.

Evidence for reduced cellular replicative capacity in SAM-P mice

The relationship between vascular cell replicative senescence and the development of atherosclerosis in humans and animal models has been discussed in detail in Chapters

One and Three. Not only is there evidence to suggest that senescent vascular cells are present in atherosclerotic lesions, but it is also thought that these cells may play an aetiological role in the development and progression of the disease (discussed further in Chapter Five).

No studies to date have looked specifically for evidence of replicative senescence in SAM vascular cells. Some research, though, has suggested that other cell types derived from SAM-P mice are more prone to replicative senescence than their counterparts from SAM-R mice. For example, a higher rate of chromosomal aberrations has been found in bone marrow cells from SAM-P/1 compared with SAM-R/1 mice [Nisitani *et al.* 1990], and the rate of increase in chromosomal aberration frequency paralleled the emergence of the ageing phenotype in each strain. Furthermore, when dermal fibroblasts isolated from SAM-P/11 neonates were grown in culture, they were able to perform fewer rounds of cell replication before reaching crisis than equivalent cells derived from SAM-R/1 neonates [Hosokawa *et al.* 1994]; as cells lost their replicative capacity they assumed the morphological features characteristic of senescent cells.

If evidence were to be found for an increased propensity of SAM-P vascular cells to cellular senescence, it would be possible to postulate a mechanism whereby this propensity could lead to the susceptibility of SAM-P mice to atherogenesis; one might for example speculate that if SAM-P arteries are lined by ECs with reduced replicative potential, the SAM-P endothelium might be less resistant to vascular atherogenic insults, if only because of an impairment of the endothelium's ability to repair any breach in its integrity.

In order to investigate cellular senescence in more detail in SAM mice in the current study, splenic cells were subjected to TRF length analysis, and aortas and skin were stained for SA-β-gal activity. The analysis of TRF length provides a useful guide to the length of the telomere itself when, as in mice, telomeres are very long. While splenic cells from SAM-P/8 mice had shorter TRFs than cells from SAM-R/1 mice, no obvious shortening of TRF length with increasing murine age was detected. These results are interesting because they do suggest a fundamental difference between the chromosomes of SAM-P and SAM-R mice generally, and the shorter TRF length observed in the mouse strain which ages more quickly certainly fits with the theory that telomere shortening may be related to replicative, and possibly organismic ageing.

On the other hand, the lack of progressive telomeric shortening with increasing age in either SAM-P or SAM-R mice would argue against a central role for telomere shortening in the ageing process of SAM mice. Indeed Kipling and Cooke detected no age-related decrease in telomere length in their study of TRF lengths in hepatocytes from various murine species [Kipling and Cooke 1990]. This finding, together with the great length of murine telomeres, and the presence of telomerase activity in some murine cells, have been cited as evidence that replicative senescence of murine cells is likely to occur via mechanisms independent of telomere shortening [Sherr and DePinho 2000, Wright and Shay 2000]. The study of telomerase-deficient mice mentioned in Chapter One also casts doubt on the relevance of telomere shortening to murine cellular senescence [Blasco *et al.* 1997].

The telomere study in this chapter and the work of Kipling and Cooke have looked only at splenic and hepatic cells; the findings in these cells may or may not be mirrored in other cell types, particularly as research in other mouse strains has suggested that there are marked differences in telomerase activity and telomere length between various tissues within individual mice [Coviello-McLaughlin and Prowse 1997]. It is therefore possible that in SAM mice there are other cell types in which telomeres do shorten with age, and the question of whether age-related telomere attrition occurs in SAM vascular cells remains open.

Another explanation for the telomere data in this chapter is that other fundamental differences between SAM-P and SAM-R mice, such as differences in oxidative status (discussed below), may affect telomerase function and/or telomere length in SAM mice, without necessarily playing a causal role in the accelerated ageing of SAM-P mice. In this respect it is of note that the emergence of replicative senescence in murine cell cultures has recently been attributed to the high sensitivity of murine cells (compared, for example, with human cells) to oxidative stress [Parrinello *et al.* 2003].

Telomere analysis in SAM splenic cells thus did not show clear-cut evidence of accelerated cellular ageing in SAM-P mice. Attention therefore turned to the detection of SA-β-gal activity in SAM tissues. The results reported by Dimri *et al.*, showing an absence of SA-β-gal staining in senescent fibroblasts from two murine strains had implied that this marker of senescence was unlikely to be helpful in the study of SAM mice [Dimri *et al.* 1995]. In fact more recent studies have shown that SA-β-gal

staining can be detected in certain murine tissue, in particular in lymphomatous cells [Schmitt *et al.* 2002] and in regenerating liver tissue [Satyanarayana *et al.* 2003].

The subsequent failure in the current study to detect SA-β-gal staining in either SAM-P of SAM-R aortas could be attributable either to a genuine absence of cellular senescence in these vessels, or to the use of an assay which was inappropriate for the study of murine vascular cells. Given the apparent ability of SA-β-gal to detect senescence in human and rabbit vascular cells (as described in Chapter Three), and in other murine tissues, it seems likely (though by no means definite) that SA-β-gal would be able to detect murine vascular cell senescence if it were present; the results in this chapter therefore imply that SAM-P aortas do not contain senescent cells. This might be predicted from the known low rate of cellular turnover in normal vascular tissue [Schwartz and Benditt 1973 and 1976, Hobson and Denekamp 1984], and it was for this reason that the SA-β-gal staining was also applied to a tissue likely to show a higher degree of proliferative activity.

Staining of SAM-P and SAM-R skin for SA-β-gal activity did show a difference between the two substrains, with markedly stronger SA-β-gal staining in SAM-P than SAM-R skin, though this staining was limited to the sebaceous and eccrine glands. Eccrine glands decrease in number and become disorganized in ageing human skin [Montagna 1965], while sebaceous glands maintain their numbers but undergo hyperplasia [Plewig and Kligman 1978]. Any inferences from the detection of SA-β-gal staining in SAM-P skin must be guarded, given the findings of Dimri *et al.* that human adult melanocytes express SA-β-gal activity independent of replicative age, and that sebaceous and eccrine gland cells express SA-β-gal activity independent of donor age [Dimri *et al.* 1995]. SA-β-gal staining was undertaken in SAM skin in the expectation that this enzyme activity might be found in the keratinocyte population, given the proliferative nature of this tissue; this turned out not to be the case. Thus in murine skin, SA-β-gal positivity does not appear to detect cellular ageing, and there is thus no clear evidence of replicative senescence in SAM skin. Nevertheless it is interesting that a difference between SAM-P and SAM-R skin is demonstrable, despite these considerations.

The results of the TRF analysis do lend support to the contention that SAM-P/8 cells have different replicative machinery from SAM-R/1 cells, but neither these results nor

those from the SA-β-gal staining of SAM skin provide evidence of an age-related accumulation of senescent cells in either strain. Given the putative role of replicative senescence both in organismic ageing and in atherosclerosis, a difference in propensity to replicative senescence between SAM strains would be an attractive explanation (at least in part) for both the ageing phenotype and the increased susceptibility to atherogenesis of SAM-P mice. In the absence of conclusive evidence of excessive replicative senescence in SAM-P mice, other strain-specific differences must be considered as aetiological factors in the increased susceptibility of SAM-P mice to atherogenesis. One such candidate may be the level of oxidative stress in SAM-P and SAM-R mice.

Differences in oxidative status between SAM-P and SAM-R mice

Several studies have pointed to differences in the levels of oxidative stress in the tissues of SAM-P and SAM-R mice. For example, SAM-P mice show higher levels of oxidatively-modified proteins in tissues such as the brain and liver, than do SAM-R mice [Butterfield *et al.* 1997, Nakamoto *et al.* 1994]; similarly, higher levels of lipid peroxidation products have been found in the brain [Choi *et al.* 1994], liver [Park *et al.* 1996] and skin [Yoshino *et al.* 1994b] of SAM-P mice. Malonyldialdehyde levels (a marker of oxidative damage) are elevated in SAM-P compared with SAM-R brain tissue [Nomura *et al.* 1989].

In accordance with this evidence of increased oxidative damage in SAM-P mice, these mice have relatively impaired antioxidant defence mechanisms; for example, in SAM-P liver and kidney tissue, mitochondrial SOD activity is lower than in SAM-R mice [Zhao *et al.* 1990, Park *et al.* 1996]. SAM-P mice also show age-dependent decreases in glutathione levels in the brain and liver [Liu and Mori 1993].

Differences in oxidative status between SAM-P and SAM-R mice may play a causative role in the accelerated ageing phenotype. The life-span of SAM-P/8 mice can be dramatically increased (from forty-two to fifty-six weeks, approximately) by intra-peritoneal administration of the free radical scavenger PBN [Edamatsu *et al.* 1995]. This prolongation of life-span is associated with an amelioration of their oxidative status [Butterfield *et al.* 1997].

There is therefore good evidence for differences in oxidative status between SAM-P and SAM-R mice. The shorter telomere length found in SAM-P mice may reflect a higher degree of oxidative stress in these mice, given the causal relationship between

increased oxidative stress and accelerated telomere attrition described in Chapter One (Section 1.5.4.1). It was suggested there that telomeres may act as sensors of cumulative oxidative damage [Serra *et al.* 2000, Toussaint *et al.* 2000a]. The shorter TRF lengths in SAM-P mice may be evidence of this phenomenon, though if that were the case, TRF length might be expected to decrease progressively with increasing organismic age.

The relevance of oxidative stress to both cellular and organismic ageing, as well as to atherosclerosis, has been discussed in detail in Chapter One. In the absence of clear evidence of accelerated cellular senescence in SAM-P mice, an abnormality in their oxidative status provides an alternative potential explanation for the observed difference in susceptibility to atherogenesis between SAM-P and SAM-R strains.

4.8 Conclusion

To summarize, the findings in this chapter suggest that SAM-P mice are more prone to atherogenesis than are SAM-R mice, implying an intrinsic link between organismic ageing and susceptibility to atherosclerosis. The difference in susceptibility to atherogenesis could not easily be explained by any observed differences in lipid profile between the two strains. Telomere and SA-β-gal studies showed differences between the two mouse strains, but did not provide conclusive evidence for the *in vivo* occurrence of replicative senescence in these mice. Nevertheless it is noteworthy that a strain of mouse with reduced cellular replicative capacity and increased oxidative stress shows both accelerated ageing and increased atherogenesis.

CHAPTER FIVE

Discussion

The overall aim of this thesis has been to explore the relationship between ageing and vascular pathophysiology. It was hoped in particular, to shed light on the mechanisms through which ageing may predispose to atherogenesis. Since associations have previously been postulated between organismic ageing and cellular senescence (as discussed in Chapter One, Section 1.4.6) and between cellular senescence and atherosclerosis (as detailed in Chapter One, section 1.4.8) it was proposed that cellular senescence might provide a mechanistic link between organismic ageing and atherosclerosis.

In order to investigate this possibility, it was first necessary to look for firm evidence that cellular senescence can occur in the vasculature. To this end, a marker of cellular senescence, SA-β-gal, was employed in a pathological situation – an artery's response to endothelial denudation – in which a cellular proliferative response is known to occur. Pilot *in vitro* studies established that this marker could detect senescence emerging among cultured vascular cells. Subsequently, use of this assay in the rabbit carotid model yielded evidence that endothelial and vascular smooth muscle cell senescence can indeed occur *in vivo* following balloon denudation. The emergence of senescent cells was augmented by repetition of the injury.

Since interpretation of these results, and of some of the data from the SAM mouse studies, depends heavily on the validity (or otherwise) of SA-β-gal as a marker of cellular senescence, it is worth considering at this stage the strengths and weaknesses of this assay in some detail, before going on to consider the implications of the results described in Chapters Three and Four.

5.1 SA-β-gal as a marker of cellular senescence

5.1.1 Possible weaknesses and limitations

Some of the limitations of SA-β-gal in the identification of senescent cells have already been mentioned in Chapter One: certain cell types in certain species do not express SA-β-gal when they senesce; conversely other cell types, including adult melanocytes, express SA-β-gal irrespective of their replicative status [Dimri *et al.* 1995].

It has been argued that in some cell types SA-β-gal expression may not necessarily indicate the irreversible cell cycle arrest which is the hallmark of cellular senescence.

Macieira-Coelho has suggested that the expression of this enzyme activity may merely reflect a prolonged resting phase in the cell cycle, no matter whether it is reversible or irreversible [Macieira-Coelho 1998]. Macieira-Coelho cited his earlier data showing that levels of lysosomal enzymes increased during prolonged resting phases of fibroblasts *in vitro*, but decreased soon after stimulation of these quiescent cultures [Macieira-Coelho *et al.* 1971]. He argued that as a result the detection of lysosomal enzymes such as β-gal would be expected to rise during any prolonged non-mitotic state, whether reversible or not, and that therefore SA-β-gal activity would be unable to distinguish between a reversible and a terminal resting phase.

While this argument seems reasonable in theory (and Macieira-Coelho presented no experimental data to prove his contention) other research suggests that at a practical level SA-β-gal is in fact able to distinguish between quiescence and senescence. Dimri *et al.* had already shown that SA-β-gal was not detected in cultures which had been made quiescent by serum deprivation, even after seven days [Dimri *et al.* 1995]. Furthermore, while low levels of β-gal staining were detectable at pH 6.0 when cells were made quiescent by confluence, this staining was less intense than that found in senescent cells, and was lost within two days of re-plating; in contrast SA-β-gal staining in senescent cells was stronger than in quiescent cells, and was not lost after re-plating [Dimri *et al.* 1995].

Another study has suggested that the expression of SA-β-gal may not be specific to replicative senescence, but may be dependent on cell density in culture, or on other causes of growth arrest [Severino *et al.* 2000]. This study confirmed that SA-β-gal activity increased in low-density cultures of proliferatively senescent cells; on the other hand β-gal activity at pH 6.0 could also be detected in supposedly immortal fibroblast cultures which had reached a high cell density, and in low-density, young, normal cultures treated with hydrogen peroxide. In the latter two situations, though, the presence of SA-β-gal staining may be a manifestation of stress-induced premature senescence: cultures with high cell densities may experience culture stress resulting from nutrient depletion, while increased oxidative stress in fibroblasts, as well as accelerating telomere shortening [von Zglinicki *et al.* 1995], is also known to precipitate SIPS and detectable SA-β-gal activity in these cells [Serrano *et al.* 1997].

In the rabbit carotid artery model, it seems unlikely that SA-β-gal activity, in endothelial cells at least, might have arisen from contact inhibition, given that these cells often neighboured discontinuities in the endothelium. Nevertheless, in this model, as with the cell culture experiments described above, the demonstration of SA-β-gal staining cannot be taken as unequivocal evidence that cells have reached replicative senescence. Instead, as mentioned in Chapter Three (Section 3.2.4.3), cells staining for SA-β-gal in the injured artery may have undergone SIPS, as a result of alterations in redox status previously shown to occur in balloon-injured arteries [Shi *et al.* 2001]. As discussed in Chapter One, the distinction between replicative and stress-induced senescence is becoming increasingly blurred, as it is becoming appreciated that these two forms of senescence share several common features and mechanisms, and may be regarded as related aspects of a cell's response to stress [Ben-Porath and Weinberg 2004].

5.1.2 Biological rationale for the ability of SA-β-gal to detect senescence

Another potential weakness of SA-β-gal as a marker of replicative senescence has been that, until recently, a mechanistic explanation for the effectiveness of the assay had not been elucidated. In particular, it was not clear whether SA-β-gal becomes detectable at pH 6.0 due to an increased expression of lysosomal β-gal, allowing detection of enzyme activity despite measurement at a suboptimal pH, or whether a particular senescent isoform of the enzyme, detectable optimally at pH 6.0, is expressed in senescent cells. With respect to the latter possibility, it is known that alternate splicing of the β-galactosidase molecule can lead to the generation of both the classic lysosomal enzyme and a protein similar (but not identical) to this enzyme [Morreau *et al.* 1989].

It has more recently been shown that the increase in SA-β-gal expression in senescent cells can in fact be attributed solely to the increase in lysosomal mass within these cells [Kurz *et al.* 2000]. In this study, the intracellular and lysosomal pH levels of young and senescent HUVECs were manipulated, and the resultant alterations in β-gal activity were studied using flow cytometry. It was found that lysosomal alkalinization, together with equilibration of the intracellular milieu to pH 6, caused a profound inhibition of the total intracellular β-gal activity. However, no matter what the intracellular and lysosomal pH, senescent cells showed levels of β-gal activity

significantly higher than in young cells. This higher level of activity correlated with higher β-gal protein levels. Acridine Orange staining showed an increase in lysosomal content with replicative age, which correlated with the rise in β-gal levels. It was concluded that SA-β-gal is a manifestation of residual lysosomal activity present at a suboptimal pH, which becomes detectable due to the increased lysosomal content of senescent cells. The same group have subsequently suggested that the increased lysosomal mass in senescent cells may result from an accumulation of autophagic vacuoles, in response to an intracellular accretion of non-degradable macromolecules and organelles [Erusalimsky and Kurz 2005].

These recent findings may help to explain why SA-β-gal does not appear to be a universal marker of cellular senescence, and why, conversely, a few non-senescent cells appear to be SA-β-gal-positive. It seems likely that this assay would be of use only in those cell types which exhibit increased lysosomal mass when (and only when) they undergo senescence. Cells with a constitutively high lysosomal content, such as phagocytes, might be expected to show SA-β-gal positivity even in the absence of senescence.

The increase in lysosomal content in senescent cells, as manifested by increased SA-β-gal staining, is relevant to considerations about the inter-relationship between apoptosis and replicative senescence. Lysosomal activation plays a significant role in cell death by apoptosis [Lockshin and Zakeri 1996], so a similar accumulation of lysosomes in senescent cells suggests a possible overlap between apoptosis and senescence. In this context it was notable that in the rabbit studies apoptotic cells did not express sufficient lysosomal activity to become SA-β-gal-positive.

DeJesus *et al.* have measured four different lysosomal enzymes (β-galactosidase, α-galactosidase A, β-glucuronidase and acid phosphatase) in young and senescent human foetal fibroblasts [DeJesus *et al.* 2002], and found that while levels of each enzyme rose with repeated passages, β-galactosidase showed the least dramatic increase of the four enzymes. Thus while a chance of cytochemistry makes it easy to assay β-galactosidase activity *in vitro* and *in vivo*, detection of other lysosomal enzymes may in the future provide more sensitive assays for cell senescence. This in itself does not invalidate SA-β-gal as a marker of senescence

5.1.3 Subsequent use of SA-β-gal to detect *ex vivo* senescence

At the time the rabbit carotid artery experiments were designed, SA-β-gal had become widely adopted as a tool to detect senescent cells *in vitro*, and was only starting to be used in the study of *ex vivo* tissue. Subsequently its value in the detection of *in vivo* senescence has if anything become increasingly accepted: tissues and organs studied include the cornea [Mishima *et al.* 1999], the prostate [Choi *et al.* 2000], the breast [te Poele *et al.* 2002], and lymphomatous masses [Schmitt *et al.* 2002], as well as liver and vascular tissue (discussed below); species investigated include mice, rats, rabbits, monkeys and humans.

SA-β-gal has been used in a study involving partial hepatectomies in telomerase-deficient mice [Satyanarayana *et al.* 2003]. The ability of the remaining hepatic cells to regenerate *in vivo* was monitored, and it was found that those cells showing SA-β-gal activity contained critically shortened telomeres and were unable to proliferate.

Since its use in the rabbit carotid model, SA-β-gal has gone on to be used in the identification of senescent vascular cells in other species. It was employed in the detection of senescent ECs in diabetic rats [Chen *et al.* 2002], and has been used as a marker of both *in vitro* and *in vivo* human VSMC senescence by Minamino *et al.* [Minamino *et al.* 2003]; in this study they showed that introduction of a *ras* allele into human VSMCs in culture led to the emergence of a senescent phenotype, including large cell size, expression of Cdk inhibitors, and also SA-β-gal-positivity; this effect appeared to be mediated via the extracellular signal-regulated kinase (ERK) signalling pathway. As will be discussed below, in the same study, the detection of co-staining for SA-β-gal and α-smooth muscle actin was taken as evidence of VSMC senescence in diseased human arteries.

In conclusion, then, SA-β-gal has become a widely accepted marker of cell senescence, whether replicative in origin or stress-induced.

5.2 Implications of vascular cell senescence for human vascular pathology

The results described in Chapter Three strongly suggest that endothelial denudation of rabbit carotid arteries leads not only to a proliferative response, but also to the emergence of senescent ECs and VSMCs in the vessel wall. It has subsequently transpired that this finding is not species-specific; SA-β-gal-positive VSMCs also

emerge in balloon-injured rat carotid arteries [Minamino *et al.* 2003]; this emergence can be enhanced by the introduction into these arteries of activated Ras protein, mirroring the promotion of a senescent phenotype in cultured VSMCs by the introduction of a *ras* allele, as mentioned above.

While senescent cells have thus been found in rabbit and rat neointimas, no such cells have to date been demonstrated in human arteries following angioplasty, so the question of whether human ECs and VSMCs senesce in this situation remains open.

5.2.1 Evidence for EC senescence in human atheroma

As mentioned earlier, however, there is now evidence that cellular senescence occurs within human atheromatous lesions. SA-β-gal-positive ECs have been demonstrated at sites overlying atherosclerotic plaques in human aorta [Vasile *et al.* 2001] and in human coronary arteries [Minamino *et al.* 2002]. In coronary arteries these cells appeared flattened and enlarged compared with ECs in non-atheromatous areas, further suggesting a senescent phenotype; it has been proposed that the specific localization of SA-β-gal-positive ECs to areas of plaque in the human coronary arteries may be evidence for a causative role of EC senescence in atherogenesis [Minamino *et al.* 2002].

5.2.2 Evidence for VSMC senescence in human atheroma

Recently the same group has detected SA-β-gal-positive VSMCs in the intima of advanced human atherosclerotic lesions [Minamino *et al.* 2003]; a few SA-β-gal-positive VSMCs were also found in the media of these vessels. The senescent intimal VSMCs showed p53 immunoreactivity in their nuclei, as well as immunohistochemical evidence of ERK activation, and expression of the pro-inflammatory cytokine interleukin-1β (IL-1β); in contrast, non-senescent VSMCs in the media did not show p53 immunoreactivity or IL-1β expression, and showed only occasional evidence of ERK activation [Minamino *et al.* 2003].

It is worth considering the various pathological implications of the emergence of cellular senescence in the arterial wall, in the context of both atherosclerosis and post-angioplasty re-stenosis.

5.2.3 Atherosclerosis as an inflammatory phenomenon

As mentioned in Chapter One, according to the response-to-injury hypothesis, the trigger for atherogenesis is a breach in the endothelium; a perpetuation of the insult may contribute to the chronicity of the atheromatous lesions. In such a situation, the endothelium's capacity to repair itself is likely to be important, and while several extrinsic factors may influence this capacity, an intrinsic limitation of EC proliferative activity would be expected to be detrimental. Conversely, replicative senescence in VSMCs might be expected to limit the extent of intimal hyperplasia seen in atherosclerotic lesions, while also retarding formation of the fibrous cap.

In addition, though, the pathological consequences of vascular cell senescence in atherogenesis may extend beyond the limitation senescence imposes on cellular proliferation; the altered functional capacity of senescent cells may also have important deleterious consequences. In order to assess these effects, it is necessary to consider in more detail the contribution of inflammation to atherogenesis.

Various lines of evidence strongly suggest a significant role for an inflammatory process in the development of atherosclerotic lesions [Libby 2002]. As has been mentioned, blood leukocytes adhere to the endothelium early in atherogenesis. This process is mediated by VCAM-1 [Cybulsky and Gimbrone 1991], and the expression of VCAM-1 by ECs appears to result from an inflammatory process in the arterial intima instigated by inflammatory cytokines including IL-1β and TNF-α, as well as by oxidized lipoproteins [Khan *et al.* 1995, Collins and Cybulsky 2001]. The recruitment of monocytes across the endothelium is then promoted by MCP-1 [Boring *et al.* 1998], and interleukin-8 [Boisvert *et al.* 1998], while lymphocytes are attracted by chemokines induced by IFN-γ [Mach *et al.* 1999]. Macrophages promote inflammation in the atheromatous plaque via the production of the pro-oxidant agent hypochlorous acid [Sugiyama *et al.* 2001], and can produce MMPs [Saren *et al.* 1996] which may contribute to plaque instability. MMPs are also produced by ECs and VSMCs, and this production is augmented by inflammatory mediators such as IL-1β, TNF-α and CD154; plaque instability may also be promoted by pro-inflammatory cytokines such as IFN-γ, which can inhibit collagen production by VSMCs [Libby and Aikawa 2002]. Thus, in the inflammatory environment, not only does destruction of the collagenous matrix increase, but the laying down of new collagen is also impaired.

There is now ample evidence to suggest that the development of cellular senescence in ECs and VSMCs renders them pro-inflammatory, and this alteration in their phenotype may therefore confer on them a pro-atherogenic role.

5.2.4 Pro-inflammatory properties of senescent ECs

It has been mentioned earlier that senescent ECs *in vitro* show increased expression of IL-1α [Maier *et al.* 1990] and ICAM-1 [Maier *et al.* 1993], both of which are over-expressed in atherosclerotic lesions [Moyer *et al.* 1991, van der Wal *et al.* 1992], and both of which promote the adherence of inflammatory cells to the endothelial surface [Bevilacqua *et al.* 1985, van der Wal *et al.* 1992].

In addition, senescent human ECs demonstrate reduced eNOS activity [Minamino *et al.* 2002]. NO produced by the normal endothelium is believed to have a variety of anti-inflammatory and anti-atherogenic properties (including the inhibition of monocyte adhesion, P-selectin expression, and MCP-1 expression [Busse and Fleming 1996]) so the appearance of senescent ECs in an atheromatous lesion might lead to the loss of this protective effect.

5.2.5 Pro-inflammatory properties of senescent VSMCs

Turning to VSMCs, there is evidence that in atheromatous lesions these cells develop an inflammatory phenotype associated with the emergence of replicative senescence. During atherogenesis, VSMCs are involved in fibrous cap formation, and the presence of this cap is thought to contribute to plaque stability. It is possible that a loss of normal VSMC function accompanying the onset of senescence may affect their ability to maintain the stability of the fibrous cap. This loss of normal function may simply lead to an inability of VSMCs to align themselves normally within the vessel wall, as discussed in Chapter Three (Section 3.2.4.3). In addition, though, other changes in VSMC function may be relevant. It is thought that the fibrous cap becomes more susceptible to rupture as a result of the depletion of matrix components by various matrix-degrading enzymes, such as proteinases and cystine and aspartate proteases [Shah 2003]. VSMCs are normally capable of synthesising extracellular matrix, and a decline in this function with senescence may contribute to plaque instability.

The Ras-induced senescence of cultured VSMCs, mentioned earlier, is associated with increased expression of pro-inflammatory cytokines and chemokines including IL-1α, IL-1β, interleukin-6 (IL-6) and MCP-1 [Minamino *et al.* 2003]. The expression of IL-

1β by intimal VSMCs in human atheromatous lesions (mentioned earlier) may have important consequences for both lesion formation and the development of plaque instability. Both these processes involve remodelling of the extracellular matrix and the degradation of elastin. Various enzymes have been implicated in this context, and these include MMPs, serine proteinases and, more recently, cysteine proteinases including cathepsins K and S. Cathepsins are lysosomal enzymes which can also function extracellularly, and which, at least in culture, are employed by macrophages to degrade extracellular elastin [Reddy *et al.* 1995]. Since macrophages and VSMCs with greatly expanded lysosomal compartments are found in atherosclerotic plaques [Sukhova *et al.* 1998], it seems reasonable to postulate that these cells may secrete increased levels of cathepsins, and that these may be involved in extracellular matrix degradation. Indeed, immunohistochemical studies of human atheromatous lesions have demonstrated that intimal VSMCs, especially those appearing to traverse the IEL, contain cathepsins K and S, while VSMCs in normal arteries contain little or no cathepsin K or S [Sukhova *et al.* 1998]. The same group has also found evidence of co-localization of cathepsin S with ECs in human atheroma [unpublished data, referred to in Sukhova *et al.* 2003]. In this context it is noteworthy that Western blotting studies have shown a dramatic up-regulation of another cathepsin, cathepsin B, in senescent (compared with pre-senescent) HUVECs [Kamino *et al.* 2003].

More recently, it has been found that when LDL receptor-deficient mice were cross-matched with cathepsin S-deficient mice, the progeny showed reduced susceptibility to atherogenesis compared with LDL receptor-deficient mice possessing normal cathepsin S activity [Sukhova *et al.* 2003]. This reduced susceptibility in cathepsin S-deficient mice was associated with dramatic reductions in the numbers of macrophages, VSMCs, and lymphocytes in the intima, as well as in the intimal content of lipid, collagen and IFN-γ.

Furthermore, when VSMCs in culture were stimulated with either IL-1β or IFN-γ, they secreted activated cathepsin S, and degraded substantial quantities of insoluble elastin [Sukhova *et al.* 1998]. Thus there is evidence not only that VSMCs in atheromatous lesions contain cathepsins K and S, but that these enzymes can be used by VSMCs to degrade elastin. It has been mentioned above that senescent VSMCs both in culture and in atheromatous lesions show increased expression of IL-1β [Minamino *et al.* 2003]. One might conclude that senescent VSMCs in atheromatous lesions, through

increased expression of IL-1β, may stimulate the secretion of cathepsins from neighbouring VSMCs, and that this may lead to degradation of the surrounding extracellular matrix, resulting in remodelling of the vessel wall and/or plaque instability.

The co-localization of IL-1β with SA-β-gal activity in intimal VSMCs [Minamino *et al.* 2003], and the fact that both β-galactosidase and cathepsins are lysosomal enzymes, together suggest close links between IL-1β expression, senescence (with its concomitant increase in lysosomal mass and therefore expression of SA-β-gal activity) and the production of cathepsins; the mechanisms underlying this association remain uncertain though. The work of Minamino *et al.* [Minamino *et al.* 2003] suggests that pro-inflammatory signals can trigger both VSMC senescence and IL-1β expression, but it remains unclear whether the expression of IL-1β leads to the development of senescence and an expansion of the lysosomal mass (and therefore increased cathepsin production), or whether increased IL-1β expression itself results from the senescence of these cells.

The pro-inflammatory properties of senescent ECs and VSMCs may provide one link in a possible vicious circle of processes involved in the initiation and propagation of atherogenesis. It has been mentioned in Chapter Three (Section 3.2.4.3) that NAD(P)H oxidase is a major enzymatic source of intracellular ROS in vascular cells [Pagano *et al.* 1995]. It transpires that hypercholesterolaemia in general [Stokes *et al.* 2001] and OxLDL in particular [Rueckschloss *et al.* 2001] are able to stimulate the generation of ROS via induction of endothelial cell NAD(P)H activity; superoxide generated in this way can then promote the adhesion of leukocytes to endothelial cells [Stokes *et al.* 2001]. Similarly, NAD(P)H activity can mediate TNF-α-induced endothelial cell production of superoxide [Li *et al.* 2002]. If the production of ROS by the endothelium, in response to either OxLDL or pro-inflammatory cytokines, then leads to the emergence of SIPS in the vessel wall, and if the emerging senescent cells themselves have pro-inflammatory properties, the resultant inflammatory response may further increase ROS generation, perpetuating the cycle.

5.2.6 Putative role of EC senescence in an artery's response to injury

Turning to post-angioplasty re-stenosis, the pathology of this phenomenon has often been studied using endothelial denudation models. These models are not ideal, though:

while angioplasty in clinical practice involves the inflation of a balloon in a localized segment of diseased artery, denudation models usually involve repeatedly drawing an inflated balloon along a segment of previously healthy artery. Despite this discrepancy, these models have suggested mechanisms through which cellular senescence could play a role in this clinically important pathological entity.

It has been postulated that a failure of re-endothelialization following luminal injury in rabbit arteries may be attributable directly to the emergence of EC senescence [Reidy *et al.* 1983]. Furthermore, as discussed in Chapter Three (Section 3.2.4.2) there is also evidence that a failure of re-endothelialization promotes neointima formation [Hutter *et al.* 2003], and that this effect may be mediated via a decline in NO synthesis by ECs [Dzau *et al.* 2002]. The demonstration in Chapter Three of rabbit EC senescence following balloon injury, combined with the known decline in eNOS activity in senescent human ECs [Minamino *et al.* 2002], suggests that human ECs may also senesce after denudation injuries (such as angioplasty), and that if they do, their senescence may promote neointimal formation via decreased eNOS expression.

5.2.7 Putative role of VSMC senescence in an artery's response to injury

The demonstration of VSMC senescence may similarly have consequences in the context of post-angioplasty re-stenosis. Here, however, the onset of VSMC senescence might be expected to be beneficial, limiting the degree of intimal hyperplasia by acting as a brake on VSMC proliferation. The situation may not be so straightforward, though. Matrix-degrading enzymes, in addition to their supposed role in atherogenesis discussed above, are thought to play an essential role in neointima formation following luminal injuries, by remodelling the extracellular matrix and permitting VSMC migration into the developing neointima [Zempo *et al.* 1996, Dollery *et al.* 1999, Johnson *et al.* 2001b]. As was argued above, in the context of atherogenesis, it seems reasonable to suspect that the expression of IL-1β by senescent VSMCs in the neointima of injured vessels may stimulate neighbouring cells to secrete matrix-degrading enzymes; the resultant breakdown of extracellular matrix may allow enhanced migration of other, non-senescent, VSMCs into this layer, accelerating neointima formation.

5.2.8 Potential widespread effect of a small number of senescent cells

It was notable in the current study that even in double-denudation vessels only a small proportion of the cross-sectional area of the vessel wall was occupied by SA-β-gal-positive cells. This finding might appear to cast doubt on the pathological significance of *in vivo* senescence in this situation. On the other hand, a few points are worth considering in this respect.

Firstly, the number of senescent cells in the vessel wall may be greater than suggested by the percentage areas provided; it is possible that more senescent cells had emerged in the six weeks following the injury, but that a proportion had been 'lost', either through shedding into the vessel lumen (while the animal was still alive, or during the harvesting process) or through a physiological process such as apoptosis (though no evidence was found of senescent cells undergoing apoptosis in this study); also, the neointima is known to contain acellular areas filled with extracellular matrix, and the existence of such areas would mean that the reported percentage areas were underestimates of the proportion of neointimal cells staining for SA-β-gal.

Secondly, because of the alteration in function known to occur in senescent cells, the significance of the presence of such cells may be out of proportion to the number of cells present. Thus if senescent cells do synthesize and release inflammatory mediators, adhesion molecules and matrix-degrading enzymes, a small number of these cells could have important influences on a much larger number of pre-senescent cells in their vicinity.

In summary, there is ample evidence to suggest that the emergence of senescent vascular cells could have pathophysiological consequences, either during the evolution of atheromatous lesions or during neointima formation following denudation injuries and angioplasty.

5.3 Organismic and cellular ageing, and atherogenesis

5.3.1 Accelerated ageing and atherogenesis

Having established that vascular cells can senesce *in vivo*, and having considered the various pathological implications of this finding, attention turned to the question of whether the emergence of vascular cell senescence could explain the association between organismic ageing and an increased susceptibility to atherosclerosis.

Clinical, pathological and experimental evidence suggests that ageing is an independent risk factor for atherosclerosis (as discussed in Chapter One, Section 1.2.3) and does not exert its influence solely through a more prolonged exposure of the organism to various pro-atherogenic factors (such as smoking and hypercholesterolaemia). Another explanation for the apparent effect of ageing on atherogenesis must therefore be sought. The SAM model was employed to look for evidence of increased cellular senescence in the context of abnormal organismic ageing, and to investigate whether abnormalities in either cellular or organismic ageing were associated with a predisposition to atherogenesis.

In these studies, it was found that mice which age at an accelerated rate (SAM-P mice) develop more extensive lipid lesions in their aortic roots than do a related strain (SAM-R mice) which age at a normal rate; the more extensive lipid lesions in SAM-P mice develop despite these mice having a lower serum cholesterol, and an equivalent HDL/total cholesterol ratio, compared with SAM-R mice. These data support the contention that accelerated organismic ageing predisposes to atherogenesis.

5.3.2 Lack of evidence for enhanced replicative senescence in SAM spleen, skin and aorta

As detailed in Chapter Four (Section 4.7.3.3) previous research has suggested differences in the *in vitro* replicative capacity of cells derived from either SAM-P or SAM-R mice, and it was expected that SAM-P cells might be more prone to senescence than their SAM-R counterparts. In fact the telomere and SA-β-gal studies described in Chapter Four showed no convincing evidence of accelerated cellular senescence in SAM-P mice. There were differences in telomere length and SA-β-gal staining between SAM-P and SAM-R mice, but these differences were found in young mice, and did not become any more accentuated as the mice of the two strains aged. Thus while telomeres were shorter in SAM-P than SAM-R mice, on average the telomere length of each strain appeared to remain constant, whatever the age of the mice. As discussed in Chapter Four, the very great length of murine telomeres suggests that senescence of murine cells is likely to occur via mechanisms other than telomere shortening; furthermore, the apparent lack of age-related shortening of SAM telomeres now suggests that telomere attrition is not aetiologically involved in the accelerated ageing of SAM-P mice. On the other hand, because of the limitations of

TRF analysis, the current study does not exclude the possibility that individual telomeres might have shortened beyond a critical length as the SAM strains aged.

The absence of any age-related accumulation of SA-β-gal-positive cells in the skin or aortas of SAM-P mice again argues against a predisposition to cellular senescence in SAM-P mice. Thus although dermal fibroblasts from SAM-P mice have a reduced *in vitro* replicative potential compared with equivalent cells from SAM-R mice [Hosokawa *et al.* 1994], the absence of progressive SA-β-gal staining in SAM-P skin suggests that *in vivo* these cells do not undergo sufficient rounds of proliferative activity to exhaust their replicative potential. The only SA-β-gal staining seen in SAM-P skin was located in sebaceous and eccrine glands, areas where, in human skin, such staining has been shown to be a non-specific (i.e. not senescence-related) finding [Dimri *et al.* 1995]; this staining was also found in young SAM-P mice, again suggesting that it is not a senescence-related phenomenon.

5.3.3 Possible interactions between telomere shortening and atherogenesis

It was proposed earlier that accelerated EC senescence may promote atherogenesis, as it may impair the endothelium's capacity for self-repair following a breach in its integrity. In fact the results of a recent study employing a genetically manipulated murine model suggest that short telomeres are associated with protection from diet-induced atherosclerosis [Poch *et al.* 2004]. Mice doubly deficient in apoE and telomerase RNA (TR) were compared with apoE-deficient mice expressing TR. The doubly deficient mice experienced greater telomere attrition but reduced atherosclerosis compared with mice expressing TR. It appeared that the reduced atherosclerosis was attributable to diminished proliferative capacity of both lymphocytes and macrophages. In other words, in this situation the development of replicative senescence in immune cells led to impaired atherogenesis, supporting the notion that atherogenesis relies on normal proliferative function in immune cells.

Conversely, though, in a small pilot study looking at TRF lengths in leukocytes from human subjects, the white cells of individuals with severe coronary artery disease contained TRFs approximately 300 bp shorter than those of age-matched controls, and equivalent in length to those of individuals with no coronary artery disease who were nearly nine years older [Samani *et al.* 2001]. This result appears to be at variance with the inferences drawn from the findings of Poch *et al.* mentioned above. The two studies can be reconciled, though, if it is postulated that atherogenesis requires

adequate proliferative activity of immune cells, but that the process of lesion formation itself exhausts the replicative potential of these cells. In the case of the SAM mice, it appears that the substrain with shorter splenic cell telomeres is in fact more prone to atherogenesis, though, as discussed, the difference in telomere length between the strains does not appear to reflect a predisposition to cellular senescence in the SAM-P mice.

5.3.4 Oxidative stress and atherogenesis in SAM mice

The lack of evidence for cellular senescence in SAM-P aortas implies that the demonstrated susceptibility of SAM-P mice to atherogenesis is not attributable to such a phenomenon. Instead other aetiologies must be sought. Evidence detailed in Chapter Four (Section 4.7.3.3) [Nomura *et al.* 1989, Zhao *et al.* 1990, Choi *et al.* 1994, Nakamoto *et al.* 1994, Yoshino *et al.* 1994b, Park *et al.* 1996, Butterfield *et al.* 1997] points to abnormalities in the oxidative status of SAM-P mice. Given the proposed role of oxidative stress in the development of atheromatous lesions [Steinberg 1995] discussed in Chapter One (Section 1.5.5), together with the higher levels of lipid peroxides found in SAM-P compared with SAM-R thoracic aortas [Yagi *et al.* 1995], it is tempting to attribute the relative athero-susceptibility of SAM-P mice to the known abnormalities in their redox status. Similarly, if the accelerated ageing of SAM-P mice is not attributable to enhanced replicative senescence in this strain, and given the proposed links between oxidative stress and shortened organismic life-span discussed in Chapter One (Section 1.5.3), it seems plausible that the high oxidative stress in SAM-P mice may also contribute to their accelerated organismic ageing.

5.3.5 Other possible interactions between organismic ageing and atherogenesis

The nature of the relationship between ageing and atherosclerosis has been discussed in some detail in Chapter One. It was suggested that atherosclerosis cannot be regarded merely as an intrinsic manifestation of the ageing process (as one might regard, for example, the emergence of wrinkled skin) (Chapter One, Section 1.2.2). The central argument in this respect is that there are human populations which age without developing appreciable levels of atherosclerosis, suggesting that ageing and atherosclerosis are not inextricably linked. On the other hand, there is also ample clinical evidence that ageing is a risk factor for atherosclerosis, and indeed that it

exerts its effect independently of other known risk factors such as smoking and diabetes mellitus (Chapter One, Sections 1.2.2 and 1.2.3).

Furthermore, evidence is emerging which suggests mechanisms through which organismic ageing may exert its influence on atherogenesis. Merat *et al.* fed a high-fat diet to young and old LDL receptor-deficient mice, and found that, despite similar plasma cholesterol levels in both groups, the older mice developed more severe aortic atherosclerotic lesions than did younger mice [Merat *et al.* 2000]. This greater degree of atherogenesis was associated with a higher level of VCAM-1 expression in the older mice. In the same study, VCAM-1 expression was also found to rise with age in C57BL/6 mice fed a normal diet, despite there being no age-related increase in plasma cholesterol in these mice. Thus, in more than one strain of mouse there appears to be an age-dependent increase in VCAM-1 expression which is not related to plasma cholesterol levels. This increased expression of VCAM-1 may render the older mice more susceptible to atherogenesis by promoting leukocyte adhesion to the endothelium.

Other mechanisms through which ageing may lead to increased susceptibility to vascular disease have been investigated in non-human primates [Wang *et al.* 2003]. During the development and progression of experimental atherosclerosis in young animals, matrix metalloproteinase-2 (MMP-2) is activated, and angiotensin II signalling is increased. Wang *et al.* therefore studied the levels of MMP-2, angiotensin II and angiotensin-converting enzyme (ACE) in the aortic walls of young and old monkeys. Aortas from the older animals had thickened intimas, as a result of increased numbers of VSMCs and more abundant matrix, compared with vessels from younger animals. The older vessels contained elevated levels of intimal MMP-2 activity; intimal angiotensin II and ACE immunofluoresence also increased, and co-localized with MMP-2. Thus mechanisms involved in experimental atherosclerosis also appeared to operate in the ageing arterial wall. They may therefore render the ageing vessel wall more prone to the development of atherosclerosis.

5.3.6 Organismic ageing: an active or a passive process?

In Chapter One (Section 1.2.3) various teleological 'explanations' for the concept of ageing were discussed. According to these theories ageing is a passive phenomenon, a design redundancy occurring as a by-product of the evolutionary imperative that genetic information must be passed from generation to generation with maximal

stringency. According to a more pragmatic argument, biological ageing can perhaps be regarded as the inevitable consequence of processes which proceed relentlessly with the passage of time, and which occur as a direct consequence of the nature of organismic biology and of the environment in which these organisms live. Thus one could argue that replicative senescence and oxidative stress, for example, are unavoidable, and indeed carry some benefit for the organism.

Replicative senescence can be regarded as essentially inevitable in the following respect: telomeres, in the absence of telomerase activity, are bound to shorten with rounds of cellular replication due to the end-replication problem [Olovnikov 1973, Levy *et al.* 1992]; it appears that after a certain degree of telomeric shortening has been achieved, a signal is triggered which prevents further cellular replication and therefore further loss of DNA. One resultant beneficial aspect of replicative senescence is that it provides a mechanism through which cells cease to divide before their chromosomal DNA is damaged, reducing the risk of cells with altered DNA passing on genetic defects to daughter cells. Indeed, it has been postulated that cell senescence may have evolved specifically as a mechanism for the suppression of tumour formation [O'Brien *et al.* 1986]. Alternatively, it has been suggested that senescence may have developed as a tool for fine-tuning tissue modelling during development [Martin 1993] and that the accompanying tumour-suppressor effect may be a felicitous incidental process.

Turning to oxidative stress, it has been mentioned that normal metabolic reactions occurring in our aerobic environment lead to the generation of ROS (Chapter One, Section 1.3.2.5). As well as their potentially deleterious effects, ROS and other free radicals are believed to play various physiological roles (such as redox-mediated amplification of immune responses, redox regulation of cell adhesion, and activation of various receptor-mediated signalling pathways) as part of normal biological function [reviewed in Dröge 2002]. In the cardiovascular system, ROS, and in particular superoxide ions, are thought to play a role in the vasculature's ability to sense hypoxia, and may also be involved in the regulation of vascular tone [reviewed in Li and Shah 2004]. Thus ROS generation may, like replicative senescence, be regarded as an unavoidable, and potentially beneficial phenomenon.

Replicative senescence and the generation of ROS, then, appear to proceed inexorably, and to have beneficial consequences in the healthy development and life of the organism.

5.3.7 Processes linking cellular and organismic ageing with atherosclerosis

It is possible to construct a network of processes involved with atherogenesis and ageing, as illustrated in Figure 5.1 overleaf. As shown, certain processes, including replicative senescence and ROS generation, may be involved both in ageing of the organism and in atherogenesis. This raises the possibility that certain clearly defined cellular and molecular processes contribute to ageing and atherosclerosis as two separate manifestations, rather than that the somewhat intangible concept of ageing exerts an actual biological influence on the histological and functional changes leading to atherogenesis.

5.4 Future experiments

5.4.1 Carotid denudation model

Future experiments may provide interesting insights into the nature of the network illustrated, and help to establish whether there is indeed a causal link between ageing and atherosclerosis.

The rabbit carotid denudation model provides the opportunity to study the consequences of mechanical injury in a species which can develop atheromatous lesions when fed a high-cholesterol diet [Orlandi *et al.* 2000]. It is known that prolonged administration of such a diet to rabbits results in focal areas of increased EC and VSMC replication in their aortas; leukocyte adhesion to these areas has also been demonstrated [Walker *et al.* 1986]. It seems reasonable to expect that this promotion of EC and VSMC replication may bring these cells closer to the limit of their replicative potential. It would therefore be interesting to repeat the rabbit denudation study after administration of a high-cholesterol diet; if the replicative potential of ECs and VSMCs has been partially expended prior to the denudation injury as a result of hypercholesterolaemia, one might predict an acceleration of the emergence of replicative senescence in the vessel wall.

Figure 5.1 Network of processes associated with atherosclerosis and ageing

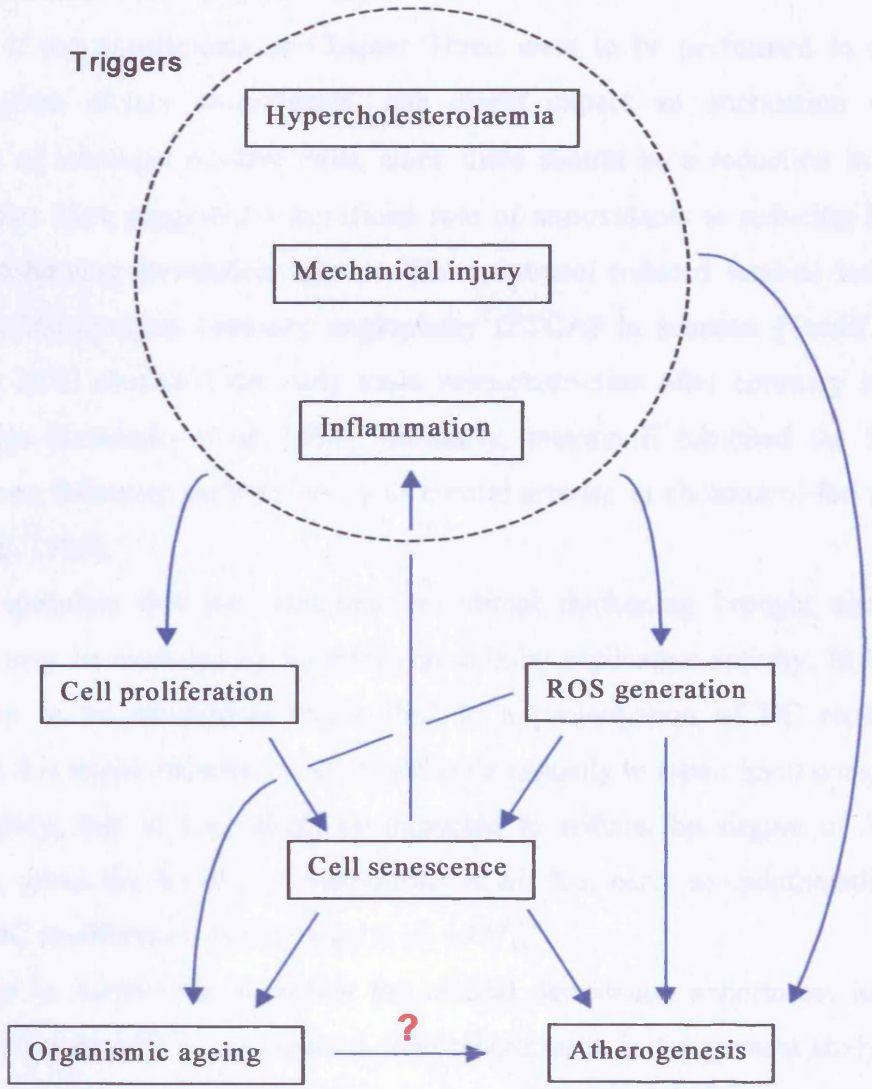

Figure 5.1 shows a network of processes associated with atherosclerosis, organismic ageing and cellular senescence. Hypercholesterolaemia, mechanical injury and inflammation have been grouped together as triggers which may, individually or in combination, initiate processes such as ROS generation and atherogenesis. The potential for positive feedback is exemplified by the putative cycle involving inflammation, ROS generation and cell senescence, discussed on page 222. It is notable that some processes which have been proposed to contribute to organismic ageing are also thought to be involved in atherogenesis. The network is not intended to be a comprehensive depiction of all the possible associations between the processes shown. The symbol ? represents the uncertainty concerning the nature of the association between organismic ageing and atherosclerosis. Abbreviation: ROS = reactive oxygen species.

Furthermore, since diet-induced hypercholesterolaemia can lead to oxidative DNA damage in the arterial wall [Martinet *et al.* 2001], hypercholesterolaemia in the rabbit denudation model might also lead to an acceleration of SIPS in vascular cells, and to a further augmentation of SA-β-gal activity.

Conversely, if the experiments of Chapter Three were to be performed in rabbits previously given dietary antioxidants, one might expect an attenuation of the development of SA-β-gal-positive cells, since there should be a reduction in SIPS. Various studies have suggested a beneficial role of antioxidants in reducing intimal hyperplasia following denudation injuries. Thus probucol reduced luminal loss after percutaneous transluminal coronary angioplasty (PTCA) in humans [Tardif *et al.* 1997], while SOD abolished the early tonic vasoconstriction after coronary balloon injury in dogs [Laurindo *et al.* 1991]. Similarly, vitamin E inhibited the intimal thickening seen following catheter injury of carotid arteries in cholesterol-fed rabbits [Konneh *et al.* 1995].

One might speculate that the reduction in intimal thickening brought about by antioxidants may be mediated by an effect on cellular replicative activity. In theory, administration of an antioxidant might lead to a prolongation of EC replicative capacity, and this might improve the endothelium's capacity to repair itself completely following injury; this in turn might be expected to reduce the degree of VSMC proliferation, given the finding of Stemerman *et al.* that early re-endothelialization inhibits VSMC proliferation [Stemerman *et al.* 1977].

It would also be informative to repeat the arterial denudation experiment in older rabbits, using young rabbits as a control. The rabbits used in the present study were sixteen to seventeen weeks old. In rabbits nearer to the end of their natural life-span, some cellular turnover may have occurred in the vessel wall during their lifetime, albeit at a low rate; the cells in the denuded vessel walls of these older animals might therefore be nearer to their replicative limit, and so the emergence of senescent cells might be more pronounced.

In these studies it would also be useful to study other potential markers of cellular senescence. SA-β-gal has now gained such acceptance as a marker of senescence that it has recently been used as a standard indicator of senescence in the evaluation of other putative markers of this cellular state [Kwak *et al.* 2004]. Nevertheless, as the validity of SA-β-gal as a marker of replicative senescence has been open to debate, it

would be helpful to look for other evidence that SA-β-gal-positive cells in the denuded arterial wall are indeed senescent. The suspected roles of the Cdk inhibitor p16 and of an alternative product of the INK4a gene locus, ARF, in the initiation of human and murine cell senescence, have been mentioned in Chapter One (Section 1.4.4.4). p16 appears to be involved in both replicative and stress-induced senescence, predominantly in humans cells; ARF on the other hand appears mainly to mediate stress-induced senescence, certainly in murine cells, and possibly in human cells [Itahana *et al.* 2004]. High levels of p16 have been found to co-exist with short telomeres in myocytes from the hearts of elderly patients with systolic heart failure, while raised levels of p16 and ARF have been shown to correlate with SA-β-gal activity in various rodent cells [Krishnamurthy *et al.* 2004]. Immunohistochemical detection of these proteins in the rabbit carotid neointima would provide further evidence of senescence in the vasculature.

The relationship between VSMC senescence and the production of cathepsins also warrants further investigation. While it is known that stimulation of VSMCs with IL-1β leads to increased production of activated cathepsin S [Sukhova *et al.* 1998], and while stimulation of VSMCs with Ras protein leads to senescence and the expression of IL-1β [Minamino *et al.* 2003], it is not as yet known whether VSMC senescence itself leads to increased production of cathepsin S. This could be investigated by growing VSMCs to senescence in culture, and then detecting cathepsins by Western blot analysis of cell lysates. One previous study of cathepsin activity in proliferating human fibroblasts has in fact shown a decline in lysosomal cathepsin activity as these cells senesced [Sitte *et al.* 2000], while another study has shown that cathepsin activity in human retinal pigment epithelial cells rises with increasing donor age [Verdugo and Ray 1997]. It is therefore not easy to predict the relationships between VSMC cathepsin activity and cellular ageing.

5.4.2 SAM model

The SAM model provides the opportunity to control for the presence of an ageing phenotype, by concomitant study of SAM-P and SAM-R strains. A weakness of the model is that the genetic differences between the two strains have not been fully elucidated. In order to gain more insights from this model into the aetiology of the ageing phenotype and into the increased susceptibility of SAM-P mice to

atherogenesis, it would be helpful to carry out a fuller characterization of the genetic differences between SAM-P and SAM-R mice.

As mentioned in Chapter Four, it would also be useful to repeat the atherogenesis experiment using a higher-cholesterol diet, in order to look for evidence of more advanced lesion formation. On the other hand, any findings from an experiment using a diet even less physiological than the Western-type diet might arguably give less reliable results.

The experiments of Poch *et al.* in which apoE-deficient mice were cross-matched with telomerase-deficient mice [Poch *et al.* 2004] have been described above. An equivalent experiment would involve cross-matching SAM-P mice and SAM-R mice with apoE-deficient mice. Cross-matching apoE-deficient mice with SAM-P mice would allow the study of the effect of imposing a senescent phenotype onto a murine strain itself susceptible to atherosclerosis, while the cross-match with SAM-R mice would provide a control. SAM-P/apoE-deficient cross-matches might be expected to have shorter telomeres than SAM-R/apoE-deficient mice, and it would be interesting to observe the effect of this difference on the relative susceptibility of each cross-matched strain to atherogenesis: while the findings of Poch *et al.* suggest that those mice with a senescent phenotype (and containing cells of decreased replicative capacity) should be relatively protected against atherogenesis (owing to the emergence of immunosenescence), the results described in Chapter Four suggest that the ageing phenotype of SAM-P mice might in fact render the SAM-P/apoE-deficient cross-matches more prone to atherogenesis than SAM-R/apoE-deficient mice. The findings might help to shed light on the relative influences of immunosenescence and other aspects of the ageing process (such as altered oxidative status) on an organism's net susceptibility to atherogenesis.

The telomere study described in Chapter Four provided only preliminary data concerning telomere length in SAM splenic cells. It would be interesting to extend this study to other cell types, and to look in more detail for any evidence of telomeric shortening in cells taken from older mice. Alternative methods for telomere length measurement, such as FACScan analysis, could be useful in this respect. Similarly, measurement of telomerase activity in SAM mice may well provide valuable insights into the relevance of telomere dynamics in murine ageing.

It has been mentioned earlier that administration of the free radical scavenger PBN to SAM-P mice can prolong their life-span [Edamatsu *et al.* 1995], suggesting an aetiological role for free radicals in the SAM-P ageing phenotype. It would be interesting to explore whether administration of PBN could attenuate the development of atheromatous lesions in SAM-P mice, and whether or not it would abolish the disparity in telomere length between SAM-P and SAM-R mice.

It would also be interesting to perform endothelial denudation experiments in SAM mice. The fact that SAM-P cells appear to be more prone to replicative senescence, and that SAM-P tissues show increased levels of oxidative stress, may have interesting influences on neointimal development and re-endothelialization in this model. The results are difficult to predict, as the effect of ageing on neointima formation is not entirely clear-cut. Thus in one study, injury to rat aortas led to significant neointima formation in young rats, but not in old rats [Chajara *et al.* 1998], while in another study, aortas from older rats responded to injury with an exaggerated proliferation of SMCs compared with aortas from younger animals [McCaffrey *et al.* 1988].

5.4.3 Human studies

In terms of human studies, the natural successor to the rabbit denudation study would be to look for evidence of senescence in human neointima. This might be possible by the study of tissue removed during certain PTCA procedures, carotid endarterectomies and aortic aneurysm repairs, or perhaps by using post-mortem samples. In terms of atherosclerosis, the studies of Minamino *et al.* [Minamino *et al.* 2002 and 2003] could be systematically repeated in adults of various chronological ages, in order to assess the effect of organismic ageing on SA-β-gal positivity in human atheromatous plaques.

5.5 Conclusion

In conclusion, the studies described in this thesis suggest that there are intimate links between certain biological processes, including replicative senescence and the damage caused by oxidative stress, which may be involved both in atherogenesis and in organismic ageing. While ageing appears to be an independent risk factor for atherosclerosis, it also seems plausible that the ageing phenotype and the development of atherosclerosis may emerge as two concomitant pathological end-points of these biological processes.

PUBLICATIONS

Articles related to this thesis published in peer-reviewed journals

van der Loo B, **Fenton MJ**, Erusalimsky JD (1998) Cytochemical detection of a senescence-associated β-galactosidase in endothelial and smooth muscle cells from human and rabbit blood vessels. Exp Cell Res 241: 309-315

Fenton M, Barker S, Kurz DJ, Erusalimsky JD (2001) Cellular senescence after single and repeated balloon catheter denudations of rabbit carotid arteries. Arterioscler Thromb Vasc Biol 21: 220-226

Fenton M, Huang H-L, Hong Y, Hawe E, Kurz DJ, Erusalimsky JD (2004) Early atherogenesis in senescence-accelerated mice. Exp Gerontol 39: 115-122

REFERENCES

Aggarwal S, Gupta S (1998) Increased apoptosis of T cell subsets in aging humans altered expression of Fas (CD95), Fas ligand, Bcl-2, and Bax. J Immunol 160: 1627-1637

Ahmed MM (1970) Age and sex differences in the structure of tunica media of coronary arteries in Chinese subjects. J Anat 106: 202

Albelda SM, Oliver PD, Romer LH, Buck CA (1990) EndoCAM: a novel endothelial cell-cell adhesion molecule. J Cell Biol 110: 1227-1237

Alcorta DA, Xiong Y, Phelps D, Hannon G, Beach D, Barret JC (1996) Involvement of the cyclin-dependent kinase inhibitor p16 (INK4a) in replicative senescence of normal human fibroblasts. Proc Natl Acad Sci USA 93: 13742-13747

Alexander K, Yang HS, Hinds PW (2003) pRb inactivation in senescent cells leads to an E2F-dependent apoptosis requiring p73. Mol Cancer Res 1: 716-728

Alheid U, Frolich JC, Forstermann U (1987) Endothelium-derived relaxing factor from cultured endothelial cells inhibits aggregation of human platelets. Thromb Res 47: 561-571

Alison MR, Sarraf CE (1992) Apoptosis: a gene-directed programme of cell death. J R Coll Physicians Lond 26: 25-35

Allsopp RC, Vaziri H, Patterson C, Goldstein S, Younglai EV, Futcher AB, Greider CW, Harley CB (1992) Telomere length predicts replicative capacity of human fibroblasts. Proc Natl Acad Sci USA. 89: 10114-10118

Anitschkow N (1913) Über die Veränderungen der Kaninchenaorta bei experimenteller Cholesterinsteatose. Beitr Path Anat Allg Path 56: 379-404

Antebi A, Culotti JG, Hedgecock EM (1998) daf-12 regulates developmental age and the dauer alternative in Caenorhabditis elegans. Development 125: 1191-1205

Assmann G, Gotto AM Jr (2004) HDL cholesterol and protective factors in atherosclerosis. Circulation 109 (23 Suppl 1): III8-III14

Atadja P, Whon H, Garkavtsev I, Veillette C, Riabowol K (1995) Increased activity of p53 in senescing fibroblasts. Proc Natl Acad Sci USA 92: 8348-8352

Aviv H, Khan MY, Skurnick J, Okuda K, Kimura M, Gardner J, Priolo L, Aviv A (2001) Age dependent aneuploidy and telomere length of the human vascular endothelium. Atherosclerosis 159: 281-287

Azuma H, Funayama N, Kubota T, Ishikawa M (1990) Regeneration of endothelial cells after balloon denudation of the rabbit carotid artery and changes in responsiveness. Japan J Pharmacol 52: 541-552

Azuma H, Niimi Y, Terada T, Hamasaki H (1995) Accelerated endothelial regeneration and intimal hyperplasia following a repeated denudation of rabbit carotid

arteries: morphological and immunohistochemical studies. Clin Exp Pharmacol Physiol 22: 748-754

Baker PB, Baba N, Boesel CP (1981) Cardiovascular abnormalities in progeria. case report and review of the literature. Arch Pathol Lab Med 105: 384-386

Balin AK, Goodman DB, Rasmussen H, Cristofalo VJ (1977) The effect of oxygen and vitamin E on the lifespan of human diploid cells in vitro. J Cell Biol 74: 58-67

Balin AK, Goodman DB, Rasmussen H, Cristofalo VJ (1978) Oxygen-sensitive stages of the cell cycle of human diploid cells. J Cell Biol 78: 390-400

Barja F, Coughlin C, Belin D, Gabbiani G (1986) Actin isoform synthesis and mRNA levels in quiescent and proliferating rat aortic smooth muscle cells in vivo and in vitro. Lab Invest 55: 226-233

Barker DJ, Osmond C (1986) Infant mortality, childhood nutrition and ischaemic heart disease in England and Wales. Lancet 1(8489): 1077-1081

Barker DJ, Winter PD, Osmond C, Margetts B, Simmonds SJ (1989) Weight in infancy and death from ischaemic heart disease. Lancet 2(8663): 577-580

Barrett TB, Gajdusek CM, Schwartz SM, McDougall JK, Benditt EP (1984) Expression of the *sis* gene by endothelial cells in culture and *in vivo*. Proc Natl Acad Sci USA 81: 6772-6774

Baumgartner HR (1972) Platelet interaction with vascular structures. Thromb Diath Haemorrh Suppl 51: 161-176

Beckman JS, Beckman TW, Chen J, Marshall PA, Freeman BA (1990) Apparent hydroxyl radical production by peroxynitrite: implications for endothelial injury from nitric oxide and superoxide. Proc Natl Acad Sci USA 87: 1620-1624

Beckman JS, Ischiropoulos H, Zhu L, van der Woerd M, Smith C, Chen J, Harrison J, Martin JC, Tsai M (1992) Kinetics of superoxide dismutase- and iron-catalyzed nitration of phenolics by peroxynitrite. Arch Biochem Biophys 298: 438-445

Beckman KB, Ames BN (1998a) Mitochondrial aging: open questions. Ann N Y Acad Sci 20: 118-127

Beckman KB, Ames BN (1998b) The free radical theory of aging matures. Physiol Rev 78: 547-581

Belt E (1952) Leonardo da Vinci's study of the aging process. Geriatrics 7: 205-210

Benditt EP, Benditt JM (1973) Evidence for a monoclonal origin of atherosclerotic plaques. Proc Natl Acad Sci USA 70: 1753-1756

Bennett MR (1999) Apoptosis of vascular smooth muscle cells in vascular remodelling and atherosclerotic plaque rupture. Cardiovasc Res 41: 361-368

Bennett MR, Evan GI, Schwartz SM (1995) Apoptosis of human vascular smooth muscle cells derived from normal vessels and coronary atherosclerotic plaques. J Clin Invest 95: 2266-2274

Ben-Porath I, Weinberg RA (2004) When cells get stressed: an integrative view of cellular senescence. J Clin Invest 113: 8-13

Ben-Porath I, Weinberg RA (2005) The signals and pathways activating cellular senescence. Int J Biochem Cell Biol 37: 961-976

Berliner JA, Territo MC, Sevanian A, Ramin S, Kim JA, Bamshad B, Esterson M, Fogelman AM (1990) Minimally modified low density lipoprotein stimulates monocyte endothelial interactions. J Clin Invest 85: 1260-1266

Bevilacqua MP, Pober JS, Wheeler ME, Cotran RS, Gimbrone MA Jr (1985) Interleukin-1 activation of vascular endothelium. Effects on procoagulant activity and leukocyte adhesion. Am J Pathol 121: 394-403

Bierman EL (1973) Fat metabolism, atherosclerosis and aging in man: a review. Mech Ageing Dev 2: 315-332

Bierman EL (1978) The effect of donor age in the in vitro lifespan of cultured human arterial smooth muscle cells. In Vitro 14: 951-955

Bilato C, Crow MT (1996) Atherosclerosis and the vascular biology of aging. Aging (Milano) 8: 221-234

Blake DA, Yu H, Young DL, Caldwell DR (1997) Matrix stimulates the proliferation of corneal endothelial cells in culture. Invest Ophth Vis Sci 38: 1119-1129

Blasco MA, Lee H-W, Hande MP, Samper E, Lansdorp PM, DePinho RA, Greider CW (1997) Telomere shortening and tumor formation by mouse cells lacking telomerase RNA. Cell 91: 25-34

Blumberg JB (1996) Status and functional impact of nutrition in older adults. In: Schneider E, Rowe J (Eds) Handbook of the Biology of Aging. Fourth Edition. New York Academic Press, New York. pp 393-414

Bochaton-Piallat M, Gabbiani F, Redard M, Desmouliere A, Gabbiani G (1995) Apoptosis participates in cellularity regulation during rat aortic intimal thickening. Am J Pathol 146: 1059-1064

Bodnar AG, Ouellette M, Frolkis M, Holt SE, Chiu C-P, Morin GB, Harley CB, Shay JW, Lichtsteiner S, Wright WE (1998) Extension of life-span by introduction of telomerase into normal human cells. Science 279: 349-352

Boisvert WA, Santiago R, Curtiss LK, Terkeltaub RA (1998) A leukocyte homologue of the IL-8 receptor CXCR-2 mediates the accumulation of macrophages in atherosclerotic lesions of LDL receptor-deficient mice. J Clin Invest 101: 353-363

Bond JA, Blaydes JP, Rowson J, Haughton MF, Smith JR, Wynford-Thomas D, Wyllie FS (1995) Mutant p53 rescues human diploid cells from senescence without inhibiting the induction of SDI1/WAF1. Cancer Res 55: 2404-2409

Boring L, Gosling J, Cleary M, Charo IF (1998) Decreased lesion formation in CCR2-/- mice reveals a role for chemokines in the initiation of atherosclerosis. Nature 394: 894-897

Bosmans JM, Kockx MM, Vrints CJ, Bult H, De Meyer GRY, Herman AG (1997) Fibrin(ogen) and von Willebrand factor deposition are associated with intimal thickening after balloon angioplasty of the rabbit carotid artery. Arterioscler Thromb Vasc Biol 17: 634-645

Bowen-Pope DF, Ross R, Seifert RA (1985) Locally acting growth factors for vascular smooth muscle cells: endogenous synthesis and release from platelets. Circulation 72: 735-740

Bragt PC, Bansberg JI, Bonta IL (1980) Antiinflammatory effects of free radical scavengers and antioxidants: further support for proinflammatory roles of endogenous hydrogen peroxide and lipid peroxides. Inflammation 4: 289-299

Brattstrom L, Wilcken DE, Ohrvik J, Brudin L (1998) Common methylene-tetrahydrofolate reductase gene mutation leads to hyperhomocysteinemia but not to vascular disease: the result of a meta-analysis. Circulation 98: 2520-2526

Breitschopf K, Zeiher AM, Dimmeler S (2001) Pro-atherogenic factors induce telomerase inactivation in endothelial cells through an Akt-dependent mechanism. FEBS Lett 493: 21-25

Breslow JL (1993) Transgenic mouse models of lipoprotein metabolism and atherosclerosis. Proc Natl Acad Sci USA 90: 8314-8318

Breslow JL (1996) Mouse models of atherosclerosis. Science 272: 685-688

Broccoli D, Young JW, de Lange T (1995) Telomerase activity in normal and malignant hematopoietic cell lines. Proc Natl Acad Sci USA 92: 9082-9086

Brooksbank BW, Balazs R (1984) Superoxide dismutase, glutathione peroxidase and lipoperoxidation in Down's syndrome fetal brain. Brain Res 318: 37-44

Brown JP, Wei W, Sedivy JM (1997) Bypass of senescence after disruption of p21 CIP1/WAF1 gene in normal diploid human fibroblasts. Science 277: 831-834

Brown MS, Goldstein JL (1983) Lipoprotein metabolism in the macrophage: implications for cholesterol deposition in atherosclerosis. Annu Rev Biochem 52: 223-261

Brown WR (1989) Molecular cloning of human telomeres in yeast. Nature 338: 774-776

Brown WT (1985) Genetics of human aging. Rev Biol Res Aging 2: 105-114

Brownlee M (1995) Advanced protein glycosylation in diabetes and aging. Annu Rev Med 46: 223-234

Bryan TM, Englezou A, Gupta J, Bacchetti S, Reddel RR (1995) Telomere elongation in immortal human cells without detectable telomerase activity. EMBO J 14: 4240-4248

Buchkovich K, Duffy LA, Harlow E (1989) The retinoblastoma protein is phosphorylated during specific phases of the cell cycle. Cell 58: 1097-1105

Buetow DE. (1985) Cell numbers vs. age in mammalian tissues and organs. In: Cristofalo VJ (Ed.) CRC Handbook of Cell Biology and Ageing. CRC Press. p1.

Buja LM, Clubb FJ Jr, Bilheimer DW, Willerson JT (1990) Pathobiology of human familial hypercholesterolaemia and a related animal model, the Watanabe heritable hyperlipidaemic rabbit. Eur Heart J 11 Suppl E: 41-52

Burchenal JEB, Keaney JF Jr, Curran-Celentano J, Gaziano JM, Vita JA (1996) The lack of effect of β-carotene on restenosis in cholesterol-fed rabbits. Atherosclerosis 123: 157-167

Burke JM, Ross R (1979) Synthesis of connective tissue macromolecules by smooth muscle. Int Rev Connect Tissue Res 8: 119-157

Bürrig K-F (1991) The endothelium of advanced arteriosclerotic plaques in humans. Arterioscler Thromb 11: 1678-1689

Busse R, Fleming I (1996) Endothelial dysfunction in atherosclerosis. J Vasc Res 33: 181-194

Butterfield DA, Howard BJ, Yatin S, Allen KL, Carney JM (1997) Free radical oxidation of brain proteins in accelerated senescence and its modulation by N-tert-butyl-α-phenylnitrone. Proc Natl Acad Sci USA 94: 674-678

Cai H, Harrison DG (2000) Endothelial dysfunction in cardiovascular diseases. Circ Res 87: 840-844

Campbell JH, Han CL, Campbell GR (2001) Neointimal formation by circulating bone marrow cells. Ann N Y Acad Sci 947: 18-24

Campisi J (1996) Replicative senescence: an old lives' tale? Cell 84: 497-500

Campisi J (2001) From cells to organisms: what can we learn about aging from cells in culture? Exp Gerontol 36: 607-618

Campisi J, Dimri G, Hara E (1996) In: Schneider E, Rowe J (Eds) Handbook of the Biology of Aging. Fourth Edition. New York Academic Press, New York. pp 121-149

Canman CE, Gilmer TM, Coutts SB, Kastan MB (1995) Growth factor modulation of p53-mediated growth arrest versus apoptosis. Genes Dev 9: 600-611

Caplan BA, Schwartz CJ (1973) Increased endothelial cell turnover in areas of *in vivo* Evans blue uptake in the pig aorta. Atherosclerosis 17: 401-417

Carew TE, Schwenke DC, Steinberg D (1987) Antiatherogenic effect of probucol unrelated to its hypocholesterolemic effect: evidence that antioxidants in vivo can selectively inhibit low density lipoprotein degradation in macrophage-rich fatty streaks and slow the progression of atherosclerosis in the Watanabe heritable hyperlipidaemic rabbit. Proc Natl Acad Sci USA 84: 7725-7729

Carrel A (1912) On the permanent life of tissues outside of the organism. J Exp Med 15: 516-528

Castellot JJ Jr, Favreau LV, Karnovsky MJ, Rosenberg RD (1982) Inhibition of vascular smooth muscle cell growth by endothelial cell-derived heparin: possible role of a platelet endoglycosidase. J Biol Chem 257: 11256-11260

Celermajer DS, Sorenson KE, Spiegelhalter DJ, Georgakopoulos D, Robinson J, Deanfield JE (1994) Aging is associated with endothelial dysfunction in healthy men years before the age-related decline in women. J Am Coll Cardiol 24: 471-476

Chait A, Ross R, Albers JJ, Bierman EL (1980) Platelet-derived growth factor stimulates activity of low density lipoprotein receptors. Proc Natl Acad Sci USA 77: 4084-4088

Chajara A, Delpech B, Courel MN, Leroy M, Basuyau JP, Levesque H. (1998) Effect of aging on neointima formation and hyaluronan, hyaluronidase and hyaluronectin production in injured rat aorta. Atherosclerosis 138: 53-64

Chamley-Campbell JH, Campbell GR, Ross R (1981) Phenotype-dependent response of cultured aortic smooth muscle to serum mitogens. J Cell Biol 89: 379-383

Chang E, Harley CB (1995) Telomere length and replicative aging in human vascular tissues. Proc Natl Acad Sci USA 92: 11190-11194

Chang ZF, Chen KY (1988) Regulation of ornithine decarboxylase and other cell cycle-dependent genes during senescence of IMR-90 human diploid fibroblasts. J Biol Chem 263: 11431-11435

Chen J, Brodsky SV, Goligorsky DM, Hampel DJ, Li H, Gross SS, Goligorsky MS (2002) Glycated collagen I induces premature senescence-like phenotypic changes in endothelial cells. Circ Res 90: 1290-1298

Chen KY, Chang ZF, Pang JH, He GS, Liu AY (1989) Polyamine metabolism and cell-cycle-dependent gene expression in IMR-90 human diploid fibroblasts during senescence in culture. Exp Gerontol 24: 523-537

Chen Q, Ames BN (1994) Senescence-like growth arrest induced by hydrogen peroxide in human diploid fibroblast F65 cells. Proc Natl Acad Sci USA 91: 4130-4134

Chen Q, Fischer A, Reagan JD, Yan LJ, Ames BN (1995) Oxidative DNA damage and senescence of human diploid fibroblast cells. Proc Natl Acad Sci USA 92: 4337-4341

Chester AH, O'Neil GS, Moncada S, Tadjkarimi S, Yacoub MH (1990) Low basal and stimulated release of nitric oxide in atherosclerotic epicardial coronary arteries. Lancet 336: 897-900

Chin JH, Azhar S, Hoffman BB (1992) Inactivation of endothelial derived relaxing factor by oxidized lipoproteins. J Clin Invest 89: 10-18

Chin L, Artandi SE, Shen Q, Tam A, Lee SL, Gottlieb GJ, Greider CW, DePinho RA (1999) p53 deficiency rescues the adverse effects of telomere loss and cooperates with telomere dysfunction to accelerate carcinogenesis. Cell 97: 527-538

Choi J, Shendrik I, Peacocke M, Peehl D, Buttyan R, Ikeguchi EF, Katz AE, Benson MC (2000) Expression of senescence-associated beta-galactosidase in enlarged prostates from men with benign prostatic hyperplasia. Urology 56: 160-166

Choi JH, Kim JI, Kim DW, Moon YS, Kim IS, Chung HY (1994) Age-related physiological changes in brain membranes of senescence accelerated mouse (SAM). In: Takeda T (Ed.) The SAM model of senescence. Elsevier Science, Amsterdam. pp 321-324

Chrest FJ, Bucholz MA, Kim YH, Kwon TK, Nordin AA (1995) Anti-CD3-induced apoptosis in T-cells from young and old mice. Cytometry 20: 33-42

Christ G, Hufnagl P, Kaun C, Mundigler G, Laufer G, Huber K, Wojta J, Binder BR (1997) Antifibrinolytic properties of the vascular wall. Dependence on the history of smooth muscle cell doublings in vitro and in vivo. Arterioscler Thromb Vasc Biol 17: 723-730

Clarkson TB, Adams MR, Weingand KW, Miller LC, Heydrick S (1987) Effect of age on atherosclerosis progression in nonhuman primates. In: Bates SR, Gangloff E (Eds) Atherogenesis and Aging. Springer-Verlag New York, Inc. Chapter 6, pp 57-71

Clarkson TB, Lehner NDM, Bullock BC, Lofland HB, Wagner WD (1976) Atherosclerosis in New World monkeys. Primates Med 9: 90-144

Clowes AW, Clowes MM, Reidy MA (1986) Kinetics of cellular proliferation after arterial injury III. Endothelial and smooth muscle growth in chronically denuded vessels. Lab Invest 54: 295-303

Clowes AW, Reidy MA, Clowes MM (1983) Kinetics of cellular proliferation after arterial injury I. Smooth muscle growth in the absence of endothelium. Lab Invest 49: 327-333

Clowes AW, Schwartz SM (1985) Significance of quiescent smooth muscle migration in the injured rat carotid artery. Circ Res 56: 139-145

Collado M, Medema RH, García-Cao I, Dubuisson MLN, Barradas M, Glassford J, Rivas C, Burgering BMT, Serrano M, Lam EW-F (2000) Inhibition of phosphoinositide 3-kinase pathway induces a senescence-like arrest mediated by $p27^{Kip1}$. J Biol Chem 275: 21960-21968

Collins T, Cybulsky MI (2001) NF-κB: pivotal mediator or innocent bystander in atherogenesis? J Clin Invest 107: 255-264

Comi P, Chiaramonte R, Maier JAM (1995) Senescence-dependent regulation of type 1 plasminogen activator inhibitor in human vascular endothelial cells. Exp Cell Res 219: 304-308

Comings DE, Okada TA (1970) Electron microscopy of human fibroblasts in tissue culture during logarithmic and confluent stages of growth. Exp Cell Res 61: 295-301

Cooper LT, Cooke JP, Dzau VJ (1994) The vasculopathy of aging. J Gerontol Biol Sci 49: B191-B196

Corda Y, Schramke V, Longhese MP, Smokvina T, Paciotti V, Brevet V, Gilson E, Geli V (1999) Interaction between Set1p and checkpoint protein Mec3p in DNA repair and telomere functions. Nat Genet 21: 204-208

Cortopassi GA, Wong A (1999) Mitochondria in organismal aging and degeneration. Biochim Biophys Acta 1410: 183-193

Cotran RS, Kumar Y, Robbins SL (1989) Diseases of aging. In: Robbins Pathologic Basis of Disease. W.B. Saunders Company, Philadelphia. pp 543-551

Counter CM, Botelho FM, Wang P, Harley CB, Bacchetti S (1994a) Stabilization of short telomeres and telomerase activity accompany immortalization of Epstein-Barr virus-transformed human B lymphocytes. J Virol 68: 3410-3414

Counter CM, Gupta J, Harley CB, Leber B, Bacchetti S (1995) Telomerase activity in normal leukocytes and in hematologic malignancies. Blood 85: 2315-2320

Counter CM, Hirte HW, Bacchetti S, Harley CB (1994b) Telomerase activity in human ovarian carcinoma. Proc Natl Acad Sci USA 91: 2900-2904

Coviello-McLaughlin GM, Prowse KR (1997) Telomere length regulation during postnatal development and ageing in Mus spretus. Nucleic Acids Res 25: 3051-3058

Cristofalo VJ (2001) "I no longer believe that cell death is programmed...", an interview with Vincent Cristofalo. Biogerontology 2: 283-290

Cristofalo VJ, Allen RG, Pignolo RJ, Martin BG, Beck JC (1998) Relationship between donor age and the replicative lifespan of human cells in culture: a reevaluation. Proc Natl Acad Sci USA 95: 10614-10619

Cristofalo VJ, Gerhard GS, Pignolo RJ. (1994) Molecular biology of aging. Surg Clin North Am 74: 1-21

Cristofalo VJ, Pignolo RJ (1993) Replicative senescence of human fibroblast-like cells in culture. Physiol Rev 73: 617-638

Cucina A, Borrelli V, Randone B, Coluccia P, Sapienza P, Cavallero A (2003) Vascular endothelial growth factor increases the migration and proliferation of smooth muscle cells through the mediation of growth factors released by endothelial cells. J Surg Res 109: 16-23

Cui C, Wani MA, Wight D, Kopchick J, Stambrook PJ (1994) Reporter genes in transgenic mice. Transgenic Res 3: 182-194

Cybulsky MI, Gimbrone MA Jr (1991) Endothelial expression of a mononuclear leukocyte adhesion molecule during atherogenesis. Science 251: 788-790

d'Adda di Fagagna F, Reaper PM, Clay-Farrace L, Fiegler H, Carr P, Von Zglinicki T, Saretzki G, Carter NP, Jackson SP (2003) A DNA damage checkpoint response in telomere-initiated senescence. Nature 426: 194-198

Dai CY, Enders GH (2000) p16 INK4a can initiate an autonomous senescence program. Oncogene 19: 1613-1622

Dart AM, Chin-Dusting JP (1999) Lipids and the endothelium. Cardiovasc Res 43: 308-322

Dartsch PC, Voisard R, Bauriedel G, Hofling B, Betz E (1990) Growth characteristics and cytoskeletal organization of cultured smooth muscle cells from human primary stenosing and restenosing lesions. Arteriosclerosis 10: 62-75

Davies MG, Hagen PO (1994) Pathobiology of intimal hyperplasia. Br J Surg 81: 1254-1269

Davies MJ, Woolf N (1993) Atherosclerosis: what is it and why does it occur? Br Heart J 69 (Supplement): S1-S11

de Haan JB, Cristiano F, Iannello R, Bladier C, Kelner MJ, Kola I (1996) Elevation in the ratio of Cu/Zn-superoxide dismutase to glutathione peroxidase activity induces features of cellular senescence and this effect is mediated by hydrogen peroxide. Human Molecular Genetics 5: 283-292

DeJesus V, Rios I, Davis C, Chen Y, Calhoun D, Zakeri Z, Hubbard K (2002) Induction of apoptosis in human replicative senescent fibroblasts. Exp Cell Res 274: 92-99

Dell'Orco RT, Mertens JG, Kruse PF Jr (1973) Doubling potential, calendar time, and senescence of human diploid cells in culture. Exp Cell Res 77: 356-360

Demple B, Harrison L (1994) Repair of oxidative damage to DNA: Enzymology and biology. Annu Rev Biochem 63: 915-948

Dice JF (1989) Altered intracellular protein degradation in aging: a possible cause of proliferative arrest. Exp Gerontol 24: 451-459

Diaz MN, Frei B, Vita JA, Keaney JF Jr (1997) Antioxidants and atherosclerotic heart disease. N Engl J Med 337: 408-416

DiCorleto PE, Bowen-Pope DF (1983) Cultured endothelial cells produce a platelet-derived growth factor-like protein. Proc Natl Acad Sci USA 80: 1919-1923

DiCorleto PE, de la Motte CA (1985) Characterization of the adhesion of the human monocytic cell line U-937 to cultured endothelial cells. J Clin Invest 75: 1153-1161

Dimri GP, Campisi J (1994a) Molecular and cell biology of replicative senescence. Cold Spring Harb Symp Quant Biol 59: 67-73

Dimri GP, Campisi J (1994b) Altered profile of transcription factor-binding activities in senescent human fibroblasts. Exp Cell Res 212: 132-140

Dimri GP, Lee X, Basile G, Acosta M, Scott G, Roskelly C, Medrano EE, Linskens M, Rubelj I, Pereira-Smith O, Peacocke M, Campisi J (1995) A biomarker that identifies senescent human cells in culture and in aging skin *in vivo*. Proc Natl Acad Sci USA 92: 9363-9367

Dimri GP, Martinez JL, Jacobs JJ, Keblusek P, Itahana K, Van Lohuizen M, Campisi J, Wazer DE, Band V (2002) The Bmi-1 oncogene induces telomerase activity and immortalizes human mammary epithelial cells. Cancer Res 62: 4736-4745

Dionisi O, Galeotti T, Terranova T, Azzi A (1975) Superoxide radicals and hydrogen peroxide formation in mitochondria from normal and neoplastic tissues. Biochim Biophys Acta 403: 292-300

Dokal I (1999) Dyskeratosis congenita. Br J Haematol 105: 11-15

Dokal I, Bungey J, Williamson P, Oscier D, Hows J, Luzzatto L (1992) Dyskeratosis congenita fibroblasts are abnormal and have unbalanced chromosomal rearrangements. Blood 80: 3090-3096

Dollery CM, Humphries SE, McClelland A, Latchman DS, McEwan JR (1999) Expression of tissue inhibitor of matrix metalloproteinases 1 by use of an adenoviral vector inhibits smooth muscle cell migration and reduces neointimal hyperplasia in the rat model of vascular balloon injury. Circulation 99: 3199-3205

Donehower LA, Harvey M, Slagle BL, McArthur MJ, Montgomery CA Jr, Butel JS, Bradley A (1992) Mice deficient for p53 are developmentally normal but susceptible to spontaneous tumours. Nature 356: 215-221

Dröge W (2002) Free radicals in the physiological control of cell function. Physiol Rev 82: 47-95

Dueland S, Drisko J, Graf L, Machleder D, Lusis AJ, Davis RA (1993) Effect of dietary cholesterol and taurocholate on cholesterol 7-α-hydroxylase and hepatic LDL receptors in inbred mice. J Lipid Res 34: 923-931

Dulic V, Drullinger LF, Lees E, Reed SI, Stein GH (1993) Altered regulation of G1 cyclins in senescent human diploid fibroblasts: accumulation of inactive cyclin E-Cdk2 and cyclin D1-Cdk2 complexes. Proc Natl Acad Sci USA 90: 11034-11038

Dumont P, Burton M, Chen QM, Gonos ES, Frippiat C, Mazarati J-B, Eliaers F, Remacle J, Toussaint O (2000) Induction of replicative senescence biomarkers by sublethal oxidative stresses in normal human fibroblast. Free Radical Biol Med 28: 361-373

Dumont P, Royer V, Pascal T, Dierick J-F, Chainiaux F, Frippiat C, Eliaers F, Remacle J, Toussaint O (2001) Growth kinetics rather than stress accelerate telomere shortening in cultures of human diploid fibroblasts in oxidative stress-induced premature senescence. FEBS Lett 502: 109-112

Dyson N (1998) The regulation of E2F by pRB-family proteins. Genes Dev 12 2245-2262

Dzau VJ, Braun-Dullaeus RC, Sedding DG (2002) Vascular proliferation and atherosclerosis: new perspectives and therapeutic strategies. Nature Med 8: 1249-1256

Edamatsu R, Mori A, Packer L (1995) The spin-trap N-tert-α-phenyl-butylnitrone prolongs the life span of the senescence accelerated mouse. Biochem Biophys Res Commun 211: 847-849

Efendy JL, Simmons DL, Campbell GR, Campbell JH (1997) The effect of the aged garlic extract, 'Kyolic', on the development of experimental atherosclerosis. Atherosclerosis 132: 37-42

Effros RB (1996) Insights on immunological aging derived from the T lymphocyte cellular senescence model. Exp Gerontol 31: 21-27

Effros RB, Walford RL (1984) T cell cultures and the Hayflick limit. Hum Immunol 9: 49-65

el-Deiry WS, Harper JW, O'Connor PM, Velculescu VE, Canman CE, Jackman J, Pietenpol JA, Burrell M, Hill DE, Wang Y (1994) WAF1/CIP1 is induced in p53-mediated G1 arrest and apoptosis. Cancer Res 54: 1169-1174

Elford J, Whincup P, Shaper AG (1991) Early life experience and adult cardiovascular disease – longitudinal and case-control studies. Int J Epidemiol 20: 833-844

Ellison DJ, Pugh DW (1955) Werner's syndrome. Br Med J 4933: 237-239

Emeson EE, Manaves V, Singer T, Tabesh M (1995) Chronic alcohol feeding inhibits atherogenesis in C57BL/6 hyperlipidemic mice. Am J Pathol 147: 1749-1758

Emeson EE, Shen M-L (1993) Accelerated atherosclerosis in hyperlipidaemic C57BL/6 mice treated with cyclosporin A. Am J Pathol 142: 1906-1915

Epstein CJ, Avraham KB, Lovett M, Smith S, Elroy-Stein O, Rotman G, Bry C, Groner Y (1987) Transgenic mice with increased Cu/Zn-superoxide dismutase activity: animal model of dosage effects in Down syndrome. Proc Natl Acad Sci USA 84: 8044-8048

Epstein CJ, Martin GM, Schultz A, Motulsky AG (1966) Werner's syndrome: a review of its symptomatology, natural history, pathologic features, genetics and relationship to the natural aging process. Medicine (Baltimore) 45: 177-221

Erusalimsky JD, Kurz DJ (2005) Cellular senescence in vivo: its relevance in ageing and cardiovascular disease. Exp Gerontol 40: 634-642

Fabricant CG, Fabricant J, Minick CR, Litrenta MM (1983) Herpes virus-induced atherosclerosis in chickens. Fed Proc 42: 2476-2479

Faggiotto A, Ross R (1984) Studies of hypercholesterolemia in the nonhuman primate. II. Fatty streak conversion to fibrous plaque. Arteriosclerosis 4: 341-356

Fairweather DS, Fox M, Margison GP (1987) The in vitro lifespan of MRC-5 cells is shortened by 5-azacytidine-induced demethylation. Exp Cell Res 168: 153-159

Fazio S, Babaev VR, Murray AB, Hasty AH, Carter KJ, Gleaves LA, Atkinson JB, Linton MF (1997) Increased atherosclerosis in mice reconstituted with apolipoprotein E null macrophages. Proc Natl Acad Sci USA 94: 4647-4652

Ferns GA, Reidy MA, Ross R (1991) Balloon catheter de-endothelialization of the nude rat carotid: Response to injury in the absence of functional T lymphocytes. Am J Pathol 138: 1045-1057

Ferns GA, Stewart-Lee AL, Änggård EE (1992) Arterial response to mechanical injury: balloon catheter de-endothelialization. Atherosclerosis 92: 89-104

Finch CE (1990) Longevity, senescence and the genome. University of Chicago Press, Chicago, IL.

Finch CE, Landfield PW (1985) Neuroendocrine and autonomic functions in aging mammals. In: Finch CE, Schneider EL (Eds): Handbook of the Biology of Aging. Second Edition. New York Academic Press, New York. p567

Fingerle J, Johnson R, Clowes AW, Majesky MW, Reidy MA (1989) Role of platelets in smooth muscle cells proliferation and migration after vascular injury in rat carotid artery. Proc Natl Acad Sci USA 86: 8412-8416

Flurkey K, Papaconstantinou J, Miller RA, Harrison DE (2001) Lifespan extension and delayed immune and collagen aging in mutant mice with defects in growth hormone production. Proc Natl Acad Sci USA 98: 6736-6741

Francis DJ, Parish CR, McGarry M, Santiago FS, Lowe HC, Brown KJ, Bingley JA, Hayward IP, Cowden WB, Campbell JH, Campbell GR, Chesterman CN, Khachigian LM (2003) Blockade of vascular smooth muscle cell proliferation and intimal thickening after balloon injury by the sulfated oligosaccharide PI-88: phosphomannopentose sulfate directly binds FGF-2, blocks cellular signaling, and inhibits proliferation. Circ Res 92: e70-e77

Frankel EN, Kanner J, German JB, Parks E, Kinsella JE (1993) Inhibition of oxidation of human low-density lipoprotein by phenolic substances in red wine. Lancet 341: 454-457

French JE, Jennings MA, Florey HW (1965) Morphological studies on atherosclerosis in swine. Ann NY Acad Sci 127: 780-799

Friedlander Y, Kark JD, Stein Y, (1985) Family history of myocardial infarction as an independent risk factor for coronary heart disease. Br Heart J 53: 382-387

Frostegard J, Ulfgren AK, Nyberg P, Hedin U, Swedenborg J, Andersson U, Hansson GK (1999) Cytokine expression in advanced human atherosclerotic plaques: dominance of pro-inflammatory (Th1) and macrophage-stimulating cytokines. Atherosclerosis 145: 33-43

Furumoto K, Inoue E, Nagao N, Hiyama E, Miwa N (1998) Age-dependent telomere shortening is slowed down by enrichment of intracellular vitamin C via suppression of oxidative stress. Life Sci 63: 935-948

Fyfe AI, Qiao J-H, Lusis AJ (1994) Immune-deficient mice develop typical atherosclerotic fatty streaks when fed an atherogenic diet. J Clin Invest 94: 2516-2520

Gavrieli Y, Sherman Y, Ben-Sasson SA (1992) Identification of programmed cell death in situ via specific labeling of nuclear DNA fragmentation. J Cell Biol 119: 493-501

Geng YJ, Libby P (1995) Evidence for apoptosis in advanced human atheroma. Colocalization with interleukin-1 beta-converting enzyme. Am J Pathol 147: 229-234

Gerhard M, Roddy MA, Creager SJ, Creager MA (1996) Aging progressively impairs endothelium-dependent vasodilation in forearm resistance vessels of humans. Hypertension 27: 849-853

Gerrity RG (1981) The role of the monocytes in atherogenesis. I. Transition of blood-borne monocytes into foam cells in fatty lesions. Am J Pathol 103: 181-190

Gerrity RG, Naito HK, Richardson M, Schwartz CJ (1979) Dietary induced atherogenesis in swine: morphology of the intima in prelesion stages. Am J Pathol 95: 775-792

Glassberg MK, Bern MM, Coughlin SR, Haudenschild CC, Hoyer LW, Antoniades HN, Zetter BR (1982) Cultured endothelial cells derived from the human iliac arteries. In Vitro 18: 859-866

Goettsch W, Lattmann T, Amann K, Szibor M, Morawietz H, Münter K, Müller SP, Shaw S, Barton M (2001) Increased expression of endothelin-1 and inducible nitric oxide synthase isoform II in aging arteries *in vivo*: implications for atherosclerosis. Biochem Biophys Res Commun 280: 908-913

Goetze S, Xi XP, Kawano Y, Kawano H, Fleck E, Hsueh WA, Law RE (1999) TNF-alpha-induced migration of vascular smooth muscle cells is MAPK dependent. Hypertension 33(1 Pt2) 183-189

Goldbourt U, Neufeld HN (1986) Genetic aspects of arteriosclerosis. Arteriosclerosis 6: 357-377

Goldstein S (1990) Replicative senescence: the human fibroblast comes of age. Science 249: 1129-1133

Goldstein S, Harley CB (1979) *In vitro* studies of age-associated diseases. Fed Proc 38: 1862-1867

Goldstein S, Niewiarowski S, Singal DP (1975) Pathological implications of cell aging in vitro. Fed Proc 34: 56-63

Gorbunova V, Seluanov A, Pereira-Smith OM (2002) Expression of human telomerase (hTERT) does not prevent stress-induced senescence in normal human fibroblasts but protects the cells from stress-induced apoptosis and necrosis. J Biol Chem 277: 38540-38549

Gossrau R, Lojda Z, Stoward PJ (1991) Glycosidases. In: Stoward PJ, Everson Pearse AG (Eds) Histochemistry: Theoretical and Applied. Churchill Livingstone, Edinburgh. pp 241-279

Greider CW (1990) Telomeres, telomerase and senescence. Bioessays 12: 363-369

Griffith JD, Comeau L, Rosenfield S, Stansel RM, Bianchi A, Moss H, de Lange T (1999) Mammalian telomeres end in a large duplex loop. Cell 97: 503-514

Groner Y, Elroy-Stein O, Avraham KB, Yarom R, Schickler M, Knobler H, Rotman G (1990) Down syndrome clinical symptoms are manifested in transfected cells and transgenic mice overexpressing the human Cu/Zn-superoxide dismutase gene. J Physiol (Paris) 84: 53-57

Groot PHE, van Vlijmen BJM, Benson GM, Hofker MH, Schiffelers R, Vidgeon-Hart M, Havekes LM (1996) Quantitative assessment of aortic atherosclerosis in ApoE*3 Leiden transgenic mice and its relationship to serum cholesterol exposure. Arterioscler Thromb Vasc Biol 16: 926-933

Grotendorst GR, Chang T, Seppä HEJ, Kleinman HK, Martin GR (1982) Platelet-derived growth factor is a chemoattractant for vascular smooth muscle cells. J Cell Physiol 113: 261-266

Groves HM, Kinlough-Rathbone RL, Richardson M, Moore S, Mustard JF (1979) Platelet interaction with damaged rabbit aorta. Lab Invest 40: 194-200

Hagen TM, Ingersoll RT, Lykkesfeldt J, Liu J, Wehr CM, Vinarsky V, Bartholomew JC, Ames BN (1999) (R)-α-lipoic acid-supplemented old rats have improved mitochondrial function, decreased oxidative damage, and increased metabolic rate. FASEB J 13: 411-418

Hagen TM, Moreau R, Suh JH, Visioli F (2002) Mitochondrial decay in the aging rat heart. Ann N Y Acad Sci 959: 491-507

Hagen TM, Vinarsky V, Wehr CM, Ames BN (2000) (R)-α-lipoic acid reverses the age-associated increase in susceptibility of hepatocytes to tert-butylhydroperoxide both in vitro and in vivo. Antiox Redox Signal 2: 473-483

Hagen TM, Yowe DL, Bartholomew JC, Wehr CM, Do KL, Park JY, Ames BN (1997) Mitochondrial decay in hepatocytes from old rats: membrane potential declines, heterogeneity and antioxidants increase. Proc Natl Acad Sci USA 94: 3064-3069

Hajjar DP (1991) Viral pathogenesis of atherosclerosis. Am J Pathol 139: 1195-1211

Hall DA (1976) Chemical and biochemical changes in connective tissues. In: The Aging of Connective Tissue. New York Academic Press, New York

Hall PA, Levison DA, Woods AL, Yu C C-W, Kellock DB, Watkins JA, Barnes DM, Gillett CE, Camplejohn R, Dover R, Waseem NH, Lane DP (1990) Proliferating cell nuclear antigen (PCNA) immunolocalization in paraffin sections: an index of cell proliferation with evidence of deregulated expression in some neoplasms. J Pathol 162: 285-294

Halliwell B, Gutteridge JMC (1989) Free Radicals in Biology and Medicine. Second Edition. Clarendon Press, Oxford

Han DKM, Haudenschild CC, Hong MK, Tinkle BT, Leon MB, Liau G (1995) Evidence for apoptosis in human atherogenesis and in a rat vascular injury model. Am J Pathol 147: 267-277

Han J, Hosokawa M, Umezawa M, Yagi H, Matsushita T, Higuchi K, Takeda T (1998) Age-related changes in blood pressure in the senescence-accelerated mouse (SAM): aged SAMP1 mice manifest hypertensive vascular disease. Lab Anim Sci 48: 256-263

Hansson GK, Björnheden T, Bylock A, Bondjers G (1981) Fc-dependent binding of monocytes to areas with endothelial injury in the rabbit aorta. Exp Mol Pathol 34: 246-252

Hansson GK, Jonasson L, Siefert PS, Stamme S (1989) Immune mechanisms in atherosclerosis. Arteriosclerosis 9: 567-578

Hara E, Smith R, Parry D, Tahara H, Stone S, Peters G (1996) Regulation of p16CDKN2 expression and its implications for cell immortalization and senescence. Mol Cell Biol 16: 859-867

Hara E, Tsurui H, Shinozaki A, Nakada S, Oda K (1991) Cooperative effect of anti-sense-Rb and antisense-p53 oligomers on the extension of life span in human diploid fibroblasts, TIG-1. Biochem Biophys Res Commun 179: 528-534

Harley CB, Futcher AB, Greider CW (1990) Telomeres shorten during ageing of human fibroblasts. Nature 345: 458-460

Harley CB, Vaziri H, Counter CM, Allsopp RC (1992) The telomere hypothesis of cellular aging. Exp Gerontol 27: 375-382

Harley CB, Villeponteau B (1995) Telomeres and telomerase in aging and cancer. Curr Opin Genet Dev 5: 249-255

Harman D (1956) Aging: a theory based on free radical and radiation chemistry. J Gerontol 2: 298-300

Harman D (1981) The aging process. Proc Natl Acad Sci USA 78: 7124-7128

Hart RW, Setlow RB (1974) Correlation between deoxyribonucleic acid excision-repair and life-span in a number of mammalian species. Proc Natl Acad Sci USA 71: 2169-2173

Harvey M, Sands AT, Weiss RS, Hegi ME, Wiseman RW, Pantazis P, Giovanella BC, Tainsky MA, Bradley A, Donehower LA (1993) In vitro growth characteristics of embryo fibroblasts isolated from p53-deficient mice. Oncogene 8: 2457-2467

Hastie ND, Dempster M, Dunlop MG, Thompson AM, Green DK, Allshire RC (1990) Telomere reduction in human colorectal carcinoma with ageing. Nature 346: 866-868

Hasty AH, Linton MF, Brandt SJ, Babaev VR, Gleaves LA, Fazio S (1999) Retroviral gene therapy in apoE-deficient mice. ApoE expression in the artery wall reduces early foam cell lesion formation. Circulation 99: 2571-2576

Haudenschild CC, Grunwald J (1985) Proliferative heterogeneity of vascular smooth muscle cells and its alteration by injury. Exp Cell Res 157: 364-370

Haudenschild CC, Schwartz SM (1979) Endothelial regeneration. II. Restitution of endothelial continuity. Lab Invest 41: 407-418

Hayflick L (1965) The limited *in vitro* life time of human diploid cell strains. Exp Cell Res 37: 614-636

Hayflick L, Moorhead PS (1961) The serial cultivation of human diploid cell strains. Exp Cell Res 25: 585-621

Heath D, Smith P, Harris P, Winson M (1973) The atherosclerotic human carotid sinus. J Pathol 110: 49-58

Heiss NS, Knight SW, Vulliamy TJ, Klauck SM, Wiemann S, Mason PJ, Poustka A, Dokal I (1998) X-linked dyskeratosis congenita is caused by mutations in a highly conserved gene with putative nucleolar functions. Nat Genet 19: 32-38

Henriksen T, Mahoney EM, Steinberg D (1981) Enhanced macrophage degradation of low density lipoprotein previously incubated with cultured endothelial cells: recognition by receptors for acetylated low density lipoproteins. Proc Natl Acad Sci USA 78: 6499-6503

Herbig U, Jobling WA, Chen BP, Chen DJ, Sedivy WE (2004) Telomere shortening triggers senescence of human cells through a pathway involving ATM, p53, and p21(CIP1), but not p16(INK4a). Mol Cell 14: 501-513

Herdeg C, Oberhoff M, Baumbach A, Schroeder S, Leitritz M, Blattner A, Siegel-Axel DI, Meisner C, Karsch KR (2003) Effects of local all-trans-retinoic acid delivery on experimental atherosclerosis in the rabbit carotid artery. Cardiovasc Res 57: 544-553

Higami Y, Shimokawa I (2000) Apoptosis in the aging process. Cell Tissue Res 301: 125-132

Higashi T, Sano H, Saishoji T, Ikeda K, Jinnouchi Y, Kanzaki T, Morisaki N, Rauvala H, Shichiri M, Horiuchi S (1997) The receptor for advanced glycation end products mediates the chemotaxis of rabbit smooth muscle cells. Diabetes 46: 463-472

Hino K, Nakamura M, Nakanishi K, Manabe M (Daiichi Pure Chemicals Co., Ltd., Tokyo, Japan) A new method for the homogeneous assay of serum HDL-cholesterol. (1996) Clin Chem 42: S299

Hobson B, Denekamp J (1984) Endothelial cell proliferation in tumours and normal tissues: continuous labelling studies. Br J Cancer 49: 405-413

Hollander W, Colombo MA, Kirkpatrick B, Paddock J (1979) Soluble proteins in the human atherosclerotic plaque. Atherosclerosis 38: 391-405

Holme I, Enger SC, Helgeland A, Hjermann I, Leren P, Lund-Larsen PG, Solberg LA, Strong JP (1981) Risk factors and raised atherosclerotic lesions in coronary and cerebral arteries. Statistical analysis from the Oslo Study. Arteriosclerosis 1: 250-256

Hoshi H, McKeehan WL (1986) Isolation, growth requirements, cloning, prostacyclin production and life-span of human adult endothelial cells in low serum culture medium. In Vitro Cell Dev Biol 22: 51-56

Hosokawa M (1994) Grading score system; a method of evaluation of the degree of senescence in senescence-accelerated mouse (SAM). In: Takeda T (Ed.) The SAM model of senescence. Excerpta Medica, Amsterdam. pp 23-28

Hosokawa M, Abe T, Higuchi K, Shimakawa K, Omori Y, Matsushita T, Kogishi K, Deguchi E, Kishimoto Y, Yasuoka K, Takeda T (1997) Management and design of the maintenance of SAM mouse strains: an animal model for accelerated senescence and age-associated disorders. Exp Gerontol 32: 111-116

Hosokawa M, Ashida Y, Nishikawa T, Takeda T (1994) Accelerated aging of dermal fibroblast-like cells from senescence-accelerated mouse (SAM). 1. Acceleration of population aging in vitro. Mech Ageing Dev 74: 65-77

Hosokawa M, Kasai R, Higuchi K, Takeshita S, Shimizu K, Hamamoto H, Honma A, Irino M, Toda K, Matsumura A, Matsushita M, Takeda T (1984) Grading score

system: a method for evaluation of the degree of senescence in senescence accelerated mouse (SAM). Mech Ageing Dev 26: 91-102

Hsiao R, Sharma HW, Ramakrishnan S, Keith E, Narayanan R (1997) Telomerase activity in normal human endothelial cells. Anticancer Res 17: 827-832

Hueper WC (1944) The anoxaemia theory. Arch Path 38: 173-181

Hutter R, Sauter BV, Reis ED, Roque M, Vorchheimer D, Carrick FE, Fallon JT, Fuster V, Badimon JJ (2003) Decreased reendothelialization and increased neointima formation with endostatin overexpression in a mouse model of arterial injury. Circulation 107: 1658-1663

Imlay JA, Chin SM, Linn S (1988) Toxic DNA damage by hydrogen peroxide through the Fenton reaction in vivo and in vitro. Science 240: 640-642

Ishibashi S, Goldstein JL, Brown MS, Herz J, Burns DK (1994) Massive xanthomatosis and atherosclerosis in cholesterol-fed low density lipoprotein receptor-negative mice. J Clin Invest 93: 1885-1893

Itahana K, Campisi J, Dimri GP (2004) Mechanisms of cellular senescence in human and mouse cells. Biogerontology 5: 1-10

Itahana K, Dimri GP, Hara E, Itahana Y, Zou Y, Desprez PY, Campisi J (2003) Control of the replicative lifespan of human fibroblasts by p16 and the polycomb protein bmi-1. Mol Cell Biol 23: 389-401

Iwasa H, Han J, Ishikawa F (2003) Mitogen-activated protein kinase p38 defines the common senescence-signalling pathway. Genes Cells 8: 131-144

Jaimes EA, Sweeney C, Raij L (2001) Effects of the reactive oxygen species hydrogen peroxide and hypochlorite on endothelial nitric oxide production. Hypertension 38: 877-883

Janssen YMW, Van-Houten B, Borm PJA, Mossman BT (1993) Biology of disease: Cell and tissue responses to oxidative damage. Lab Invest 69: 261-274

Jarvik LF, Falek A, Kallman FJ, Lorge I (1960) Survival trends in a senescent twin population. Am J Hum Genet 12: 170-179

Jauchem JR, Lopez M, Sprague EA, Schwartz CJ (1982) Mononuclear cell chemoattractant activity from cultured arterial smooth muscle cells. Exp Mol Pathol 37: 166-174

Jilka RL, Weinstein RS, Takahashi K, Parfitt AM, Manolagas SC (1996) Linkage of decreased bone mass with impaired osteoblastogenesis in a murine model of accelerated senescence. J Clin Invest 97: 1732-1740

Johnson CP, Baugh R, Wilson CA, Burns J (2001a) Age related changes in the tunica media of the vertebral artery: implications for the assessment of vessels injured by trauma. J Clin Pathol 54: 139-145

Johnson JL, van Eys GJJM, Angelini GD, George SJ (2001b) Injury induces dedifferentiation of smooth muscle cells and increased matrix-degrading

metalloproteinase activity in human saphenous vein. Arterioscler Thromb Vasc Biol 21: 1146-1151

Johnson LK, Longenecker JP (1982) Senescence of aortic endothelial cells in vitro: influence of culture conditions and preliminary characterization of the senescent phenotype. Mech Ageing Dev 18: 1-18

Johnson TM, Yu ZX, Ferrans VJ, Lowenstein RA, Finkel T (1996) Reactive oxygen species are downstream mediators of p53-dependent apoptosis. Proc Natl Acad Sci USA 93: 11848-11852

Jonasson L, Holm J, Hansson GK (1988) Cyclosporin A inhibits smooth muscle cell proliferation in the vascular response to injury. Proc Natl Acad Sci USA 85: 2303-2306

Jonasson L, Holm J, Skalli O, Bondjers G, Hansson GK (1986) Regional accumulations of T cells, macrophages, and smooth muscle cells in the human atherosclerotic plaque. Arteriosclerosis 6: 131-138

Joris I, Zand T, Nunnari JJ, Krolikowski FJ, Majno G (1983) Studies on the genesis of atherosclerosis. I. Adhesion and emigration of mononuclear cells in the aorta of hypercholesterolaemic rats. Am J Pathol 113: 341-358

Kamenz J, Seibold W, Wohlfrom M, Hanke S, Heise N, Lenz C, Hanke H (2000) Incidence of intimal proliferation and apoptosis following balloon angioplasty in an atherosclerotic rabbit model. Cardiovasc Res 45: 766-776

Kamino H, Hiratsuka M, Toda T, Nishigaki R, Osaki M, Ito H, Inoue T, Oshimura M (2003) Searching for genes involved in arteriosclerosis: proteomic analysis of cultured human umbilical vein endothelial cells undergoing replicative senescence. Cell Struct Funct 28: 495-503

Kannel WB, McGee DL (1979) Diabetes and cardiovascular disease. The Framingham Study. JAMA 241: 2035-2038

Kedziora J, Bartosz G (1988) Down's syndrome: a pathology involving the lack of balance of reactive oxygen species. Free Radic Biol Med 4: 317-330

Kent S (1976) Is diabetes a form of accelerated aging? Geriatrics 140: 149-151

Kenyon C (1996) Ponce d'elegans: genetic quest for the fountain of youth. Cell 84: 501-504

Kerr JFR (1971) Shrinkage necrosis: a distinct mode of cellular death. J Pathol 105: 13-21

Khan BV, Parthasarathy SS, Alexander RW, Medford RM (1995) Modified low density lipoprotein and its constituents augment cytokine-activated vascular cell adhesion molecule-1 gene expression in human vascular endothelial cells. J Clin Invest 95: 1262-1270

Kim H, You S, Farris J, Kong B-W, Christman SA, Foster LK, Foster DN (2002) Expression profiles of p53-, $p16^{INK4a}$-, and telomere-regulating genes in replicative

senescent primary human, mouse, and chicken fibroblast cells. Exp Cell Res 272: 199-208

Kim NW, Piatyszek MA, Prowse KR, Harley CB, West MD, Ho PL, Coviello GM, Wright WE, Weinrich SL, Shay JW (1994) Specific association of human telomerase activity with immortal cells and cancer. Science 266: 2011-2015

Kim SH, Kaminker P, Campisi J (1999) TIN2, a new regulator of telomere length in human cells. Nat Genet 23: 382-383

Kipling D, Cooke HJ (1990) Hypervariable ultra-long telomeres in mice. Nature 347: 400-402

Kita T, Nagano Y, Yokode M, Ishii K, Kume N, Ooshima A, Yoshida H, Kawai C (1987) Probucol prevents the progression of atherosclerosis in Watanabe heritable hyperlipidaemic rabbit, an animal model for familial hypercholesterolaemia. Proc Natl Acad Sci USA 84: 5928-5931

Kjeldsen K, Wanstrup J, Astrup P (1968) Enhancing influence of arterial hypoxia on the development of atheromatosis in cholesterol-fed rabbits. J Atheroscl Res 8: 835-845

Knekt P, Ritz J, Pereira MA, O'Reilly EJ, Augustsson K, Fraser GE, Goldbourt U, Heitmann BL, Hallmans G, Liu S, Pietinen P, Spiegelman D, Stevens J, Virtamo J, Willett WC, Rimm EB, Ascherio A (2004) Antioxidant vitamins and coronary heart disease risk: a pooled analysis of 9 cohorts. Am J Clin Nutr 80: 1508-1520

Kocher O, Skalli O, Bloom WS, Gabbiani G (1984) Cytoskeleton of rat aortic smooth muscle cells. Normal conditions and experimental intimal thickening. Lab Invest 50: 645-652

Kockx MM, De Meyer GR, Jacob WA, Bult H, Herman AG (1992) Triphasic sequence of neointimal formation in the cuffed carotid artery of the rabbit. Arterioscler Thromb 12: 1447-1457

Kohn RR (1977) Chapter 12. Heart and Cardiovascular System. In: Finch CE, Hayflick L (Eds) The Handbook of the Biology of Aging. Van Nostrand Reinhold Company, New York. pp 281-317

Kohn RR (1978) Principles of Mammalian Aging. Second Edition. Prentice-Hall Inc., Englewood Cliffs, NJ.

Kohno A, Yonezu T, Matsushita M, Irino M, Higuchi K, Higuchi K, Takeshita S, Hosokawa M, Takeda T (1985) Chronic food restriction modulates the advance of senescence in the senescence accelerated mouse (SAM). J Nutr 115: 1259-1266

Koldovsky O, Asp NG, Dahlqvist A (1969) A method for the separate assay of "neutral" and "acid" beta-galactosidase in homogenates of rat small-intestinal mucosa. Anal Biochem 27: 409-418

Kollum M, Kaiser S, Kinscherf R, Metz J, Kubler W, Hehrlein C (1997) Apoptosis after stent implantation compared with balloon angioplasty in rabbits. Role of macrophages. Arterioscler Thromb Vasc Biol 17: 2383-2388

Komura S, Yoshino K, Ohishi N, Yagi K (1994) Serum lipid peroxide level of the senescence-accelerated mouse. In: Takeda T (Ed.) The SAM model of senescence. Elsevier Science, Amsterdam. pp 141-144

Konneh MK, Rutherford C, Li SR, Änggard E, Ferns GAA (1995) Vitamin E inhibits the intimal response to balloon catheter injury in the carotid artery of the cholesterol-fed rabbit. Atherosclerosis 113: 29-39

Kraemer R (2000) Regulation of cell migration in atherosclerosis. Curr Atheroscler Rep 2: 445-452

Krimpenfort P, Quon KC, Mooi WJ, Loonstra A, Berns A (2001) Loss of p16Ink4a confers susceptibility to metastatic melanoma in mice. Nature 413: 83-86

Krishnamurthy J, Torrice C, Ramsey MR, Kovalev GI, Al Regaiey K, Su L, Sharpless NE (2004) Ink4a/Arf expression is a biomarker of aging. J Clin Invest 114: 1299-1307

Kritchevsky SB, Shimakawa T, Tell GS, Dennis B, Carpenter M, Eckfeldt JH, Peacher-Ryan H, Heiss G (1995) Dietary antioxidants and carotid artery thickness. The ARIC Study. Atherosclerosis Risk in Communities Study. Circulation 92: 2142-2150

Kugiyama K, Kerns SA, Morrisett JD, Roberts R, Henry PD (1990) Impairment of endothelium-dependent arterial relaxation by lysolecithin in modified low-density lipoprotein. Nature 344: 160-162

Kulju KS, Lehman JM (1995) Increased p53 protein associated with aging in human diploid fibroblasts. Exp Cell Res 217: 336-345

Kumazaki T, Robetorye RS, Robetorye SC, Smith JR (1991) Fibronectin expression increases during in vitro cellular senescence: correlation with increased cell area. Exp Cell Res 195: 13-19

Kurokawa T, Ozaki N, Ishibashi S (1998) Difference between senescence-accelerated prone and resistant mice in response to insulin in the heart. Mech Ageing Dev 102: 25-32

Kuro-o M, Matsumura Y, Aizawa H, Kawaguchi H, Suga T, Utsugi T, Ohyama Y, Kurabayashi M, Kaname T, Kume E, Iwasaki H, Iida A, Shiraki-Iida T, Nishikawa S, Nagai R, Nabeshima YI (1997) Mutation of the mouse klotho gene leads to a syndrome resembling ageing. Nature 390: 45-51

Kurose I, Higuchi H, Miura S, Saito H, Watanabe N, Hokari R, Hirokawa M, Takaishi M, Zeki S, Nakamura T, Ebinuma H, Kato S, Ishii H (1997) Oxidative stress-mediated apoptosis of hepatocytes exposed to acute ethanol intoxication. Hepatology 25: 368-378

Kurtin PJ, Pinkus GS (1985) Leukocyte common antigen–a diagnostic discriminant between hematopoietic and nonhematopoietic neoplasms in paraffin sections using monoclonal antibodies: correlation with immunologic studies and ultrastructural localization. Hum Pathol 16: 353-365

Kurz DJ, Decary S, Hong Y, Erusalimsky JD (2000) Senescence-associated (beta)-galactosidase reflects an increase in lysosomal mass during replicative ageing of human endothelial cells. J Cell Sci 113: 3613-3622

Kurz DJ, Decary S, Hong Y, Trivier E, Akhmedov A, Erusalimsky JD (2004) Chronic oxidative stress compromises telomere integrity and accelerates the onset of senescence in human endothelial cells. J Cell Sci 117: 2417-2426

Kurz DJ, Hong Y, Trivier E, Huang HL, Decary S, Zang GH, Luscher TF, Erusalimsky JD (2003) Fibroblast growth factor-2, but not vascular endothelial growth factor, upregulates telomerase activity in human endothelial cells. Arterioscler Thromb Vasc Biol 23: 748-754

Kwak IH, Kim HS, Choi OR, Ryu MS, Lim IK (2004) Nuclear accumulation of globular actin as a cellular senescence marker. Cancer Res 64: 572-580

Langille BL, Reidy MA, Kline RL (1986) Injury and repair of endothelium at sites of flow disturbances near abdominal aortic coarctations in rabbits. Arteriosclerosis 6: 146-154

Lansdorp PM (2000) Repair of telomeric DNA prior to replicative senescence. Mech Ageing Dev 118: 23-34

Laurindo FR, da Luz PL, Uint L, Rocha TF, Jaeger RG, Lopes EA (1991) Evidence for superoxide radical-dependent coronary vasospasm after angioplasty in intact dogs. Circulation 83: 1705-1715

Lavrovsky Y, Chatterjee B, Clark RA, Roy AK (2000) Role of redox-regulated transcription factors in inflammation, aging and age-related diseases. Exp Gerontol 35: 521-532

LeBoeuf RC, Doolittle MH, Montcalm A, Martin DC, Reue K, Lusis AJ (1990) Phenotypic characterization of the Ath-1 gene controlling high density lipoprotein levels and susceptibility to atherosclerosis. J Lipid Res 31: 91-101

Lecka-Czernik B, Moerman EJ, Jones RA, Goldstein S (1996) Identification of gene sequences overexpressed in senescent and Werner syndrome human fibroblasts. Exp Gerontol 31: 159-174

Lee AC, Fenster BE, Ito H, Takeda K, Bae NS, Hirai T, Yu ZX, Ferrans VJ, Howard BH, Finkel T (1999) Ras proteins induce senescence by altering the intracellular levels of reactive oxygen species. J Biol Chem 274: 7936-7940

Lee MS, Gallagher RC, Bradley J, Blackburn EH (1993) In vivo and in vitro studies of telomeres and telomerase. Cold Spring Harb Symp Quant Biol 58: 707-718

Lefrancois L, Thomas ML, Bevan MJ, Trowbridge IS (1986) Different classes of T lymphocytes have different mRNAs for the leukocyte-common antigen, T200. J Exp Med 163: 1337-1342

Levy MZ, Allsopp RC, Futcher AB, Greider CW, Harley CB (1992) Telomere end-replication problem and cell ageing. J Mol Biol 225: 951-960

Li B, Comai L (2000) Functional interaction between Ku and the Werner syndrome protein in DNA end processing. J Biol Chem 275: 39800

Li H, Reddick RK, Maeda N (1993) Lack of apoA-I is not associated with increased susceptibility to atherosclerosis in mice. Arterioscler Thromb 13: 1814-1821

Li J-M, Mullen AM, Yun S, Wientjes F, Brouns GY, Thrasher AJ, Shah AM (2002) Essential role of the NADPH oxidase subunit p47(phox) in endothelial cell superoxide production in response to phorbol ester and tumour necrosis factor-alpha. Circ Res 90: 143-150

Li J-M, Shah AM (2004) Endothelial cell superoxide generation: regulation and relevance for cardiovascular pathophysiology. Am J Physiol Regul Integr Comp Physiol 287: R1014-R1030

Libby P (2002) Inflammation in atherosclerosis. Nature 420: 868-874

Libby P, Aikawa M (2002) Stabilization of atherosclerotic plaques: new mechanisms and clinical targets. Nat Med 8: 1257-1262

Libby P, Warner SJC, Friedman GB (1988) Interleukin-1: a mitogen for human vascular smooth muscle cells. J Exp Med 165: 1316-1331

Lin AH, Castle CK, Melchior GW, Marotti KR (1995) The effect of population density on the development of experimental atherosclerosis in female mice. Atherosclerosis 11: 85-88

Lindner V, Reidy MA (1991) Proliferation of smooth muscle cells after vascular injury is inhibited by an antibody against basic fibroblast growth factor. Proc Natl Acad Sci USA 88: 3739-3743

Lindner V, Reidy MA, Fingerle J (1989) Regrowth of arterial endothelium. Denudation with minimal trauma leads to complete endothelial regrowth. Lab Invest 54: 556-563

Lingner J, Hughes TR, Shevchenko A, Mann M, Lundblad V, Cech TR (1997) Reverse transcriptase motifs in the catalytic subunit of telomerase. Science 276: 561-567

Lipetz J, Cristofalo V (1972) Ultrastructural changes accompanying the aging of human diploid cells in culture. J Ultrastruct Res 39: 43-56

Lipman RD, Taylor A (1987) The *in vivo* replicative potential and cellular morphology of human lens epithelial cells derived from different aged donors. Curr Eye Res 6: 1453-1457

Lipton BA, Parthasarathy S, Ord VA, Clinton SK, Libby P, Rosenfeld ME (1995) Components of the protein fraction of oxidized low density lipoprotein stimulate interleukin-1 alpha production by rabbit arterial macrophage-derived foam cells. J Lipid Res 36: 2232-2242

Liu J, Mori A (1993) Age-associated changes in superoxide dismutase activity, thiobarbituric acid reactivity, and reduced glutathione level in brain and liver in SAM: a comparison with ddY mice. Mech Ageing Dev 71: 23-30

Liu MW, Roubin GS, King SB 3rd (1989) Restenosis after coronary angioplasty: potential biological determinants and role of intimal hyperplasia. Circulation 79: 1374-1387

Lockshin RA, Zakeri Z (1996) The biology of cell death and its relationship to aging. In: Holbrook N, Martin GR, Lockshin RA (Eds) Cellular Aging and Cell Death. Wiley-Liss, New York. pp 167-180

Luce MC, Bunn CL (1989) Decreased accuracy of protein synthesis in extracts from aging human diploid fibroblasts. Exp Gerontol 24: 113-125

Ludmer PL, Selwyn AP, Shook TL, Wayne RR, Mudge GH, Alexander RW, Ganz P (1986) Paradoxical vasoconstriction induced by acetylcholine in atherosclerotic coronary arteries. N Engl J Med 315: 1046-1051

Lundberg AS, Hahn WC, Gupta P, Weinberg RA (2000) Genes involved in senescence and immortalization. Curr Opin Cell Biol 12: 705-709

Lupu F, Bergonzelli GE, Heim DA, Cousin E, Genton CY, Bachmann F, Kruithof EK (1993) Localization and production of plasminogen activator inhibitor-1 in human healthy and atherosclerotic plaques. Arterioscler Thromb 13: 1090-1100

Luscher TF, Dohi Y, Tschudi M (1992) Endothelium-dependent regulation of resistance arteries: alterations with aging and hypertension. J Cardiovasc Pharmacol 19 Suppl 5: S34-S42

Lusis AJ (2000) Atherosclerosis. Nature 407: 233-241

Lutgens E, de Muinck ED, Kitslaar PJEHM, Tordoir JHM, Wellens HJJ, Daemen MJAP (1999) Biphasic pattern of cell turnover characterizes the progression from fatty streaks to ruptured human atherosclerotic plaques. Cardiovasc Res 41: 473-479

Lykkesfeldt J, Hagen TM, Vinarsky V, Ames BN (1998) Age-associated decline in ascorbic acid concentration, recycling, and biosynthesis in rat hepatocytes – reversal with (R)-alpha-lipoic acid supplementation. FASEB J 12: 1183-1189

McCaffrey TA, Nicholson AC, Szabo PE, Weksler ME, Weksler BB (1988) Aging and arteriosclerosis. The increased proliferation of arterial smooth muscle cells isolated from old rats is associated with increased platelet-derived growth factor-like activity. J Exp Med 167: 163-174.

McConnell BB, Starborg M, Brookes S, Peters G (1998) Inhibitors of cyclin-dependent kinases induce features of replicative senescence in early passage human fibroblasts. Curr Biol 8: 351-354

McCormick JJ, Maher VM (1988) Towards an understanding of the malignant transformation of diploid human fibroblasts. Mutat Res. 199: 273-91

MacDonald K, Rector TS, Braunlan EA, Coubo SH, Olivari MT (1989) Association of coronary artery disease in cardiac transplant recipients with cytomegalovirus infection. Am J Pathol 64: 359-362

McEachern MJ, Blackburn EH (1995) Runaway telomere elongation caused by telomerase RNA gene mutations. Nature 376: 403-409

McGill HC Jr (1968) The geographic pathology of atherosclerosis. Baltimore: Williams & Wilkins. pp 1-193

McGill HC Jr (1984) George Lyman Duff memorial lecture. Persistent problems in the pathogenesis of atherosclerosis. Arteriosclerosis 4: 443-451

McGill HC Jr (1988) The cardiovascular pathology of smoking. Am Heart J 115: 250-257

McGill HC Jr, Geer JC, Strong JP (1963). Natural history of human atherosclerotic lesions. In: Sandler M, Barne GH (Eds) Atherosclerosis and its origin. Academic Press, New York. pp 39-65

McMurray HF, Parrott DP, Bowyer DE (1991) A standardized method of culturing aortic transplants, suitable for the study of factors affecting the phenotypic modulation, migration and proliferation of aortic smooth muscle cells. Atherosclerosis 86: 227-237

Mach F, Sauty A, Iarossi AS, Sukhova GK, Neote K, Libby P, Luster AD (1999) Differential expression of three T lymphocyte-activating CXC chemokines by human atheroma-associated cells. J Clin Invest 104: 1041-1050

Maciag T, Hoover GA, Stemerman MB, Weinstein R (1981) Serial propagation of human endothelial cells *in vitro*. J Cell Biol 91: 420-426

Macieira-Coelho A (1998) Markers of "cell senescence". Mech Ageing Dev 103: 105-109

Macieira-Coelho A, Garcia-Giralt E, Adrian M (1971) Changes in lysosomal associated structures in human fibroblasts kept in resting stage. Proc Soc Exp Biol Med 138: 712-718

Maier JA, Voulalas P, Roeder D, Maciag T (1990) Extension of the life-span of human endothelial cells by an interleukin-1alpha antisense oligomer. Science 249: 1570-1574

Maier JAM, Statuto M, Ragnotti G (1993) Senescence stimulates U937-endothelial cell interactions. Exp Cell Res 208: 270-274

Majno G, Joris I (1995) Apoptosis, oncosis, and necrosis: an overview of cell death. Am J Pathol 146: 3-15

Malik N, Francis SE, Holt CM, Gunn J, Thomas GL, Shepherd L, Chamberlain J, Newman CM, Cumberland DC, Crossman DC (1998) Apoptosis and cell proliferation after porcine coronary angioplasty. Circulation 98: 1657-1665

Manderson JA, Mosse PRL, Safstrom JA, Young SB, Campbell GR (1989) Balloon catheter injury to rabbit carotid artery. I. Changes in smooth muscle phenotype. Arteriosclerosis 9: 289-298

Mangoni AA, Jackson SH (2002) Homocysteine and cardiovascular disease: current evidence and future prospects. Am J Med 112: 556-565

Marciniak RA, Johnson FB, Guarante L (2000) Dyskeratosis congenita, telomeres and human ageing. Trends Genet 16: 193-195

Marotti KR, Castle CK, Boyle TP, Lin AH, Murray RW, Melchior GW (1993) Severe atherosclerosis in transgenic mice expressing simian cholesteryl ester transfer protein. Nature 364: 73-75

Martin GM (1993) Clonal attenuation: causes and consequences. J Gerontol 48: B171-B172

Martin GM, Sprague CA, Epstein CJ (1970) Replicative life-span of cultivated human cells. Effects of donor's age, tissue, and genotype. Lab Invest 23: 86-92

Martin JF, Booth RF, Moncada S (1991) Arterial wall hypoxia following thrombosis of the vasa vasorum is an initial lesion in atherosclerosis. Eur J Clin Invest 21: 355-359

Martin TR, Altman LC, Albert RK, Henderson WR (1984) Leukotriene B4 production by human alveolar macrophage: a potential mechanism for amplifying inflammation in the lung. Am Rev Respir Dis 129: 106-111

Martinet W, Knaapen MW, De Meyer GR, Herman AG, Kockx MM (2001) Oxidative DNA damage and repair in experimental atherosclerosis are reversed by dietary lipid lowering. Circ Res 88: 648-650

Masutomi K, Yu EY, Khurts S, Ben-Porath I, Currier JL, Metz GB, Brooks MW, Kaneko S, Murakami S, DeCaprio JA, Weinberg RA, Stewart SA, Hahn WC (2003) Telomerase maintains telomere structure in normal human cells. Cell 114: 241-253

Mather M, Rottenberg H. (2000) Aging enhances the activation of the permeability transition pore in mitochondria. Biochem Biophys Res Commun 273: 603-608

Matsumura T, Zerrudo Z, Hayflick L (1979) Senescent human diploid cells in culture: survival, DNA synthesis and morphology. J Gerontol 34: 328-334

Matsumura Y, Aizawa H, Shiraki-Iida T, Nagai R, Kuro-o M, Nabeshima Y (1998) Identification of the human klotho gene and its two transcripts encoding membrane and secreted klotho protein. Biochem Biophys Res Commun 242: 626-630

Matsunaga H, Handa JT, Aotaki-Keen A, Sherwood W, West MD, Hjelmeland LM (1999) Beta-galactosidase histochemistry and telomere loss in senescent retinal pigment epithelial cells. Invest Ophthalmol Vis Sci 40: 197-202

Matsushita H, Chang E, Glassford AJ, Cooke JP, Chiu CP, Tsao PS (2001) eNOS activity is reduced in senescent human endothelial cells: Preservation by hTERT immortalization. Circ Res 89: 793-798

Mazzone T, Jensen M, Chait A (1983) Human arterial wall cells secrete factors that are chemotactic for monocytes. Proc Natl Acad Sci USA 80: 5094-5097

Medrano EE, Yang F, Boissy R, Farooqui J, Shah V, Matsumoto K, Nordlund JJ, Park HY (1994) Terminal differentiation and senescence in the human melanocyte: repression of tyrosine-phosphorylation of the extracellular signal-regulated kinase 2 selectively defines the two phenotypes. Mol Biol Cell 5: 497-509

Mendez MV, Stanley A, Park HY, Shon K, Phillips T, Menzoian JO (1998) Fibroblasts cultured from venous ulcers display cellular characteristics of senescence. J Vasc Surg 28: 876-883

Merat S, Fruebis J, Sutphin M, Silvestre M, Reaven PD (2000) Effect of aging on aortic expression of the vascular cell adhesion molecule-1 and atherosclerosis in murine models of atherosclerosis. J Gerontol A Biol Sci Med Sci 55: B85-B94

Merry BJ (2000) Calorie restriction and age-related oxidative stress. Ann N Y Acad Sci 908: 180-198

Metcalfe JA, Parkhill J, Campbell L, Stacey M, Biggs P, Byrd PJ, Taylor AM (1996) Accelerated telomere shortening in ataxia telangiectasia. Nat Genet 13: 350-353

Meyerson M, Counter CM, Eaton EN, Ellisen LW, Steiner P, Caddle SD, Ziaugra L, Beijersbergen RL, Davidoff MJ, Liu Q, Bacchetti S, Haber DA, Weinberg RA (1997) hEST2, the putative human telomerase catalytic subunit gene, is up-regulated in tumor cells and during immortalization. Cell 90: 785-795

Miller NE (1987) Associations of high-density lipoprotein subclasses and apolipoproteins with ischemic heart disease and coronary atherosclerosis. Am Heart J 113: 589-597

Millis AJ, Hoyle M, McCue HM, Martini H (1992) Differential expression of metalloproteinase and tissue inhibitor of metalloproteinase genes in aged human fibroblasts. Exp Cell Res 201: 373-379

Minamino T, Mitsialis SA, Kourembanas S (2001) Hypoxia extends the life span of vascular smooth muscle cells through telomerase activation. Mol Cell Biol 21: 3336-3342

Minamino T, Miyauchi H, Yoshida T, Ishida Y, Yoshida H, Komuro I (2002) Endothelial cell senescence in human atherosclerosis. Role of telomere in endothelial dysfunction. Circulation 105: 1541-1544

Minamino T, Yoshida T, Tateno K, Miyauchi H, Zou Y, Toko H, Komuro (2003) Ras induces vascular smooth muscle cell senescence and inflammation in human atherosclerosis. Circulation 108: 2264-2269

Miquel J, Economos AC, Fleming J, Johnson JE Jr (1980) Mitochondrial role in aging. Exp Gerontol 15: 575-591

Mirault ME, Tremblay A, Pothier F (1992) Phenotypes of transgenic mice overexpressing glutathione peroxidase. Proc Am Assoc of Cancer Res 183: 1095A

Mishima K, Handa JT, Aotaki-Keen A, Lutty GA, Morse LS, Hjelmeland LM (1999) Senescence-associated beta-galactosidase histochemistry for the primate eye. Invest Ophthalmol Vis Sci 40: 1590-1593

Mitchell JR, Wood E, Collins K (1999) A telomerase component is defective in the human disease dyskeratosis congenita. Nature 492: 551-555

Moncada S, Herman AG, Higgs EA, Vane JR (1977) Differential formation of prostacyclin (PGX or PGI_2) by layers of the arterial wall: an explanation for the anti-thrombotic properties of vascular endothelium. Thromb Res 11: 323-344

Mondello C, Petropoulou C, Monti D, Gonos ES, Franceschi C, Nuzzo F (1999) Telomere length in fibroblasts and blood cells from healthy centenarians. Exp Cell Res 248: 234-242

Montagna W (1965) Morphology of the ageing skin: the cutaneous appendages. In: Montagna W (Ed.) Advances in the Biology of the Skin. Pergamon Press, Oxford. Chapter 6 pp 1-16

Moore S, Belbeck LW, Richardson M, Taylor W (1982) Lipid accumulation in the neointima formed in normally fed rabbits in response to one or six removals of the aortic endothelium. Lab Invest 47: 37-42

Morel DW, Di Corleto PE, Chisolm GM (1984) Endothelial and smooth muscle cells alter low density lipoprotein *in vitro* by free radical oxidation. Arteriosclerosis 4: 357-364

Morreau H, Galjart NJ, Gillemans N, Willemsen R, van der Horst GT, d'Azzo A (1989) Alternative splicing of beta-galactosidase mRNA generates the classic lysosomal enzyme and a beta-galactosidase-related protein. J Biol Chem 264: 20655-20663

Moyer CF, Sajuthi D, Tulli H, Williams JK (1991) Synthesis of IL-1 Alpha and IL-1 Beta by arterial cells in atherosclerosis. Am J Pathol 138: 951-960

Mugge A, Forstermann U, Lichtlen PR (1991) Platelets, endothelial-dependent responses and atherosclerosis. Ann Med 23: 545-550

Murnane JP, Sabatier L, Marder BA, Morgan WF (1994) Telomere dynamics in an immortal human cell line. EMBO J 13: 4953-4962

Mustard JF, Packham MA (1975) Platelets, thrombosis and drugs. Drugs 9: 19-76

Mutoh T, Naoi M, Nagatsu T, Takahashi A, Matsuoka Y, Hashizume Y, Fujiki N (1988) Purification and characterization of human liver beta-galactosidase from a patient with the adult form of GM1 gangliosidosis and a normal control. Biochim Biophys Acta 964: 244-253

Naderi J, Hung M, Pandey S (2003) Oxidative stress-induced apoptosis in dividing fibroblasts involves activation of p38 MAP kinase and over-expression of Bax: resistance of quiescent cells to oxidative stress. Apoptosis 8: 91-100

Nagai R, Nabeshima YI (1997) Mutation of the mouse klotho gene leads to a syndrome resembling ageing. Nature 390:45-51.

Nakamoto H, Nakamura A, Goto S, Hosokawa M, Fujisawa H, Takeda T (1994) Accumulation of oxidatively modified proteins in senescence-accelerated mouse SAMP11 and SAMR1. In: Takeda T (Ed.) The SAM Model of Senescence. Elsevier Science, Amsterdam. pp 137-140

Nakashima Y, Plump AS, Raines EW, Breslow JL, Ross R (1994) ApoE-deficient mice develop lesions of all phases of atherosclerosis throughout the arterial tree. Arterioscler Thromb 14: 133-140

Napoli C, D'Armiento FP, Mancini FP, Postiglione A, Witztum JL, Palumbo G, Palinski W (1997) Fatty streak formation occurs in human fetal aortas and is greatly enhanced by maternal hypercholesterolaemia. Intimal accumulation of low density lipoprotein and its oxidation precede monocyte recruitment into early atherosclerotic lesions. J Clin Invest 100: 2680-2690

Navab M, Berliner JA, Watson AD, Hama SY, Territo MC, Lusis AJ, Shih DM, Van Lenten BJ, Frank JS, Demer LL, Edwards PA, Fogelman AM (1996) The Yin and Yang of oxidation in the development of the fatty streak. A review based on the 1994 George Lyman Duff Memorial Lecture. Arterioscler Thromb Vasc Biol 16: 831-842

Newby AC, Zaltsman AB (1999) Fibrous cap formation or destruction – the critical importance of vascular smooth muscle cell proliferation, migration and matrix formation. Cardiovasc Res 41: 345-360

Nichols WW, Buynak EB, Bradt C, Hill R, Aronson M, Jarrell BE, Mueller SN, Levine EM (1987) Cytogenetic evaluation of human endothelial cell cultures. J Cell Physiol 132: 453-462

Nigg EA (1995) Cyclin-dependent protein kinases: key regulators of the eukaryotic cell cycle. Bioessays 17: 471-480

Niimi Y, Azuma H, Hirakawa K (1994) Repeated endothelial removal augments intimal thickening and attenuates EDRF release. Am J Physiol 266: H1348-H1356

Nishina PM, Wang J, Toyofuku W, Kuypers FA, Ishida BY, Paigen B (1993) Atherosclerosis and plasma and liver lipids in nine inbred strains of mice. Lipids 23: 599-605

Nisitani S, Hosokawa M, Sasaki MS, Yasuoka K, Naiki H, Matsushita T, Takeda T (1990) Acceleration of chromosomal aberrations in senescence-accelerated strains of mice. Mutat Res 237: 221-228

Noda A, Ning Y, Venable SF, Pereira-Smith OM, Smith JR (1994) Cloning of senescent cell-derived inhibitors of DNA synthesis using an expression screen. Exp Cell Res 211: 90-98

Nomura Y, Wang BX, Qi SB, Namba T, Kaneko S (1989) Biochemical changes related to aging in the senescence-accelerated mouse. Exp Gerontol 24: 49-55

Nusbaum TJ, Graves JL, Mueller LD, Rose MR (1993) Fruit fly aging and mortality. Science 269: 1567

O'Brien W, Stenman G, Sager R (1986) Suppression of tumor growth by senescence in virally transformed human fibroblasts. Proc Natl Acad Sci USA 83: 8659-8663

Odagiri Y, Uchida H, Hosokawa M, Takemoto K, Morley AA, Takeda T (1998) Accelerated accumulation of somatic mutations in the senescence-accelerated mouse. Nat Genet 19: 116-117

Ofir R, Wong AC, McDermid HE, Skorecki KL, Selig S (1999) Position effect of human telomeric repeats on replication timing. Proc Natl Acad Sci USA 96: 11434-11439

Okada AA, Dice JF (1984) Altered degradation of intracellular proteins in aging human fibroblasts. Mech Ageing Dev 26: 341-356

Okamoto R, Hatani M, Tsukitani M, Suehiro A, Fujino M, Imai N, Takano S, Watanabe Y, Fukuzaki H (1983) The effect of oxygen on the development of atherosclerosis in WHHL rabbits. Atherosclerosis 47: 47-53

Okuda K, Khan MY, Skurnick J, Kimura M, Aviv H, Aviv A (2000) Telomere attrition of the human abdominal aorta: relationships with age and atherosclerosis. Atherosclerosis 152: 391-398

Olovnikov AM (1973) A theory of marginotomy. The incomplete copying of template margin in enzymic synthesis of polynucleotides and biological significance of the phenomenon. J Theor Biol 41: 181-190

Orgel LE (1963) The maintenance of the accuracy of protein synthesis and its relevance to ageing. Proc Natl Acad Sci USA 49: 517-521

Orlandi A, Marcellini M, Spagnoli LG (2000) Aging influences development and progression of early aortic atherosclerotic lesions in cholesterol-fed rabbits. Arterioscler Thromb Vasc Biol 20: 1123-1136

Packer L, Fuehr K (1977) Low oxygen concentration extends the lifespan of cultured human diploid cells. Nature 267: 423-425

Pagano PJ, Ito Y, Tornheim K, Gallop PM, Tauber AI, Cohen RA (1995) An NADPH oxidase superoxide-generating system in the rabbit aorta. Am J Physiol 268: H2274-H2280

Paigen B, Mitchell D, Reue K, Morrow A, Lusis AJ, LeBoeuf RC (1987a) Ath-1, a gene determining atherosclerosis susceptibility and high density lipoprotein levels in mice. Proc Natl Acad Sci USA 84: 3763-3767

Paigen B, Morrow A, Brandon C, Mitchell D, Holmes P (1985) Variation in susceptibility to atherosclerosis among inbred strains of mice. Atherosclerosis 57: 65-73

Paigen B, Morrow A, Holmes P, Mitchell D, Williams RA (1987b) Quantitative assessment of atherosclerotic lesions in mice. Atherosclerosis 68: 231-240

Palinski W, Rosenfeld ME, Ylä-Herttuala S, Gurtner GC, Socher SS, Butler SW, Parthasarathy S, Carew TE, Steinberg D, Witztum JL (1989) Low density lipoprotein undergoes oxidative modification *in vivo*. Proc Natl Acad Sci USA 86: 1372-1376.

Palinski W, Tangirala RK, Miller E, Young SG, Witztum JL (1995) Increased autoantibody titers against epitopes of oxidized LDL in LDL receptor-deficient mice with increased atherosclerosis. Arterioscler Thromb Vasc Biol 15: 1569-1576

Paneth N, Susser M (1995) Early origin of coronary heart disease (the "Barker hypothesis"). BMJ 310: 411-412

Pang JH, Chen KY (1994) Global change of gene expression at late G1/S boundary may occur in human IMR-90 diploid fibroblasts during senescence. J Cell Physiol 160: 531-538

Parhami F, Fang ZT, Fogelman AM, Andalibi A, Territo MC, Berliner JA (1993) Minimally modified low density lipoprotein-induced inflammatory responses in endothelial cells are mediated by cyclic adenosine monophosphate, J Clin Invest 92: 471-478

Park JW, Choi CH, Kim MS, Chung MH (1996) Oxidative status in senescence-accelerated mice. J Gerontol 51A: B337-B345

Park WY, Hwang CI, Kang MJ, Seo JY, Chung JH, Kim YS, Lee JH, Kim H, Kim KA, Yoo HJ, Seo JS (2001) Gene profile of replicative senescence is different from progeria or elderly donor. Biochem Biophy Res Commun 282: 934-939

Parkes TL, Elia AJ, Dickinson D, Hilliker AJ, Phillips JP, Boulianne GL (1998) Extension of Drosophila lifespan by overexpression of human SOD1 in motorneurons. Nat Genet 19: 105-106

Parrinello S, Samper E, Krtolica A, Goldstein J, Melov S, Campisi J (2003) Oxygen sensitivity severely limits the replicative lifespan of murine fibroblasts. Nature Cell Biol 5: 741-747

Parthasarathy S, Printz DJ, Boyd D, Joy L, Steinberg D (1986) Macrophage oxidation of low density lipoprotein generates a modified form recognized by the scavenger receptor. Arteriosclerosis 6: 505-510

Pearson TA, Wang A, Solez K, Heptinstall RH (1975) Clonal characteristics of fibrous plaques and fatty streaks from human aorta. Am J Pathol 81: 379-387

Perlman H, Maillard L, Krasinski K, Walsh K (1997) Evidence for the rapid onset of apoptosis in medial smooth muscle cells after balloon injury. Circulation 95: 981-987

Peter M (1997) The regulation of cyclin-dependent kinase inhibitors (CKIs). Prog Cell Cycle Res 3: 99-108

Petersen S, Saretzki G, von Zglinicki T (1998) Preferential accumulation of single-stranded regions in telomeres of human fibroblasts. Exp Cell Res 239: 152-160

Pisciotta AV, Westring DW, DePrey C, Walsh B (1967) Mitogenic effect of phytohaemagglutinin at different ages. Nature 215: 193-194

Pitas RE (1990) Expression of the acetyl low density lipoprotein receptor by rabbit fibroblasts and smooth muscle cells. Up-regulation by phorbol esters. J Biol Chem 265: 12722-12727

Plewig G, Kligman AM (1978) Proliferative activity of the sebaceous glands of the aged. J Invest Dermatol 70: 314-317

Plump AS, Smith JD, Hayek T, Aalto-Setala K, Walsh A, Verstuyft JG, Rubin EM, Breslow JL (1992) Severe hypercholesterolaemia and atherosclerosis in apolipoprotein E-deficient mice created by homologous recombination in ES cells. Cell 71: 343-353

Poch E, Carbonell P, Franco S, Díez-Juan A, Blasco MA, Andrés V (2004) Short telomeres protect from diet-induced atherosclerosis in apolipoprotein E-null mice. FASEB J 18: 418-420

Pollman MJ, Hall JL, Gibbons GH (1999) Determinants of vascular smooth muscle cell apoptosis after balloon angioplasty injury. Influence of redox state and cell phenotype. Circ Res 84: 113-121

Ponten J (1976) The relationship between in vitro transformation and tumor formation in vivo. Biochim Biophys Acta 458: 397-422

Poole JCF, Florey HW (1958) Changes in the endothelium of the aorta and the behaviour of macrophages in experimental atheroma of rabbits. J Pathol Bacteriol 75: 245-253

Poot M, Esterbauer H, Rabimovitch PS, Hoehn H (1988) Disturbance of cell proliferation by two model compounds of lipid peroxidation contradicts causative role in proliferative senescence. J Cell Physiol 137: 421-429

Qiao J-H, Xie P-Z, Fishbein MC, Kreuzer J, Drake TA, Demer LL, Lusis AJ (1994) Pathology of atheromatous lesions in inbred and genetically engineered mice. Genetic determination of arterial calcification. Arterioscler Thromb 14: 1480-1497

Quinn MT, Parthasarathy S, Fong LG, Steinberg D (1987) Oxidatively modified low density lipoproteins: potential role in recruitment and retention of monocyte/macrophage during atherogenesis. Proc Natl Acad Sci USA 84: 2995-2998

Quinn MT, Parthasarathy S, Steinberg D (1988) Lysophosphatidylcholine: a chemotactic factor for human monocytes and its potential role in atherogenesis. Proc Natl Acad Sci USA 85: 2805-2809

Radomski MW, Palmer RM, Moncada S (1987) Endogenous nitric oxide inhibits human platelet adhesion to vascular endothelium. Lancet 2: 1057-1058

Rattan SI (1991) Protein synthesis and the components of protein synthetic machinery during cellular aging. Mutat Res 256: 115-125

Rauskolb C, Irvine KD (1999) Notch-mediated segmentation and growth control of the Drosophila leg. Dev Biol 210: 339-350

Reddick RL, Zhang SH, Maeda N (1994) Atherosclerosis in mice lacking apo E. Evaluation of lesional development and progression. Arterioscler Thromb 14: 141-147

Reddy VY, Zhang Q-Y, Weiss SJ (1995) Pericellular mobilization of the tissue-destructive cysteine proteinases, cathepsins B, L, and S, by human monocyte-derived macrophages. Proc Natl Acad Sci USA 92: 3849-3853

Refsum H, Ueland PM, Nygard O, Vollset SE (1998) Homocysteine and cardiovascular disease. Annu Rev Med 49: 31-62

Regnstrom J, Nilsson J, Tornvall P, Landou C, Hamsten A (1992) Susceptibility to low-density lipoprotein oxidation and coronary atherosclerosis in man. Lancet 339: 1183-1186

Reidy MA (1985) Biology of disease. A reassessment of endothelial injury and arterial lesion formation. Lab Invest 53: 513-520

Reidy MA (1988) Endothelial regeneration. VIII. Interaction of smooth muscle cells with endothelial regrowth. Lab Invest 59: 36-43

Reidy MA, Clowes AW, Schwartz SM (1983) Endothelial regeneration V. Inhibition of endothelial regrowth in arteries of rat and rabbit. Lab Invest 49: 569-575

Reidy MA, Schwartz SM (1981) Endothelial injury and regeneration. III. Time course of intimal changes after small defined injury to rat aortic endothelium. Lab Invest 44: 301-308

Reidy MA, Silver M (1985) Endothelial regeneration VII. Lack of intimal proliferation after defined injury in the rat aorta. Am J Pathol 118: 173-177

Reidy MA, Standaert D, Schwartz SM (1982) Inhibition of endothelial cell regrowth. Cessation of aortic endothelial cell replication after balloon catheter denudation. Arteriosclerosis 2: 216-220

Repin VS, Dolgov VV, Zaikina OE Novikov ID, Antonov AS, Nikolaeva MA, Smirnov VN (1984) Heterogeneity of endothelium in human aorta. A quantitative analysis by scanning electron microscopy. Atherosclerosis 50: 35-52

Reveillaud I, Niedzwiecki A, Bensch KG (1991) Expression of bovine superoxide dismutase in *Drosophila melanogaster* augments resistance to oxidative stress. Mol Cell Biol 11: 632-640

Rheinwald JG, Hahn WC, Ramsey MR, Wu JY, Guo Z, Tsao H, De Luca M, Catricala C, O'Toole KM (2002) A two-stage, p16(INK4A)- and p53-dependent keratinocyte senescence mechanism that limits replicative potential independent of telomere status. Mol Cell Biol 22: 5157-5172

Rigotti A, Trigatti BL, Penman M, Rayburn H, Herz J, Krieger M (1997) A targeted mutation in the murine gene encoding the high density lipoprotein (HDL) receptor scavenger receptor class B type I reveals its key role in HDL metabolism. Proc Natl Acad Sci USA 94: 12610-12615

Rittling SR, Brooks KM, Cristofalo VJ, Baserga R (1986) Expression of cell cycle-dependent genes in young and senescent WI-38 fibroblasts. Proc Natl Acad Sci USA 83: 3316-3320

Rohme D (1981) Evidence for a relationship between longevity of mammalian species and life spans of normal fibroblasts in vitro and erythrocytes in vivo. Proc Natl Acad Sci U S A. 78: 5009-5013

Rosen EM, Mueller SN, Noveral JP, Levine EM (1981) Proliferative characteristics of clonal endothelial cell strains. J Cell Physiol 107: 123-137

Rosenfeld ME (1998) Inflammation, lipids, and free radicals: lessons learned from the atherogenic process. Semin Reprod Endocrinol 16: 246-261

Rosenfeld ME, Faggiotto A, Ross R (1985) The role of the mononuclear phagocyte in primate and rabbit models of atherosclerosis. Proceedings of the Fourth Leiden Conference on Mononuclear Phagocytes. The Hague: Martinus Nijhoff. pp 795-802

Rosenthal D, Stevens SL, Skillern CS, Wellons ED, Robinson K, Matsuura JH, Gannon BJ (2002) Topical application of beta-radiation to reduce intimal hyperplasia after carotid artery balloon injury in rabbit. A possible application for brachytherapy in vascular surgery. Cardiovasc Radiat Med 3: 16-19

Ross R (1986) The pathogenesis of atherosclerosis – an update. N Engl J Med 314: 488-500

Ross R, Glomset JA (1976) The pathogenesis of atherogenesis. N Engl J Med 295: 369-377, 420-425.

Ross R, Glomset J, Kariya B, Harker L (1974) A platelet-derived serum factor that stimulates the proliferation of arterial smooth muscle cells *in vitro*. Proc Natl Acad Sci USA 71: 1207-1210

Roy AK (1997) Transcription factors and aging. Mol Med 3: 496-504

Rubin EM, Krauss RM, Spangler EA, Verstuyft JG, Clift SM (1991) Inhibition of early atherogenesis in transgenic mice by human apolipoprotein AI. Nature 353: 265-267

Rubin EM, Smith DJ (1994) Atherosclerosis in mice: getting to the heart of a polygenic disorder. Trends Genet 10: 199-203

Rudolph KL, Chang S, Lee HW, Blasco M, Gottlieb GJ, Greider C, DePinho (1999) Longevity, stress response, and cancer in aging telomere-deficient mice. Cell 96: 701-712

Rueckschloss U, Galle J, Holtz J, Zerkowski HR, Morawietz H (2001) Induction of NAD(P)H oxidase by oxidized low-density lipoprotein in human endothelial cells. Circulation 104: 1767-1772

Sacher GA (1977) Life table modification and life prolongation. In: Finch CE, Hayflick L (Eds) Handbook of the Biology of Aging. Van Nostrand Reinhold Company, New York. p582

Sage J, Mulligan GJ, Attardi LD, Miller A, Chen S, Williams B, Theodorou E, Jacks T (2000) Targeted disruption of the three Rb-related genes leads to loss of G(1) control and immortalization. Genes Dev 14: 3037-3050

Sager R (1991) Senescence as a mode of tumor suppression. Environ Health Perspect 93: 59-62

Saito Y, Yamagishi T, Nakamura T, Ohyama Y, Aizawa H, Suga T, Matsumara Y, Masuda H, Kurabayashi M, Kuro-o M, Nabeshima Y, Nagai R (1998) Klotho protein protects against endothelial dysfunction. Biochem Biophys Res Commun 248: 324-329

Samani NJ, Boultby R, Butler R, Thompson JR, Goodall AH (2001) Telomere shortening in atherosclerosis. Lancet 358: 472-473

Saren P, Welgus HG, Kovanen PT (1996) TNF-alpha and IL-1beta selectively induce expression of 92-kDa gelatinase by human macrophages. J Immunol 157: 4159-4165

Saretzki G, Sitte N, Merkel U, Wurm RE, von Zglinicki T (1999) Telomere shortening triggers a p53-dependent cell cycle arrest via accumulation of G-rich single stranded DNA fragments. Oncogene 18: 5148-5158

Satyanarayana A, Wiemann SU, Buer J, Lauber J, Dittmar KE, Wustefeld T, Blasco MA, Manns MP, Rudolph KL (2003) Telomere shortening impairs organ regeneration by inhibiting cell cycle re-entry of a subpopulation of cells. EMBO J 22: 4003-4013

Sawamura T, Kume N, Aoyama T, Moriwaki H, Hoshikawa H, Aiba Y, Tanaka T, Miwa S, Katsura Y, Kita T, Masaki T (1997) An endothelial receptor for oxidized low-density lipoprotein. Nature 386: 73-77

Schleicher ED, Wagner E, Nerlich AG (1997) Increased accumulation of the glycoxidation product N(epsilon)-(carboxymethyl)lysine in human tissues in diabetes and aging. J Clin Invest 99: 457-468

Schmidt AM, Hori O, Chen JX, Li JF, Crandall J, Zhang J, Cao R, Yan SD, Brett J, Stern D (1995) Advanced glycation endproducts interacting with their endothelial receptor induce expression of vascular cell adhesion molecule-1 (VCAM-1) in cultured human endothelial cells and in mice. A potential mechanism for the accelerated vasculopathy of diabetes. J Clin Invest 96: 1395-1403

Schmidt AM, Yan SD, Brett J, Mora R, Nowygrod R, Stern D (1993) Regulation of human mononuclear phagocyte migration by cell surface-binding proteins for advanced glycation end products. J Clin Invest 91: 2155-2168

Schmidt HH, Hill S, Makariou EV, Feuerstein IM, Dugi KA, Hoeg JM (1996) Relation of cholesterol-year score to severity of calcific atherosclerosis and tissue deposition in homozygous familial hypercholesterolemia. Am J Cardiol 77: 575-580

Schmitt CA, Fridman JS, Yang M, Lee S, Baranov E, Hoffman RM, Lowe SW (2002) A senescence program controlled by p53 and p16INK4a contributes to the outcome of cancer therapy. Cell 109: 335-346

Schneider EL, Mitsui Y (1976) The relationship between in vitro aging and in vivo human age. Proc Natl Acad Sci USA 73: 3584-3588

Schneider JE, Berk BC, Gravanis MB, Santoian EC, Cipolla GD, Tarazona N, Lassegue B, King SB (1993) Probucol decreases neointimal formation in a swine model of coronary artery balloon injury. A possible role for antioxidants in restenosis. Circulation 88: 628-637

Schneiderman J, Sawdey MS, Keeton MR, Bordin GM, Berstein EF, Dilley RB, Loskutoff DJ (1992) Increased type 1 plasminogen activator inhibitor gene expression in atherosclerotic human arteries. Proc Natl Acad Sci USA 89: 6998-7002

Schober A, Knarren S, Lietz M, Lin EA, Weber C (2003) Crucial role of stromal cell-derived factor-1α in neointimal formation after vascular injury in apolipoprotein E-deficient mice. Circulation 108: 2492-2497

Schwartz CJ, Valente AJ, Sprague EA, Kelley JL, Nerem RM (1991) The pathogenesis of atherosclerosis: an overview. Clin Cardiol 14 : I1-I16

Schwartz RS, Huber KC, Murphy JG, Edwards WD, Camrud AR, Vlietstra RE, Holmes DR (1992) Restenosis and the proportional neointimal response to coronary artery injury: results in a porcine model. J Am Coll Cardiol 19: 267-274

Schwartz SM, Benditt EP (1973) Cell replication in the aortic endothelium: a new method for study of the problem. Lab Invest 28: 699-707

Schwartz SM, Benditt EP (1976) Clustering of replicating cells in aortic endothelium. Proc Natl Acad Sci USA 73: 651-653

Schwartz SM, Benditt EP (1977) Aortic endothelial cell replication. I. Effects of age and hypertension in the rat. Circ Res 41: 248-255

Schwartz SM, Gajdusek CM, Reidy MA (1980) Maintenance of integrity in aortic endothelium. Fed Proc 39: 2618-2625

Scott-Burden T, Vanhoutte PM (1993) The endothelium as a regulator of vascular smooth muscle proliferation. Circulation 87 (Suppl V): V51-V55

Seluanov A, Gorbunova V, Falcovitz A, Sigal A, Milyavsky M, Zurer I, Shohat G, Goldfinger N, Rotter V (2001) Change of the death pathway in senescent human fibroblasts in response to DNA damage is caused by an inability to stabilize p53. Mol Cell Biol 21: 1552-1564

Serra V, Grune T, Sittle N, Saretzki G, von Zglinicki T (2000) Telomere length as a marker of oxidative stress in primary human fibroblast cultures. Ann N Y Acad Sci 908: 327-330

Serrano M, Lin AW, McCurrach ME, Beach D, Lowe SW (1997) Oncogenic ras provokes premature cell senescence associated with accumulation of p53 and p16INK4a. Cell 88: 593-602

Seshadri T, Campisi J (1990) Repression of c-fos transcription and an altered genetic program in senescent human fibroblasts. Science 247: 205-209

Severino J, Allen RG, Balin S, Balin A, Cristofalo VJ (2000) Is beta-galactosidase staining a marker of senescence in vitro and in vivo? Exp Cell Res 257: 162-171

Shah PK (2003) Mechanisms of plaque vulnerability and rupture. J Am Coll Cardiol 41(4 Suppl S): 15S-22S

Shanahan CM, Weissberg PL, Metcalfe JC (1993) Isolation of gene markers of differentiated and proliferating vascular smooth muscle cells. Circ Res 73: 193-204

Shay JW, Pereira-Smith OM, Wright WE (1991a) A role for both RB and p53 in the regulation of human cellular senescence. Exp Cell Res 196: 33-39

Shay JW, Wright WE, Werbin H (1991b) Defining the molecular mechanisms of human cell immortalization. Biochim Biophys Acta 1072: 1-7

Shelton DN, Chang E, Whitter PS, Choi D, Funk WD (1999) Microarray analysis of replicative senescence. Curr Biol 9: 939-945

Sherr CJ (1996) Cancer cell cycles. Science 274: 1672-1677

Sherr CJ, DePinho RA (2000) Cellular senescence: Mitotic clock or culture shock? Cell 102: 407-410

Sherwood SW, Rush D, Ellsworth JL, Schimke RT (1988) Defining cellular senescence in IMR-90 cells: a flow cytometric analysis. Proc Natl Acad Sci USA 85: 9086-9090

Shi Y, Niculescu R, Wang D, Patel S, Davenpeck KL, Zalewski A (2001) Increased NAD(P)H oxidase and reactive oxygen species in coronary arteries after balloon injury. Arterioscler Thromb Vasc Biol 21: 739-745

Shi Y, O'Brien JE, Fard A, Mannion JD, Wang D, Zalewski A (1996) Adventitial myofibroblasts contribute to neointimal formation in injured porcine coronary arteries. Circulation 94: 1655-1664

Shin WS, Hong YH, Peng HB, De Caterina R, Libby P, Liao JK (1996) Nitric oxide attenuates vascular smooth muscle cell activation by interferon-gamma. The role of constitutive NF-kappa B activity. J Biol Chem 271: 11317-11324

Siegler R, Rich MA (1963) Unilateral thymic lymphoma in AKR mice. Trans N Y Acad Sci 25: 590-597

Sies H (1991) Oxidative Stress II: Oxidants and Antioxidants. Academic Press, London

Sies H (1993) Strategies of antioxidant defence. Eur J Biochem 215: 213-219

Sitte N, Merker K, Von Zglinicki T, Grune T, Davies KJ (2000) Protein oxidation and degradation during cellular senescence of human BJ fibroblasts: part I – effects of proliferative senescence. FASEB J 14: 2495-2502

Smith GS, Walford RL (1977) Influence of the main histocompatibility complex on ageing in mice. Nature 270: 727-729

Smith JR, Pereira-Smith OM (1996) Replicative senescence: implications for in vivo aging and tumor suppression. Science 273: 63-67

Smith JR, Pereira-Smith OM, Schneider EL (1978) Colony size distributions as a measure of in vivo and in vitro aging. Proc Natl Acad Sci USA 75: 1353-1356

Smith JR, Whitney RG (1980) Intraclonal variation in proliferative potential of human diploid fibroblasts: stochastic mechanism for cellular aging. Science 207: 82-84

Smith S, Giriat I, Schmitt A, de Lange T (1998) Tankyrase, a poly(ADP-ribose) polymerase at human telomeres. Science 282: 1484-1487

Smogorzewska A, de Lange T (2002) Different telomere damage signaling pathways in human and mouse cells. EMBO J 21: 4338-4348

Smogorzewska A, van Steensel B, Bianchi A, Oelmann S, Schaefer MR, Schnapp G, de Lange T (2000) Control of human telomere length by TRF1 and TRF2. Mol Cell Biol 20: 1659-1668

Sohal RS, Allen RG (1990) Oxidative stress as a causal factor in differentiation and aging: a unifying hypothesis. J Gerontol 25: 499-522

Sohal RS, Sohol BH, Brunk UT (1990) Relationship between antioxidant defenses and longevity in different mammalian species. Mech Ageing Dev 53: 217-227

Sohal RS, Svensson I, Sohol BH, Brunk UT (1989) Superoxide anion radical production in different animal species. Mech Ageing Dev 49: 129-135

Sohal RS, Weindruch R (1996) Oxidative stress, caloric restriction and aging. Science 273: 59-63

Southgate K, Newby AC (1990) Serum-induced proliferation of rabbit aoritc smooth muscle cells from the contractile state is inhibited by 8-Br-cAMP but not 8-Br-cGMP. Atherosclerosis 82: 113-123

Souza HP, Souza LC, Anastacio VM, Pereira AC, Junqueira M de L, Krieger JE, da Luz PL, Augusto O, Laurindo FRM (2000) Vascular oxidant stress early after balloon injury: evidence for increased NAD(P)H oxidoreductase activity. Free Radic Biol Med 28: 1232-1242

Sparrow CP, Doebber TW, Olszewski J, Wu MS, Ventre J, Stevens KA, Chao YS (1992) Low density lipoprotein is protected from oxidation and the progression of atherosclerosis is slowed in cholesterol-fed rabbits by the antioxidant N,N'-diphenyl-phenylenediamine. J Clin Invest 89: 1885-1891

Spencer NF, Poynter ME, Im SY, Daynes RA (1997) Constitutive activation of NF kappa B in an animal model of aging. Int Immunol 9: 1581-1588

Stadtman ER (1992) Protein oxidation and aging. Science 257: 1220-1224

Staiano-Coico L, Darzynkiewicz Z, Melamed M, Weksler ME (1984) Immunological studies of aging. IX. Impaired proliferation of T lymphocytes detected in elderly humans by flow cytometry. J Immunol 132: 1788-1792

Stanulis-Praeger BM (1987) Cellular senescence revisited: a review. Mech Aging Dev 38: 1-48

Stary HC, Blankenhorn DH, Chandler AB, Glagov S, Insull W Jr, Richardson M, Rosenfeld ME, Schaffer SA, Schwartz CJ, Wagner WD, Wissler RW (1992) A definition of the intima of human arteries and of its atherosclerosis-prone regions. A report from the Committee on Vascular Lesions of the Council on Arteriosclerosis, American Heart Association. Arterioscler Thromb 12: 120-134

Stary HC, Chandler AB, Glagov S, Guyton JR, Insull W Jr, Rosenfeld ME, Schaffer SA, Schwartz CJ, Wagner WD, Wissler RW (1994) A definition of initial, fatty streak, and intermediate lesions of atherosclerosis. A report from the Committee on Vascular Lesions of the Council on Arteriosclerosis, American Heart Association. Arterioscler Thromb 14: 840-856

Stary HC, Malinow MR (1982) Ultrastructure of experimental coronary artery atherosclerosis in cynomolgus monkeys. A comparison with the lesions of other primates. Atherosclerosis 43: 151-175

Stationary Office (1996) Mortality Statistics for England and Wales. Series DH2 number 23, ISBN 0 11 6210257

Stavri GT, Hong Y, Zachary IC, Breier G, Baskerville PA, Ylä-Herttuala S, Risau W, Martin JF, Erusalimsky JD (1995) Hypoxia and platelet-derived growth factor BB synergistically upregulate the expression of vascular endothelial growth factor in vascular smooth muscle cells. FEBS Lett 358: 311-315

Stein GH, Beeson M, Gordon L (1990) Failure to phosphorylate the retinoblastoma gene product in senescent human fibroblasts. Science 249: 666-669

Stein GH, Drullinger LF, Robetorye RS, Pereira-Smith OM, Smith JR (1991) Senescent cells fail to express cdc2, cycA, and cycB in response to mitogen stimulation. Proc Natl Acad Sci USA 88: 11012-11016

Stein GH, Dulic V (1995) Origins of G1 arrest in senescent human fibroblasts. Bioessays 17: 537-543

Stein GH, Namba M, Corsaro CM (1985) Relationship of finite proliferative lifespan, senescence, and quiescence in human cells. J Cell Physiol 122: 343-349

Steinberg D (1983) Lipoproteins and atherosclerosis: a look back and a look ahead. Arteriosclerosis 3: 293-301

Steinberg D (1995) The oxidative modification hypothesis of atherogenesis: strengths and weaknesses. In: Woodford FP, Davignon J, Sniderman A (Eds) Atherosclerosis X. Elsevier Science, Amsterdam.

Steinberg D, Parthasarathy S, Carew TE, Khoo JD, Witztum JL (1989) Beyond cholesterol: modifications of low density lipoprotein that increase its atherogenicity. N Engl J Med 320: 915-924

Stemerman MB, Spaet TH, Pitlick F, Cintron J, Lejnieks I, Tiell ML (1977) The pattern of reendothelialization and intimal thickening. Am J Pathol 87: 125-142

Stemerman MB, Weinstein R, Rowe JW, Maciag T, Fuhro R, Gardner R (1982) Vascular smooth muscle cell growth kinetics in vivo in aged rats. Proc Natl Acad Sci USA 79: 3863-3866

Stenmark KR, Gerasimovskaya E, Nemenoff RA, Das M (2002) Hypoxic activation of adventitial fibroblasts: role in vascular remodeling. Chest 122: 326S-334S.

Stewart-Phillips JL, Lough J (1991) Pathology of atherosclerosis in cholesterol-fed, susceptible mice. Atherosclerosis 90: 211-218

Stokes J 3rd, Kannel WB, Wolf PA, Cupples LA, D'Agostino RB (1987) The relative importance of selected risk factors for various manifestations of cardiovascular disease among men and women from 35 to 64 years old: 30 years of follow-up in the Framingham Study. Circulation 75: V65-V73

Stokes KY, Clanton EC, Russell JM, Ross CR, Granger N (2001) NAD(P)H oxidase-derived superoxide mediates hypercholesterolemia-induced leukocyte-endothelial cell adhesion. Circ Res 88: 499-505

Strong JP, McGill HC Jr (1962) The natural history of coronary atherosclerosis. Am J Pathol 40: 37-49

Sugiyama S, Okada Y, Sukhova GK, Virmani R, Heinecke JW, Libby P (2001) Macrophage myeloperoxidase regulation by granulocyte macrophage colony-stimulating factor in human atherosclerosis and implication in acute coronary syndromes. Am J Pathol 158: 879-891

Sukhova GK, Shi G-P, Simon DI, Chapman HA, Libby P (1998) Expression of the elastolytic cathepsins S and K in human atheroma and regulation of their production in smooth muscle cells. J Clin Invest 102: 576-583

Sukhova GK, Williams JK, Libby P (2002) Statins reduce inflammation in atheroma of nonhuman primates independent of effects on serum cholesterol. Arterioscler Thromb Vasc Biol 22: 1452-1458

Sukhova GK, Zhang Y, Pan JH, Wada Y, Yamamoto T, Naito M, Kodama T, Tsimikas S, Witztum JL, Lu ML, Sakara Y, Chin MT, Libby P, Shi GP (2003) Deficiency of cathepsin S reduces atherosclerosis in LDL receptor-deficient mice. J Clin Invest 111: 897-906

Suttorp N, Toepfer W, Roka L (1986) Antioxidant defence mechanisms of endothelial cells: glutathione redox cycle versus catalase. Am J Physiol 251: C671-C680

Szilard L (1959) A theory of aging. Nature 184: 957-958

Takeda T, Hosokawa M, Higuchi K, (1991) Senescence-accelerated mouse (SAM): a novel murine model of accelerated senescence. J Am Geriatr Soc 39: 911-919

Takeda T, Hosokawa M, Higuchi K (1994a) Senescence-accelerated mouse (SAM). A novel murine model of aging. In: Takeda T (Ed.) The SAM model of senescence. Excerpta Medica, Amsterdam. pp 15-22

Takeda T, Hosokawa M, Higuchi K, Hosono M, Akiguchi I, Katoh H (1994b) A novel murine model of aging, senescence-accelerated mouse (SAM) Arch Gerontol and Geriatr 19: 185-192

Takeda T, Hosokawa M, Takeshita S, Irino M, Higuchi K, Matsushita T, Tomita Y, Yasuhira K, Hamamoto H, Shimizu K, Ishii M, Yamamuro T (1981) A new murine model of accelerated senescence. Mech Ageing Dev 17: 183-194

Tangirala RK, Casanada F, Miller E, Witztum JL, Steinberg D, Palinski W (1995a) Effect of the antioxidant N,N-diphenyl 1,4-phenylenediamine (DPPD) on atherosclerosis in ApoE-deficient mice. Arterioscler Thromb Vasc Biol 15: 1625-1630

Tangirala RK, Rubin EM, Palinski W (1995b) Quantitation of atherosclerosis in murine models: correlation between lesions in the aortic origin and in the entire aorta, and differences in the extent of lesions between sexes in LDL receptor-deficient and apolipoprotein E-deficient mice. J Lipid Res 36: 2320-2328

Tardif JC, Coté G, Lesperance J, Bourassa M, Lambert J, Doucet C, Bilodeau L, Nattel S, Guise P (1997) Probucol and multivitamins in the prevention of restenosis after coronary angioplasty. Multivitamins and Probucol Study Group. N Engl J Med 337: 365-372.

Tassin J, Malaise E, Courtois Y (1979) Human lens cells have an in vitro proliferative capacity inversely proportional to the donor age. Exp Cell Res 123: 388-392

Taylor KE, Glagov S, Zarins CK (1989) Preservation and structural adaptation of endothelium over experimental foam cell lesions. Quantitative ultrastructural study. Arteriosclerosis 9: 881-894

te Poele RH, Okorokov AL, Jardine L, Cummings J, Joel SP (2002) DNA damage is able to induce senescence in tumor cells in vitro and in vivo. Cancer Res 62: 1876-1883

Tepper CG, Seldin MF, Mudryj M (2000) Fas-mediated apoptosis of proliferating, transiently growth arrested, and senescent normal human fibroblasts. Exp Cell Res 260: 9-19

Tesco G, Vergelli M, Amaducci L, Sorbi S (1993) Growth properties of familial Alzheimer skin fibroblasts during in vitro aging. Exp Gerontol 28: 51-58

Thompson KV, Holliday R (1975) Chromosome changes during in vitro ageing of MRC-5 human fibroblasts. Exp Cell Res 96 :1-6

Thornton SC, Mueller SN, Levine EM (1983) Human endothelial cells: use of heparin in cloning and long-term serial cultivation. Science 222: 623-625

Thweatt R, Murano S, Fleischmann RD, Goldstein S (1992) Isolation and characterization of gene sequences overexpressed in Werner syndrome fibroblasts during premature replicative senescence. Exp Gerontol 27: 433-440

Tokunaga O, Fan J, Watanabe T (1989) Atherosclerosis- and age-related multinucleated variant endothelial cells in primary culture from human aorta. Am J Pathol 135: 967-976

Toussaint O, Medrano EE, von Zglinicki T (2000a) Cellular and molecular mechanisms of stress-induced premature senescence (SIPS) of human diploid fibroblasts and melanocytes. Exp Gerontol 35: 927-945

Toussaint O, Remacle J, Clark BF, Gonos ES, Franceschi C, Kirkwood TB (2000b) Biology of ageing. Bioessays 22: 954-956

Tschudi MR, Barton M, Bersinger NA, Moreau P, Cosentino F, Noll G, Malinski T, Luscher TF (1996) Effect of age on kinetics of nitric oxide release in rat aorta and pulmonary artery. J Clin Invest 98: 899-905

Tsukamoto A, Kaneko Y, Yoshida T, Han K, Ichinose M, Kinura S (1998) 2-Methoxyestradiol, an endogenous metabolite of estrogen, enhances apoptosis and beta-galactosidase expression in vascular endothelial cells. Biochem Biophys Res Commun 248: 9-12

Ungvari Z, Csiszar A, Edwards JG, Kaminski PM, Wolin MS, Kaley G, Koller A (2003) Increased superoxide production in coronary arteries in hyperhomocysteinaemia: role of tumor necrosis factor-alpha, NAD(P)H oxidase, and inducible nitric oxide synthase. Arterioscler Thromb Vasc Biol 23: 418-424

van der Wal AC, Das PK, Tigges AJ, Becker AE (1992) Adhesion molecules on the endothelium and mononuclear cells in human atherosclerotic lesions. Am J Pathol 141: 1427-1433

Vasile E, Tomita Y, Brown LF, Kocher O, Dvorak HF (2001) Differential expression of thymosin beta-10 by early passage and senescent vascular endothelium is modulated by VPF/VEGF: evidence for senescent endothelial cells in vivo at sites of atherosclerosis. FASEB J 15: 458-466

Vaziri H, Benchimol S (1996) From telomere loss to p53 induction and activation of a DNA-damage pathway at senescence: the telomere loss/DNA damage model of cell aging. Exp Gerontol 31: 295-301

Vaziri H, Benchimol S (1998) Reconstitution of telomerase activity in normal human cells leads to elongation of telomeres and extended life span. Curr Biol 8: 279-282

Vaziri H, Schachter F, Uchida I, Wei L, Zhu X, Effros R, Cohen D, Harley CB (1993) Loss of telomeric DNA during aging of normal and trisomy 21 human lymphocytes. Am J Hum Genet 52: 661-667

Vaziri H, West MD, Allsopp RC, Davison TS, Wu YS, Arrowsmith CH, Poirier GG, Benchimol S (1997) ATM-dependent telomere loss in aging human diploid fibroblasts and DNA damage lead to the post-translational activation of p53 protein involving poly(ADP-ribose) polymerase. EMBO J 16: 6018-6033

Verdugo ME, Ray J (1997) Age-related increase in activity of specific lysosomal enzymes in the human retinal pigment epithelium. Exp Eye Res 65: 231-240

Verheyen AK, Vlaminckx EM, Lauwers FM, Saint-Guillain ML, Borgers MJ (1988) Identification of macrophages in intimal thickening of rat carotid arteries by cytochemical localization of purine nucleoside phosphorylase. Arteriosclerosis 8: 759-767

Verma IM, Stevenson J (1997) IkappaB kinase: beginning, not the end. Proc Natl Acad Sci USA 94: 11758-11760

Vikhert AM, Zhdanov VS (1975) Kaltsinoz koronarnykh arteri serdtsa. Kardiologiya 15: 102-108

Virmani R, Avolio AP, Mergner WJ, Robinowitz M, Herderick EE, Cornhill JF, Guo SY, Liu TH, Ou DY, O'Rourke M (1991) Effect of aging on aortic morphology in populations with high and low prevalence of hypertension and atherosclerosis. Comparison between occidental and Chinese communities. Am J Pathol 139: 1119-1129

Vlaicu R, Niculescu F, Rus HG, Cristea A (1985) Immunohistochemical localization of the terminal C5b-9 complement complex in human aortic fibrous plaque. Atherosclerosis 57: 163-177

Vlassara H, Fuh H, Donnelly T, Cybulsky M (1995) Advanced glycation endproducts promote adhesion molecule (VCAM-1, ICAM-1) expression and atheroma formation in normal rabbits. Mol Med 1: 447-456

von Zglinicki T, Pilger R, Sitte N (2000) Accumulation of single-strand breaks is the major cause of telomere shortening in human fibroblasts. Free Radic Biol Med 28: 64-74

von Zglinicki T, Saretzki G, Döcke W, Lotze C (1995) Mild hyperoxia shortens telomeres and inhibits proliferation of fibroblasts: a model for senescence? Exp Cell Res 220: 186-193

Wagner M, Hampel B, Bernhard D, Hala M, Zwerschke W, Jansen-Dürr P (2001) Replicative senescence of human endothelial cells in vitro involves G1 arrest, polyploidization and senescence-associated apoptosis. Exp Gerontol 36: 1327-1347

Wakita K, Lord JM, Tokuhisa T (1991) A method for detecting the expression of a toxic gene in cultured cells. Anal Biochem 198: 224-227

Walford R (1969) The immunologic theory of aging. Munksgaard, Copenhagen

Walker LN, Reidy MA, Bowyer DE (1986) Morphology and cell kinetics of fatty streak lesion formation in the hypercholesterolemic rabbit. Am J Pathol 125: 450-459

Walzem RL, Watkins S, Frankel EN, Hansen RJ, German JB (1995) Older plasma lipoproteins are more susceptible to oxidation: a linking mechanism for the lipid and oxidation theories of atherosclerotic cardiovascular disease. Proc Natl Acad Sci USA 92: 7460-7464

Wang E (1995) Senescent human fibroblasts resist programmed cell death, and failure to suppress bcl2 is involved. Cancer Res 55: 2284-2292

Wang M, Takagi G, Asai K, Resuello RG, Natividad FF, Vatner DE, Vatner SF, Lakatta EG (2003) Aging increases aortic MMP-2 activity and angiotensin II in non-human primates. Hypertension 41: 1308-1316

Warner HR, Hodes RJ, Pocinki K (1997) What does cell death have to do with aging? J Am Geriatr Soc 45: 1140-1146

Watanabe T, Fan J (1998) Atherosclerosis and inflammation mononuclear cell recruitment and adhesion molecules with reference to the implication of ICAM-1/LFA-1 pathway in atherogenesis. Int J Cardiol 66 Suppl 1: S45-S53

Wautier JL, Wautier MP, Schmidt AM, Anderson GM, Hori O, Zoukourian C, Capron L, Chappey O, Yan SD, Brett J (1994) Advanced glycation end products (AGEs) on the surface of diabetic erythrocytes bind to the vessel wall via a specific receptor inducing oxidant stress in the vasculature: a link between surface-associated AGEs and diabetic complications. Proc Natl Acad Sci USA 91: 7742-7746

Wei W, Herbig U, Wei S, Dutriaux A, Sedivy JM (2003) Loss of retinoblastoma but not p16 function allows bypass of replicative senescence in human fibroblasts. EMBO Rep 4: 1061-1065

Weidinger FF, McLenachan JM, Cybulsky MI, Gordon JB, Rennke HG, Hollenberg NK, Fallon JT, Ganz P, Cooke JP (1990) Persistent dysfunction of regenerated endothelium after balloon angioplasty of rabbit iliac artery. Circulation 81: 1667-1679

Weinberg RA (1995) The retinoblastoma protein and cell cycle control. Cell 81: 323-330

Weingand KW, Clarkson TB, Adams MR, Bostrom AD (1986) Effects of age and/or puberty on coronary artery atherosclerosis in cynomolgus monkeys. Atherosclerosis 62: 137-144

Weinstein DB, Carew TE, Steinberg D (1976) Uptake and degradation of low density lipoprotein by swine and arterial smooth muscle cells with inhibition of cholesterol biosynthesis. Biochim Biophys Acta 424: 404-421

Weiss N, Keller C, Hoffman U, Loscalzo J (2002) Endothelial dysfunction and atherothrombosis in mild hyperhomocysteinaemia. Vasc Med 7: 227-239

Welbourn CR, Goldman G, Paterson IS, Valeri CR, Shepro D, Hechtman HB (1991) Pathophysiology of ischaemia reperfusion injury: central role of the neutrophil. Br J Surg 78: 651-655

West MD, Pereira-Smith OM, Smith JR (1989) Replicative senescence of human skin fibroblasts correlates with a loss of regulation and overexpression of collagenase activity. Exp Cell Res 184: 138-147

Whisnant JP, Homer D, Ingall TJ, Baker HL Jr, O'Fallon WM, Wievers DO (1990) Duration of smoking is the strongest predictor of severe extracranial carotid artery atherosclerosis. Stroke 21: 707-714

Wissler RW, Vesselinovitch D (1977) Atherosclerosis in nonhuman primates. Adv Vet Sci Comp Med 21: 351-420

Witztum JL (1993) Murine models for study of lipoprotein metabolism and atherosclerosis. J Clin Invest 92: 536-537

Witztum JL (1994) The oxidation hypothesis of atherosclerosis. Lancet 344: 1363-1364

Witztum JL, Steinberg D (1991) Role of oxidized LDL in atherogenesis. J Clin Invest 88: 1785-1792

Wong H, Riabowol K (1996) Differential CDK-inhibitor gene expression in aging human fibroblasts. Exp Gerontol 31: 311-325

Woolf N (1977) Aspects of atherogenesis. Br J Hosp Med 18: 286-293

Wright HP (1968) Endothelial mitosis around aortic branches in normal guinea-pigs. Nature 220: 78-79

Wright WE, Piatyszek MA, Rainey WE, Byrd W, Shay JW (1996) Telomerase activity in human germline and embryonic tissues and cells. Dev Genet 18: 173-179

Wright WE, Shay JW (2000) Telomere dynamics in cancer progression and prevention: fundamental differences in human and mouse telomere biology. Nat Med 6: 849-851

Wyllie AH (1992) Apoptosis and the regulation of cell numbers in normal and neoplastic tissues: an overview. Cancer Metastasis Rev 11: 95-103

Xiong Y, Hannon GJ, Zhang H, Casso D, Kobayashi R, Beach D (1993) p21 is a universal inhibitor of cyclin kinases. Nature 366: 701-704

Xu D, Neville R, Finkel T (2000) Homocysteine accelerates endothelial cell senescence. FEBS Lett 470: 20-24

Xu HJ, Zhou Y, Ji W, Perng GS, Kruzelock R, Kong CT, Bast RC, Mills GB, Li J, Hu SX (1997) Reexpression of the retinoblastoma protein in tumor cells induces senescence and telomerase inhibition. Oncogene 15: 2589-2596

Yagi K, Komura S, Sasaguri Y, Yoshino K, Ohishi N (1995) Atherogenic change in the thoracic aorta of the senescence-accelerated mouse. Atherosclerosis 118: 233-236

Yagi K, Yoshino K, Komura S, Kondo K, Ohishi N (1988) Lipid peroxide levels in the senescence-accelerated mouse. J Clin Biochem Nutr 5: 21-27

Yang J, Chang E, Cherry AM, Bangs J, Chang E, Cherry AM, Bangs CD, Oei Y, Bodnar A, Bronstein A, Chiu CP, Herron GS (1999) Human endothelial cell life extension by telomerase expression. J Biol Chem 274: 26141-26148

Ye X, Meeker HC, Kozlowski P, Carp I (2002) Increased c-Fos protein in the brains of scrapie-infected SAMP8, SAMR1, AKR and C57BL mice. Neuropath Appl Neurobiol 28: 358-366

Ylä-Herttuala S, Palinski W, Rosenfeld ME, Parthasarathy S, Carew TE, Butler S, Witztum JL, Steinberg D (1989) Evidence for the presence of oxidatively modified low density lipoprotein in atherosclerotic lesions of rabbit and man. J Clin Invest 84: 1086-1095

Yoshino K, Komura S, Ohishi N, Yagi K (1994a) Serum lipid and lipoprotein levels in the senescence-accelerated mouse. J Clin Biochem Nutr 17: 89-94

Yoshino K, Komura S, Okada T, Ohishi N, Yagi K (1994b) Skin lipid peroxide level of the senescence-accelerated mouse. In: Takeda T (Ed.) The SAM model of senescence. Elsevier Science, Amsterdam. pp 145-148

Yost JC, Herman IM (1988) Age-related and site-specific adaptation of the arterial endothelial cytoskeleton during atherogenesis. Am J Pathol 30: 595-604

Zarins CK, Glagov S, Giddens DP (1990) What do we find in human atherosclerosis that provides insight into the hemodynamic factors in atherogenesis? In: Glagov S, Newman WP, Schaffer SA (Eds) Pathobiology of the Human Atherosclerotic Plaque. Springer-Verlag, New York. pp 317-332

Zemel PC, Sowers JR (1990) Relation between lipids and atherosclerosis: epidemiological evidence and clinical implications. Am J Cardiol 66: 7I-12I

Zempo N, Koyama N, Kenagy RD, Lea HJ, Clowes AW (1996) Regulation of vascular smooth muscle cell migration and proliferation in vitro and in injured rat arteries by a synthetic matrix metalloproteinase inhibitor. Arterioscler Thromb Vasc Biol 16: 28-33

Zhang L, Aviv H, Gardner JP, Okuda K, Patel S, Kimura M, Bardeguez A, Aviv A (2000) Loss of chromosome 13 in cultured human vascular endothelial cells. Exp Cell Res 260: 357-364

Zhang SH, Reddick RL, Burkey B, Maeda N (1994) Diet-induced atherosclerosis in mice heterozygous and homozygous for apolipoprotein E gene disruption. J Clin Invest 94: 937-945

Zhang SH, Reddick RL, Piedrahita JA, Maeda N (1992) Spontaneous hypercholesterolaemia and arterial lesions in mice lacking apolipoprotein E. Science 258: 468-471

Zhao X-H, Awaya A, Kobayashi H, Ohnuki T, Tokumitsu Y, Nomura Y (1990) Effects of repeated administration of facteur thymique sérique (FTS) on biochemical changes related to aging in senescence-accelerated mouse (SAM). Japan J Pharmacol 53: 311-319

Zhdanov VS, Lifshits AM, Vikhert AM (1973) Atherosclerosis of the aortic arch. Kardiologiya 13: 47-52

Zhu BH, Ueno M, Matsushita T, Fujisawa H, Seriu N, Nishikawa T, Nishimura Y, Hosokawa M (2001) Effects of aging and blood pressure on the structure of the thoracic aorta in SAM mice: a model of age-associated degenerative vascular changes. Exp Gerontol 36: 111-124